



Dipl.-Ing. Christian Höller

# **Approaches and Concepts to Increase the Economic Efficiency of Selective Laser Melting**

## **Doctoral Thesis**

to achieve the university degree of

Doktor der technischen Wissenschaften

submitted to

**Graz University of Technology**

Supervisor and Examiner

Univ.-Prof. Dipl.-Ing. Dr.techn. Rudolf Pichler

Institute of Production Engineering

Head: Univ.-Prof. Dipl.-Ing. Dr.techn. Franz Haas

External Examiner

Prof. Dr.-Ing. Michael Zäh

Institute for Machine Tools and Industrial Management

Technical University of Munich

Graz, September 2020



## Statutory Declaration

I declare that I have authored this thesis independently, that I have not used other than the declared sources/resources, and that I have explicitly indicated all material which has been quoted either literally or by content from the sources used. The text document uploaded to TUGRAZonline is identical to the present doctoral thesis.

14/09/2020

---

Date

---

Signature

*The important thing is not to stop questioning.  
Curiosity has its own reason for existence.*

– Albert Einstein –

---

## Preface

This thesis was carried out during my profession as research associate at the Institute of Production Engineering (IFT) at Graz University of Technology.

First of all, I want to thank my supervisor Univ.-Prof. Dipl.-Ing. Dr.techn. Rudolf Pichler for the opportunity to work on the fascinating topic of selective laser melting in his research group. I really appreciate his professional guidance, constructive suggestions and the space he gave me for conducting my research. I also want to express my gratitude to Univ.-Prof. Dipl.-Ing. Dr.techn. Franz Haas, for the possibility of writing this thesis at his institute and his support during my research activities. Also, I would like to thank Prof. Dr.-Ing. Michael Zäh, for being part of the thesis committee, his valuable recommendations and for his review of my thesis.

I want to thank all of my past and present colleagues at the IFT for the cooperative and supportive atmosphere in the last four and a half years. I want to express my special gratitude to Philipp Schwemberger, my office and SLM workmate, for his continuous support. I really appreciate your valuable contributions to this thesis and our strong collaboration. Special thanks to the members of the “Forscherexpress”, Philipp, Thomas, Martin, Georg and Matthias. I am pleased to be part of this group and to share my thoughts and time with you. You enriched my time at the IFT, but also my personal life.

I very much appreciate the opportunity to teach and guide several students during my working activities. In particular, I want to mention Christopher, Stefan, Georg, Klemens and Thomas who were always open for my ideas and worked on their topics conscientiously.

I have greatly benefited from the projects I was involved during the past years. Therefore, I would like to offer my thanks to my project partners for the fruitful cooperation and the many insights I have gained.

Finally, I would like to extend my gratitude to my family and to my girlfriend Lisa. Thank you all for your patience and for your encouragement to find and go my own way.

---

## Abstract

Selective laser melting (SLM) – as a leading metal-based additive manufacturing (AM) process – carves its way from prototyping to production. Despite its high growth rates and disruptive potential, the dissemination of SLM within the manufacturing industry is still limited. Low productivity and a lack of comprehensive knowledge about the potentials lead to economic disadvantages compared to established production technologies. This thesis addresses the ongoing issue of economic efficiency with selected approaches along the SLM process chain.

Success in SLM starts with the selection of the right parts. For this, a screening process model (SPM) was developed and tested in an industrial environment. In addition, the economic impact of design for additive manufacturing (DfAM) was examined. For this purpose, lifecycle costing (LCC) was elaborated for a use case from the aviation industry. Out of this, the importance of cost considerations in early development stages was studied analytically by elaborating representative build job simulations. Moving further along the SLM process chain, the increase in productivity during the step of processing was demonstrated experimentally for 316L stainless steel. For this, SLM test specimens were created with advanced parameter configurations. The evaluation of the fabricated samples was based on three criteria: build-up rate, minimum downskin angle and relative density. The economic impact of the advanced parameter configurations was verified by comparing the manufacturing costs of altered parameters with those of standard parameters. As a last approach, the novel concept of direct machining (DM) is introduced. Direct machining is the subtractive post-processing of SLM parts directly on the build platform. First, its feasibility was examined and verified by machining experiments. Based on a theoretical load model, DM was further enhanced and additional experiments were conducted. Finally, the economic potential of DM as third presented approach was evaluated.

The results of this work show that all the concepts developed along the SLM process chain can increase the economic efficiency. A structured and quantifiable selection process leads to parts that utilize the full technical potential of SLM and that are economically reasonable at the same time. Moving further, the developed parameter configurations led to cost advantages of approx. 45 % due to a faster build-up rate and an improved downskin angle. Finally, results confirm the feasibility of direct machining as a promising concept for economic post-processing.

---

## Kurzfassung

Selektives Laserschmelzen (SLM) gilt als das führende additive Fertigungsverfahren für metallische Bauteile. Trotz hoher Wachstumsraten und des Innovationspotentials ist die Verbreitung von SLM innerhalb der Fertigungsindustrie noch sehr begrenzt. Die geringe Produktivität, aber auch fehlendes Wissen rund um die technologischen Möglichkeiten, führen zu ökonomischen Nachteilen gegenüber traditionellen Fertigungstechnologien. Die vorliegende Arbeit begegnet diesem Problem mit ausgewählten Ansätzen entlang der SLM Prozesskette.

Erfolg mit SLM beginnt bei der Auswahl von geeigneten Bauteilen. Dazu wurde ein strukturiertes Modell zur Bauteilauswahl (screening process model, SPM) entwickelt und im industriellen Umfeld getestet. Darüber hinaus wurde der ökonomische Nutzen eines Ansatzes, der Bauteile speziell für die additive Fertigung optimiert (DfAM), anhand von Lebenszykluskostenrechnungen (life cycle costing, LCC) untersucht. Die Notwendigkeit von Kostenüberlegungen in frühen Stadien der Produktentwicklung wurde durch Simulationen bestätigt. Im nächsten Schritt der Prozesskette wurde die Produktivitätssteigerung während des Bauprozesses für 316L Edelstahl experimentell überprüft. Dazu wurden SLM Probenkörper mit weiterentwickelten Parameterkonfigurationen hergestellt. Für die Evaluierung wurden drei Kriterien herangezogen: Aufbaurate, minimaler Überhangwinkel und relative Dichte. Zusätzlich wurden die positiven ökonomischen Auswirkungen durch den Vergleich der Herstellkosten mit jenen der Standard SLM Parameter verifiziert. Der letzte Ansatz zur Produktivitätssteigerung ist das neuartige Konzept des „direct machining“ (DM). DM beschreibt die subtraktive Nachbearbeitung von SLM Bauteilen direkt auf der Bauplattform. Zuerst wurde die Realisierbarkeit experimentell nachgewiesen. Basierend auf einem theoretischen Modell wurde DM anschließend weiterentwickelt und untersucht. Abschließend wurde der wirtschaftliche Nutzen von DM als letztes vorgestelltes Konzept evaluiert.

Die Resultate zeigen, dass die entwickelten Ansätze aus dieser Arbeit die Wirtschaftlichkeit von SLM steigern. Ein strukturierter und messbarer Auswahlprozess führt zu Bauteilen, die das volle technische und ökonomische Potenzial von SLM nutzen. Während des Bauprozesses gelang es, durch höhere Aufbauraten und verbesserte Überhangwinkel Kostenvorteile von ca. 45 % zu erzielen. Abschließend zeigte auch das entwickelte Konzept des direct machining vielversprechende Resultate hinsichtlich ökonomischer SLM Nachbearbeitung.

---

# Table of Contents

<b>1</b>	<b>Introduction.....</b>	<b>1</b>
1.1	Problem Statement and Motivation.....	3
1.2	Research Aims and Objectives.....	5
1.3	Structure of the Thesis .....	6
<b>2</b>	<b>Theoretical Background.....</b>	<b>9</b>
2.1	Basics of Additive Manufacturing.....	9
2.2	AM-Process Chain.....	13
2.3	Economic Relevance of AM and its Potentials .....	18
2.4	Limitations of AM .....	23
2.5	Selective Laser Melting – State of the Art.....	24
2.5.1	Process Fundamentals of SLM.....	25
2.5.2	Economic Aspects – Challenges for SLM as Manufacturing Technology.....	30
2.5.3	Process-related Challenges.....	31
2.5.4	Information-related Challenges .....	38
<b>3</b>	<b>Costs and Economic Appraisal of SLM.....</b>	<b>43</b>
3.1	Cost Considerations of SLM .....	43
3.1.1	Present Cost Calculations and Cost Models.....	43
3.1.2	Lifecycle Cost Considerations.....	47
3.1.3	Summary of Chapter 3.1.....	50
3.2	The IFT Cost Model.....	51
3.3	Cost Evaluation of Selected Build Jobs .....	56
3.3.1	Methodology .....	56
3.3.2	Example 1: Jet Engine Bracket.....	58
3.3.3	Example 2: Filter Head.....	62
3.3.4	Example 3: Pipe Section.....	64
3.3.5	Micro Economies of Scale .....	67
3.3.6	Discussion of the Cost Evaluation of Selected Build Jobs.....	69
3.4	Screening, Selection and Transfer Model for SLM.....	71
3.4.1	Use Case 1: Starting with SLM.....	72
3.4.2	Use Case 2: Experienced SLM Users.....	79
3.4.3	Discussion of the Presented Use Cases.....	85
3.5	Lifecycle Costs – Case Study .....	87
3.5.1	Redesign for SLM .....	88
3.5.2	Lifecycle Costs.....	89



---

3.5.3	Lifecycle Costs within the VDI 2225-3 .....	92
3.5.4	Discussion of the LCC Case Study .....	93
3.6	Summary of Chapter 3 .....	94
<b>4</b>	<b>Parameter Optimization for SLM – “316L Economy” .....</b>	<b>96</b>
4.1	Effect of Parameter Settings on the Productivity.....	96
4.2	Preliminary Studies .....	98
4.3	Studies on 316L Economy .....	101
4.3.1	Methodology .....	101
4.3.2	Test Series 1 – Improvement of the Downskin Angle.....	102
4.3.3	Test Series 2 – Investigation of the Relative Density .....	106
4.4	Economic Evaluation of 316L Economy and Discussion.....	111
4.5	Summary of Chapter 4.....	115
<b>5</b>	<b>Direct Machining as a New Approach to Economic Post-Processing.....</b>	<b>116</b>
5.1	Initial Situation .....	116
5.1.1	The Geometrical Accuracy of SLM.....	116
5.1.2	The Concept of Direct Machining .....	120
5.2	Feasibility Study of Direct Machining – DM1 .....	122
5.3	Modelling of Direct Machining .....	127
5.3.1	Cutting Forces for Plain Face Milling.....	127
5.3.2	Cutting Forces for Direct Machining .....	131
5.4	Optimization of Support Structures for Direct Machining – DM2 .....	133
5.4.1	Experimental Setup .....	133
5.4.2	Results and Discussion of the Milling Experiments .....	137
5.5	Economic Evaluation of Direct Machining.....	143
5.6	Summary of Chapter 5.....	149
<b>6</b>	<b>Conclusion and Outlook .....</b>	<b>150</b>
6.1	Pre-Processing: Costs and Economic Appraisal.....	150
6.2	Processing: 316L Economy.....	151
6.3	Post-Processing: Direct Machining.....	152
6.4	Synthesis of the Approaches.....	153
6.5	Outlook and Future Tasks .....	155
	<b>List of Figures .....</b>	<b>158</b>
	<b>List of Tables .....</b>	<b>162</b>
	<b>References .....</b>	<b>164</b>
	<b>Appendix .....</b>	<b>175</b>

---

## List of Symbols

Symbol	Unit	Designation
$A$	$\text{mm}^2$	undeformed chip cross section
$a$	mm	grid distance
$a_p$	mm	cutting depth
$b$	mm	chip thickness
$C_{\text{Add}}$	€	additional costs
$C_{\text{BP,L}}$	€	labor costs, build process
$C_{\text{BP,M}}$	€	machine costs, build process
$C_{\text{Ene}}$	€	energy costs
$C_{\text{Gas}}$	€	gas costs
$C_{\text{Manf}}$	€	total manufacturing costs
$C_{\text{Mat}}$	€	material costs
$C_{\text{Pos,L}}$	€	labor costs, post-processing
$C_{\text{Pos,M}}$	€	machine costs, post-processing
$C_{\text{Pre,HS}}$	€	specific hardware and software costs, pre-processing
$C_{\text{Pre,L}}$	€	labor costs, pre-processing
$C_{\text{SP,L}}$	€	labor costs, setup preparation
$C_{\text{SP,M}}$	€	machine costs, setup preparation
$C_{\text{SR,L}}$	€	labor costs, setup removal
$C_{\text{SR,M}}$	€	machine costs, setup removal
$e_t$	mm	perpendicular distance to the neutral axis
$E_V$	$\text{J}/\text{mm}^3$	volumetric energy density
$F$	N	machining force
$f$	mm	feed
$F_a$	N	active force
$F_c$	N	cutting force
$F_{\text{cm}}$	N	average cutting force
$F_{\text{cmz}}$	N	average cutting force per tooth
$F_{\text{cN}}$	N	perpendicular component of the cutting force
$F_f$	N	feed force
$F_p$	N	passive force
$F_{\text{res}}$	N	resulting force out of $F_x$ and $F_y$
$f_z$	mm	feed per tooth
$h$	mm	chip thickness
$h_{\text{c,b}}$	mm	bottom cutting height
$h_{\text{c,t}}$	mm	top cutting height

---

$h_s$	mm	hatch spacing
$h_s$	mm	support height
$I_x$	$\text{mm}^4$	second moment of inertia, x-axis
$I_y$	$\text{mm}^4$	second moment of inertia, y-axis
$I_{x,y}$	$\text{mm}^4$	second moment of inertia, x- and y-axis
$K_0$	€	initial investment, NPV
$k_c$	$\text{N}/\text{mm}^2$	specific cutting force
$k_{c,1.1}$	$\text{N}/\text{mm}^2$	unit specific cutting force
$K_t$	€	cash inflow-outflow, NPV
$l_z$	mm	layer thickness
$M_b$	Nm	bending moment
$m_c$	-	exponent of cutting force
$n_{b,i}$	#	actual number of parts on the build platform
$n_{b,max}$	#	maximum number of possible parts on the build platform
$P_L$	W	laser power
$r$	%	discount rate, NPV
$t$	mm	grid thickness
$t_b$	h	total build time
$t_{bci}$	h	total build time per customer, collective
$t_{bi}$	h	total build time per customer, solo
$t_w$	s	waiting time
$u_t$	-	utilization factor
$V_b$	$\text{cm}^3$	build volume, part
$V_B$	$\text{cm}^3$	total build volume
$v_c$	m/min	cutting speed
$v_f$	mm/min	feed speed
$\dot{V}_{Pr}$	$\text{cm}^3/\text{h}$	practical build-up rate
$v_s$	mm/s	scanning speed
$\dot{V}_{Th}$	$\text{cm}^3/\text{h}$	theoretical build-up rate
$w$	mm	total grid width
$z_{iE}$	-	number of cutting edges in operation
$\delta$	°	downskin angle
$\varphi$	°	entry angle
$\kappa$	°	cutting tool angle
$\sigma_b$	$\text{N}/\text{mm}^2$	bending stress
$\tau$	$\text{N}/\text{mm}^2$	shear stress

---

## List of Abbreviations

<b>Abbreviation</b>	<b>Designation</b>
ABC	activity-based costing
AD	Additive.Designer
AI	artificial intelligence
AM	additive manufacturing
AMT	advanced manufacturing technologies
B	block support structure
C	cross support structure
CAD	computer-aided design
CAM	computer-aided manufacturing
CM	conventional manufacturing (see TM)
CNC	computerized numerical control
CT	computer tomography
DfAM	design for additive manufacturing
DfM	design for manufacturing
DM	direct machining
DMLS	direct metal laser sintering (see SLM)
EBM	electron beam melting
EoS	economies of scale
FDM	fused deposition modeling
FEA	finite element analysis
FF	feasibility factor
FL	filling level
GD&T	geometric dimensioning and tolerancing
HPDC	high-pressure die-casting
IFT	Institut für Fertigungstechnik (Institute of Production Engineering)
IM	injection molding
IoT	internet of things
LBM	laser beam melting (see SLM)
LCC	lifecycle costing
L-PBF	laser-powder bed fusion (see SLM)
M	medium filling level
m-AMTM	metal additive manufacturing transfer model
m-EoS	micro economies of scale
MM	Materialise Magics
NPV	net present value

---

OEF	optimization enabling factor
OEM	original equipment manufacturer
PC	parameter configuration
PLM	product lifecycle management
R	rod support structure
RM	rapid manufacturing
RP	rapid prototyping
RT	rapid tooling
S	strong filling level
SLA	stereolithography (AM process)
SLM	selective laser melting
SLS	selective laser sintering
SM	separate machining
SME	small and medium-sized enterprises
SPM	screening process model
ST	support type
STL	stereolithography or standard transformation/triangle language
TBJ	test build job
TD ABC	time-driven activity-based costing
TM	traditional manufacturing (see CM)
W	weak filling level



# 1 INTRODUCTION

The term “manufacturing”, from a technological perspective, can be regarded as the transformation of a starting material, or of single components, into a finished part. The manufacturing process uses a combination of labor, power, machinery and tools. From an economic perspective, manufacturing means the increase of value by one or more processing operations. While it originally derives from the two Latin terms “manus” (hand) and “factus” (made), manufacturing has left the made-by-hand-state today. <sup>1</sup>

Nowadays, modern manufacturing means using advanced technologies. Along with the so-called 4th industrial revolution, digitalization is entering the shop floor.<sup>2</sup> Artificial intelligence (AI), the internet of things (IoT) or cloud computing are constantly changing the world of production to meet the rising demand for individualized and customized products.<sup>3, 4</sup> Related to this, additive manufacturing (AM) is stated as one of the key technologies when it comes to advanced manufacturing technologies (AMT). <sup>5,6</sup>

Additive manufacturing is defined as the “process of joining materials to make parts from 3D model data, usually layer upon layer, as opposed to subtractive manufacturing and formative manufacturing methodologies”<sup>7</sup>. The layer-by-layer buildup of raw material is the basic principle of several AM processes and at the same time its greatest advantage. It allows a near-net-shape production without the use of specific tools or fixtures. With AM, typical boundaries of conventional manufacturing (CM), such as undercuts from formative manufacturing (e.g. casting) or cavities from subtractive manufacturing, (e.g. milling) can be left aside. The resulting freedom of design allows to create parts and products that cannot be manufactured in conventional ways – or at least not under reasonable economic

---

<sup>1</sup> Cf. Groover (2013) pp. 1–4.

<sup>2</sup> Cf. Gehrke et al. (2015) p. 6.

<sup>3</sup> Cf. Jardim-Goncalves et al. (2011) pp. 725–726.

<sup>4</sup> Cf. Tao et al. (2017) pp. 1079–1082.

<sup>5</sup> Cf. Wang (2018).

<sup>6</sup> Cf. Esmailian et al. (2016) pp. 93–95.

<sup>7</sup> ISO/ASTM 52900:2015 (2015) p. 1.

conditions. Furthermore, AM is seen as a disruptive technology that can change business models and industrial branches substantially<sup>8, 9, 10, 11</sup>

AM – informally often called 3D-printing – has its origins in the manufacturing of prototypes and started in the mid-1980s. Originally, AM should enable the fast creation of physical objects to visualize design ideas and to support product development. This process is widely known as rapid prototyping (RP). Today, AM has found its way into the industry as a manufacturing technology for high-quality end products. This shift from prototyping to manufacturing is based on the successful use of AM parts in various industrial sectors and branches. For example, customization and individualization are the primary reasons for the use of AM in medicine. Medical uses – from patient-specific implants to the bioprinting of organs – as well as the related research in this field, have significantly increased in number in the past years.<sup>12</sup> Metal-based AM processes can produce highly stressed parts for automotive and aerospace industry. One of the most quoted examples is the fuel nozzle of the GE Aero LEAP engine. It combines the main advantages of AM such as part integration, a lightweight design and the use of complex materials. GE targets a series production of 32,000 pieces per year.<sup>13</sup> From an economic perspective, the global market size of AM has been continuously increasing over the past years. The market size of AM is predicted to have more than doubled, from US\$ 15.8 billion in 2020 to US\$ 35.8 billion, in 2024.<sup>14</sup>

The transformation from prototyping to manufacturing requires the use of adequate AM processes. Selective laser melting (SLM) is the leading AM process concerning the production of metal parts. For that, a high-intense laser beam locally melts a metal powder layer by layer. After solidification, the single layers are joined together which results in the parts having relative densities >99 %, with excellent mechanical and technical properties.<sup>15</sup> Therefore, SLM enables the production of parts for the direct use in the industry. However, SLM must overcome certain challenges to become a well-established manufacturing technology.

---

<sup>8</sup> Cf. Hannibal/Knight (2018).

<sup>9</sup> Cf. Savolainen/Collan (2020).

<sup>10</sup> Cf. Zäh (2013) p. 13; p. 125.

<sup>11</sup> Cf. Gebhardt/Hötter (2016) pp. 1–6.

<sup>12</sup> Cf. Javaid/Haleem (2018).

<sup>13</sup> Cf. Milewski (2017) pp. 7–8.

<sup>14</sup> Cf. Forbes (2019).

<sup>15</sup> Cf. Gebhardt (2011) pp. 42–43.



### 1.1 Problem Statement and Motivation

As already stated, SLM offers great opportunities as a manufacturing technology. Despite the high growth rates of the AM market, SLM is still a niche manufacturing technology of metal parts. The market share of metal AM systems and hardware (including SLM machines) can be estimated to make up only 2 % of the world machine-tool market which is around US\$ 87.1 billion, excluding parts and accessories.<sup>16, 17, 18</sup>

The reasons for the small proportion of SLM in the manufacturing industry are diverse. First of all, SLM is a rather new manufacturing technology. Today, the successful use of SLM parts in various industrial sectors underlines the already stated shift from rapid prototyping to direct manufacturing. However, an overall acceptance of SLM as an adequate manufacturing technology – alongside traditional ones such as casting or milling – is still missing.

As typical for a young technology, SLM has to overcome certain obstacles. Firstly, knowledge about the capabilities of the technology needs to be acquired and disseminated. SLM related knowledge starts with the design process. Only specific design considerations can lead to suitable parts and products that use the full potential of SLM. This specific knowledge about the reasonable use of AM – not only limited to SLM – is widely known as design for additive manufacturing (DfAM). Only the appropriate use of DfAM can “add value” or “increase functionality” – two frequently used terms – of AM parts and products. Still, the quantification of possible benefits of AM products is difficult. Nevertheless, when it comes to the comparison of AM to traditional manufacturing technologies, a more holistic approach than the simple evaluation based on the manufacturing cost will be necessary. Otherwise, the often cited “added value” through AM will not be considered in its full dimension.

Furthermore, the finding of suitable SLM products is major challenge today. Again, a deep understanding of the technology and its possibilities is necessary to produce successful SLM parts. This is especially true for companies that are new to the field of AM, which has not yet been explored in great detail. Additionally, AM professionals (academic and non-academic), who can support the development of suitable products, are still underrepresented in Central European companies. A broader knowledge base leads to a greater number of successful SLM

---

<sup>16</sup> Cf. German Machine Tool Builders' Association (2019) p. 80.

<sup>17</sup> Cf. IDC (2020).

<sup>18</sup> Cf. Ampower (2019).

use cases. Due to that, awareness would rise further and SLM could become more deeply rooted in the world of manufacturing.

Apart from the lack of awareness, an economic barrier prevents the use of SLM in large quantities. Due to the low productivity, SLM is mainly restricted to small-series production and branches that require complex parts of high value, such as medicine or aerospace.<sup>19</sup> Slow build-up rates for SLM as well as the high initial costs for machine and equipment lead to high processing costs. This makes SLM parts barely competitive within classical serial production.

The limited productivity is a well-known, and probably the greatest, challenge for SLM as a manufacturing technology. Therefore, great efforts are made to increase it. One approach towards higher build-up rates is the adjustment of the machine parameters. As an example, higher laser power or larger beam diameters are reported as possible solutions for better economic efficiency, also based on higher build-up rates.<sup>20,21</sup> To achieve an economic benefit, an in-depth knowledge about parameters and their impact on the part properties is essential. Furthermore, the adjustment of the parameters must be made possible for the user by the machine manufacturer. Although the influence of SLM parameters on the build-up rate is well reported for some materials, their positive influence on the overall manufacturing costs is rarely explored and described.

In SLM process chain, post-processing of the manufactured parts is an important phase. The limited geometrical tolerances and part properties (e.g. surface roughness) prevent direct use of SLM parts in their as-built state for industrial applications. Additionally, support structures, which are required for the manufacturing process, have to be removed. Thus, additional process steps like CNC machining or polishing must be conducted to achieve high quality parts. These steps increase the manufacturing costs significantly. Post-processing is reported as one of the major bottlenecks of the SLM technology when it comes to higher productivity and only few tangible concepts are available to achieve a higher grade of automatization so far. The challenging task is to enable a higher grade of automatization without impairing the strengths of SLM, such as complexity and individualization.

---

<sup>19</sup> Cf. Cordovilla et al. (2018).

<sup>20</sup> Cf. Schleifenbaum et al. (2010).

<sup>21</sup> Cf. Buchbinder et al. (2011).

The SLM process offers great opportunities but still there is some work to do. The goal is to develop SLM into a fully recognized and accepted manufacturing technology alongside the traditional ones. On the one hand, a broad knowledge base of the right use and suitable applications as well as a deep process understanding would result in more and more SLM products with added value. On the other hand, higher productivity would lead to less manufacturing costs and increase the competitiveness of SLM as a manufacturing technology.

### **1.2 Research Aims and Objectives**

The overarching aim of this doctoral thesis is to improve the economic efficiency of the SLM process with selected approaches and concepts. First of all, the whole process chain of SLM needs to be investigated. The process chain of SLM generally consists of three consecutive steps: pre-processing; processing and post-processing. One research question (RQ) for each process step is developed and elaborated in order to cover the whole process chain. Secondly, only approaches and concepts that are based on the existing infrastructure at the Institute of Production Engineering (IFT) of Graz University of Technology will be discussed. The reason for this is the transferability of it to the typical (industrial) SLM users. The typical user operates one SLM machine and usually expands its existing business model with it. That means that the high initial investment into the SLM equipment already burdens the budget. Thus, there are fewer financial resources to invest in – if so available – additional equipment to achieve a higher economic efficiency. Therefore, all presented measures in this thesis are applicable to a broad spectrum of SLM users. Finally, this doctoral thesis will support the strategic course of the IFT regarding its SLM research agenda.

The first objective of this thesis is an overall analysis of the process chain of selective laser melting, from which a cost model is developed, allowing the determination of the main cost drivers of SLM. Based on this, the possible potential for an increase of process efficiency is investigated. In the following paragraphs, three research questions following the main SLM process chain are elaborated:

#### **1. Pre-Processing**

**RQ1: “How can pre-processing – and design for additive manufacturing (DfAM) in particular – positively influence the economic perspective on SLM parts?”**

DfAM is undoubtedly a key factor for the successful use of SLM as a manufacturing technology. Still, DfAM related benefits (e.g. part consolidation) and their positive economic effects are hard to quantify. Furthermore, a comprehensible and quantifiable selection of suitable SLM parts for DfAM is challenging as well. For this, a self-developed part screening process model and economic appraisal in an early stage should emphasize the role of pre-processing for successful SLM parts.

### **2. Processing**

**RQ2: “How can the choice of newly developed parameters for 316L stainless steel have a positive influence on economic efficiency?”**

Open SLM systems allow a broad variety and flexibility in the adjustment of the machine parameters for the scanning process. It should be investigated whether self-developed machine parameters can increase the economic efficiency compared to the provided standard parameters for stainless steel 316L. It is postulated, that advanced parameters can lead to higher build-up rates while the mechanical properties remain comparable. Higher build-up rates directly decrease the manufacturing costs and therefore positively influence the economic efficiency.

### **3. Post-Processing**

**RQ3: “How can the step of subtractive post-processing be made more efficient?”**

SLM manufactured parts show limited accuracy and geometrical tolerances in the as-built state. Therefore, CNC machining is the state-of-the art post-processing technology used to overcome these limitations. A novel approach, named direct machining (DM) will be introduced and its feasibility will be validated. Direct machining is supposed to reduce the clamping and handling time for post-processing CNC machining. The resulting decrease in manufacturing time should lead to higher economic efficiency.

## **1.3 Structure of the Thesis**

This chapter and Figure 1.1 give an overview of the structure of the thesis and its content.

In chapter 2, the state of the art of AM and SLM is covered. In the first part of the chapter, the classification and process chain of AM is discussed as well as the economic potential and limitations. The second part presents the current state of SLM from a technical and an

economic point of view. Finally, process- and information-related challenges of SLM are addressed.

Chapter 3 covers research question 1 (RQ1) concerning costs and the economic appraisal of SLM. Based on the IFT cost model, main cost drivers for the SLM process are determined in this chapter. Additionally, the cost evaluation of selected build jobs is presented and the term “micro-economies of scale” is introduced. In the second part of the chapter, the importance of the selection process of suitable AM components and their economic evaluation is discussed based on two use cases from the industry. Along with this, the developed metal additive manufacturing transfer model (m-AMTM) and the screening process model (SPM) are described. In the last part, a case study explores the difference between conventional and additive manufacturing regarding life cycle costing.

In chapter 4, research question 2 (RQ2) will be discussed. This chapter gives insight into the methodology and experimental investigation of our advanced machine parameters for 316L, internally called “316L economy”. Simulations show the influence of 316L economy on the build-up rate and build time. Additionally, a positive effect on the amount of support structure was found and is discussed in this chapter. The findings from the investigations of 316L economy are evaluated in terms of their economic advantages.

Chapter 5 focuses on research question 3 (RQ3). Post-processing via CNC machining improves the quality of SLM parts but also causes additional costs. The new approach of direct machining will be introduced and explained. Milling experiments demonstrate the feasibility of this concept. Additionally, the optimization of the support structures for direct machining is discussed and its economic impact is analyzed.

As chapters 3,4 and 5 are very different in content, their results will be discussed and summarized separately within the respective chapter. The covered topics and the conducted results are concluded in chapter 6 where also an outlook on the context-related future tasks of SLM is provided.

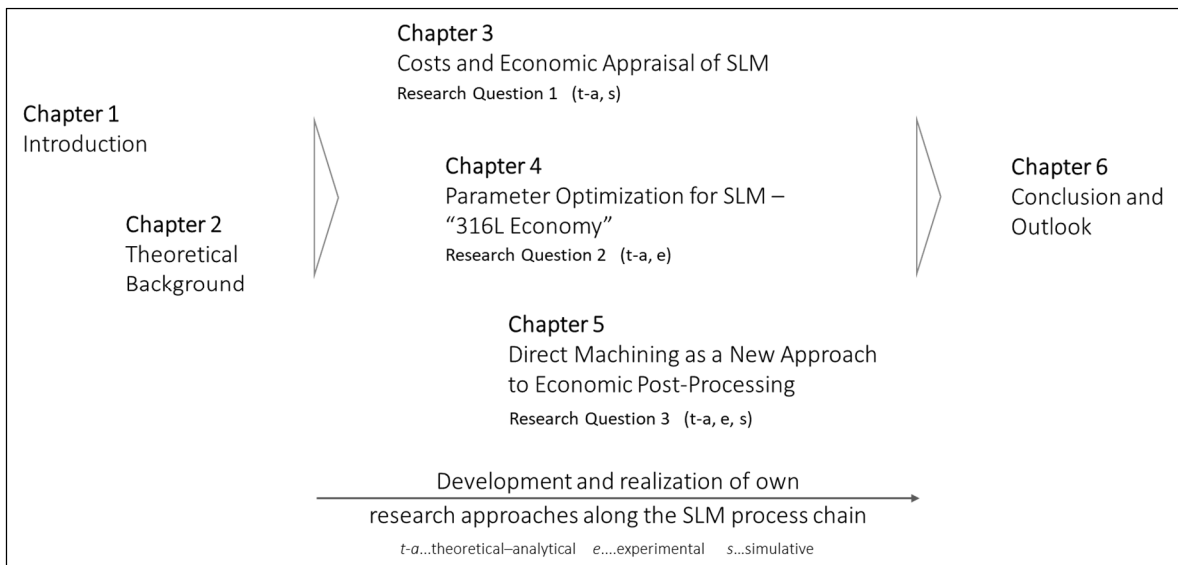


**Figure 1.1:** Basic structure of the thesis;  
Source: own representation.

## 2 THEORETICAL BACKGROUND

Chapter 2 provides theoretical background for this thesis. It gives an overview of additive manufacturing and its subordinate process of SLM. The chapter describes the state of the art focusing on the economic aspects. For reasons of clarity, the specific state of the art regarding the elaborated research approaches (Figure 1.1) will be described within the corresponding chapters 3, 4 and 5.

### 2.1 Basics of Additive Manufacturing

This chapter outlines the topic of AM. With the general principle of AM, a classification and distinction of AM as a manufacturing technology will be provided. A special focus of this chapter lies on the economic part of AM. Starting with the process chain of AM, the economic potential and possible limitations are discussed in the later subchapters.

As already mentioned, additive manufacturing is the process of joining raw material – typically layer by layer – based on 3D model data. In addition to the term additive manufacturing, other names can be used synonymously, such as additive layer manufacturing, solid freeform fabrication or more informally, 3D printing. The German standard VDI 3405<sup>22</sup>, however, clearly distinguishes between AM and 3D printing. According to them, 3D printing is a special AM process based on the deposition of a binder or the co-polymerization of a powder.

AM as a manufacturing technology can be classified in different ways. One possibility is that AM can be regarded as a third manufacturing category beside subtractive and formative manufacturing (Figure 2.1). In subtractive manufacturing, the desired shape of a part is achieved by selected removal of material from a part while in its raw state. Related manufacturing technologies are for instance drilling, milling or grinding. For formative manufacturing, the desired geometry of a part is reached by using external forces, pressure or heat. Typical formative technologies are forging, casting or injection molding. Both,

---

<sup>22</sup> Cf. VDI 3405:2014-12 (2014) p. 15.

subtractive and formative manufacturing technologies are often referred to as traditional manufacturing (TM) or conventional manufacturing (CM) technologies.<sup>23, 24, 25</sup>

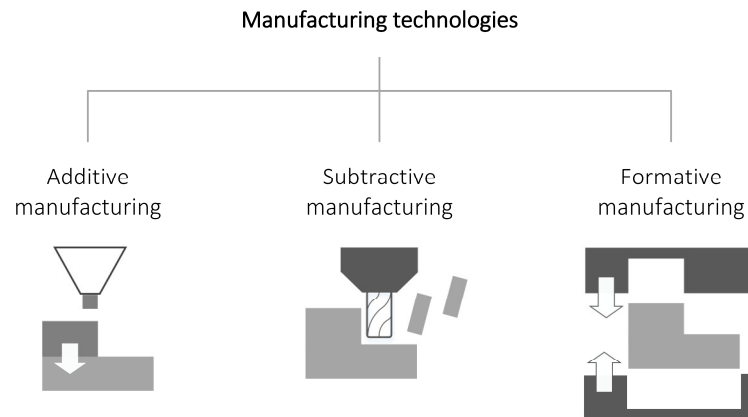


**Figure 2.1:** Basic classification of manufacturing technologies;  
Source: own representation.

Another typical and well-established classification of AM as manufacturing technology can be made according to the standard DIN 8580<sup>26</sup>. The standard classifies the different manufacturing processes into six main categories (Figure 2.2) which can be further divided into subcategories. In the literature, AM is usually assigned to the first category “primary forming”. However, this categorization only applies to certain AM processes.<sup>27</sup> The reason for this is the different mechanism that determines how the single layers are connected. For instance, SLM – where the layers are melted together – can be categorized into the subcategory 4.6 of DIN 8580 “Joining through welding”.<sup>28,29</sup> At the moment, there is an ongoing revision on the DIN 8580 standard. One of the main reasons for this is the clear inclusion of AM into the categories of DIN 8580.<sup>30</sup>

---

<sup>23</sup> Cf. Burns (1993) p. 3.

<sup>24</sup> Cf. ISO/ASTM 52900:2015 (2015) p. 12.

<sup>25</sup> Cf. Gebhardt (2011) p. 1.

<sup>26</sup> DIN 8580:2003-09 (2003).

<sup>27</sup> Cf. Kumke (2018) p. 9.

<sup>28</sup> Cf. Krauss (2017) p. 7.

<sup>29</sup> Cf. Berger et al. (2019) p. 10.

<sup>30</sup> DIN-Normenausschuss Technische Grundlagen (2018).



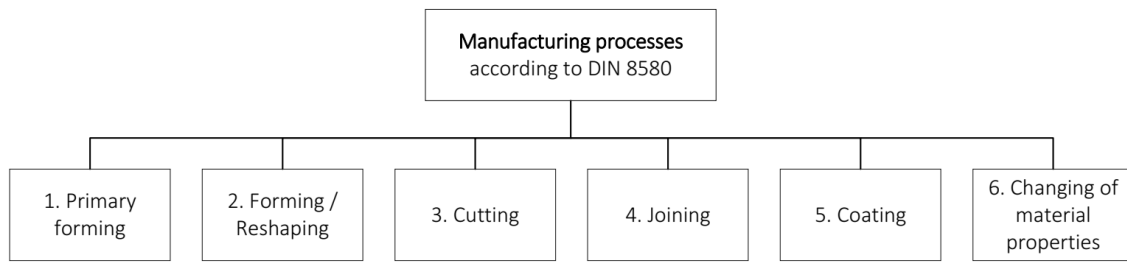


**Figure 2.2:** Main categories of manufacturing technologies based on DIN 8580;  
Source: own representation, based on DIN 8580:2003-09 (2003).

A more detailed subdivision can be made for AM as manufacturing technology itself. AM includes many different processes – like SLM – that can be distinguished in different ways, for instance based on the technology, on the used raw material or based on their application. The ISO/ASTM 52900 standard classifies the AM processes into seven main technological categories (Table 2.1). Since the development of new AM processes is very dynamic, an ultimate classification is difficult to represent. Therefore, the author focuses on the well-established classification of ISO/ASTM 52900 with own additions throughout this thesis.

**Table 2.1:** Classification of AM processes into seven categories according to ISO/ASTM 52900 with a brief explanation and processable materials; Source: own representation, based on <sup>31,32</sup>.

Technology	Mechanism	Raw materials				
		ME	PL	PA	CE	FS
1. Binder jetting	A liquid bonding agent selectively joins powder material together	X	X		X	X
2. Direct energy deposition	Thermal energy fuses raw material by melting as the material is deposited	X				
3. Material extrusion	Raw material is selectively dispensed through a nozzle or orifice		X			
4. Material jetting	Droplets of the raw material are selectively deposited and built together		X			X
5. Powder bed fusion	Thermal energy selectively fuses the raw material inside a powder bed	X	X		X	X
6. Sheet lamination	Single layers (sheets) of raw material are bonded together to form the AM part	X	X	X		
7. Vat photo-polymerization <sup>1</sup>	Liquid photopolymers in a vat is selectively cured by light-activated polymerization		X		X	

Raw material: *ME* Metals; *PL* Plastics; *PA* Paper; *CE* Ceramics; *FS* Foundry sand

<sup>1</sup> Including DLP (Direct Light Processing)

<sup>31</sup> Cf. VDI 3405:2014-12 (2014) p. 8.

<sup>32</sup> Cf. ISO/ASTM 52900:2015 (2015) pp. 2–3.

At the moment, the most relevant technology for metal AM, according to its market share, is powder bed fusion.<sup>33</sup> Powder bed fusion of metals includes the processes of SLM and electron beam melting (EBM). EBM uses an electron beam as an energy source to melt the metal powder. On the one hand, the main advantage is the higher build-up rates compared to SLM. On the other hand, SLM can produce finer geometries and has a better dimension accuracy compared to EBM.<sup>34</sup>

Hopkinson, Hague & Dickens divided AM processes based on the used initial state of the raw material.<sup>35</sup> According to the authors, the raw material can be in a liquid-, powder- or solid state. A connection between their classification and the ISO/ASTM classification is presented in Figure 2.3.

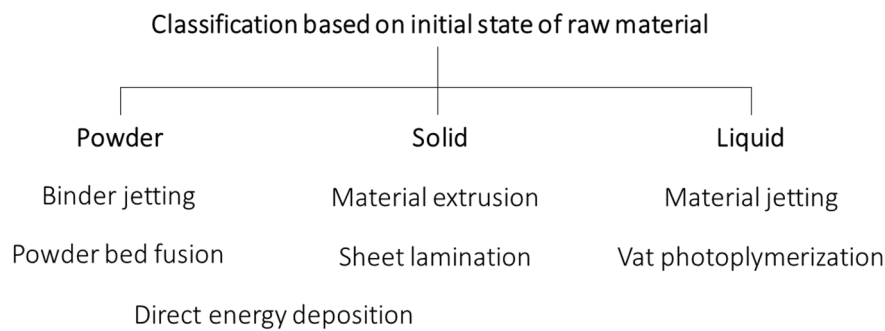


**Figure 2.3:** Classification of AM processes based on the initial state of raw material;  
Source: own representation.

Another division of AM can be made based on the application of AM. Besides Rapid prototyping (RP), as origin of AM, rapid manufacturing (RM) and rapid tooling (RT) have been established as main categories of different applications for AM.<sup>36</sup> These three categories can be defined as follows:

**Rapid prototyping:** According to the VDI 3405 standard, RP is the “additive fabrication of parts with limited functionality, but with sufficiently well-defined specific characteristics”<sup>37</sup>. RP is used to make prototypes, (scale) models or mock-ups from the digital into the physical but they do not meet the overall specifications of the targeted final product. Prototypes are made to evaluate certain criteria, such as haptic behavior, geometrical proportions, or

---

<sup>33</sup> Cf. SmarTech Analysis (2019).

<sup>34</sup> Cf. Bhavar et al. (2017).

<sup>35</sup> Cf. Hopkinson et al. (2006) pp. 57–79.

<sup>36</sup> Cf. Zäh (2013) pp. 9–10.

<sup>37</sup> Cf. VDI 3405:2014-12 (2014) p. 4.

physical properties such as temperature resistance. The word “rapid” indicates a fast availability of prototypes which can support the product development and can decrease the development time.<sup>38,39</sup>

**Rapid manufacturing:** According to the VDI 3405, RM is the “additive fabrication of end products”<sup>40</sup>. The term “end product” means that the manufactured parts meet all the required specifications and are suitable for series production. One of the main characteristics – and simultaneously one of the main advantages – is the tool-less manufacturing of products. Additional post-processing of the RM parts, such as blasting or machining, could be necessary to fulfill all customer requirements.<sup>41,42</sup>

**Rapid tooling:** The VDI 3405 defines RT as “the use of additive technologies and processes to fabricate end products which are used as tools, molds and mold inserts”<sup>43</sup>. RT enables the manufacturing of complex tools within a short period. Gebhardt subdivides RT into prototype tooling and direct tooling, depending on the targeted application. Direct tooling leads to molds and tools for later end products in serial production quality. Whereas prototype tooling is used to create temporary molds for small series or – as the name suggests – for the fabrication of prototypes.<sup>44</sup>

As this chapter indicates, AM can be classified in different ways and from different perspectives (material, application field, binding mechanism etc.). However, AM as a manufacturing technology is highly dynamic and new developments are constantly expanding the technology. Nevertheless, from a general perspective, the described classifications are widely used and well established.

## 2.2 AM-Process Chain

Despite the large number of different AM processes, their general process chain is similar. The previously mentioned main process steps of pre-processing, processing and post-

---

<sup>38</sup> Cf. Gebhardt/Hötter (2016) p. 7, pp. 291-307.

<sup>39</sup> Cf. Berger et al. (2019) pp. 27–29.

<sup>40</sup> Cf. VDI 3405:2014-12 (2014) p. 4.

<sup>41</sup> Cf. Hopkinson et al. (2006) p. 1.

<sup>42</sup> Cf. Berger et al. (2019) p. 35.

<sup>43</sup> Cf. VDI 3405:2014-12 (2014) p. 4.

<sup>44</sup> Cf. Gebhardt (2011) pp. 12–16.

processing can be subdivided further (Figure 2.4). The different process steps are explained in the following chapter.<sup>45, 46, 47, 48</sup>

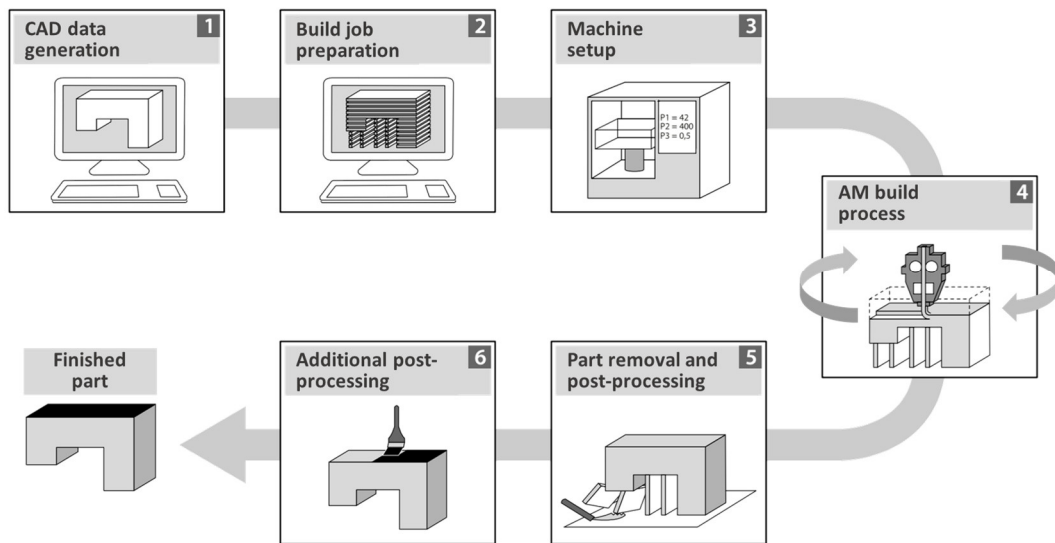


**Figure 2.4:** General process chain of AM;  
Source: modified from Kumke (2018) p. 10.

### 1. CAD data preparation:

The first step is the creation of suitable CAD (computer-aided design) data which can be done in several different ways. The most common way is the design of models with CAD software. The design of these CAD models can be based on an already existing design (redesign) or it can be a new design. But there are also other specific cases of data origin, such as geometries out of reverse engineering or medical imaging procedures, like computed tomography (CT).

### 2. Build job preparation:

The CAD data of the future parts has to be prepared for AM. First of all, the CAD data – which generally is a volume model – has to be converted into an STL file format. The acronym STL stands for stereolithography, although several other definitions for it are also used in specific literature, such as standard transformation/triangle language. The STL file

---

<sup>45</sup> Cf. Zäh (2013) pp. 14–19.

<sup>46</sup> Cf. Gebhardt (2011) pp. 3–5.

<sup>47</sup> VDI 3405:2014-12 (2014).

<sup>48</sup> Cf. Chua/Leong (2014) pp. 19–29.

format is the standard interface between CAD and several different AM systems from the beginning of AM up to now.<sup>49, 50</sup>

The STL file format approximates the surface of 3D-geometries with triangles. The size of these triangles mainly determines the accuracy of this approximation and deviation between target geometry (CAD) and the STL geometry. These deviations, based on the approximation, can be visible on the finished AM part, especially on round and curved surfaces. Despite this weakness, the STL file format is still the standard interface between CAD and AM systems.

After converting the CAD file into an STL format, the digital positioning of the parts on the build platform can take place. This process is also known as nesting and should be as effective as possible, because of the limited space on the build platform of AM systems. It is well known, that the chosen location and orientation can influence the part properties significantly. This results in anisotropic material behavior and in a variation of mechanical properties such as surface roughness or geometrical accuracy. Additionally, the position and orientation of the parts on the build platform determines the required amount of support structures. Support structures have two main tasks: They fixate the parts on the build platform and allow a better heat dissipation during the AM process. Support structures can be generated automatically by the preparation software or can be placed manually by the user. As stated above, the positioning of the parts on the build platform can greatly influence the build process, the economic efficiency as well as the part properties. This is especially true for metal AM processes like SLM. Although modern software can support the preparation, the knowledge and experience of qualified employees is essential.

After the right positioning of the parts and the definition of the support structures, the machine parameters for the build process can be defined. This step depends strongly on the used AM system. But even for similar AM systems, like SLM machines, the adjustment possibilities of machine parameters vary. Open systems allow the user to freely adjust important parameters such as laser power, laser speed or scanning strategy. This flexibility allows the operator to influence the part properties (e.g. relative density) or the build process (e.g. build-up rate) significantly.

---

<sup>49</sup> Cf. Kai et al. (1997) p. 566.

<sup>50</sup> Cf. Klahn et al. (2018) p. 38.

The last step of the build job preparation is called slicing. The preparation software slices – as the name indicates – the parts on the build platform into AM layers, based on the defined layer thickness adjusted in the previous step. Slicing creates contour information for the AM system for the layer generation. As an example, slicing defines the movement vectors of the laser system for each layer based on the scanning strategy for the SLM process. After finishing the slicing, the created data file can be transferred to the AM machine and the build job preparation is finished.

### 3. Machine setup:

As for every manufacturing process, a proper setup of the machine is essential. For AM systems, machine setup mainly focuses on the physical tasks of preparing the machine. This can include for instance the provision of the raw material, the adjustment of the recoater system or heating up the build platform. The setup also includes digital tasks, such as loading the prepared data from step 2 or the adjustment of process parameters, such as the nozzle temperature of material jetting systems or the waiting time of the recoater system for SLM machines.

### 4. Build process:

During the build process, the part is created layer-by-layer by the AM machine. This additive fabrication happens usually fully automatically based on the provided contour information from step 2. For complex and difficult geometries, the responsible operator monitors the progress of the build process. Today, different possibilities of inline process monitoring systems help to decrease the required presence time of the operator at the machine. However, the operator generally only has limited options of intervention in case of process difficulties. The reason for this is that only few parameters are adjustable during the build job. This can lead to the damage of the affected parts or termination whole build process.

### 5. Part removal and post-processing:

After the build process, the single parts or the whole build platform can be removed from the machine. Previously, surplus and unused raw material should be gathered for later sieving or disposal. After the removal of the parts, the machine can be cleaned and prepared for the next build job. At this stage, the parts can still be directly attached to the build platform directly and/or through the support structures, depending on the AM system. This can lead to a more or less rigid connection between the AM part and the build platform. Therefore, the degree of effort for the full removal of the parts from the support structures

and the build platform can vary widely for different AM systems. After removing the support structures, the AM parts should be cleaned of remaining material residues. Depending on the AM process, more intense chemical cleaning or impregnation can be necessary. To conclude, post-processing in stage 5 includes all tasks which are required to get a usable AM part.

### 6. Additional post-processing / finishing:

Additional post-processing and finishing help to improve the AM part properties and/or add value to them. For instance, (micro-) blasting decreases the surface roughness, heat treatment helps to improve the mechanical properties and coating can close pores on the surface. Since each additional post-processing task requires resources, the necessity for it should be clearly given.

Coming back to the more general division of the AM process chain into pre-processing, processing and post-processing. The author suggests the following definition for the term processing: "Processing includes all process steps where the AM machine is not available for further build jobs. This concerns the layer-by-layer production (AM build process) as well as all necessary tasks before and after the AM build process with the AM machine." This differs from the definition of the VDI 3405 standard. The VDI standard defines the term "in-processing", which is an indication of only the build process (step 4).

Related to the provided definition, pre-processing includes all process steps that are located chronically before processing. Regarding Figure 2.4, the CAD data generation (step 1) and the build job preparation (2) are part of pre-processing. Pre-processing ends with the machine setup, when the AM machine is occupied with processing the received data or necessary setup tasks (e.g. recoater adjustment).

Post-processing includes all tasks which take place right after processing. Post-processing starts when the parts have been removed from the AM machine and the machine is ready to process a new build job (step 5 and step 6, Figure 2.4).

It should be noted that the presented process steps are representative for the various AM processes. In detail, every AM process has its own process characteristics and requirements.

### 2.3 Economic Relevance of AM and its Potentials

In the following chapter, the potentials of AM and their economic relevance with focus on the value chain will be described.

As already stated in chapter 1, the initial reason for the invention of AM was the fast creation of physical models (prototypes) to support the product development process.<sup>51</sup> Developing from rapid prototyping into rapid manufacturing, AM has found its way into serial production. When it comes to the advantages and potentials of AM, two points always emerge: complexity for free and lot size independence (“individualization for free”<sup>52</sup>). AM has a fundamentally different relationship between costs, lot size and part complexity compared to conventional manufacturing processes (Figure 2.5).

For conventional manufacturing, such as casting or milling, every increase of complexity (e.g. more complex shape, number of cavities etc.) also increases the manufacturing costs. Complexity for free describes the extensive independence of the manufacturing costs from the part complexity (Figure 2.5, left). This allows a high degree of design freedom and can lead to highly innovative products. Furthermore, AM allows a high flexibility in production. This results from the nearly independent relationship between unit costs and production volume (Figure 2.5, right). For conventional manufacturing, unit costs decrease with increasing lot sizes because of the economies of scale effect. AM does not require high initial investments into part specific tools, molds etc. and enables an economic production of individual parts and small series with a high grade of customization.<sup>53, 54,55</sup>

---

<sup>51</sup> Cf. Berger et al. (2019) pp. 37–38.

<sup>52</sup> Poprawe et al. (2015) p. 50.

<sup>53</sup> Cf. Brecher (2015) pp. 50–51.

<sup>54</sup> Cf. Klahn et al. (2018) pp. 14–15.

<sup>55</sup> Cf. Poprawe et al. (2015) pp. 50–51.



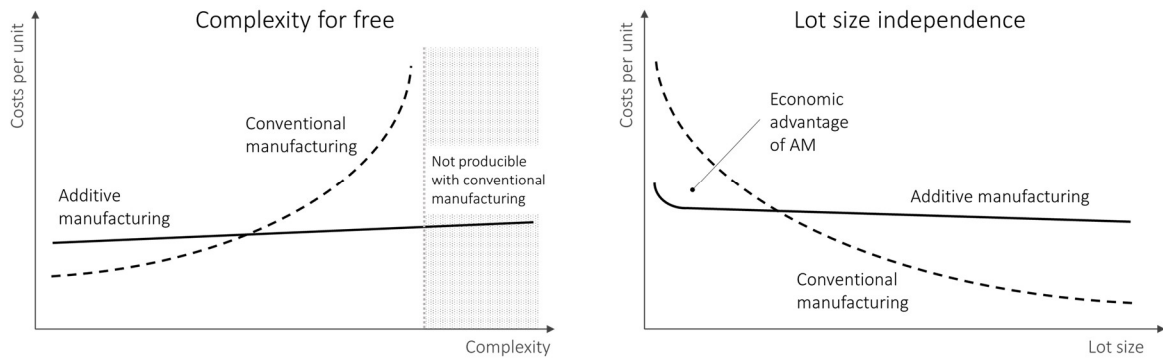


**Figure 2.5:** Relationship between costs and complexity (left) and production volume (right) of AM and CM;

Source: own representation, adapted from Klahn et al. (2018) p. 14 and Poprawe et al. (2015) p. 51.

The use of AM in a company should be driven by economic aspects and the reasonable use along the value chain. Klahn et al. identified two main processes inside a company that could be influenced positively by AM: the product development process and order processing. The authors define possible drivers for the value creation based on the two discussed beneficial characteristics of AM, complexity for free and independence from lot size (Figure 2.5 and Table 2.2).

**Table 2.2:** Specific AM benefits as driver for added value; Source: cf. Klahn et al. (2018) p. 71.

	Product development	Order processing
<b>Complexity for free</b>	Function-driven product design	Integration of functionalities and components
<b>Lot size independence</b>	Simplification of the physical product generation	Variety of variants and short time to market

Regarding the product development process, the freedom of design leads to a function-driven product design. The function of a product can be prioritized as AM allows the manufacturing of sophisticated shapes and design without remarkable additional costs. In contrast to this, conventional manufacturing follows a production-driven approach, where the used manufacturing process limits the product design significantly. The second reason for value creation within the product development process is the simplification of the physical product generation for testing purposes. The cost independence of lot sizes allows to create single components, prototypes or small series for product testing and further

developments<sup>56</sup>. This can accelerate the product development and reduce the time to market – which is widely reported as a major benefit of AM.<sup>57, 58, 59</sup>

When it comes to order processing, complexity for free can help to reduce the number of components required for a product. This is often referred to as integrated design. Integrated design for AM can mean the integration of functionalities and/or the integration of two or more components into a single part (part consolidation). The benefit for the order processing is clear: fewer components decrease the assembly time and reduce the handling time (e.g. for commissioning). This can result in shorter lead times and an increase of production efficiency. The second driver for value creation within the order processing is the broad variety of variants due to the independence of lot sizes. This enables a highly flexible and adaptable lot size one production. Furthermore, AM does not require tools and fixtures and allows a near net shape manufacturing. This enables a high degree of individualization and customization and makes it easy to offer different product variants cost efficiently. In order to do that, design changes and late customer interventions can be handled and processed very effectively.<sup>60, 61, 62</sup>

Klahn et al. further discuss eight fields of application of AM along the value chain of a typical OEM (original equipment manufacturer)<sup>63</sup>. The authors described the impact and possible benefits of using AM in different phases of the value chain. This approach is not restricted to OEMs only – it could also be applied to typical SMEs (small and medium-sized enterprises) that offer product development and manufacturing. These eight application fields are described briefly in the following paragraphs.

---

<sup>56</sup> Cf. Gebhardt/Hötter (2016) pp. 294–295.

<sup>57</sup> Cf. Klahn et al. (2018) p. 72.

<sup>58</sup> Cf. Kritzinger et al. (2018b).

<sup>59</sup> Cf. Gebhardt/Hötter (2016) pp. 294–295.

<sup>60</sup> Cf. Klahn et al. (2018) p. 72.

<sup>61</sup> Cf. Hopkinson et al. (2006) p. 3; 167–168.

<sup>62</sup> Cf. Campbell et al. (2013) pp. 2–3.

<sup>63</sup> Cf. Klahn et al. (2018) pp. 72–94.

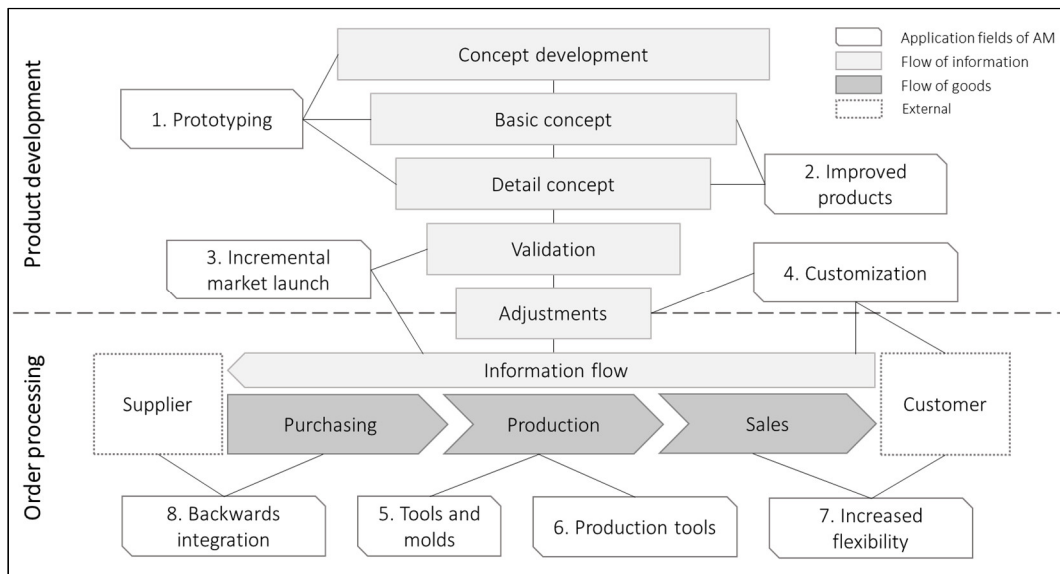


**Figure 2.6:** Fields of application and possible benefits of AM along the value chain;  
Source: own representation, adapted from Klahn et al. (2018) p. 73.

### 1. Prototyping:

AM allows the production of prototypes in different degrees of maturity. This enables fast testing and validation of new product ideas. Prototyping supports the product development process in early stages which can decrease the development costs significantly. Prototypes can also help to meet the customer demands earlier and can improve the communication between departments internally.

### 2. Improved products:

AM enables the design and manufacturing of completely new products. The freedom of design and the possible integration of components and functionalities can improve the performance of a product and add value to it. Since AM is a generally expensive manufacturing technology, a cost-benefit analysis has to support the use of AM for production.

### 3. Incremental market launch:

The launch of a new product on the market involves risks and uncertainties and requires financial efforts. With AM, pilot series can be produced which can be tested on the market. No cost intensive tools or fixtures are necessary and adjustments based on the customer feedback can be made immediately. Additionally, the time to market can be reduced as a further competitive advantage.

### 4. Customization:

AM enables highly individualized manufacturing without any additional cost to meet the customer's demand. Different variants of the same product can be manufactured simultaneously during the same build job. Design changes can be realized easily and can be immediately implemented into the order processing.

### 5. Tools and molds:

Rapid tooling, as explained in chapter 2.1, allows the production of tools and molds for conventional manufacturing. Again, fast availability is a major benefit here. It can lead to a shortening of possible downtimes due to damaged or missing tools and molds. Additionally, the already discussed freedom of design allows an increased functionality. For instance, optimized cooling channels can reduce the cooling time and further shorten the takt time of the casting process. As a consequence, the production costs can be reduced.

### 6. Production tools:

AM allows the manufacturing of production tools within a short time. These tools are not necessary for the manufacturing itself (like molds) but they support the production process. This, again, can result in better workplace ergonomics and higher throughput. Production tools can be regarded as assistive tools, like templates, jigs or fixtures for transportation.

### 7. Increased flexibility:

Small lot sizes and changing part properties require a flexible or even agile manufacturing system. AM enables benefits based on diversification, also known as economies of scope. Economies of scope decrease the overall production costs by increasing the variety of products. Together with a digital production system, lead times can be reduced and the order processing can be simplified. Additionally, time consuming adjustments or re-assembling of product lines are not applicable to AM.

### 8. Backwards integration:

With AM, a company can reduce its dependency on their suppliers and the market. It changes the make-or-buy situation and can bring back value creation inside the company. Complex products, which were formerly external parts, can be realized with AM inside the company. Furthermore, this reduces the necessary efforts in coordination with suppliers and makes the order processing easier.

Of course, potentials of AM have been widely reported in scientific literature. There are different classifications and listings available. It is obvious that the potentials described above do not cover all possible benefits of AM. For this, AM includes too many different processes with their own potentials and characteristics. However, a structured approach – for instance based on the value chain – can help to identify possible potentials enabled by AM. For further details, the author references to relevant literature <sup>64, 65, 66, 67</sup>.

### 2.4 Limitations of AM

Apart from the various advantages, AM also has process-specific and economic disadvantages. In the following chapter, disadvantages and limitations of AM with relevance to the thesis' topic will be discussed.

#### 1. Economic efficiency and productivity:

The production of high quantities with AM is very cost-intensive (Figure 2.5, right). Slow build-up rates paired with high initial investments into the machinery lead to high production costs, especially for SLM. Additionally, long cycle times make it difficult to integrate AM into a modern production chain. This is also true when it comes to the software infrastructure: AM requires special software solutions which makes the integration into established product lifecycle management (PLM) systems difficult. Furthermore, the lack of automatization – especially for AM post-processing – lead to high labor costs. Another limitation is the size of the building chamber. It determines the maximum number of parts as well as the maximum part size. Concerning the material cost, raw material for AM is generally more expensive than the material equivalent for conventional manufacturing. However, the price of the raw material should not be overstated when it comes to production costs. Whereas build speed and the degree of automatization influence the productivity significantly.

#### 2. Part properties:

Anisotropic material properties are one of the major issues concerning AM. Depending on the build orientation, mechanical properties (i.e. yield strength, relative density, etc.) vary

---

<sup>64</sup> Klahn et al. (2018).

<sup>65</sup> Kritzinger et al. (2018a).

<sup>66</sup> Hopkinson et al. (2006).

<sup>67</sup> Lachmayer et al. (2016).

for different load directions. This is also true for the surface roughness, which can be unsatisfyingly rough, depending on the AM process. Likewise, the geometrical accuracy of AM is limited. Process specific mechanisms (i.e. distortion, warping etc.) cause inaccuracies of manufacturing and can prevent to meet the required geometrical tolerances. This in turn requires more effort in post-processing. Additionally, the part quality and its properties are not supposed to be repetitive for AM. Process simulation and monitoring can increase the stability, but AM is far from reaching a comparable reproducibility to established conventional manufacturing processes.

### 3. Knowledge:

AM is a young manufacturing technology compared to the well-established conventional processes, such as turning, forging or casting. AM as a manufacturing technology is constantly evolving and so is the knowledge about it. This also affects the way of designing parts. Although first guidelines for the right design for additive manufacturing (DfAM) are available, their dissemination among the AM users is yet to come. This also includes the educational and training sector. Successful usage of AM – from a technical and economic perspective – requires knowledge about the (design) possibilities and appropriate fields of application. It begins with the processability of AM materials and ends with the recycling of the AM part after its – hopefully beneficial – life cycle. However, knowledge of AM does not only affect the companies directly involved in AM. It also affects decision makers which are responsible for standardization and the specification of general valid guidelines for the industry. Uniform standards regarding quality assurance and certification for AM are still under development.

However, the described limitations should be seen exemplarily for AM. For process-specific limitations, reference is made to relevant literature. The research questions RQ1-3 from chapter 1.2 have been developed out of the limitations mentioned above. A specific theoretical background to the research questions is provided in the following SLM-related chapters.

## **2.5 Selective Laser Melting – State of the Art**

The classification of SLM within the seven basic AM processes has already been discussed in chapter 2.1. In this chapter, the principle of SLM and its main characteristics will be

explained. According to the VDI 3405<sup>68</sup>, SLM is referred to as laser beam melting (LBM). Other common terms are laser-powder bed fusion (L-PBF) or direct metal laser sintering (DMLS). Uniform terminology in the field of AM is not fully established yet and therefore different names for SLM are common. Due to the broad acceptance in business and academia, the author will use the term SLM in this doctoral thesis consistently.

### 2.5.1 Process Fundamentals of SLM

SLM started – as typical for AM – as a RP technology in the mid-1990s in Germany, at the company F&S Stereolithographietechnik GmbH.<sup>69</sup> Since then, SLM has evolved from rapid prototyping to a manufacturing technology for valuable end products (rapid manufacturing). From a technical perspective, SLM works with the same layer-by-layer principle as every AM technology. Therefore, the pre-processing and post-processing are quite similar to the already described steps in chapter 2.2. The process characteristic of SLM regarding the build process (step 4, Figure 2.4) can be seen in Figure 2.7 and will be explained in the following paragraphs.

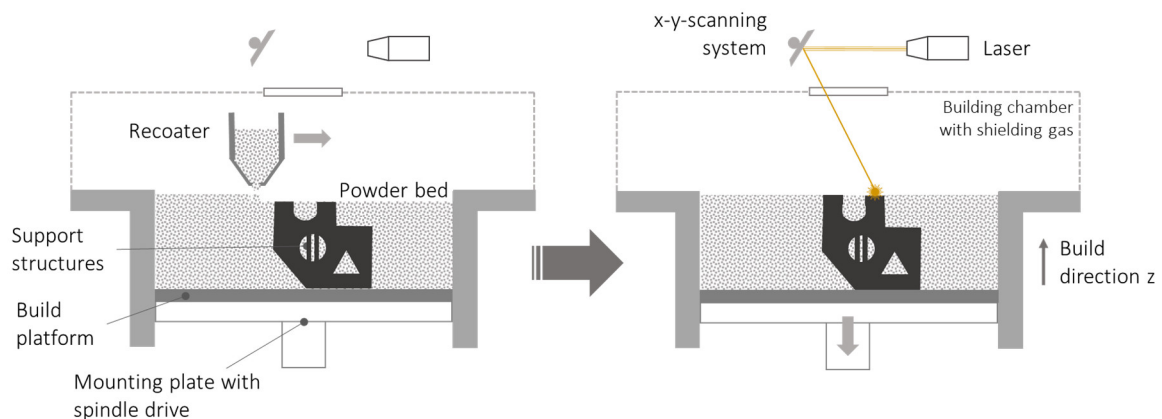


**Figure 2.7:** Schematic principle of the SLM build process – layer-by-layer sequence;  
Source: own representation.

The initial setup includes the preparation of the build platform and leveling of the recoater. After that, the building chamber is floated with shielding gas (Argon or Nitrogen). If the oxygen level inside the building chamber drops to a predefined threshold, the first layer of powder is applied by the recoater (Figure 2.7, left). When the powder is applied uniformly, the laser starts to scan the defined paths provided by contour data from the slicing process

<sup>68</sup> Cf. VDI 3405:2014-12 (2014) p. 10.

<sup>69</sup> Cf. Gebhardt/Hötter (2016) p. 176.

(Figure 2.7, right). The laser beam is directed by a scanning system. The scanning system consists of a collimator, a movable mirror system and a lens and navigates the laser on the powder bed in  $x$ - and  $y$ -direction. When the laser spot hits the powder, it selectively melts the surrounding powder particles and fuses them with the build platform (layer 1) or to the previous layer ( $n-1$ ). After the laser has scanned the pre-set path for the actual layer, the spindle drive lowers the build platform according to adjusted layer thickness. Then again, a new layer of powder is applied and the process of laser scanning can take place for the new layer (Figure 2.7, left to right). This sequence is repeated until all designated layers have been scanned and melted together. Then the SLM part is finished and post-processing procedures can start.<sup>70, 71, 72</sup>

It is widely reported that SLM can create parts with up to 99.9 % relative density.<sup>73, 74, 75</sup> This is a key factor for rapid manufacturing of end products with good mechanical properties. However, only the right adjustment of the machine parameters for the melting process can lead to optimal dense SLM parts. For SLM, the most common parameters are: laser power ( $P_L$ ), scanning speed ( $v_s$ ), hatch spacing ( $h_s$ ) and the layer thickness ( $l_z$ ). The laser beam selectively melts the powder particles when scanning the powder bed at a predefined scanning speed. The distance between two melting tracks is defined as hatch spacing. After solidification, the melt tracks merge with the preceding layer and the part solidifies through this (Figure 2.8). The influence of these major parameters will be described in the following paragraph.

---

<sup>70</sup> Cf. Gu et al. (2012) pp. 135–138.

<sup>71</sup> Cf. Yap et al. (2015) p. 2.

<sup>72</sup> Cf. VDI 3405:2014-12 (2014) pp. 10–11.

<sup>73</sup> Cf. Gu et al. (2012) p. 137.

<sup>74</sup> Cf. Kruth et al. (2005) pp. 31–35.

<sup>75</sup> Cf. Fayazfar et al. (2018) pp. 102–108.



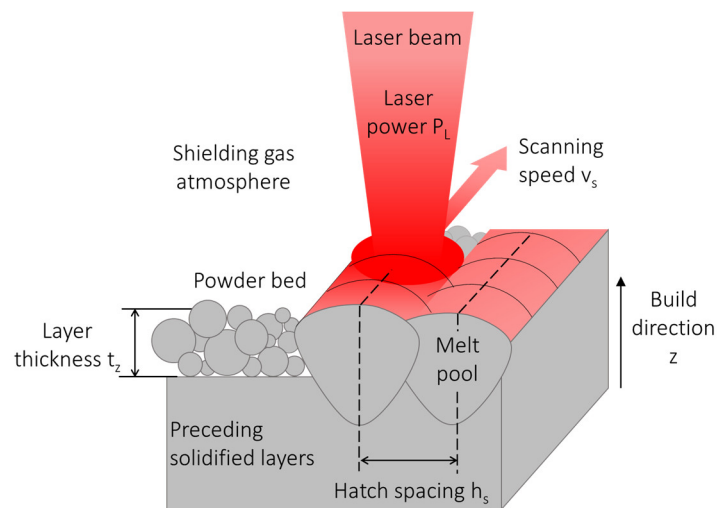


**Figure 2.8:** Schematic melting process and basic parameters for SLM;  
Source: own representation.

Laser power ( $P_L$ ): As already mentioned, the energy source for the melting process of SLM is a mid- or high-power laser system, typically ranging from 100 W to 1 kW.<sup>76</sup> Common laser types for SLM are ytterbium-doped fiber lasers (Yb-fiber lasers) and Nd:YAG solid-state lasers (neodymium-doped yttrium aluminum garnet). For metal AM, both laser types show significant advantages in contrast to CO<sub>2</sub> lasers due to their compact design and good energy absorptance of the metal powder because of the short wavelength. Furthermore, they enable a larger process window and a smaller spot size compared to CO<sub>2</sub> lasers.<sup>77,78</sup>

The laser power significantly influences the quality of the melting process. On the one hand, low laser power, especially in combination with high scanning speeds, results in high porosity. One related phenomenon to this is the balling effect, an insufficient connection of the melted powder to the previous layer that results in discontinuous melt tracks.<sup>79</sup> Related to this, low  $P_L$  can result in an incomplete melting of powder particles which leads to the formation of pores in between the layers. These pores are known as lack of fusion defects.<sup>80</sup>

---

<sup>76</sup> Cf. Gebhardt/Hötter (2016) pp. 526–534.

<sup>77</sup> Cf. Lee et al. (2017).

<sup>78</sup> Cf. Ferrage et al. (2017) p. 12.

<sup>79</sup> Cf. Li et al. (2012).

<sup>80</sup> Cf. Sola/Nouri (2019).

On the other hand, too high laser power combined with low scanning speed can lead to material evaporation during the melting process which again leads to porosity. This is known as the keyhole effect<sup>81</sup> or keyhole mode<sup>82</sup>.

Scanning speed ( $v_s$ ): The speed at which the laser moves over the powder bed is defined as scanning speed. As already indicated above, the scanning speed influences energy input and therefore the formation of the melt pool. From an economic point of view, the scanning speed influences the build time. Faster scanning speeds lead to higher build-up rates which further can decrease the manufacturing costs. This will be specifically elaborated on in chapter 2.5.2.

Hatch spacing ( $h_s$ ): The distance between two parallel melt tracks is referred to as hatch spacing. To achieve a high relative density, the hatch spacing should be adjusted properly so that the melt tracks overlap. For that, the spot size of the laser beam needs to be considered. Figure 2.8 shows the overlapping of the two melt pools as representative for the melt tracks. If the hatch spacing is too wide, the melt tracks cannot fuse and porosity and/or unmelted powder can remain in between. Nevertheless, this effect may be desired. SLM allows the production of parts with graded porosity. Porous structures can support the osseointegration – the connection between bone tissue and medical implants.<sup>83</sup> Apart from this, the porous structures – for instance by the variation of the hatch spacing – can be used for technical elements such as porous filters.<sup>84</sup> In contrast to that, a too narrow hatch spacing can lead to an excessive high energy input.

Layer thickness ( $l_z$ ): The layer thickness, which usually ranges from 20-100  $\mu\text{m}$ <sup>85</sup>, greatly influences the SLM process in different ways. First of all, the layer thickness determines the geometrical resolution of the SLM to a large extent. On the one hand, the stair-step or stair stepping effect – a well-known issue with layer-by-layer fabrication – becomes more influential for higher layer thicknesses. The stair-step effect describes the geometrical deviations between the CAD contour and real contour of the AM part. Using small layer thickness leads to higher resolutions and therefore decreases the stair-step effect (Figure 2.9). Furthermore, SLM parts built with a small layer thickness tend to show less surface

---

<sup>81</sup> Cf. Yap et al. (2015) p. 10.

<sup>82</sup> Cf. Sola/Nouri (2019) p. 6.

<sup>83</sup> Cf. Goharian (2019) pp. 143–144.

<sup>84</sup> Cf. Yadroitsev et al. (2009).

<sup>85</sup> Cf. Gupta (2019) p. 4.

roughness.<sup>86</sup> On the other hand, the layer thickness can influence the build time significantly. A higher layer thickness increases the build-up rate. More details about this relationship will be provided in chapter 3.3. However, only parameters that are well adapted to the layer thickness allow a flawless melting process.

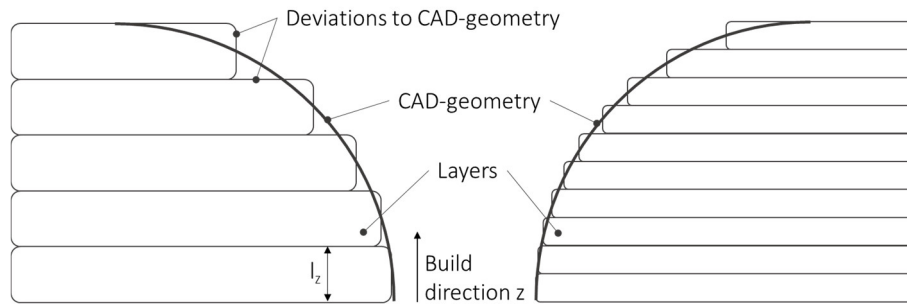


**Figure 2.9:** Stair-step effect for high layer thickness (left) and small layer thickness (right); Source: own representation.

The range of processable materials with SLM is constantly expanding. Furthermore, the available materials strongly depend on the SLM machine manufacturer. Table 2.3 provides an overview of selected materials for the SLM process and application examples for them. A comprehensive review of SLM materials can be found in Yap et al. (2015).

**Table 2.3:** Selection of processable materials for SLM; Source: based on Yap et al. (2015).

Material group and example	Description	Fields of application
<b>Ferrous metals</b>		
316L	Stainless steel	Aerospace (e.g. turbine blades <sup>87</sup> ) Biomedical applications <sup>88</sup> Chemical industry (e.g. heat exchanger <sup>89</sup> )
17-4 PH	Martensitic precipitation-hardened stainless steel	Aerospace and defense <sup>90</sup> Medical <sup>91</sup>
• Tool steels		
1.2709	Maraging tool steel	Tooling <sup>92, 93</sup>
H13/H20	Martensitic tool steel	Molds
<b>Non-ferrous metals</b>		
• Titanium alloys		

<sup>86</sup> Cf. Savalani/Pizarro (2016) p. 120.

<sup>87</sup> Cf. Yakout et al. (2018).

<sup>88</sup> Cf. Lodhi et al. (2019).

<sup>89</sup> Cf. Brischetto et al. (2017) p. 126.

<sup>90</sup> Cf. Hu et al. (2017).

<sup>91</sup> Cf. Gu et al. (2013).

<sup>92</sup> Cf. Kempen et al. (2011).

<sup>93</sup> Cf. Yasa et al. (2010).

Material group and example	Description	Fields of application
Ti6Al4V Grade 5 / Grade 23	High strength titanium-alloy	Biomedical and dental applications <sup>94</sup> Lightweight structures
<ul style="list-style-type: none"> <li>• Aluminum alloys AlSi10Mg</li> </ul>	Hardenable aluminum-alloy	Automotive and aerospace <sup>95</sup> Lightweight structures
<ul style="list-style-type: none"> <li>• Nickel-based alloys Inconel 625 / 718</li> </ul>	Precipitation-hardenable nickel-chromium-alloy	High temperature applications (gas turbine blades, aircraft engines, energy etc.)
Hastelloy X	Nickel-chromium-iron-alloy	Aircraft engines and gas turbine components
<ul style="list-style-type: none"> <li>• Other metals CoCr28Mo6</li> </ul>	High temperature resistant Co-Alloy	Biomedical (implants and prostheses) <sup>96</sup> Heat exchangers
CuSn10	Copper-tin alloy (bronze)	Housings and bearings Chemical and electrical industry <sup>97</sup>
<ul style="list-style-type: none"> <li>• Ceramics TCP</li> </ul>	Tricalcium-phosphate	Bone substitute implant <sup>98</sup>
<ul style="list-style-type: none"> <li>• Composites TiC/Ti5Si3</li> </ul>	Titanium carbide/titanium silicide	High temperature structural applications

Depending on the SLM machine, the adjustable process parameters are manifold. Apart from the main parameters presented in this chapter, roughly 100 to 200 further parameters influence the scanning process.<sup>99, 100</sup> Where necessary, a further explanation will be provided within the relevant chapters of this thesis.

### 2.5.2 Economic Aspects – Challenges for SLM as Manufacturing Technology

SLM is the leading metal-based AM technology and allows the manufacturing of close to fully dense parts with good mechanical properties. Various studies have shown, that the mechanical properties of parts manufactured with SLM can be compared to those manufactured traditionally out of conventional raw material. In combination with the process specific advantages mentioned in chapter 2.3, SLM could change manufacturing significantly. Regarding SLM, as stated in chapter 1.1, only a small percentage of the world wide tool market is attributed to metal-based AM systems. The reasons for this are mainly

---

<sup>94</sup> Cf. Yadroitsev et al. (2014).

<sup>95</sup> Cf. Kempen et al. (2012).

<sup>96</sup> Cf. Hedberg et al. (2014).

<sup>97</sup> Cf. Afshari et al. (2017).

<sup>98</sup> Cf. Hoeges et al. (2009).

<sup>99</sup> Cf. Kurzynowski et al. (2012) p. 5.

<sup>100</sup> Cf. SLM Solutions Group AG (2020b).

based on economic aspects and decisions. This chapter discusses the economic background of SLM as a base for the latter described approaches in this thesis.

A lot of research in the past focused on the process related mechanism of SLM. Major goals were parameter studies to improve the material characteristics – such as relative density – of the SLM parts. Furthermore, studies focused on the development of improvements on existing powder of raw materials or on the development of new materials and alloys for the SLM process. From a process perspective, SLM has evolved a lot since its beginning in the mid-1990ies. However, the process still appears immature compared to the established manufacturing processes such as forging or casting. However, this should not come as a surprise, especially when comparing the time of development of these technologies. AM – and SLM in particular – are rather recent technologies in relation to forging or casting. Their first appearance can be traced back to the Bronze Age, around 4000-1000 B.C<sup>101, 102</sup>.

Today, successful use cases in the industry have helped to improve the awareness of SLM as manufacturing technology. Furthermore, the increasing media reporting has fixed AM as a possible way of manufacturing of parts into people's minds. And yet, SLM has not been established according to its potentials within the industry. The reasons for this are diverse and will be discussed in the following chapters. The author suggests dividing these reasons into two main groups:

- 1) Process related challenges
- 2) Information related challenges

Both will be described in the next sections.

### 2.5.3 Process-related Challenges

SLM is reported as a manufacturing technology with limited productivity. This is seen as a major drawback concerning its industrial use.<sup>103, 104, 105</sup> First of all, the term “productivity” should be defined and clarified in this thesis.

Productivity is broadly defined and used very situationally depending on the related context (e.g. business economics, production science, economics etc.). However, production can be

---

<sup>101</sup> Cf. Industrieverband Massivumformung e.V. (2014).

<sup>102</sup> Cf. Ravi (2006) p. 14.

<sup>103</sup> Cf. Gusarov et al. (2018).

<sup>104</sup> Cf. Cordovilla et al. (2018) p. 1.

<sup>105</sup> Cf. Bremen et al. (2011) p. 25.

regarded as the quotient of output to input. In other words, the amount of resources used (input) in relation to the generated result (output) from a quantitative point of view. The reference parameters for input and output can be chosen according to the given context. For instance, in the field of production, the output can be measured in units and the input could be the production time (e.g. measured in minutes) or the required use of material (e.g. measured in kg). By modifying the input and output factors, the productivity can be increased or decreased.<sup>106, 107, 108</sup>

$$\text{Productivity} = \frac{\text{Quantity of output}}{\text{Resource input}}$$

Examples:  
Product (e.g. units)  
Money (e.g. revenue)

Examples:  
Machinery (e.g. processing time)  
Material (e.g. kg of raw material)

**Figure 2.10:** General definition of productivity with examples for output and input;  
Source: own representation, adapted from Durdyev et al.<sup>109</sup>

Also, the term economic efficiency needs to be clarified. Economic efficiency is related to an optimal state of a production or service market. Basically, it means getting the maximum output with minimum input (e.g. costs). The use of costs within the definition would be the bridge to the German term “Wirtschaftlichkeit”. In contrast to productivity, Wirtschaftlichkeit evaluates input to output in monetary terms only. Economic efficiency within this thesis should be understood as seeking for the optimum of the SLM production process – for instance by increasing the productivity. Increasing the economic efficiency means improving the ratio between useful output to input in a measurable way. Where it is reasonable and possible, costs should be used as the basis of assessment.<sup>110, 111</sup>

In the past, several concepts and measures have been developed to increase productivity. For instance, multiple laser systems can significantly increase the build-up rates.<sup>112</sup> Other concepts that can increase the productivity would be the use of larger build chamber sizes or

---

<sup>106</sup> Cf. Organisation for Economic Co-operation and Development (2001) p. 11.

<sup>107</sup> Cf. Frenz (1963) p. 11.

<sup>108</sup> Cf. Prokopenko (1987) p. 3.

<sup>109</sup> Cf. Durdyev et al. (2018).

<sup>110</sup> Cf. Petrou (2014).

<sup>111</sup> Cf. Gabler Wirtschaftslexikon (2020).

<sup>112</sup> Cf. Wong et al. (2019).

the parallelization of the machine setup.<sup>113</sup> Poprawe et al. (2015) investigated different concepts and possibilities to achieve higher productivity. They identified three basic concepts:

- 1) Increase of the build chamber size
- 2) Parallelization of the SLM processes
- 3) Increase of the laser power / process development

Number 1) and 2) can be counted to hardware related measures. They require adjustment or enlargement of the existing SLM system. In the past years, the build chamber size has increased steadily. Larger build chambers mean that more parts can be manufactured at the same time or that the maximum part size can be extended. Today, two typical representative machines with large build chamber sizes are the SLM 800 with 500 x 280 x 875 mm<sup>3</sup> and the Concept Laser X Line 2000R with 800 x 400 x 500 mm<sup>3</sup> build volume.<sup>114, 115</sup> According to Poprawe et al., the second possibility to increase the productivity is the parallelization of the SLM process. Parallelization describes the setup of the build platform being done separately from the build chamber so that the machine is occupied less due to necessary handling operations. The other type of parallelization is the use of multiple laser systems. Instead of a single laser, two or more laser melt the powder at the same time. Modern SLM machines, such as the EOS M 400-4, use four laser beam sources at the same time.<sup>116</sup> In their study, Poprawe et al. show that the use of a multiple laser system can be an effective way to increase the productivity – despite the high initial investment in these machines.

The third concept is the use of high laser power. Poprawe et al. increased the laser power  $P_L$  from 300 W to 1 kW. For this, the laser beam focus has to be increased too, in order to prevent vaporization and overheating of the processing zone. By further adjusting the scanning speed and layer thickness, they were able to increase the build-up rate for 1.2709 maraging steel from 3 mm<sup>3</sup>/s up to 15 mm<sup>3</sup>/s. At the same time, mechanical properties like yield strength, tensile strength, and breaking elongation stayed in the same ranges compared to those processed by the conventional 300 W system. These findings lead to an important point: The role of the build-up rate in order to evaluate the productivity of SLM.

---

<sup>113</sup> Cf. Poprawe et al. (2015) pp. 51–52.

<sup>114</sup> SLM Solutions Group AG (2020a).

<sup>115</sup> GE Additive (2020).

<sup>116</sup> EOS GmbH (2019).

The theoretical build-up rate for SLM can be calculated as follows:

$$\dot{V}_{Th} = v_s \cdot h_s \cdot l_z \quad (2.1)$$

The theoretical build-up rate is a measure for the build speed. It can be regarded as comparative value between different SLM systems and is typically expressed in  $\text{cm}^3/\text{h}$ . As can be seen in the equation (2.1), the theoretical build-up rate depends on the scanning speed ( $v_s$  in  $\text{mm}/\text{s}$ ), hatch spacing ( $h_s$  in  $\text{mm}$ ) and the layer thickness ( $l_z$  in  $\text{mm}$ ). An increase of these multipliers leads directly to a higher theoretical build-up rate. However, a good melting process depends on the right adjustment of these parameters. Setting them too high for the sake of increasing the build-up rate would lead to insufficient melting of the powder particles and furthermore to the already described balling or lack of fusion effects. The reason for this is that the energy input of the laser is not powerful enough to ensure a proper melting process. To counteract this, the use of high-power laser systems – as described above on the example of Poprawe et al. – is a good way to increase the build-up rate and keep the relative density in high ranges. The relationship between laser power ( $P_L$ ) and the other parameters  $v_s$ ,  $h_s$ , and  $l_z$  is described by the volumetric energy density  $E_V$ <sup>117, 118</sup>:

$$E_V = \frac{P_L}{v_s \cdot h_s \cdot l_z} \quad (2.2)$$

$E_V$  (in  $\text{J}/\text{mm}^3$ ) is a frequently investigated parameter and probably the most established measure to describe the SLM process in related literature<sup>119</sup>. It is a measure for the average energy input during processing. Depending on the processed material, a certain process window of  $E_V$  allows to produce SLM parts with high relative density. On the one hand, if the  $E_V$  is set too high, excessive energy input can lead to the described material vaporization (keyhole-effect) and porosity as a consequence. On the other hand, too low  $E_V$  leads again to porosity because of insufficient melting in the process zone. However, the outcome is clear: increasing the theoretical build-up rate (denominator in equation (2.2)) requires an increase of  $P_L$  to enable an adequate process window for  $E_V$ . This relationship will be further described and investigated in chapter 4.

---

<sup>117</sup> Cf. Gu et al. (2012) p. 157.

<sup>118</sup> Cf. Thijs et al. (2010) p. 3305.

<sup>119</sup> Cf. Gu et al. (2013) p. 1.



Apart from the theoretical build-up rate  $\dot{V}_{Th}$ , a more practical definition of the build-up rate is presented in this thesis. This practical build-up rate,  $\dot{V}_{Pr}$ , is determined by dividing the total build volume ( $V_B$  in  $cm^3$ ) by the total build time ( $t_b$  in h):

$$\dot{V}_{Pr} = \frac{V_B}{t_b} \quad (2.3)$$

The total build time  $t_b$  is the time between start and finish of the build job. The total build volume  $V_B$  includes all volumes of the built parts and of the required support structures – in other words, all material that was molten by the laser on the build platform. The determination of  $\dot{V}_{Pr}$  can be calculated in two different ways. First, the experimental way, where  $t_b$  needs to be determined for the real build job. This can be easily done with the help of the log files of the build job where the times of start and finish are clearly listed. The other way is the build job simulation done by a preparation software. Based on the sliced file, the software calculates the required build time. However, for both ways,  $V_B$  can be determined through the use of the preparation software, which lists the required volume of the parts and the support structure.

The differences between  $\dot{V}_{Th}$  and  $\dot{V}_{Pr}$  are manifold. The theoretical build-up rate  $\dot{V}_{Th}$  is only applicable to one single scanning line. The reason for this is the scanning strategy of the laser. The scanning strategy describes the movement of the laser on a single layer and it is usually very diverse. The scanning strategy requires various steps in order to finish a single layer:

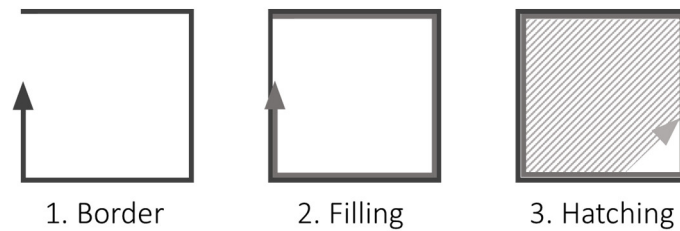


**Figure 2.11:** Schematic sequence of the laser scanning;  
Source: own representation.

Figure 2.11 shows a typical sequence of the scanning process of a single layer. At first, the outer contour, called border contour, is exposed to the laser. The border contour limits the part geometry from the powder bed. Next, the laser system scans the filling contour. It can be seen as a transition zone to the hatching contour. The hatching contour fills the inner area of the part. Typically, these three contour types are created with different parameters for  $P_L$ ,

$v_s$ , and  $h_s$ . Therefore, the volumetric energy density  $E_V$  as well as the theoretical build-up rate  $\dot{V}_{Th}$  vary within a layer.

In addition to that, different scanning patterns for the hatching contour are selectable by the operator. Three typical hatching patterns can be seen in Figure 2.12. Compared to the standard pattern, stripes and chessboard pattern are supposed to lead to a more homogeneous temperature distribution on the layer. As a result, residual stresses can be reduced and mechanical properties can be improved.<sup>120, 121</sup>

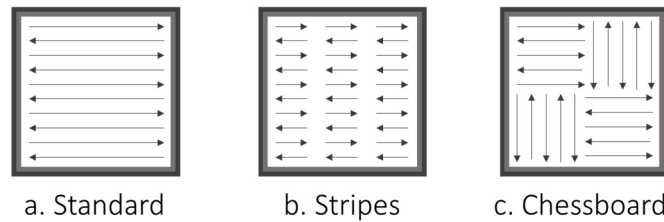


**Figure 2.12:** Selection of typical hatching patterns for SLM;  
Source: own representation.

This uneven motion sequence of the laser brings  $\dot{V}_{Th}$  to its limits. The complex movements of the laser necessary to create a single layer cannot be covered fully by this approach. Furthermore, there are additional processing times during the build process which are not directly related to the scanning process of the laser. First, the recoater takes time to apply fresh powder before the scanning process starts (recoater time  $t_r$ ). After the scanning process has finished, an additional waiting time ( $t_w$ ) can be set. This waiting time allows the parts to cool down before the recoater applies the fresh powder for the new layer. Both,  $t_r$  and  $t_w$  cannot be covered by the approach of  $\dot{V}_{Th}$ .

In contrast, the practical build-up rate  $\dot{V}_{Pr}$  does not require detailed information on the scanning strategy. Furthermore,  $\dot{V}_{Pr}$  takes the movement of the recoater and the waiting time into account. However, this approach also has a major drawback:  $\dot{V}_{Pr}$  very much depends on the build job configuration. The chosen parts, their orientation, the amount of support structures etc. influence the determination of  $\dot{V}_{Pr}$ . Additionally, a variation of the waiting time or the termination of a single part during the build job would influence  $\dot{V}_{Pr}$ .

<sup>120</sup> Cf. Jhabvala et al. (2010).

<sup>121</sup> Cf. Kranz (2017) pp. 15–16.

significantly. Nevertheless,  $\dot{V}_{Pr.}$  reflects real build job conditions better than  $\dot{V}_{Th}$  and can be considered as benchmark value for parameter studies.

But how can higher build-up rates increase the productivity of SLM? There is a broad agreement in scientific literature that the main cost driver for SLM are machine costs based on the processing time.<sup>122, 123</sup> High initial machine investments paired with slow build-up rates lead to high machine costs due to their influence on the machinery hourly rate. Faster build-up rates directly decrease the manufacturing time and furthermore the manufacturing costs – the main cost driver for SLM. Therefore, the importance to increase the build-up rates should be emphasized. As stated at the beginning of this chapter, productivity is the relationship between output to the required input. Higher build-up rates clearly decrease the required input, because less processing time and less times of occupancy of the machine is necessary. So, without a doubt, there is a positive impact of the build-up rate on the economic efficiency.

### **Summary of this Chapter of Process-related Challenges and Contribution of the Thesis to the Reported Issues:**

SLM offers great opportunities for manufacturing but the lack of productivity is one of the major drawbacks of the technology. The selection of parameters influences the build-up rate for SLM and furthermore the overall productivity of the technology.

This thesis contributes to the discussed topics in this chapter in several ways. First, the cost structure of SLM is analyzed and critical cost drivers are identified. From a theoretical and analytical perspective, chapter 3 describes the simulative investigation of different SLM parameters and their influence on the manufacturing costs. Related to this, the term micro-economy of scale is introduced and explained. Furthermore, chapter 4 shows the experimental part of increasing the build-up rate by adjusting the most relevant parameters for 316L stainless steel. Additionally, productivity will be positively influenced through better performance of the overhang structures. This comprehensive combination of simulative and experimental investigations extends the present knowledge. However, this thesis will not provide an in-depth study of mechanical and microstructural properties. The focus of this thesis is the investigation of the economic impact using advanced parameters. Productivity and economic efficiency will also be covered in chapter 5 where a novel

---

<sup>122</sup> Cf. Lindemann et al. (2012).

<sup>123</sup> Cf. Brecher/Özdemir (2017) p. 25.

approach for post-processing is introduced. This approach increases the productivity by decreasing the handling time. Specific literature for chapter 3, 4 and 5 that has not been covered yet will be discussed in the relevant chapters.

### 2.5.4 Information-related Challenges

As shown in chapter 2.2, AM can positively contribute to the value chain of a company. The potential benefits are various and AM can offer new possibilities to create value for a company (Figure 2.6). Successful use cases and examples of the effective use of AM in an industrial context are reported in the examined literature<sup>124, 125, 126, 127</sup>.

Despite the various benefits that AM can bring, its dissemination within the industry is still limited. For the successful use of AM, knowledge about its possibilities and capabilities is necessary. Knowledge generally can be defined as “[...] what makes possible the transformation of information into instructions. Knowledge can be obtained either by transmission from another who has it, by instruction, or by extracting it from experience”<sup>128</sup>. As expressed in this definition, experience – either made by oneself or by others – is import for gaining knowledge. And for a young manufacturing technology like AM, extensive experience must be gathered first.

This is especially true for SLM. On one hand, the process mechanism of SLM is rather complex compared to other AM processes. The finished SLM parts can be strongly influenced by the process parameters – from porous structures to full dense parts. On the other hand, SLM is – as already described – an expensive manufacturing technology. Components must therefore be economically reasonable and more importantly, be free of defects. The number of publications regarding SLM have significantly increased since the introduction of the technology.<sup>129</sup> This growing interest helps to advance the technology further and to gain technology-based knowledge.

In the past years, research focused intensively on the design of appropriate SLM parts that are created using the new possibilities of manufacturing. This concept is widely known as design for additive manufacturing (DfAM). There currently is no clear definition for DfAM.

---

<sup>124</sup> Cf. Klahn et al. (2018) pp. 153–181.

<sup>125</sup> Lachmayer et al. (2016).

<sup>126</sup> Gibson et al. (2015).

<sup>127</sup> Cf. Chua/Leong (2014) pp. 355–464.

<sup>128</sup> Rowley (2007) p. 166.

<sup>129</sup> Cf. Yap et al. (2015) 16-17.

It includes – depending on the source – different approaches and techniques. For Rosen et al., the objectives of DfAM should be to “maximize product performance through the synthesis of shapes, sizes, hierarchical structures, and material compositions, subject to the capabilities of AM technologies”<sup>130</sup>. Tang and Zhao defined DfAM as “Design for Additive Manufacturing is a type of design methods whereby functional performance and/or other key product life-cycle considerations such as manufacturability, reliability and cost can be optimized subjected to the capabilities of additive manufacturing technologies”<sup>131</sup>. Both definitions show what DfAM is all about: Using the capabilities and opportunities of AM for innovative product development. This is sometimes referred to as “additive thinking” within the AM community. In contrast to that, design for manufacturing (DfM) describes how a product has to be designed for trouble-free and cost-efficient conventional manufacturing. While DfM can be seen as a restrictive approach, DfAM has a clear orientation towards capabilities of (additive) manufacturing.<sup>132</sup>

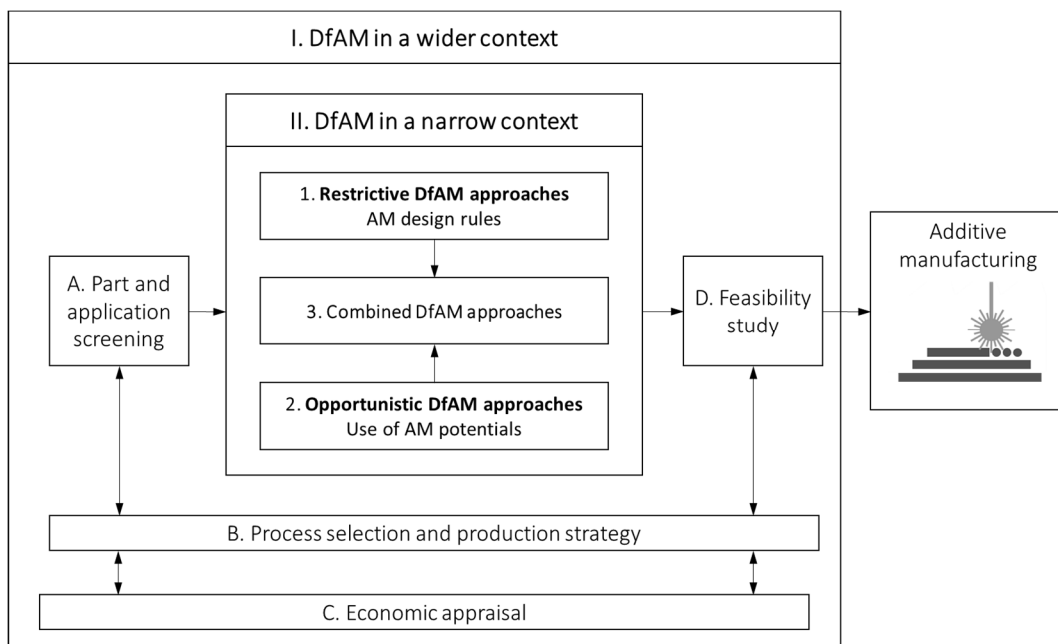


**Figure 2.13:** Classification of DfAM approaches;  
 Source: own representation, adapted and modified from Kumke (2018) p. 43.

Kumke conducted an in-depth study of DfAM approaches. The author made a distinction between DfAM in a narrow and in a wider context:

<sup>130</sup> Gibson et al. (2015) p. 411.

<sup>131</sup> Tang/Zhao (2016).

<sup>132</sup> Cf. Kumke (2018) pp. 34–42.

### **I. DfAM in a narrow context:**

It describes DfAM approaches that support the product development with guidelines and design rules. A further subdivision can be made based on Laverne et al.<sup>133</sup> and Kumke<sup>134</sup>:

1. Restrictive DfAM approaches: This approach includes manufacturing restrictions and design rules for AM. Although there is a great design freedom for AM, there are rules to be followed, including maximum overhang structures, minimum wall thicknesses and feature sizes, etc. Also, material related considerations, like basic processability, mechanical properties or anisotropic behavior must be taken into account.<sup>135</sup>

2. Opportunistic DfAM approaches: This approach focuses on the unique possibilities and capabilities offered by AM (e.g. freedom of design). The exploitation of AM potentials extends the mere use of design rules to a higher level of AM design. For this, the analysis of successful use cases, the use of AM databases or AM specific creativity techniques can serve as knowledgebase to this approach. Concrete examples are topology optimization, part and function consolidation and bionic and lattice structures.

3. Combined DfAM approaches: This includes the opportunistic and restrictive approach to enable a design that fully justifies the use of AM. As an example, the use of topology optimization with considerations regarding minimum requirements for support structures can be named. Kumke notes that a lot of existing DfAM approaches are very task specific and cannot fully serve as a tool for supporting the designer for any parts.

### **II. DfAM in a wider context:**

It extends the concept of DfAM beyond the actual design process. For instance, the part and application screening (step A, Figure 2.13) should determine parts which are suitable for the use of DfAM approaches.

A. Part and application screening: This process is supposed to identify parts and designs for which AM can be considered. The selection process depends on AM relevant criteria and should be quantifiable.

---

<sup>133</sup> Cf. Laverne et al. (2015) 21701/2-3.

<sup>134</sup> Cf. Kumke (2018) pp. 42–56.

<sup>135</sup> Cf. Chekurov (2019) pp. 1–4.

B. Process selection and production strategy: Based on selected parts and applications, a suitable AM process can be found. This step should support the decision making regarding the production process, based on criteria such as part size, lot size etc.

D. Feasibility study: This study investigates the manufacturability of selected parts for defined AM production systems. It should identify, whether part and production system fit together. Furthermore, related approaches can support considerations towards build orientation, modular fabrication etc.

But what makes a part a successful AM part? The success of an SLM part is defined during the design process. DfAM helps to create parts that use the opportunities of the SLM technology. However, even the most innovative and well-designed parts have to conquer economic evaluations.<sup>136</sup> Related to SLM – or AM in general – the terms “added value” or “increased functionality” appear. These terms are often used in relation to DfAM. But the question is: How can those vague terms be quantified? The decision about SLM as a possible manufacturing technology is based on financial consideration in most cases. So how can these vague terms be transformed into measurable characteristics?

To answer these questions, the schematic approach of Kumke has been extended by the author. The point C. Economic appraisal (Figure 2.13) has been added by the author of this thesis. It emphasizes the importance of the economic aspect of SLM parts. Designer, engineers and other involved employees need to estimate the expected costs of parts fabricated through SLM. As already stated, DfAM should enable the unique possibilities and opportunities of AM. So how can these advanced design possibilities be considered? Economic appraisal means more than just calculating the manufacturing costs. It means the quantification of benefits enabled by SLM and the cost consideration beyond the manufacturing costs. The reason for this is that selected SLM enabled benefits can only be taken into account over the whole lifecycle of a part. It is important that DfAM makes economic sense. The author's approach to this topic is discussed in chapter 3.

---

<sup>136</sup> Cf. Ehrlenspiel et al. (2014) pp. 1–2.

### **Summary of this Chapter of Information-related Challenges and Contribution of the Thesis to the Reported Issues:**

The successful use of SLM starts with the choice of parts that justify the use of this (expensive) manufacturing technology, not only from a technical, but also from an organizational and an economic point of view. Knowledge about opportunities and limitations of SLM is seen as essential for the use of it.

This will be shown and discussed based on two business cases from the industry. For these cases, a part screening model was developed and is presented in chapter 3. The part screening model supports the selection process of suitable SLM parts in a quantifiable way and serves to enhance the knowledge about the right use of SLM within a company. Additionally, both business cases show how the integration of SLM into a company can take place and how awareness of the technology can be established. From an economic point of view, SLM has to challenge conventional manufacturing when it comes to costs. Chapter 3 discusses how SLM can add value to a product and how the term added value could be made quantifiable. For this, selected approaches of cost-benefit analysis and life cycle costing (LCC) are applied on a specific use case. Based on this, SLM will be compared to conventional manufacturing with regard to costs. This thesis does not provide own research findings concerning DfAM-related techniques or design guidelines. These topics are already well elaborated and recommendable literature is widely available (among others: <sup>137, 138, 139, 140, 141</sup>). This thesis focuses on the importance of SLM knowledge and how this knowledge can be transformed into economic benefits – at best in an early design stage. The classification of the topics examined in this thesis can be made based on the modified scheme by Kumke (Figure 2.13). Contributions regarding the part screening process, process selection and production strategy (Figure 2.13, step A and B) as well as regarding the economic appraisal (Figure 2.13, step C) can be found in chapter 3. Again, specific findings from literature related to these topics are covered in the corresponding chapters.

---

<sup>137</sup> Zäh et al. (2018).

<sup>138</sup> Kumke (2018).

<sup>139</sup> Kranz (2017).

<sup>140</sup> Adam (2015).

<sup>141</sup> Yang/Zhao (2015).



## **3 COSTS AND ECONOMIC APPRAISAL OF SLM**

This chapter discusses SLM from a holistic, economic point of view. Firstly, cost specific aspects, such as cost models and lifecycle costing (LCC), are described based on existing scientific literature in chapter 3.1. In chapter 3.2, the development of an own cost model apart from the available models in the literature is introduced. In chapter 3.3, three representative build jobs are investigated from a cost perspective. The relationship between manufacturing costs and lot size is analyzed. Along with this, the debatable question whether economies of scale exist for SLM or not, is discussed. Additionally, the main cost drivers along the SLM process chain are identified by the use of the IFT cost model. Chapter 3.4 focuses on the economic impact of the SLM pre-processing step. The importance of reasonable part selection processes and accompanying cost considerations is presented based on two use cases from the industry. In chapter 3.5, a holistic approach to assess the part costs for SLM based on lifecycle costs is presented. For this, a case study that compares SLM with conventional manufacturing is elaborated. Chapter 3.6 summarizes the main findings of the chapter.

### **3.1 Cost Considerations of SLM**

As already stated in chapter 2.4, a major limitation of AM is the lack of productivity and economic efficiency. This is especially true for SLM since it requires a high initial investment into the machine and necessary equipment. Paired with slow build rates, this can easily lead to higher manufacturing costs of SLM compared to conventional manufacturing costs. In order to produce economically reasonable parts, considerations about their costs and benefits have to be established. To challenge SLM parts with conventional manufacturing, cost calculation is an essential task. This not only allows to determine the price of a part but also helps to identify costs drivers along the production process. Resulting from this, measures to increase the productivity can be developed.

#### **3.1.1 Present Cost Calculations and Cost Models**

In the following chapter, relevant cost models for AM and SLM are discussed.

Hopkinson and Dickens<sup>142</sup> compared the costs of three different AM processes (fused deposition modeling (FDM), selective laser sintering (SLS) and stereolithography (SLA)) with conventional manufacturing (injection molding (IM)). The authors investigated whether the mentioned AM processes can be used more economically than IM for two different RM parts (a small lever and a medium-sized cover part). For their cost analysis, Hopkinson and Dickens divided the costs into three types: machine costs, labor costs and material costs. The authors named the machine costs as major part for the manufacturing costs of the AM parts. However, according to their study, AM processes can compete with IM up medium production volumes when it comes to costs per part (Figure 3.1).

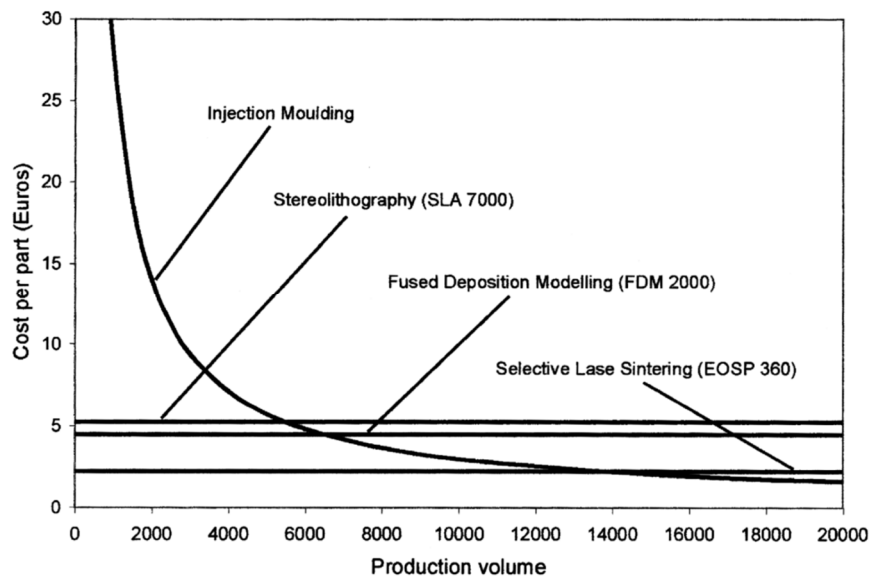


**Figure 3.1:** Cost comparison of AM with IM for the small lever;  
Source: Hopkinson and Dickens (2003) p. 38.

An interesting aspect of the graph is the fact that there is a straight linear relationship between costs per part and the production volume. This indicates that positive scale effects are not achievable with AM. This will be discussed more closely in chapter 3.3.

Hopkinson and Dickens present a well elaborated comparison between AM and CM. However, several assumptions of their cost model make it unusable at the IFT. First, the model only considers fully utilized build platforms with identical parts. Therefore, the manufacturing flexibility of AM is not taken into account. Second, pre- and post-processing steps and important overhead costs are not covered in the cost calculation.

<sup>142</sup> Hopkinson/Dickens (2003).

Ruffo et al.<sup>143</sup> advanced the model of Hopkinson and Dickens based on the lever part. One major point of criticism is the inaccuracy for low production volumes of the model of Hopkinson and Dickens. Ruffo et al. chose a full cost model and divided the costs into direct and indirect costs including overhead costs for administration and production. Especially the consideration of indirect costs for low production volumes lead to a entirely different relationship between costs per part and lot size. The resulting saw tooth shape of the cost curve can be seen in Figure 3.2.

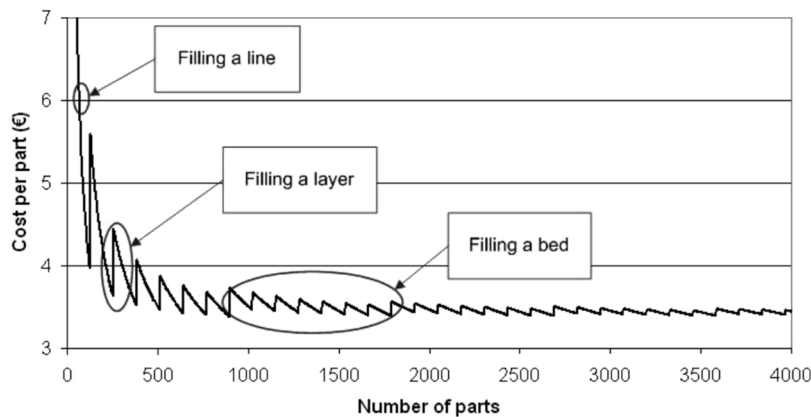


**Figure 3.2:** Saw tooth curve of costs per part for the lever;  
Source: Ruffo et al. (2006) p. 1423.

The distribution of indirect costs to the parts increases the accuracy especially for low production volumes. This approach has been extended by Ruffo and Hague<sup>144</sup> in their subsequent study. In this study, they conquered especially their second major criticism point on the model of Hopkinson and Dickens: saying that the model is only valid for identical parts on the build platform. In their study of 2007, Ruffo and Hague analyzed the split of the total manufacturing costs into different components on the same build platform. AM allows to manufacture different components (of different customers) simultaneously which can lead to economic benefits. The concept of the distribution of indirect costs of Ruffo and Hague has also been considered for the development of the IFT cost model (see chapter 3.2). However, there are some limitations to the cost model of Ruffo and Hague (2007). First, the model is based on the SLS process where parts can be built up directly in the powder bed. This allows the arrangement of parts on top of each other in z-direction. This is not possible for SLM where parts have to be connected with rigid support structures. Furthermore, a lack

<sup>143</sup> Ruffo et al. (2006).

<sup>144</sup> Ruffo/Hague (2007).

of flexibility of the model is detectable. To distribute the costs among different parts, the model needs an accurate calculation of costs of a high production volume in advance. Last, pre- and post-processing have not been taken into account within the model.

Rickenbacher et al.<sup>145</sup> developed a cost model especially for SLM. The cost model allows the calculation of the total costs per part, including also pre- and post-processing. Additionally, the calculation for different parts (size, geometry, complexity, etc.) – that are manufactured simultaneously on the same build platform – is possible with this model. Where possible, an aliquot distribution of indirect costs (e.g. gas consumption, separation from build platform, etc.) on the different parts is performed. A special focus was set on a fair distribution of costs. For this, an algorithm was developed by Rickenbacher et al. This algorithm takes the different build heights into account so that parts with small build heights will not be overpriced. Furthermore, the authors used their model to identify cost drivers. As other authors before, Rickenbacher et al. identified the machine costs based on the build time as main cost driver along the process chain. Because of its comprehensibility, the cost model of Rickenbacher et al. served as basis for the development of the IFT cost model (chapter 3.2).

Pilli et al.<sup>146</sup> investigated costs for SLM with PH1 stainless steel. They used their cost model to analyze the effect of build platform utilization and the cost structure of exemplary parts. According to the authors, cost savings for a fully utilized build platform were between 81 to 92 % compared to the built of a single component. Furthermore, the cost share of the machine costs was very dominating. More than 95 % of the part costs can be attributed to the machine costs, the rest to material and energy. Nevertheless, the model of Piili et al. (2015) is greatly simplified in some points. Personnel costs are not included and also pre- and post-processing are not sufficiently discussed.

Schröder et al.<sup>147</sup> chose a process-based approach for their cost model. This approach considers all job-relevant activities that cause costs. They especially emphasize the necessity of including possible waste and the recycling of the material and the use of quality monitoring activities. Schröder et al. identified seven main process steps, ranging from planning and design to a quality check at the end. All of these process steps have sub-processes with their own cost calculation. This makes the cost model very comprehensive and detailed. It allows 77 variables to be edited. In their study, Schröder et al. performed a

---

<sup>145</sup> Rickenbacher et al. (2013).

<sup>146</sup> Piili et al. (2015).

<sup>147</sup> Schröder et al. (2015).

sensitivity analysis for two different products. These two products vary in size (small and huge) and in required quantity (1 and 1000). Results show that the machine investment has the highest influence on the part costs. Also, the degree of utilization and the layer thickness were highly influential. All three influence factors can be attributed to what is generally known as machine costs. This confirms findings from previous studies by other authors. For a small product with a lot size of 1000 parts, post-processing was the most influential factor – a high potential for further process optimization according to the authors.

Findings from literature confirm – as already stated by the author – that the machine costs for processing is the major cost driver when it comes to SLM. Costs for material, energy and gas contribute only little to the overall costs of SLM. Costs for post-processing are highly individual and strongly depend on the related part. However, these costs are also reported as important cost drivers for SLM in the literature.

The high manufacturing flexibility of SLM also results in a flexible process sequence. This requires an adaptable but also comprehensive approach along the whole process chain. It is essential that pre- and post-processing are also included. For this, a detailed process-based approach like in Schröder et al. is recommended by the author.

#### **3.1.2 Lifecycle Cost Considerations**

The last chapter described the necessity of cost models for AM. Despite their differences, these cost models have something in common – they do not cover the full lifecycle of AM parts. This chapter serves as a brief overview of lifecycle-based approaches and their influence on SLM.

SLM has the reputation of being an expensive manufacturing technology, especially in comparison to conventional manufacturing. Cost assessment based on manufacturing costs often turn out to be disadvantageous for AM. In this context, AM-related benefits such as part consolidation, lightweight design etc. are not taken into account. The reason for this is that most benefits enabled by AM show their effects not until the use phase. For instance, part consolidation can lead to less maintenance effort or decrease the probability of leakage. Furthermore, the lightweight AM design of aircraft parts decreases the fuel consumption. Some benefits can have a direct monetary impact (less fuel consumption means less fuel costs). but some AM benefits can be hard to be assessed in a monetary way. For instance, the

positive effects of patient specific AM implants in the medical field are not easy to quantify.<sup>148</sup>

<sup>149</sup>

As a possible approach, the quantification of AM enabled benefits can be realized through lifecycle costing (LCC). Ehrlenspiel et al. (2007) defined that “lifecycle costs are those seen by the product user as the sum of all costs starting from the purchase and during the use (product life span) of a product (plant, machine, device, apparatus, etc.).”<sup>150</sup>

According to Ehrlenspiel et al., LCC consists of:

- **Initial costs** (purchasing price)
- **One-time costs** (e.g. for transportation and installation)
- **Operation costs** (e.g. for energy and supplies)
- **Maintenance costs** (e.g. for inspection and repair)
- **Other costs** (e.g. insurance and taxes)

LCC extends the cost perspective beyond manufacturing and total costs (Figure 3.3). It can be seen that lifecycles costs affect the user (customer) of a part or product. For instance, operating costs do not affect the manufacturer of AM parts at all. But then, why would a manufacturer be interested in LCC? The reason is that life cycle costs can be seen as selling point for the manufacturer. Lifecycle costs make cost-benefit considerations quantifiable – an important issue for capital goods where decisions are not exclusively based on the purchase price.<sup>151</sup>

---

<sup>148</sup> Cf. Lindemann et al. (2012) pp. 177–178.

<sup>149</sup> Cf. Zäh (2013) p. 121.

<sup>150</sup> Ehrlenspiel et al. (2007) p. 111.

<sup>151</sup> Cf. Ehrlenspiel et al. (2007) 5-6; 114-115.

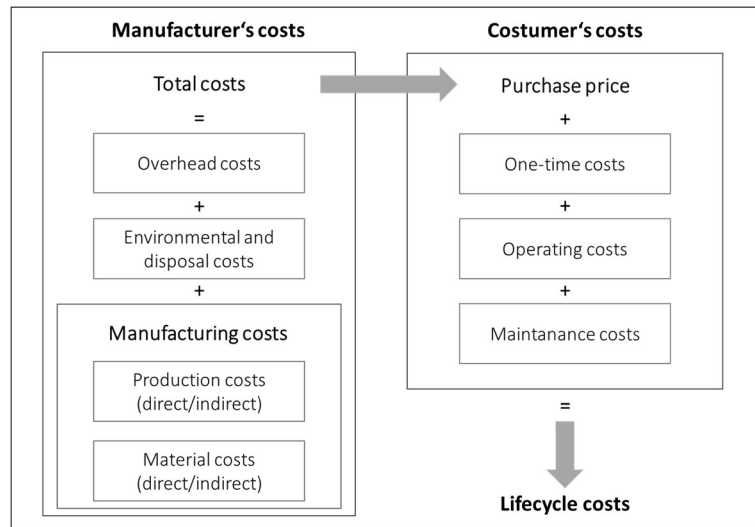


**Figure 3.3:** Schematic structure of the lifecycle costs;  
 Source: own representation, modified from Ehrlenspiel et al. (2007) p. 113.

Klahn et al. (2018) discussed the importance of lifecycle-based cost-benefit approach to fully consider the benefits of AM. According to the authors, a comprehensive AM design can lower the operating costs. Therefore, design decisions for AM directly influence the lifecycle costs. LCC allows the manufacturer to evaluate the impact of design decisions on the customer. Despite a possible higher purchasing price compared to CM, AM can generate economic benefits, along the lifecycle of products, for the customer. According to Klahn et al., these benefits are called “benefits of higher order” and have to be taken into account within the balance of a business case.<sup>152</sup> For the authors, a benefit of the first order can be reached when AM decreases the manufacturing costs during production within the manufacturing company. Currently, this is rarely the case. However, a positive example is presented in chapter 3.4.1.

A benefit of second order appears during the use phase of the product. For instance, AM manufactured molds with internal cooling channels increase the productivity, or the lightweight AM parts decrease the fuel consumption. Usually, the customer benefits from that over a longer period of time. Benefits of third order include the positive impact of AM manufactured parts on other (non-) AM parts. For instance, an AM manufactured cutter head with increased cooling capabilities generates parts with better surface roughness. Thus,

<sup>152</sup> Cf. Klahn et al. (2018) p. 95.

the capabilities of AM have to be considered beyond the production process to qualify their beneficial use.

Lindemann et al.<sup>153</sup> emphasize the importance of lifecycle considerations for AM. According to the authors, the estimation of AM-enabled benefits requires a lifecycle-based approach to take the advantages of the technology into account. In their study, the authors present the cost calculation of an exemplary SLM part with regard to different influence factors (build-up rate, utilization rate, material costs and machine investment). The whole process chain from pre- to post-processing was considered. Machine costs are found to be the main influence factor on the manufacturing costs (44.5 to 78.5 %). However, the authors did not cover lifecycle considerations quantitatively because their cost model ends with post-processing. While lifecycle considerations are stated within the study, they were not executed.

#### **3.1.3 Summary of Chapter 3.1**

Knowledge about costs of AM is essential for two reasons. First, to calculate the total costs of a product and to determine a selling price. Second, to identify cost drivers along the process chain of production. In the literature, machine costs were found to be the main cost driver for AM. Based on this, process optimizations can be developed and executed. However, for both tasks, the cost model has to be accurate. Present cost models of the literature do not fulfil the requirements of the IFT completely. Therefore, an own cost model has been developed based on findings from the models of Rickenbacher et al. (2013) and Schröder et al. (2015). This model is briefly presented in chapter 3.2 and applied in chapter 3.3.

However, in some situations, a highly accurate determination of costs is not necessary. For instance, in early stages of the product development, a rough estimation of costs can help to decide whether the use of SLM makes sense from an economic point of view. For these considerations, a fast but sufficiently accurate estimation is enough. An approach based on the practical build-up rate  $\check{V}_{Pr}$  is presented in chapter 3.4.1.

Cost considerations in AM – and especially for SLM – should go beyond the exclusive consideration of manufacturing costs (internal) or purchasing price (external). The importance of LCC and its ability to take the benefits of AM into account was stated and

---

<sup>153</sup> Lindemann et al. (2012).



presented in this chapter. Two examples of LCC are presented in this thesis: in chapter 3.4.1, LCC considerations made exemplarily quantified. In chapter 3.5, a use case for LCC and cost-benefit analysis is presented. For the sake of completeness, it should be noted that the terms total cost of ownership (TCO) and LCC are used sometimes interchangeably. The author uses the term LCC consistently in this thesis.

## 3.2 The IFT Cost Model

In the following chapter, the mentioned IFT cost model will be described fundamentally. The cost model was developed by Georg Quinz and the author of this thesis in 2016. Since then, the cost model has been developed further and adapted to the requirements at the IFT and its academic context. On the one hand, the cost model serves as a calculation basis for the pricing of parts and the budgeting of industrial and academic projects at the institute. On the other hand, the model is used for the evaluation and quantification of the developed approaches towards higher economic efficiency – also used in this thesis (see chapter 3.3 and chapter 4). In this chapter, only the key points of the IFT cost model will be discussed. For deeper insight, the author refers to the thesis of Georg Quinz<sup>154</sup>.

As already stated, AM allows the production of highly individual parts and is usually used for small batch sizes. Therefore, the composition of the manufacturing process frequently varies. Process steps – for instance during post-processing – that are required for product A may be omitted for product B although both products are manufactured at the same build platform and at the same time. This flexibility in production demands a flexible costing method that allows a source-based allocation of costs to the AM products.<sup>155</sup>

The IFT cost model is based on the German term “Prozesskostenrechnung”, a costing method that can be attributed to activity-based costing (ABC).<sup>156</sup> This approach for AM as a cost calculation method is also reported in the literature. Lindemann et al. (2012) used the approach of time-driven activity-based costing (TD ABC). This method allows an allocation of costs based on the time that a process takes. The authors separated the AM process into four main processes to calculate their costs: preparation, production, removal and post-processing. Krauss et al. (2011) also emphasized the inclusion of the whole AM process chain

---

<sup>154</sup> Quinz (2016).

<sup>155</sup> Cf. Krauss et al. (2011) p. 2.

<sup>156</sup> Cf. Horsch (2020) p. 269.

for cost considerations. The authors calculated the process times and -costs based on subprocesses with individual levels of details.

The IFT cost model follows the division of pre-processing, processing and post-processing of the SLM process chain described in chapter 2.2. Similar to Krauss et al., these main process steps are further divided into subprocesses to achieve a higher level of detail for the determination of process times and -costs. In the following Figure 3.4, the main cost positions along the process chain for the IFT cost model are listed.

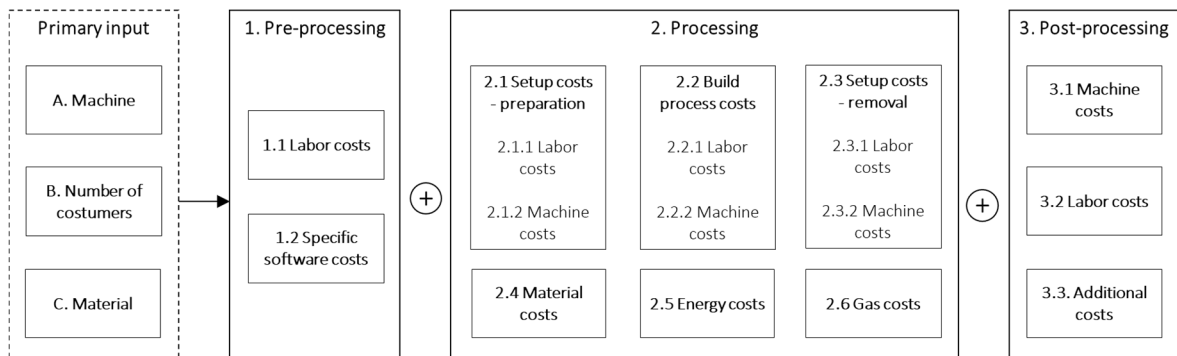


**Figure 3.4:** Main types of costs along the SLM process chain for the calculation of the manufacturing costs with IFT cost model;  
Source: own representation.

The calculation done with the IFT cost model starts with the selection of primary variables and input of necessary data (Table 3.1). After that, the single cost positions along the process chain can be edited. In the following tables, a basic description of input variables and cost positions is provided and their main reference values for the calculations are listed.

**Table 3.1:** Primary input variables for the IFT cost model.

Primary input	Description
A. Machine	Selection of the SLM machine if more than one is available
B. Build job data	Includes important basic data for the build job, for instance: <ul style="list-style-type: none"> <li>○ Part specific: number of parts, volume (parts, support structures), build time</li> <li>○ Number of customers: defines the number of different input customers with parts on the same build platform. For each customer, a separate input mask is opened</li> </ul>
C. Material	Selection of the available raw material for the chosen machine from A.

**Table 3.2:** Main type of costs for step 1: pre-processing.

Costs	Important reference values	Description
<b>1. Pre-processing</b>		
1.1 Labor Costs $C_{Pre,L}$	<ul style="list-style-type: none"> <li>▪ Working time (h)</li> <li>▪ Staff's hourly rate (€/h)</li> </ul>	Labor costs for pre-processing tasks like CAD data generation, topology optimization, build job preparation etc.
1.2 Specific hardware and software costs $C_{Pre,HS}$	<ul style="list-style-type: none"> <li>▪ Utilization time (h)</li> <li>▪ Lump sum</li> </ul>	Software costs (license, maintenance etc.) for special required software (e.g. for topology optimization or simulation), calculated with overhead allocation

**Table 3.3:** Main type of costs for step 2: processing.

Costs	Important reference values	Description
<b>2. Processing</b>		
2.1. Setup costs – preparation $C_{SP}$		
2.1.1 Labor costs $C_{SP,L}$	<ul style="list-style-type: none"> <li>▪ Working time (h)</li> <li>▪ Staff's hourly rate (€/h)</li> </ul>	Labor costs for setting up the machine for the SLM process, e.g. powder sieving and filling, recoater adjustment, loading of data e.g.
2.1.2 Machine costs $C_{SP,M}$	<ul style="list-style-type: none"> <li>▪ Setup time (h)</li> <li>▪ Machine hour rate (€/h)</li> </ul>	Costs during setup when the machine is occupied, for instance by settings of the operator or specific preparation processes that are ongoing (e.g. pre-heating of the build platform)
2.2 Build process costs $C_{BP}$		
2.2.1 Labor costs $C_{BP,L}$	<ul style="list-style-type: none"> <li>▪ Working time (h)</li> <li>▪ Staff's hourly rate (€/h)</li> </ul>	Labor costs during the build process, for instance for supervision, necessary adjustment or refilling of powder
2.2.2 Machine costs $C_{BP,M}$	<ul style="list-style-type: none"> <li>▪ Total build time (h)</li> <li>▪ Machine hour rate (€/h)</li> </ul>	Machine costs during the processing (= fabrication of the parts)
2.3 Setup costs – removal $C_{SR}$		
2.3.1 Labor Costs $C_{SR,L}$	<ul style="list-style-type: none"> <li>▪ Working time (h)</li> <li>▪ Staff's hourly rate (€/h)</li> </ul>	Includes costs for removal of the build platform (unpacking), cleaning of the build chamber, etc.
2.3.2 Machine Costs $C_{SR,M}$	<ul style="list-style-type: none"> <li>▪ Setup time (h)</li> <li>▪ Machine hour rate (€/h)</li> </ul>	Costs during cleaning, unpacking etc. when the SLM machine is occupied
2.4 Material costs $C_{Mat}$	<ul style="list-style-type: none"> <li>▪ Total build volume (<math>cm^3</math>)</li> <li>▪ Purchase price (€/kg)</li> </ul>	Includes direct costs for powder consumption. A surcharge for scrap material as not reusable powder can be included
2.5 Energy costs $C_{Ene}$	<ul style="list-style-type: none"> <li>▪ Setup time (h)</li> <li>▪ Total build time (h)</li> <li>▪ Power consumption (W)</li> <li>▪ Energy price (€/kWh)</li> </ul>	Energy costs caused by the SLM machine and its periphery (e.g. vacuum cleaner). The power consumption during the SLM process was tested experimentally
2.6 Gas Costs $C_{Gas}$	<ul style="list-style-type: none"> <li>▪ Total build time (h)</li> <li>▪ Gas consumption - processing (l/min)</li> <li>▪ - floating (l)</li> <li>▪ Gas price (€/m<sup>3</sup>)</li> </ul>	Costs due to necessary consumption of shielding gas during the process. It includes the initial floating of the building chamber and the ongoing consumption during the build process (values are taken from SLM280HL datasheet)

**Table 3.4:** Main type of costs for step 3: post-processing.

Costs	Important reference values	Description
<b>3. Post-processing</b>		
3.1 Machine costs $C_{Pos,M}$	<ul style="list-style-type: none"> <li>▪ Setup time (h)</li> <li>▪ Machine hour rate (€/h)</li> </ul>	Includes the costs of the different machines that are used for post-processing, e.g. heat treatment, CNC machining, quality inspection etc.
3.2 Labor Costs $C_{Pos,L}$	<ul style="list-style-type: none"> <li>▪ Working time (h)</li> <li>▪ Staff's hourly rate (€/h)</li> </ul>	Labor costs during post-processing, for instance for the removal of support structures, inspection, or reprocessing of the build platform
3.3 Additional Costs $C_{Add}$	<ul style="list-style-type: none"> <li>▪ individual, e.g. purchase price (€)</li> </ul>	Additional costs include costs that have not been considered before. For instance, costs for external services of post-processing, special equipment for the build job (e.g. filter), recycling costs etc.

The cost model allows the allocation of costs directly to the parts and customers to a high degree. Indirect costs (overhead), for instance for administration, marketing, IT or operating costs, are regulated within the guidelines of Graz University of Technology. These overhead costs can be added into the IFT cost model as an additional cost item. This approach can also be applied to other organizations when using the IFT cost model.

A more detailed execution of the IFT cost model will not be explained in this thesis. Its application is demonstrated in chapter 3.3 and 4. However, one particular example – the cost distribution within a single build platform – will be described in the following paragraphs. It is a common procedure for SLM to fill a build platform with parts of different customers (the reason for this is explained in the following chapter, see utilization). Nevertheless, a fair cost distribution for all concerned customers should be targeted.

In contrast to the complex algorithm of Rickenbacher et al. (2013), a simpler approach for the IFT cost model was developed. The target value for the cost distribution is the total build time  $t_b$  which strongly influences the total manufacturing costs. As already stated, the total build volume can easily be calculated with the preparation software. The proportionate allocation of the build time for each customer ( $t_{bci}$ ) is calculated as follows:

$$t_{bci} = t_{bi} \cdot \frac{t_b}{\sum_{i=0}^n t_{bi}} \quad (3.1)$$

Where  $t_{bi}$  is the total build time (h) for the customer  $i$  if the build job would be carried out exclusively for the customer  $i$  without any other customer's parts on the build platform. This shall be illustrated with an example:

It is assumed that the SLM parts of three customers 1, 2 and 3 can be manufactured at the same time on the same build platform. The first step is to simulate the total build time with the preparation software for each customer based on the assumption that the build job would be done exclusively for the customer. For example:

- Customer 1:  $t_{b1} = 6.5$  h
- Customer 2:  $t_{b2} = 14$  h
- Customer 3:  $t_{b3} = 9.5$  h

However, if the components of all customers are manufactured on the same build platform, it is assumed that the total build time  $t_b$  takes 20 h. With the equation (3.3), the partial build time for customer 1 within the collective build job can be calculated:

$$t_{bc1} = 6.5 \cdot \frac{20}{6.5 + 14 + 9.5} = 4.33 \text{ h} \quad (3.2)$$

Using that equation, the partial build times for customer 2 and 3 can be calculated:

- $t_{bc2} = 9.33$  h
- $t_{bc3} = 6.33$  h

It can be seen that the joint production of the components lowers the build times for each customer significantly (-33 %). For the IFT cost model, the  $t_b$  is an important calculation factor that co-determines many costs, such as the machine costs during processing  $C_{BP,M}$ , the supervision time of the operator  $C_{BP,LS}$  or the gas costs  $C_{Gas}$ . Therefore, a causation-based allocation of costs can be achieved. Furthermore, a fair passing on of cost advantages to each customer – due to the joint production of components – can be made possible.

The IFT costs model was created as a spreadsheet in Microsoft Excel and can be edited easily. Where no definite numbers (e.g. setup time) are available, the program provides advice based on calculations from input values such as total build time or part volume.<sup>157</sup> Of course, the cost model also has its limitations. For the use in an industrial context, overhead costs (e.g. for sales, administration, logistics etc.) and profit margins have to be included additionally. However, the advantage of the IFT cost model lies in the combination of clarity and adequate accuracy paired with high adaptability at the same time.

---

<sup>157</sup> Quinz (2016).

### 3.3 Cost Evaluation of Selected Build Jobs

In this chapter, the evaluation of the cost structure for three different SLM parts is presented. The evaluation has three main purposes. First, it helps to determine the main cost drivers for SLM. Of course, knowledge about cost drivers for SLM is available in related literature. However, findings from the literature should be verified by the self-developed cost model. Second, the relationship between costs and lot size will be discussed. It is postulated, that there is no linear and constant relationship between costs and production volume (lot size) as shown in various references (<sup>158, 159, 160</sup>). The author expects a degressive relationship as other reviewed literature reports (<sup>161, 162, 163</sup>). Related to this, the term “micro economies of scale” will be presented and explained. Third, the investigation based on these three representative parts will show the impact of selected parameters on the build time – and further on the manufacturing costs.

#### 3.3.1 Methodology

These investigations were carried out by simulation. No physical build job was necessary to determine the manufacturing costs. The reason for this is that the fictive build time can be predicted easily with the preparation software after slicing. As software for the build job preparation, Materialise Magics (vers.21) was used. In order to qualify the build time prediction of Materialise Magics, 18 different build jobs within a time range of 20 months were analyzed. It showed that the real build time of the physical build job differs from the simulative approach by the software. On average, the computed build job took 11.53 % longer than the real build job (Table 3.5). This difference was considered for the later simulative-based cost calculation for the three parts. All real build jobs were carried out with the SLM 280HL (single laser, 400 W, SLM Solutions AG) machine. Only build jobs without manual interventions during the build job were taken into account for this study.

---

<sup>158</sup> Cf. Hopkinson/Dickens (2003) p. 38.

<sup>159</sup> Cf. Atzeni/Salmi (2012) p. 1154.

<sup>160</sup> Cf. Poprawe et al. (2015) p. 51.

<sup>161</sup> Cf. Zäh (2013) pp. 141–148.

<sup>162</sup> Cf. Lindemann et al. (2012) p. 185.

<sup>163</sup> Cf. Ruffo et al. (2006).

**Table 3.5:** Comparison of computed and real build time for 18 build jobs.

<b>Build job Nr.</b>	<b>Computed build time in hh:mm</b>	<b>Real build time in hh:mm</b>	<b>Difference in %</b>
20170620	12:41	11:08	12.22
20170613	06:06	05:34	8.74
20170607	09:37	08:28	11.96
20170531	15:29	13:39	11.84
20170427	08:26	07:25	12.06
20170315	16:14	14:33	10.37
20170307	11:47	10:44	8.91
20170222	15:28	13:44	11.21
20170217	01:12	01:04	11.11
20170208	41:12	36:15	12.01
20170131	04:46	04:15	10.84
20170112	15:08	13:18	12.11
20170110	14:15	12:34	11.81
20161220	08:59	07:55	11.87
20161206	15:51	14:10	10.62
20161129	07:48	06:42	14.10
20161027	05:11	04:32	12.54
20161024	05:11	04:30	13.18
MV			11.53
± SD			1.32
95% C.I.			0.61

The selection of the three different part types is based on their different size, shape and the possible lot size on the build platform. They represent typical parts for SLM with specific characteristics such as lattice structures, cavities or topology optimized geometries. As already mentioned, parameters were varied for this investigation (see Table 3.6). The number of parts on the build platform (lot size) varied between one part and a full build platform. This provides information about the cost behavior within a single build platform. Apart from the lot size, the layer thickness was varied between 30  $\mu\text{m}$  and 50  $\mu\text{m}$ . Both values of layer thickness are in the typical range for the 280HL SLM machine. For comparability reasons, standard parameter configurations, provided by the manufacturer SLM, were chosen. These parameter sets are supposed to lead to high relative densities. The third parameter that was varied, was the waiting time ( $t_w$ ). The waiting time – as a reminder – is the time between the start of the scanning process and the beginning of the recoating process. When the scanning process needs less time than the preset  $t_w$ , the process is on hold and allows the parts on the build platform to cool down. The layer thickness and waiting time were chosen as modifiable parameters as they can be easily adjusted by even unexperienced

users of SLM Solutions AG machines. A more comprehensive look at the impact of parameter variation is discussed in chapter 4. Also, additional calculations for the studies within this chapter are available in the Appendix (Table A 1 to Table A 3).

**Table 3.6:** Overview of parameter variation for the three investigated parts.

Part name	Lot size	Layer thickness	Waiting time
	in no. of parts	in $\mu\text{m}$	in s
1. Jet engine bracket	1; 5; 10; 16	30; 50	0; 30
2. Filter head	1; 3; 6; 8	30; 50	0; 30
3. Pipe section	1; 30; 59; 88; 117	30; 50	0; 30

For this study, only the manufacturing costs in accordance with the German designation “Herstellkosten” are considered. The term Herstellkosten can be translated to English either as “manufacturing costs” or with “production costs”. Sometimes, both are used interchangeably.<sup>164</sup> Manufacturing costs in this thesis include direct costs for material and manufacturing as well as possible overhead costs for both. It is also assumed that the parts are manufactured in the presented state. That means that possible development costs (e.g. CAD, FEA) are not considered. Furthermore, costs for distribution and administration are not considered.

### 3.3.2 Example 1: Jet Engine Bracket

The jet engine bracket has its origin in the GE Jet Engine Bracket Challenge<sup>165</sup>. The GE Bracket Challenge was a design contest where an existing bracket was optimized towards maximum lightweight for AM. Engineers all over the world have submitted their solution via the online platform GrabCAD. One of these brackets has been used for this investigation.<sup>166</sup> This bracket includes interesting lattice structures and complex shapes – both predestined for being fabricated with SLM. The bracket was scaled down to 1:4 to investigate the effect of increasing lot sizes better. The brackets represent a small to medium sizes, but complex, part for SLM. Additionally, the bracket requires a high amount of support structure which will be influential on the labor costs. As material, 316L was exemplarily considered.

<sup>164</sup> Averkamp (2020).

<sup>165</sup> Morgan et al. (2016).

<sup>166</sup> GrabCAD (2013).



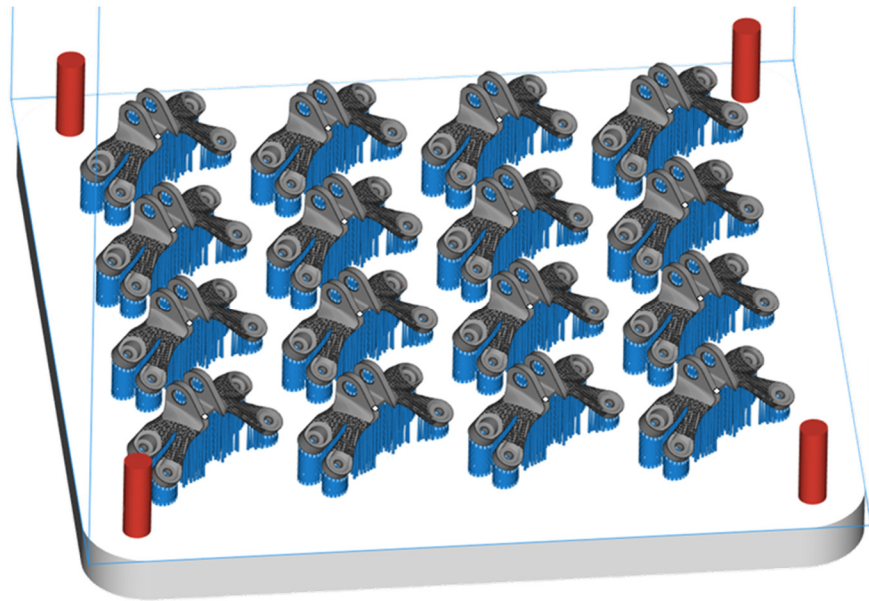


**Figure 3.5:** Overview of the prepared jet engine brackets (16 parts) for SLM;  
Source: own representation.

A maximum of 16 brackets can be arranged on a single build platform (Figure 3.5). An overview of the simulated build times, depending on the lot size and selected parameters, is shown in Table 3.7. It can be immediately seen that there is a wide relative deviation of build times for small lot sizes. As expected, a small layer thickness ( $l_z = 30 \mu\text{m}$ ) combined with a long waiting time ( $t_w = 30 \mu\text{s}$ ) results in long build times – especially for small lot sizes. The negative effect of the  $t_w$  on the build time decreases with increasing lot sizes. The reason is that the scanning process for a single layer takes longer than the preset waiting time. In that case,  $t_w$  does not influence the build time.

**Table 3.7:** Parameter configuration and simulated build times for the jet engine bracket.

Configuration		Build time of the build job in hh:mm			
Layer thickness $l_z$ in $\mu\text{m}$	Waiting time $t_w$ in s	Number of parts			
		1	3	6	8
30	0	03:28	07:44	13:04	19:27
30	30	12:45	13:09	16:20	21:37
50	0	02:35	06:46	11:56	18:11
50	30	08:16	08:48	13:10	18:56

But what would happen in terms of time and costs if the required amount of parts exceeds one build platform? To answer this question, the lot size has been extended to 48 brackets.

This means three full build platforms for the SLM 280HL machine. The pure build time by machine can be calculated by looking at Table 3.7. Three full build platforms mean three times the build time for 16 parts. However, additional time for the changing of the build platform and the setup of the machine between each build job have to be taken into account. The effects on the manufacturing costs will be discussed at the end of this chapter.

With knowledge of the build times, the manufacturing costs can be calculated with the IFT cost model (Table A 1, Appendix). Exemplarily, the cost share of the manufacturing costs of a single bracket is shown in Figure 3.6. As parameter configuration, the most promising configuration with regard to the economic perspective ( $l_z = 50 \mu\text{m}$  /  $t_w = 0 \text{ s}$  / 16 parts) has been chosen. On the one hand, the share of labor costs (45.2 %) shows to be rather high – even higher than the machine costs. The main reason for this is the time-consuming removal of the support structures of this part. As shown in Figure 3.5, the parts have to be supported extensively due to their build orientation and all of these support structures have to be removed at a certain point. On the other hand, the share of material consumption is rather low. Only 2 % of costs are caused by material consumption.

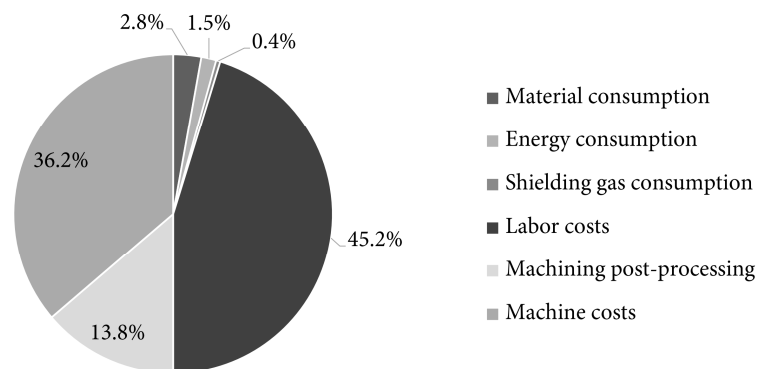


**Figure 3.6:** Cost shares of manufacturing costs of one jet engine bracket ( $l_z = 50 \mu\text{m}$  /  $t_w = 0 \text{ s}$  / 16 parts);

Source: own representation.

Coming now to the influences of different parameter settings on the manufacturing costs. For this, all four investigated parameter configurations are compared in a common chart. A non-linear relationship between manufacturing costs per part (y-axis) and the lot size (x-axis) is clearly visible. This behavior contradicts findings from related literature. The curves of manufacturing costs correspond to the saw-tooth profile from Ruffo et al.<sup>167</sup>. Similar to

<sup>167</sup> Cf. Ruffo et al. (2006) p. 1423.

this study, the outlier up represents the additional costs for setting up a new build platform. A closer look to the different curves reveals, that parameter settings clearly influence the manufacturing costs. This effect is most visible with small lot sizes. For a low utilization of the build platform, the waiting time  $t_w$  is highly influential on the manufacturing costs because of the increase of the build time. The scanning process of the laser takes less time than the adjusted waiting time. That means, that the whole SLM process stands still during this time, which adds to the build time.

The layer thickness also influences the manufacturing costs significantly. For building the same part height in z-direction, more than 1.6 times more layers are required for the  $l_z = 30 \mu\text{m}$  build job. This is directly related to the number of waiting times, recoating times and scanning times for each layer. However, this effect becomes smaller with increasing lot sizes. There are multiple reasons for this. On the one hand, fixed costs for e.g. pre-processing or machine setup can be distributed to more parts. On the other hand, the build time does not increase linearly with increasing lot sizes. Especially the fixed times for recoating and waiting remain the same for one part as for a full build platform. More than that, as already stated, the effect of  $t_w$  can be neglected for large lot sizes.

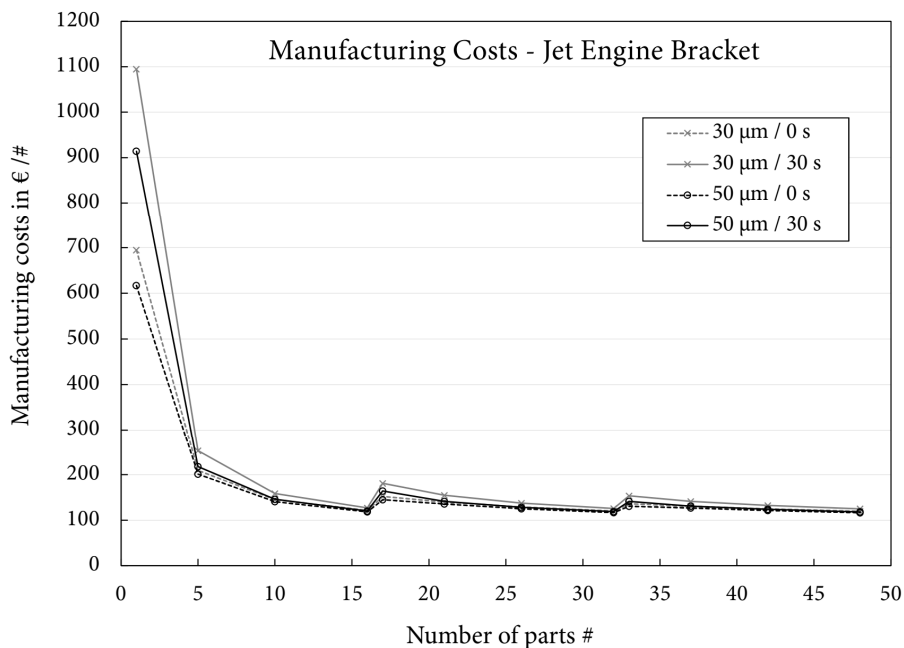


**Figure 3.7:** Influence of different parameter configurations on the relationship between manufacturing costs and lot size for the jet engine bracket;

Source: own representation.

Figure 3.7 also reveals that the manufacturing costs of the jet engine bracket asymptotically approach a lower limit value when the build platform is fully utilized. That means, a further decrease of manufacturing costs can only be achieved by additional measures. For instance, the use of machines with larger build chambers would allow more parts to be manufactured at the same time. This would decrease the manufacturing costs per part. Another measure would be to decrease the build time by using a faster set of parameters. This approach was studied and is presented in chapter 5. However, Figure 3.6 shows that a major part of the manufacturing costs for the jet engine bracket is caused by manual labor for post-processing. An approach to decrease these costs is presented in chapter 5.

### 3.3.3 Example 2: Filter Head

The filter head has been developed within an industrial project at the IFT. In this section, the filter head should represent a topologically optimized part with medium size. Because of its complex shapes created by the optimization, SLM can be a valuable manufacturing technology. In total, 8 parts can be arranged on a single build platform for the SLM 280HL machine (Figure 3.8). As material, 316L has been chosen again.

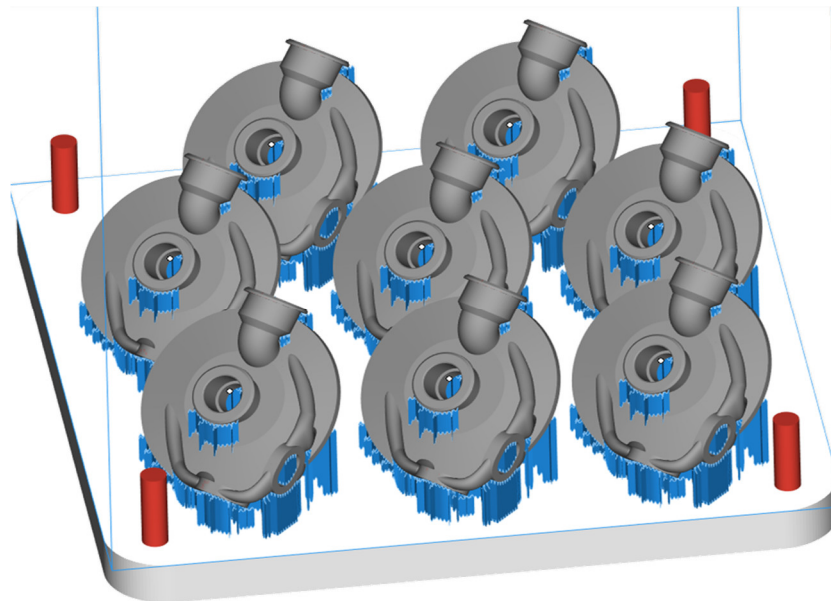


**Figure 3.8:** Overview of the prepared filter heads (8 parts) for SLM;  
Source: own representation.

As in the example of the jet engine bracket before, the build time is calculated for different parameter configurations (Table 3.8). Again, the build jobs performed with  $l_z = 50 \mu\text{m}$  and  $t_w = 0 \text{ s}$  can be seen as the most promising ones when it comes to the decreasing of build

time. Similar to the jet engine bracket, the effect of the  $t_w$  on the build time decreases with increasing lot size, but it does not become obsolete for both selected  $l_z$ .

**Table 3.8:** Parameter configuration and simulated build times for the filter head.

Configuration		Build time of the build job in hh:mm			
Layer thickness $l_z$ in $\mu\text{m}$	Waiting time $t_w$ in s	Number of parts			
		1	3	6	8
30	0	11:16	23:24	41:34	53:35
30	30	27:57	30:35	45:24	56:19
50	0	07:53	17:18	31:23	40:42
50	30	17:11	21:17	33:30	42:04

A closer look at the cost share for one filter head (Figure 3.9) shows different results compared to the cost share of the jet engine bracket (Figure 3.6). The largest share of costs concerns the machine costs (53.9 %) due to the longer build time. Although support structures are necessary, their removal is less intensive in relation to the size of the filter head. The cost share of CNC post-processing (7.3 %) results from the machining of functional surfaces, such as sealing and connecting surfaces. Nonetheless, material-, gas- and energy consumption still play a minor role to the manufacturing costs.

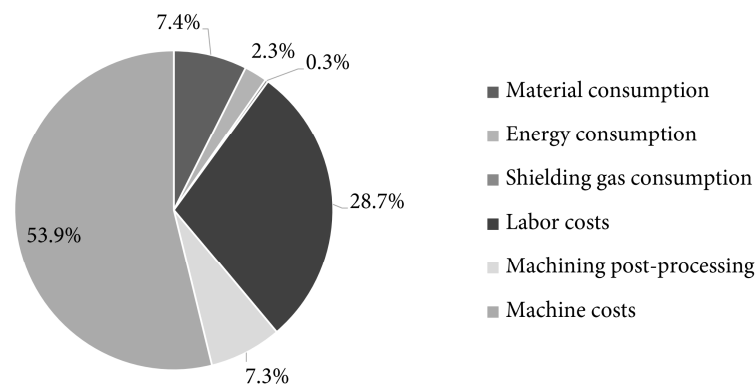


**Figure 3.9:** Cost shares of manufacturing costs of one filter head ( $l_z = 50 \mu\text{m}$  /  $t_w = 0\text{s}$  / 8 parts); Source: own representation.

Again, to investigate the effect of producing three full build platforms, the simulation of the manufacturing costs has been extended to a lot size of 24 parts (see Table A 2, Appendix). This means three fully utilized build platforms. Figure 3.10 shows the results from this investigation. The sawtooth effect for all parameter configurations is clearly visible again. Compared to the jet engine bracket, there is a bigger difference in costs per part between the

single configurations. Especially the cost advantage for  $l_z = 50 \mu\text{m}$  is clearly visible. This can be explained by the smaller number of total layers needed for the filter head.

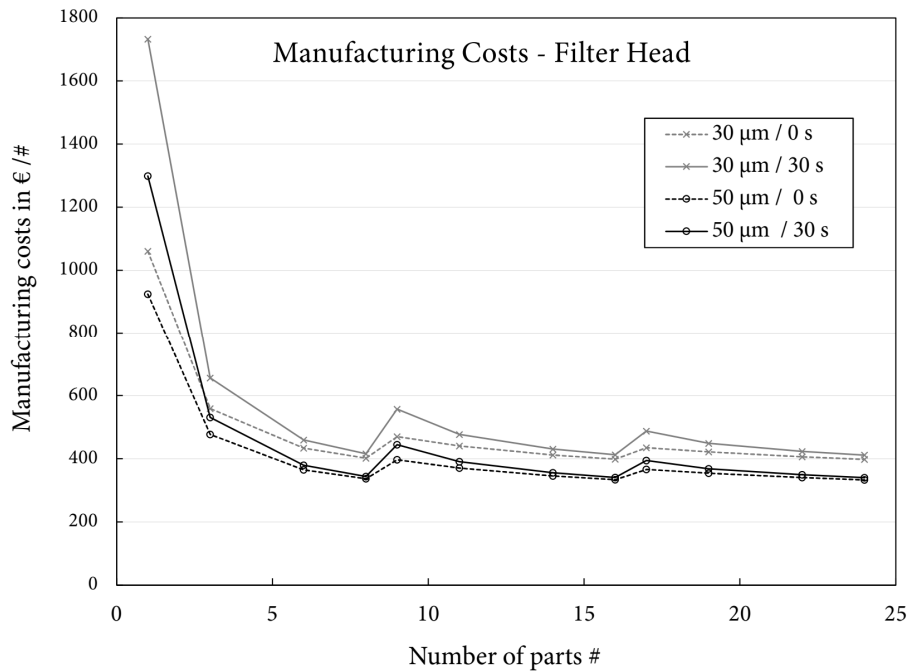


**Figure 3.10:** Influence of different parameter configurations on the relationship between manufacturing costs and lot size for the filter head;  
Source: own representation.

Here again, the line chart clearly shows the asymptotical approach of the manufacturing costs towards a minimum value. Nevertheless, as shown for the jet engine bracket, the fabrication of a single part – especially for the  $l_z = 30 \mu\text{m} / t_w = 30 \text{ s}$  configuration – results in high manufacturing costs per part.

### 3.3.4 Example 3: Pipe Section

The last part in this study of manufacturing costs is a pipe section. The pipe section is a test part for the testing of pressure, leak tightness and tensile strength made of 316L. It is not an end product for SLM but it can be seen as a test specimen for further investigation of possible hydraulic applications for SLM. The reason why it has been chosen for this study is because of its advanced height ( $h = 100 \text{ mm}$ ). Furthermore, the small dimensions in x and y direction allow a great number of pipe sections to be manufactured at the same time. Figure 3.11 shows a fully utilized build platform with 117 pipe sections.

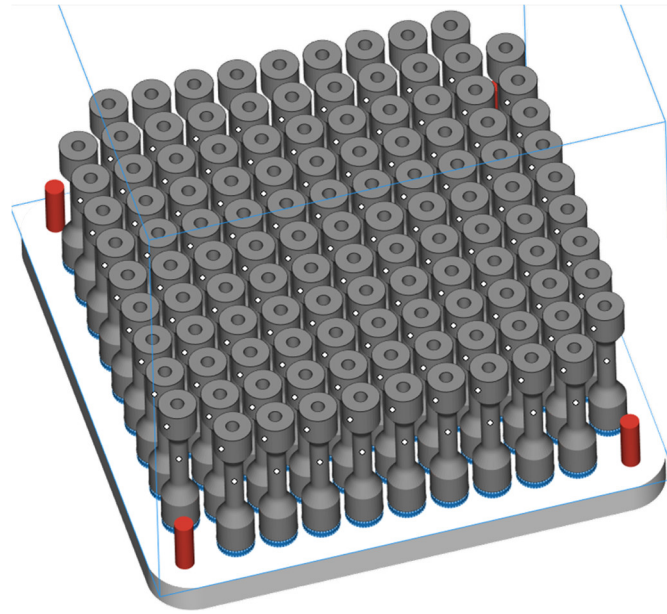


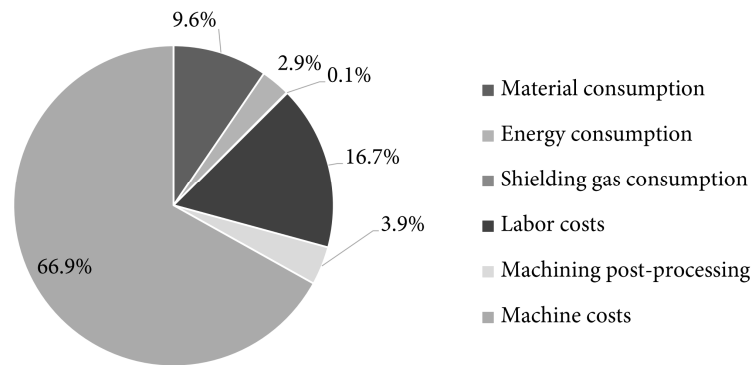
**Figure 3.11:** Overview of the prepared pipe sections (117 parts) for SLM;  
Source: own representation.

The parameter configuration for the pipe section remained the same, as already described, for the jet engine bracket and the filter head. Table 3.9 shows an enormous increase in build time regarding a single build platform. The SLM process for 117 pipe sections using a layer thickness of 30  $\mu\text{m}$  would last more than ten consecutive days. Furthermore, the waiting time does influence the build time for each parameter configuration. The effect disappears just after reaching a lot size of 30 parts.

**Table 3.9:** Parameter configuration and simulated build times for the pipe section.

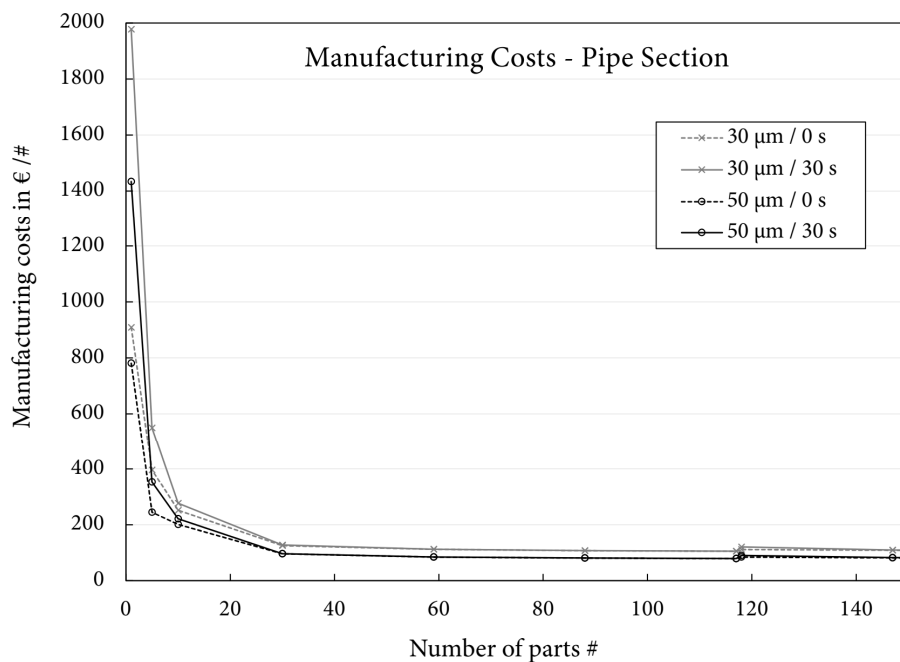
Configuration		Build time of the build job in hh:mm				
Layer thickness	Waiting time	Number of parts				
$l_z$ in $\mu\text{m}$	$t_w$ in s	1	30	59	88	117
30	0	8:48	70:45	133:08	194:41	256:41
30	30	35:19	72:13	133:08	194:41	256:41
50	0	5:37	49:09	92:58	136:19	180:00
50	30	21:49	49:19	92:58	136:19	180:00

Figure 3.12 shows the cost share of the manufacturing costs for a single pipe section ( $l_z = 50 \mu\text{m} / t_w = 0 \text{ s} / 117 \text{ parts}$ ). With a share of 2/3 of the manufacturing costs, the machine costs are dominating. Obviously, this is due to wide expansion in z-direction. Whereas post-processing is simple for this part.



**Figure 3.12:** Cost shares of manufacturing costs of one pipe section ( $l_z = 50 \mu\text{m} / t_w = 0\text{s} / 117$  parts);  
Source: own representation.

Concerning the pipe section, the decrease of manufacturing costs when using a full build platform is tremendous. Manufacturing costs of € 1977.80 (1 part) are reduced to € 107.59 (117 parts) for the configuration of  $l_z = 30 \mu\text{m} / t_w = 0\text{s}$  (see Table A 1, Appendix). This means a decrease of approx. 95 %. Furthermore, the manufacturing costs for a single pipe section differ widely for the different chosen parameter configurations.



**Figure 3.13:** Influence of different parameter configurations on the relationship between manufacturing costs and lot size for the pipe section;  
Source: own representation.



The manufacturing costs for the most efficient parameter configuration ( $l_z = 50 \mu\text{m} / t_w = 0 \text{ s}$ ) are only approx. 40 % of those with  $l_z = 30 \mu\text{m}$  and  $t_w = 0 \text{ s}$  for one part. This cost advantage decreases significantly with increasing number of parts. But for the pipe section, cost advantages for the parts with a layer thickness of  $50 \mu\text{m}$  remain prevalent, independent from the lot size.

#### 3.3.5 Micro Economies of Scale

There are controversial opinions on whether or not an economies of scale effect for SLM exists. Economies of scale (EoS) is the decrease of the average costs per unit (output) with increasing scale of output produced by a company.<sup>168</sup>

As a typical example for production, the high expenses for tools and molds for a special product of a company lead to high fixed costs. This leads to the typical relationship shown in Figure 2.5, right for conventional manufacturing. If these costs spread over a large quantity of output, an economic advantage be generated. However, EoS is typically related to mass production.<sup>169</sup> Thus, the question arises which for good reason is whether this effect is also achievable for AM – or SLM in particular. For Lipson and Kurman, EoS does not exist for AM.<sup>170</sup> For Piller et al., the missing economies of scale for AM can be a big advantage for AM. The reason for this is that AM allows the manufacturing to happen more closely to the customer. The independence from large production quantities lower the boundaries to start production and enables manufacturing products which are individualized and close to the customer's needs.<sup>171</sup> Baumers et al. (2016) clearly state, that EoS for AM exists. In their work, the authors investigated the influence of two metal-AM production systems (EBM and SLM) on the production costs. They showed, that process related EoS can be achieved by increasing machine throughput. Higher throughput can be reached by increasing the available build volume. As a result, the average costs per part can be reduced. Baumers et al. further highlight the importance of the development of machines with more capacities and new AM processes that can increase the productivity further.<sup>172</sup>

The findings from this chapters are in line with the findings of Baumers et al. (2016). The author of this thesis also postulates that economies of scale are achievable with SLM. The

---

<sup>168</sup> Cf. OECD (1993) pp. 39–40.

<sup>169</sup> Cf. Lipson/Kurman (2013) p. 26.

<sup>170</sup> Cf. Lipson/Kurman (2013) p. 27.

<sup>171</sup> Cf. Piller et al. (2015).

<sup>172</sup> Cf. Baumers et al. (2016).

reason for this is that the fixed costs (e.g. machine costs based on the hourly rate, labor, etc.) can be distributed across a larger number of parts. But in contrast to Baumers et al., EoS was noted for an existing SLM system with a given build chamber. There was no additional machine or equipment necessary to see the cost advantages. A fully utilized build platform leads to an increase of the throughput and a significant decrease of the average part costs. Compared to the common use of EoS for mass production, EoS, in this context, is used for a very narrow range of production: a single build platform of a single machine. Since this effect takes place – compared to the original use of EoS for mass production – on a very small scale, the author suggests the following term for it: “Micro-economies of scale” (m-EoS). Micro-economies of scale describe the achievement of cost benefits with an increasing utilization rate of SLM for a single build platform.

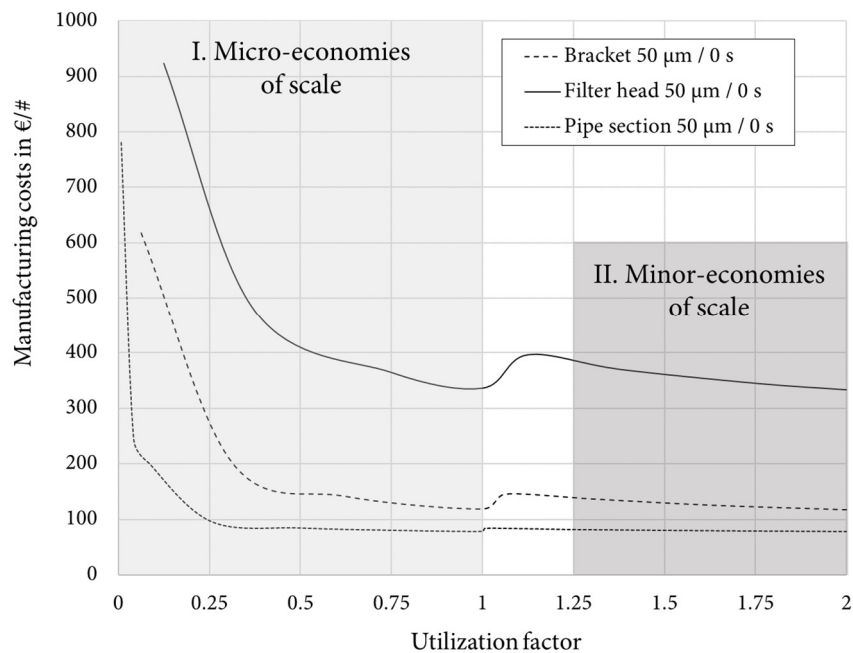


**Figure 3.14:** Cost comparison for three different parts and micro-economies of scale effect; Source: own representation.

Figure 3.14 shows the cost-utilization relationship of the three described SLM parts of this chapter. For all three parts, the same parameter set ( $l_z = 50 \mu\text{m}$  and  $t_w = 0 \text{ s}$ ) was used to enable data comparison. Related to this, a utilization factor ( $u_t$ ) is used. The utilization factor describes the relationship between the actual number of parts in total ( $n_{b,i}$ ) and the maximum possible parts of the same type on one build platform ( $n_{b,\text{max}}$ ).

$$u_t = \frac{n_{b,i}}{n_{b,max}} \quad (3.3)$$

If  $u_t$  is 1, the build platform is fully utilized. This is the point where the lowest costs per unit can be detected for the first build platform. To produce more parts of the same type, a new build job has to be set up. It should be noted that “fully utilized” refers to the build platform (x- and y- direction), not to the build chamber (including z-direction). The reason for this is that the stacking of parts in z-direction is very uncommon and unpracticable for SLM because of the necessary support structures.

For all three parts, m-EoS can be achieved (Figure 3.14). However, m-EoS is limited to the very first build platform. After the manufacturing costs have dropped significantly for the first build platform, a further decrease is only slightly present. In order to do that, the positive effect of m-EoS on the decrease of the manufacturing costs is much smaller or even neglectable (II: Minor-economies of scale). To further decrease the costs per unit for the existing system, the process has to be made more efficient. For instance, by decreasing the build time with advanced parameters (see chapter 4) or efficient post-processing (see chapter 5). Another option to achieve this would be using the positive effects of the learning curve as Baumers and Holweg<sup>173</sup> suggest. An expert user can also drop the costs per unit significantly, for instance due to less build failures, the economic use of support structures or less required setup time.

### 3.3.6 Discussion of the Cost Evaluation of Selected Build Jobs

Apart from the confirmation of EoS for SLM, other findings from this chapter are worth discussing.

#### 1. Utilize Your Build Platform

From a cost perspective, the manufacturing of a single part with SLM is highly inefficient. Fixed costs for labor, machine etc. are directly attributed to the part which makes them usually very expensive. A higher degree of utilization of the SLM platform is recommendable. Of course, this can also be reached through the fabrication of different parts (for different customers) at the same time. No matter easily EoS is achievable for SLM, one thing is certain:

---

<sup>173</sup> Baumers/Holweg (2019).

The often presented and cited complete independence of the manufacturing costs from the lot size is not given. The fabrication of a single part on the platform can be very expensive.

#### 2. Watch Your Parameters

As clearly shown for all three parts, SLM parameters influence the build time and therefore the manufacturing costs. If possible, the usage of an increased layer thickness is recommendable. It enables cost benefits independently from the lot size. Also, the influence of the waiting time should be emphasized. It can increase the build time significantly – most of all for a build job where the degree of utilization is small. As shown in this chapter, the amount of scanning time per layer determines if the set waiting time comes into effect. The waiting time is – at least in the expert mode – freely selectable by the operator for the used machine for SLM Solutions, which makes sense for research and development. From an economic and industrial perspective, it should be integrated and determined along with the SLM slicing process during pre-processing. The reason for this is – as the author hypothesizes – that there is optimal  $t_w$  depending on the actual layer based on factors such as heat transfer and manufacturing time.

#### 3. Know Your Cost Drivers

The cost structures of all three investigated parts differ from each other (Figure 3.15). General statements about the composition of costs for SLM can only be indicative. A study of the individual SLM part (and its lot size!) has to be conducted to determine its individual costs structure. However, findings from this chapter confirm that machine cost and labor are the dominating cost drivers for SLM. Although powder for SLM is much more expensive than raw material for conventional manufacturing of the same alloy, its impact on the overall costs should not be over-estimated as only a small proportion of the manufacturing costs can be attributed to the powder – especially for small and medium sized parts.

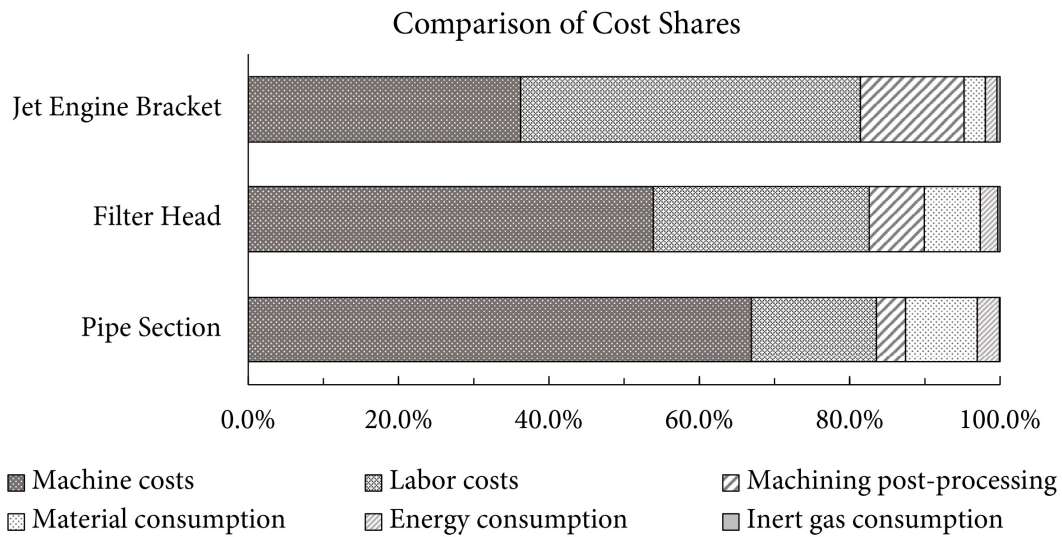


**Figure 3.15:** Comparison of cost shares of the three representative SLM parts of this chapter;  
Source: own representation.

Concerning the points above, an in-depth study of the positive influence of advanced parameters is presented in chapter 4. Furthermore, post-processing and its associated labor as important cost driver is discussed more closely in chapter 5, where a self-developed approach is also presented.

### 3.4 Screening, Selection and Transfer Model for SLM

As described in chapter 2, DfAM is seen as a key factor to make use of the unique possibilities that SLM offers. However, the mere realization of DfAM during the product development is not enough. First of all, an important issue has to be addressed for a successful product development for SLM:

#### Is it the right part for DfAM?

The decision whether the concerned part is principally suitable for DfAM or not, has to be made based on the task (redesign or new design). Since DfAM requires (financial) efforts for its realization (engineering, software etc.), it must be ensured, that only reasonable parts are processed and this decision should be made in a structured and quantifiable way. This ensures that the decision for or against a part is comprehensible within a company. In order to do that, a defined part screening process should be done at the beginning of a possible SLM (or AM in general) project. This approach is also listed in the extended scheme of Kumke (Figure 2.13) as step A. – part and application screening.

The question about the suitability of parts for further optimization is covered in two use cases that are based on projects at the IFT that the author was involved in. The two presented use cases had different initial situations. For use case 1, SLM has been considered and investigated as potential manufacturing technology for components of their innovative products. Whereas for use case 2, SLM has already been in use for several years within the company. The selection of the appropriate part for AM means also including economic considerations (Figure 2.13, step C). For this, cost estimations for potential SLM components accompanied the selection process and were elaborated for both use cases.

Both use cases help to answer one general question: How can SLM (or AM in general) be implemented successfully in a company?

#### **3.4.1 Use Case 1: Starting with SLM**

The following chapter focuses on the part selection process and the economic appraisal within this project and the findings from it. This project was carried out together with Stefan Karanovic, who used findings from the project for his master's thesis<sup>174</sup>.

##### **3.4.1.1 Initial Situation**

The presented use case is based on a project with a large-sized engineering company that is a global player in the automotive industry. The development of solutions for testing and simulation is one of their core businesses. AM has been considered as potential manufacturing technology for their measurement devices. The company did not own a SLM machine at the same time the project was carried out. The aim was to investigate the possibilities of AM – and SLM in specific – for the company and their products. Additionally, awareness for AM should be created.

##### **3.4.1.2 Project Realization**

From a superordinate perspective, the transfer of SLM as a manufacturing technology into the company was one of the main challenges. Until the start of the project, knowledge and experience with AM was mainly limited to the field of plastic processing for prototyping. From the very beginning, a structured and scientific approach was followed, as only comprehensible and fact-based results can lead to awareness and acceptance within the involved departments and beyond. Findings and learnings from this project are collected in

---

<sup>174</sup> Karanovic (2018).

the internal AM knowledge platform of the company. The platform serves as knowledge base for further developments and use cases. In this chapter, special focus will be put on the component selection for the SLM redesign. It should be noted that, similar to the use case 2 (chapter 3.4.2), only existing components were considered for the redesign.

The first step of the component selection was the definition of key criteria and the development of an assessment method. Four key criteria were identified:

- 1. Unique selling proposition (USP):** Does the use of AM lead to unique benefits that would not have been achievable with conventional manufacturing? This is closely related to DfAM-related features such as lightweight design, increased functionality, or part consolidation.
- 2. Cost-benefit:** This criterion states that it is necessary to compare the AM design with the conventional part from an economic perspective. Achievable advantages should be compared to the expected higher manufacturing costs. As feasible, a lifecycle cost (LCC) analysis should be performed.
- 3. Design of Experiment (DoE):** Experimental investigations on a scientific basis of the redesigned components should lead to quantifiable findings and results. These results should not only aim to qualify the related use case but also to extend the AM knowledge platform for further projects.
- 4. Manufacturability:** describes to what extent the targeted technical properties of the part can be achieved with AM.

The evaluation of the key criteria above is based on two factors. On the one hand, the optimization enabling factor (OEF) rates the key criteria for the possible AM component between 1 (very low potential) and 5 (high potential). On the other hand, the realizability of the key criteria is rated by the feasibility factor (FF), again between 1 (unlikely) and 5 (very likely). A rating of 0 for the OEF or the FF would lead to the immediate knock-out of the investigated part. The score for each of the four key criteria is determined by multiplying the OEF with the FF. At maximum, a total score of 100 can be achieved. An exemplary scheme of the assessment method for potential AM components is provided in Table 3.10.

**Table 3.10:** Scheme of the developed assessment method with exemplary rating.

Key criteria	Optimization enabling factor (OEF) (1-5)	Feasibility factor (FF) (1-5)	Score OEF x FF
USP	4	3	12
Cost-benefit	3	5	15
DoE	5	4	20
Manufacturability	4	3	12
<b>Total score:</b>			<b>59</b>

In addition to the described assessment method in this use case, another important question needs to be answered. Since relevant components for the optimization for AM are used in corrosive environment, their corrosion resistance has to be ensured. Therefore, primary studies on the corrosion resistance of considered SLM materials were conducted. For this, several test specimens were created to test the corrosion behavior of SLM manufactured 316L and AlSi10Mg with inductively coupled plasma optical emission spectroscopy and potentiodynamic polarization scan. After these tests had shown promising results for the corrosion behavior of both materials, the component selection was continued using the assessment method.

After the selection process, two promising components could be identified. One of these two components will be described more clearly as it shows the importance of a holistic approach on the AM design and cost considerations very well. The part – or more precise the assembly – is used as inlet-outlet manifold within an innovative measurement device. The initial design consists of 43 single parts (see Figure 3.16). The inlet-outlet manifold scored 72 points out of 100 in the assessment which is in the required top third of the ranking. A cost estimation was performed for rating the cost criteria. The approach will be explained briefly in the following paragraphs. For the estimation, a few assumptions were made: First, the volume of the future optimized manifold ( $V_{b,opt}$ ) was estimated with 30 % (including supports) of the initial volume of  $169 \text{ cm}^3$  due to the possible part consolidation and minimization:

$$V_{b,opt} = 169 \text{ cm}^3 \cdot 0.3 = 50.7 \text{ cm}^3 \quad (3.4)$$

Based on experimental data of past build jobs with the SLM 280HL at the IFT, the practical build-up rate  $\dot{V}_{Pr}$  for 316L with a layer thickness of  $50 \mu\text{m}$  was determined with  $9.69 \text{ cm}^3/\text{h}$ . With that value, the build time of one optimized manifold was approximated:



$$t_{b,opt} = \frac{50.7}{9.69} = 5.23 \text{ h per component} \quad (3.5)$$

With an hourly machine rate of 80 €/h – based on findings from the IFT cost model and from the examined literature<sup>175, 176</sup> – the costs for the build process were calculated:

$$C_{BP} = 5.23 \cdot 80 = 418.40 \text{ €} \quad (3.6)$$

The processing costs are considered with 70 % of the total costs<sup>177</sup>, which leads to total manufacturing costs ( $C_{Manf}$ ) of:

$$C_{Manf} = \frac{418.40}{0.7} = 597.71 \text{ €} \quad (3.7)$$

Of course, this is only a rough but also quick cost estimation. It should give an idea of the cost range of the potential component. Compared to manufacturing costs of the initial design (415 €), the estimated costs are higher. However, additional expected benefits for the future optimized SLM part, such as part consolidation, were not taken into account at this stage of the selection. These benefits can only be reasonably quantified when the final AM design is elaborated. Additionally, the build-up rate was chosen conservatively to account for the uncertain amount of necessary support structures. The estimated costs of approx. 600 € encouraged to proceed with the redesign of the inlet-outlet manifold as a potential use case.

A function driven approach is a key point for AM design.<sup>178</sup> Production driven aspects – such as manufacturability – do not have to be prioritized in the design phase for AM. A clear focus should be put on fully understanding the required functions and the interaction of the component with its surrounding. This perspective can lead to the often cited DfAM approach of part consolidation.<sup>179, 180</sup> At best, part consolidation enables both of the following aspects: integration of parts and integration of functions into an optimized AM component. After the redesign, a validation with finite element analysis (FEA) was performed to ensure stability and mechanical strength.

---

<sup>175</sup> Cf. Rickenbacher et al. (2013) p. 213.

<sup>176</sup> Cf. Barclift et al. (2016) p. 2021.

<sup>177</sup> Cf. Lindemann et al. (2012) p. 187.

<sup>178</sup> Cf. Klahn et al. (2018) pp. 118–128.

<sup>179</sup> Schmelzle et al. (2015).

<sup>180</sup> Kim/Moon (2020).

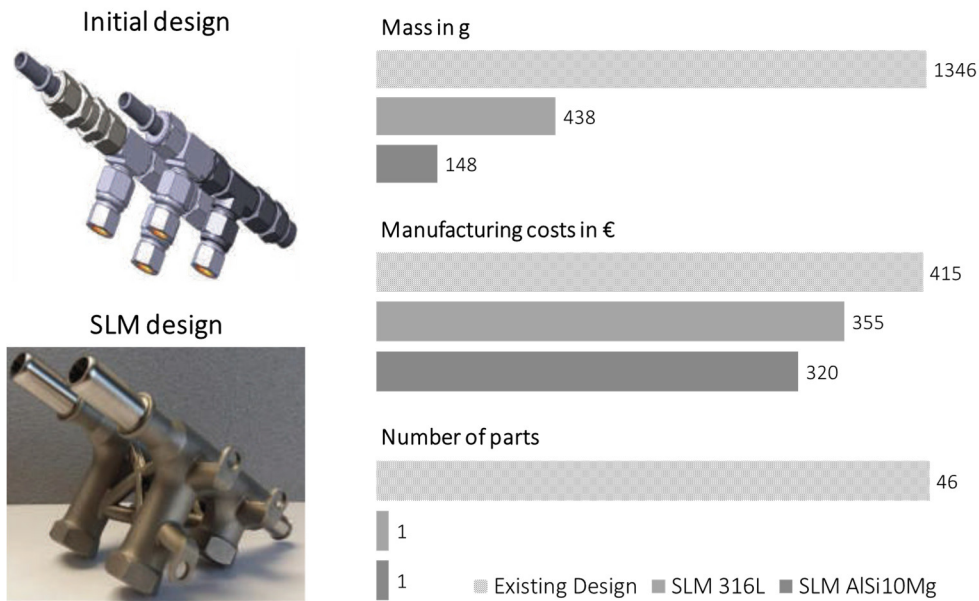


**Figure 3.16:** Comparison of the initial design and the optimized SLM design. All values in the graph are related to one component;  
 Source: own representation; modified from Karanovic (2018), p. 99.

Figure 3.16 shows the comparison between the initial inlet-outlet manifold and the redesign, manufactured with SLM. As stated above, two different materials (316L and AlSi10Mg) were chosen due to their good corrosion resistance in the primary studies. The redesigned component is much lighter (-89 % for AlSi10Mg, -67 % for 316L) than the Existing design. Part consolidation led to a reduction of the part number from 43 to only one part – by enabling all the necessary functions of the manifold. Additionally, a new function could be added to the design: The attachment points for the connection with the housing were integrated into the design.

Figure 3.16 also shows that the manufacturing costs are lower than those of the initial manifold. This means a cost advantage from the very beginning. The provided numbers of the manufacturing costs are based on an offer by an external company. Compared to the estimated costs (598 €) before, the offered prices are significantly lower (355 € for 316L, based on a lot size of 50 parts). It is expected that the reason for this is mainly based on the very rough estimation with a relatively low build-up rate compared to the external provider. The external provider uses a SLM 500 system with multiple laser systems where a significantly higher build-up rate can be expected.

From a cost perspective, the SLM optimized inlet-outlet manifold is very promising. This contrasts with the widely spread opinion that SLM has higher manufacturing costs than traditional manufacturing. Useful part consolidation and a beneficial small lot size (50 parts) lead to clear cost advantages compared to the initial design. Although the evaluation based on the manufacturing costs would already justify the use of SLM, lifecycle considerations were elaborated for further discussion. For this, possible benefits for the optimized SLM design were collected (Table 2.1). These benefits were classified according to their potential economic impact, whether they are direct monetary or indirect monetary benefits. Direct monetary means that the enabled benefits through AM can be clearly quantified in terms of money (e.g. fewer labor costs for assembling, reduced fuel consumption due to lightweight design etc.). Whereas the positive impact of indirect monetary benefits cannot be easily determined in a monetary way.

**Table 3.11:** Overview of direct monetary (DM) and indirect monetary (IDM) benefits for SLM inlet-outlet manifold.

Benefit	Effect	Description	DM	IDM
<b>Part consolidation (43 to 1)</b>	Less assembly time	- Reduced labor cost for assembling	x	
		- Less spare parts needed	x	
	Reduced risk of failure (leakage)	- Minimization of downtime	x	
		- Increased company reputation due to innovative use of AM		x
	Supply chain cost reduction	- Reduced handling costs	x	
	- Reduced transportation costs - Reduced supplier management costs	x x		
<b>Reduced mass</b>	Weight reduction from 1346 g to 148 g	- Competitive advantage		x
		- Lighter connecting components (e.g. housing) - positive influence on the measurement accuracy	x	x
<b>Miniaturized design</b>	Size reduction from 237 x 55 x 67 mm <sup>3</sup> to 127 x 70 x 57 mm <sup>3</sup>	- Contribution to the overall system miniaturization		x
		- Enabling a system redesign to gain competitive advantages		x
<b>Function driven design</b>	Manifold cost reduction from 415 € to 320 €	- Reduced manufacturing costs	x	
		- Reduced labor costs for assembling	x	
	Integration of housing mount	- Mounting structure cost reduction	x	
		- Less spare parts needed	x	
Stiffer coupling components	- Lighter supporting components (housing)	x		

Direct monetary benefits can be considered for lifecycle cost assessment. This assessment has not been part of this project in detail. However, an estimation of the positive cost impact was elaborated exemplarily. For this, the cost advantage of two positive effects of part consolidation were investigated:

- less assembly time
- supply chain cost reduction

First, less assembly time leads to reduced labor costs. Second, costs within the supply chain can be saved due to reduced handling (e.g. commissioning), transportation and management costs. A rough calculation that takes these considerations into account is provided in Table 3.12 and Table 3.13. Following assumptions were made:

Required manifolds per year:	100
Purchasing sequence:	2 times per year
Hourly rate for assembling (labor):	50 €/h
Supply chain cost per order:	40 €

**Table 3.12:** Estimation of assembly and supply chain costs for the initial manifold.

<b>Initial inlet-outlet manifold</b>		
Assembly time manifold	45 min	37.50 €/#
Number of suppliers for 43 parts	5	
Estimated supply chain costs for 50 manifolds	200 €	4.00 €/#
Manufacturing costs per manifold		415.00 €/#
<b>Total</b>		<b>465.50 €/#</b>

**Table 3.13:** Estimation of assembly and supply chain costs for the optimized SLM manifold.

<b>SLM inlet-outlet manifold (AlSi10Mg)</b>		
Assembly time manifold	15 min	12.50 €/#
Number of suppliers for 1 part	1	
Estimated supply chain costs for 50 manifolds	40 €	0.80 €/#
Manufacturing costs per manifold		320.00 €/#
<b>Total</b>		<b>333.30 €/#</b>

The estimation of additional costs for assembly and the supply chain shows that the increase of costs is more significant for the initial manifold (+50.50 €/#) than for the optimized SLM

manifold (+13.30 €/#). This supports the benefits of part consolidation in a quantifiable way and increases the cost advantage of the SLM manifold additionally.

As next step, a prototype of the optimized inlet-outlet manifold was manufactured with SLM (Figure 3.16). The manifold was tested and its functionality was investigated experimentally. The manifold showed good results in the conducted leak tightness tests in a climatic chamber (-20 °C to +80 °C). Furthermore, its dynamic behavior in the shaker experiments was satisfying.

In this project, two SLM prototypes were methodically developed – from the component selection and cost evaluation to the experimental testing. This chosen holistic approach was necessary to create awareness and fundamental knowledge of SLM within the company. Starting with this project, the company's SLM activities have been expanded since.

#### **3.4.2 Use Case 2: Experienced SLM Users**

The following chapter focuses on the part selection process and the strengthening of SLM inside the company during this project and the findings resulting from it. This project was carried out together with Christopher Michael Leitner, who used findings from the project for his master's thesis<sup>181</sup>.

##### **3.4.2.1 Initial Situation**

The first investigated use case comes from a project together with a Styrian company, which is globally known for producing innovative measurement devices. There is a big difference to the use case 1 from the previous chapter: The company had been using a SLM machine for 5 years when the project started. For Austrian conditions, they were One of the first companies to use SLM technology Even though there already was awareness of the capabilities and knowledge of the SLM technology among the company and its workers, the machine was not fully utilized for neither internal nor external projects. Also, the product range of the company was predestinated for SLM as highly complex components in small and medium quantities are used in their measurement devices.

---

<sup>181</sup> Leitner (2020).

### 3.4.2.2 Project Realization

The main goal was to find a way to increase the utilization of the SLM machine within the company. Two promising internal strategies have resulted from an economic analysis:

- 1) Create awareness for AM-design
- 2) Expand the AM-product portfolio

Based on both strategies, key factors for the successful use of SLM were defined. These key factors are: product portfolio, employees, product design and equipment. A methodical approach for the implementation of the strategy containing the key factors had to be found. The reason for this is that a methodical approach – in the sense of a guideline – delivers a structured procedure. To do that, the transfer model of Klahn et al. (2018) was extended and tailored to the company. Klahn et al. emphasize the role of the first pilot projects (called pilots) carried out with a new technology (the model is not only restricted to AM) inside a company. Unfortunately, the SLM pilot project in this company had been carried out a few years ago and was – as expected – not very successful. This led to additional skepticism toward SLM within the company and its employees.

#### **The Metal AM Transfer Model:**

However, the goal was to create awareness and to extend the present product portfolio of SLM parts. Therefore, the metal AM transfer model (m-AMTM) was created (Figure 3.17). The m-AMTM leads to internal SLM pilots in a comprehensible and structured way. In the end, not only potential and reasonable SLM parts should be created, but also the awareness for the technology should be increased.<sup>182</sup>

---

<sup>182</sup> Cf. Lindemann et al. (2015) pp. 216–217.

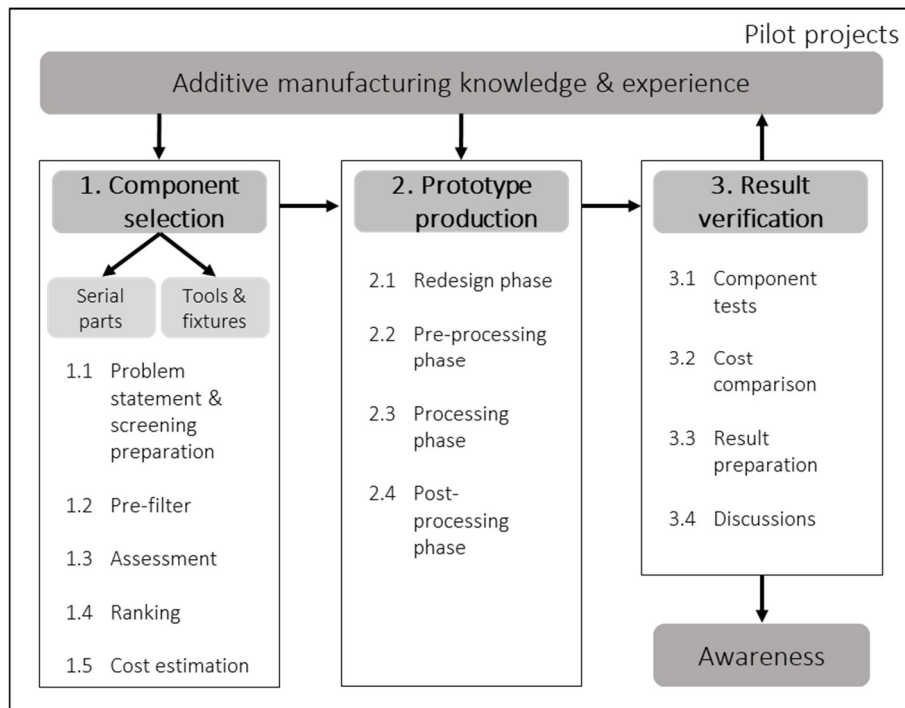


**Figure 3.17:** The metal-AM transfer model (m-AMTM) for use case 2;  
 Source: cf. Leitner (2020) p. 33.

The selection of components is the first important step of the m-AMTM. This can be compared with step A. Part and Application Selection of the model of Kumke (see Figure 2.13). Again, here the importance of the selection of suitable components as first step for further development towards fabrication with SLM should be emphasized. As already stated, this component selection should be reasonable and quantifiable in the best way possible. Within this project, a part screening model has been developed to select promising pilots (Figure 3.18). For this, the screening model of Lindemann et al.<sup>183</sup> has been modified and adjusted to the characteristics of the involved company.

<sup>183</sup> Lindemann et al. (2015).

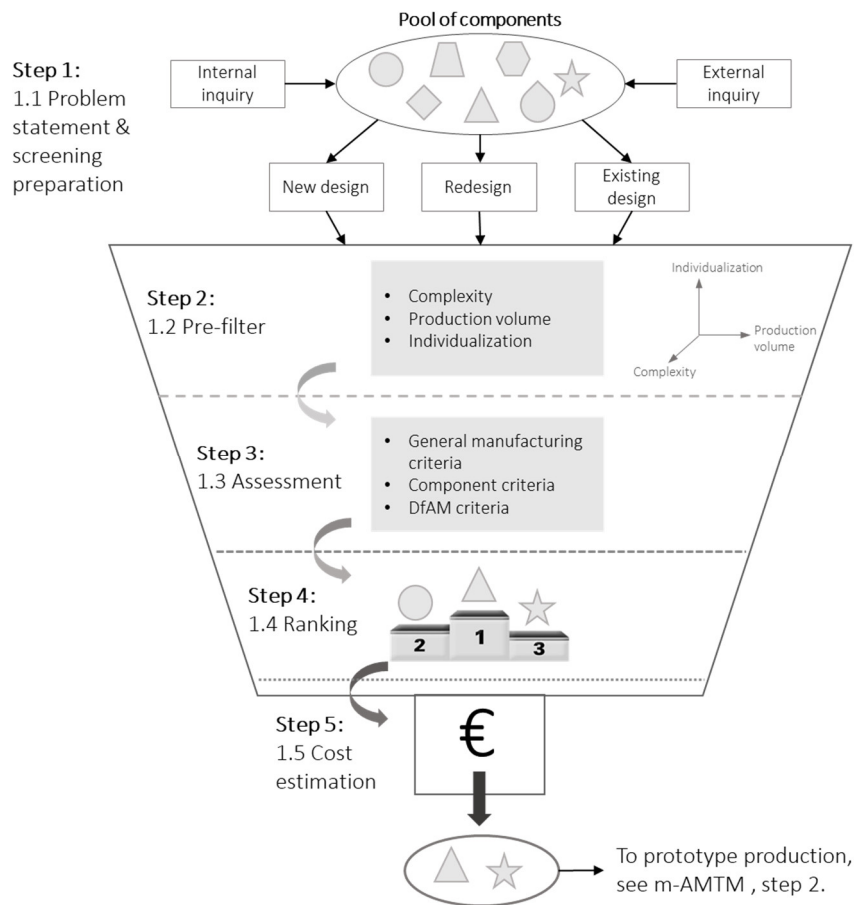


**Figure 3.18:** Screening process model (SPM) for suitable AM components;  
Source: own representation, cf. Leitner (2020).

The screening process model (SPM) allows a stage-to-stage selection of suitable components for AM. The SPM is not restricted to SLM – it can be adjusted to the considered AM process. Each investigated component starts at step 1. If a component does not fulfill the requirements of a single step of the SPM, it is no longer considered as pilot for AM fabrication. The single steps will be explained briefly in the following:

**ad 1.1 Problem statement & screening preparation**

Step 1 can be regarded as a preparation phase during the screening process. It consists of four major tasks:

- a) Collection of problem relevant information: This includes a basic requirement analysis. The order comes from an internal (company) or external (customer) demand. The main difference between these is the level of scope: Where external orders tend to be specific,



internal demands can be vague, like in the present use case (“higher utilization of SLM machine”).

b) Restriction of the search field: A broad problem statement from a) should be restricted in order to decrease the number of components to be examined. For the present use case, an ABC-analysis helped to identify products that contribute most to the annual turnover of the company.

c) Determination of filter criteria: To filter possible components, reasonable criteria had to be determined. The use of the model of Connor et al.<sup>184</sup> has proven its worth. It classifies products into eight different categories (e.g. mass customization) according to three aspects: production volume, part complexity and individualization. Resulting from this, the model shows whether or not the use of AM is expected to be beneficial.

Other filter criteria could be the available build chamber size or mandatory criteria regarding surface tolerances. The selection of criteria highly depends on the scope of the problem statement from a). For instance, criteria differ whether a new design or a redesign is considered. For this, the “hierarchy of problem statement”-approach was developed during this project. The hierarchy of problem statement can be seen in Figure A 1, Appendix.

d) Providing a checklist of criteria and definition of the assessment method: The developed filter criteria for the screening process should be reasonable for both, involved and non-involved personnel. For this, the selected criteria have to be documented and explained. The rating should be clearly described and objectified in the best possible way.

#### **ad 1.2 Pre-filter**

In step 2 of the SPM, a pre-filter is applied to the potential AM components. As useful pre-filter, the “Three Axis Model of Manufactured Products” from Connor et. al.<sup>185</sup> can be used to assess the potential AM components at this stage. As a possible outcome, a product can be withdrawn because it is a typical part for mass manufacturing according to the model.

#### **ad 1.3 Assessment**

In the third step, the remaining components are assessed and rated according to the defined criteria from step 1. This step is similar to the approach of Lindeman et al. (2015). To each

---

<sup>184</sup> Conner et al. (2014).

<sup>185</sup> Cf. Conner et al. (2014) p. 66.

criterion, between 1 (worst) and 5 (best) points can be assigned. A rating of 0 means that a mandatory criterion is not fulfilled. That leads to an immediate withdrawal of the investigated component from the selection process. Additionally, a weighting factor for the criteria is strongly recommended. This is also included in the assessment sheet. An example of the assessment of step 3 can be seen in Figure A 2, Appendix.

#### **ad 1.4 Ranking**

The assessment in step 3 leads to a final value for the investigated components. This value needs to be higher than a defined limit value. Otherwise, the component will not be considered for step 5 and will be withdrawn from the selection process. In this project, the limit value was set to 65 % of the maximum value possible.

#### **ad 1.5 Cost estimation**

The last step of the SPM is the cost estimation. The cost estimation should clarify whether the remaining components are economically reasonable. Since the ultimate part geometry is not determined in this phase for a new- or redesigned component, assumptions have to be made. Simplified calculations can be made based on the practical build-up rate  $\dot{V}_{PR}$ , as in use case 1 in the previous chapter. With surcharge factors for pre- and post-processing, a sufficient accurate estimation can be reached.

Once the last step is done, the SPM is completed. The technical and economic potential has been assessed and the potential components are moving on to the next stage of the m-AMTM, step 2: prototype production (Figure 3.17).

Without a doubt, the selection process of suitable components is essential for the successful use of AM. The process should fulfill two basic requirements:

- 1) **Comprehensibility:** The single steps should be equally understandable to AM experts and novices. The criteria have to be clear and transparent.
- 2) **Quantification:** A determination of suitable components has to be made based on quantifiable measures. Assessment and rating leads to a comparative that serves as a clear decision basis.

However, the selection of components is only one part – and the first step of the m-AMTM – when it comes to the use of AM in a company. The implementation of a new technology requires knowledge and a structured approach. Pilot projects help to create awareness and

to gain knowledge inside a company. This can be transferred to further internal and external AM projects. The presented use case shows the importance of a structured approach – like the presented m-AMTM or SPM. With the consequent use of the SPM, promising SLM components have been identified within the product portfolio of the company. Afterwards, those components were redesigned, fabricated and tested according to steps 2 and 3 of the m-AMTM (see Figure 3.17).

#### **3.4.3 Discussion of the Presented Use Cases**

Nevertheless, similar findings and recommendations can be concluded from both use cases:

##### **1. The Use of a Methodical Approach**

Especially the introduction phase of a new technology can become critical in a company. After a situation analysis (internal and external), a methodology should be developed.<sup>186</sup> The methodical approach has to consider the human factor as well. SLM offers great possibilities and can change – and also enhance – the present value chain of the company (see chapter 2.3). Employees are therefore required to get involved into the possibilities of the new technology – at best within successful SLM pilot projects that are embedded in an implementation methodology. The methodology ensures comprehensibility and the gaining of knowledge.

In use case 1, a special focus was put on the scientific validation of SLM as a possible manufacturing technology. Out of it, knowledge of SLM was gained which is broadly applicable and not limited to the chosen pilot projects. All of this knowledge about SLM is available at the internal AM knowledge platform that different departments have access to. In use case 2, the implementation methodology was more comprehensive than in the use case 1. A specific transfer model – the m-AMTM – was developed. The transfer model should ensure a “re-start” of the SLM technology for the company. It expands the already present AM knowledge in the company with a systematical approach. The use of systematical implementation methodologies as presented in this chapter or in models from related literature, such as the experience transfer model (ETM)<sup>187</sup>, are strongly recommended by the author.

---

<sup>186</sup> Cf. Klahn et al. (2018) p. 183.

<sup>187</sup> Leutenecker-Twelsiek et al. (2018).

## 2. The Importance of the First Projects

The importance of pilot projects following an implementation methodology – as Klahn et al.<sup>188</sup> suggest – can be confirmed by the author. Four main requirements regarding pilot projects can be identified:

- Moderate complexity
- Short project duration
- Involvement of employees
- Methodical approach

Findings from use case 2 indicate that all of these four points were not sufficiently considered when the SLM process was introduced in the company. This led to skepticism and to a lack of belief in the technology. This explains the unsatisfactory utilization of the machine.

In use case 1, attention was paid that the first pilot parts deliver – as called within the company- “quick wins”. That means that the two selected and optimized components were created and tested in relatively short time (approx. 3 months) with a manageable use of resources. Nevertheless, a methodical approach was followed that allows clear statements about benefits and limitations of SLM for the company.

## 3. Selection and Quantification

For use case 1, a simple scheme based on four key criteria was chosen. Nevertheless, the application of this scheme led to two very promising components for the pilot projects. For use case 2, the process of component selection was expanded. The selection process model (SPM) considers different initial situations and problem statements. Possible components undergo a defined process and are rated in the end. Findings from both use cases show that a methodical selection based on a quantifiable rating helps to identify promising components but also makes the selection comprehensible for the involved employees and departments.

Besides the technological benefits of SLM parts, costs can be regarded as the essential criterion for or against AM. Therefore, cost estimations were included into the selection process to assess potential parts in an early design stage from a cost perspective. In this context, SLM enabled benefits have to be taken into account for the economic appraisal beyond the manufacturing costs.

---

<sup>188</sup> Cf. Klahn et al. (2018) 183-189.

This chapter emphasizes the importance of a methodical component selection and the accompanying economic appraisal. Their applicability is not limited to pilot projects. Both should be seen as important amendments for the already well established DfAM techniques (Figure 2.13) and can also be used for advanced SLM product development.

### 3.5 Lifecycle Costs – Case Study

Even the most innovative SLM products can fail to success on the market, despite the reasonable use of DfAM. The reason for this is mainly based on economic decisions when the manufacturing costs or purchasing prices cannot compete with those of conventional manufacturing. For a better evaluation, the importance of lifecycle costs (LCC) has been stated in chapter 3.1.2. In this chapter, the use of LCC based on a case study from the literature is presented. This case study was created with Klemens Hochreiter during an internal project at the IFT<sup>189</sup>.

Atzeni and Salmi (2012) compared the costs of AM (SLM process) with CM (HPDC – high-pressure die-casting) within a case study of a part for aviation. They wanted to find out up to what production volume SLM remains competitive from a cost perspective. For this, they calculated the manufacturing costs (without pre-processing) for both manufacturing technologies for a scale model (1:5) of the main landing gear of a Piaggio P.180 Avanti II airplane.

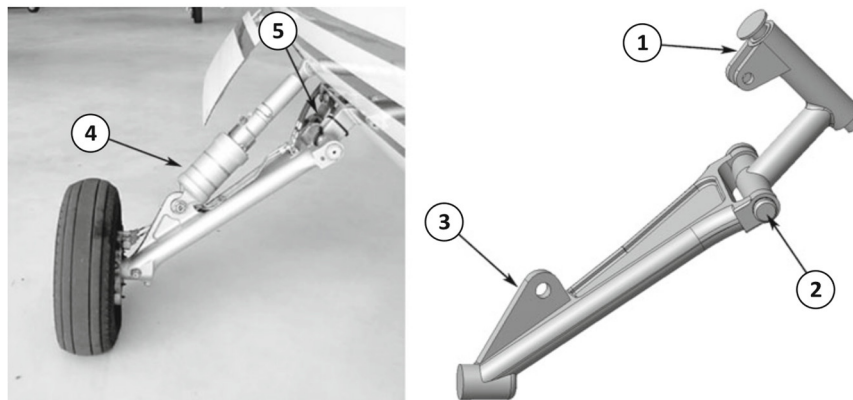


**Figure 3.19:** Main landing gear of the Piaggio P.180 Avanti II airplane;  
Source: Atzeni and Salmi (2012) p. 1151.

---

<sup>189</sup> Hochreiter (2018).

The authors redesigned the main landing gear according to DfAM principles. Due to several boundary conditions (e.g. coupling requirements), only the major support component (component 1) remained in the focus for the redesign. The authors achieved a more homogeneous stress distribution but did not reduce the weight – one of the actual main objectives in aviation for the use of AM. Furthermore, the cost calculation was finished with the determination of total costs. LCC, to quantify possible benefits, was not investigated in this study of Atzeni and Salmi.

#### 3.5.1 Redesign for SLM

Due to the mentioned limitations – the missing weight reduction and LCC – the study of Atzeni and Salmi (2012) was extended by the author of this thesis. For this, only the c was considered for the case study. The aim was to analyze the lifecycle and to compare the LCC for SLM and CM. Following assumptions were made:

- A scale of 1:2 was chosen to fit the SLM 280HL at the IFT
- low production volume of the airplane (236 units until 2018)<sup>190</sup>
- For CM, milling and welding was considered, material AlSi10Mg, five single components per part
- redesign with AM based on DfAM principles, material Scalmalloy® (Al-Mg-Sc-Zr-Alloy)

The redesign was done with Solid Edge ST8 and the FEA was performed with PTC Creo Simulate 3.0. In total, seven different design variants were created. In the end, design 8 was the most promising one for SLM. A comparison to the design for CM (design 1) can be seen in Figure 3.20.

---

<sup>190</sup> Kingsley-Jones (2018).

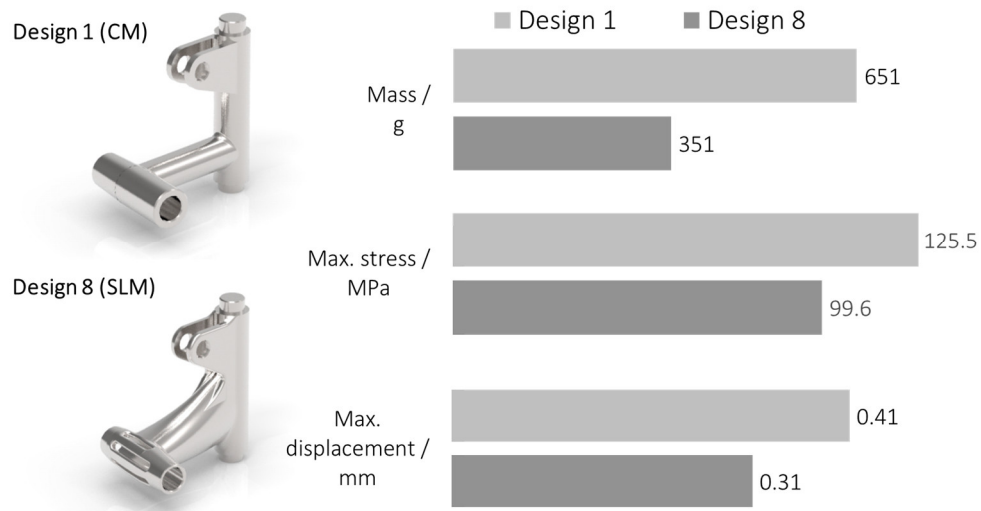


**Figure 3.20:** Comparison between design 1 (CM) and design 8 (SLM) for the major support component;  
Source: own representation, based on Hochreiter (2018).

The redesign resulted in a significant decrease of mass (-46 %). The maximum of the von Mises-stress was decreased (-21 %) as same was the maximum displacement (-24 %). Additionally, part consolidation of five parts with the design 1 (three rods, two hinges) to one single part was achieved.

### 3.5.2 Lifecycle Costs

As already stated in chapter 3.1.2, LCC extends the cost perspective beyond the total costs to the use phase of a part or product. For this case study, the reduced weight and the part consolidation are expected to lead to economic benefits during the use phase.

For LCC, defined procedures are available (<sup>191</sup>, among others). However, within this thesis, a simplified individual approach – similar to the majority of researchers in AM – is used. Also, Ehrlenspiel et al. noted the mainly individual approach when calculating the LCC.<sup>192</sup> In order to calculate the LCC for both designs, the process chain from design to the recycling of the main component was analyzed. The single steps for both designs and the caused costs – based on a single part – can be found in Figure A 3 and Figure A 4 in the Appendix.

<sup>191</sup> VDI 2884 (2005).

<sup>192</sup> Cf. Ehrlenspiel et al. (2007) p. 114.

For the conventional design 1, a practically feasible production process including engineering, purchasing, production and transport was chosen. Both, direct costs (e.g. for CNC turning and heat treatment) and indirect costs (e.g. storage and engineering) were considered and estimated to calculate the total costs. For the use phase, the installation (3 hours per part) and the maintenance were taken into account. According to safety regulations, the main landing gear has to be checked every 12 years or after every 6,000 take-off and landing cycles – whatever comes first. The technician has to check for cracks, abrasion and controls the weld seams. A use phase of 30 years or 35,000 take-off and landing cycles are expected for the airplane. Based on that, five obligatory maintenance activities were estimated. One maintenance activity was estimated with a duration of two hours.<sup>193</sup>

Compared to the conventional design 1, design 8 consists of a lightweight single SLM component. This leads to differences for the lifecycle of the major support component. In total, fewer steps have to be fulfilled for the production of the SLM component. However, the SLM build process increases the production costs significantly. Cost savings due to less time for purchasing or production engineering cannot outweigh the high SLM machine costs. Concerning the use phase of the SLM component, the same time for installation as for design 1 is estimated. Due to part consolidation and a more homogeneous stress distribution within the design 8, less effort for maintenance can be expected.<sup>194</sup> For this, 15,000 take-offs and landings or every 15 years, professional service has to be conducted. This leads to only two service activities for the SLM component. Without weld seams, the maintenance activity is expected to take less time (1.5 hours).

The major difference between design 1 and 8 in the use phase results from cost savings due to less fuel consumption for the lighter SLM design 8. The fuel savings were calculated with the modified Breguet Range Equation. According to it, fuel savings per flight of 0.107 l were calculated. This appears to be very little. But over a lifespan of 35,000 cycles or 30 years, this results in cost savings of 1,862 € (two major support components per airplane, kerosene price 1.88 € /gallon). This calculation is based on the investigated scale model. With a 1:1 scale, weight savings of 2.4 kg can be achieved per component for the SLM design 8. This would lead to calculated cost savings of 14,887 € over the lifespan of an airplane.

---

<sup>193</sup> RUAG Group (2020).

<sup>194</sup> Cf. Ameri et al. (2019) p. 541.



To calculate the LCC from the aspects mentioned above, the net present value (NPV) method<sup>195</sup> was used. This method compares the monetary impact of different design considerations over the lifecycle. For this, the NPV method assesses not only the initial investment but also the future earnings and costs of an investment. This leads to a comprehensible approach to compare and evaluate different investments or design considerations. The NPV can be calculated as follows:

$$NPV = K_0 + \sum_{t=1}^n \frac{K_t}{(1+r)^t} \quad (3.8)$$

Where  $K_0$  is the initial investment (e.g. total costs or purchasing price),  $K_t$  is the net cash inflow-outflow during a period  $t$ , and  $r$  is the discount rate to consider earnings out of an alternative investment. The calculation of the NPV for design 1 and 8, is summarized in the following table:

**Table 3.14:** Summarized calculation of the NPV for design 1 and design 8

	<b>Design 1</b>	<b>Design 8</b>
Initial costs (production and installation) $K_0$	-895 €	-1,660 €
Maintenance costs per service	-170 €	-128 €
Fuel savings p.a.	---	31 €
Discount rate	4 %	4 %
<b>NPV</b>	<b>-1,366.47 €</b>	<b>-1,246.41 €</b>

For the calculation of the NPV, costs and savings were considered. Per definition, costs have a negative sign in the calculation. Thus, a higher NPV can be seen as advantageous. Table 3.14 shows a marginally higher NPV for design 8, despite the significantly higher initial costs due to the expensive SLM process. This indicates – if only slightly – the beneficial use of design 8 over the lifespan from an economic perspective. A decision exclusively based on the initial costs would have been misleading. It is noteworthy that the calculations above are based on 1:2 scale model. For the original size – which would be manufacturable with a large SLM machine (e.g. SLM500) – the NPV would be even more beneficial.

<sup>195</sup> Cf. Klahn et al. (2018) pp. 69–70.

### 3.5.3 Lifecycle Costs within the VDI 2225-3

For this case study, a further well-established instrument for cost-benefit analysis was investigated. The VDI 2225<sup>196</sup> describes a procedure to compare alternatives (products, designs etc.) from an economical and technical perspective. The procedure is used during the development process to evaluate different proposed solutions. The technical rating is based on a five-part scale. A feature can be rated between unsatisfying (0 points) to very good (4 points). Compared to the ideal design (4 points for every technical criterion), the technical value (x-axes) can be determined. For the economic value, the VDI 2225 suggests considering the minimal purchasing price at the market to calculate the manufacturing costs. Since the CM design 1 would have clearly the lowest purchasing price, it was set as the reference in this use case to calculate the economic value (y-axis). The idea behind the method is that a lower economic value for one solution can be compensated with a high technical value and vice versa.

The calculation of the economic value is based on the manufacturing costs. As a result, LCC is not considered within the VDI 2225. Therefore, the influence of the LCC on the VDI 2225 method is studied. The results can be seen in Figure 3.21. The dash dotted line is called the development line. Along this line, the same technical and economic value is given. The calculation of the technical and economic value is provided in the Table A 4 and Table A 5 in the Appendix.

---

<sup>196</sup> VDI 2225 Part 3:1998-11 (1998).

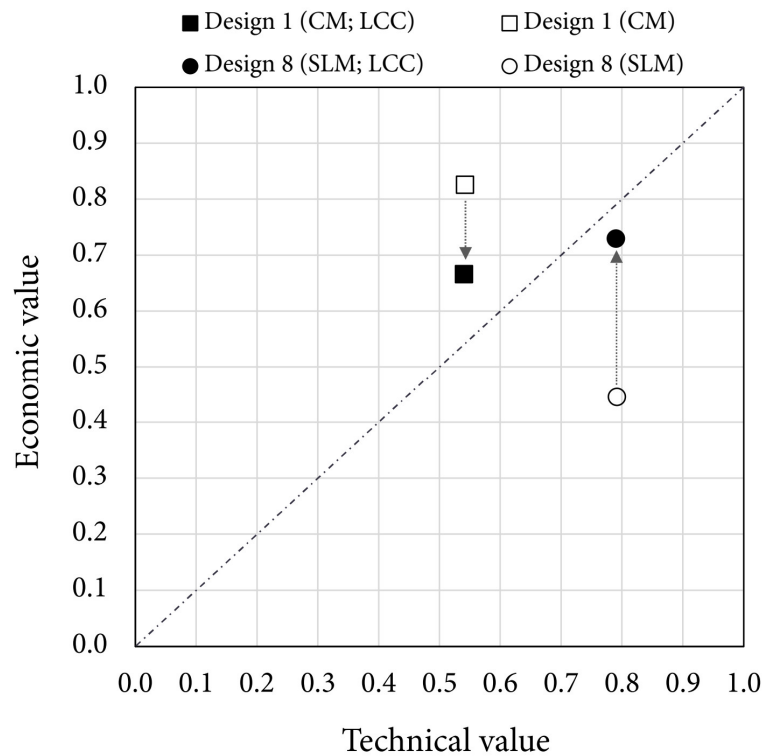


**Figure 3.21:** Evaluation according to VDI 2225 for design 1 and design 8. The direction of the dotted arrow marks the impact of the LCC;  
Source: Own representation, based on VDI 2225.

With the consideration of LCC, the evaluation for design 1 and design 8 significantly changes because of the new resulting economic value. According to the method of VDI 2225, design 8 is clearly preferable as it is closer to the ideal solution (economic and technical value of 1). Without the LCC consideration in this method, the use of SLM would have been more questionable.

### 3.5.4 Discussion of the LCC Case Study

This case study was elaborated to calculate and compare the LCC of an aviation part manufactured with SLM and CM. The positive impact of SLM enabled benefits on the LCC was shown. For this, the calculation of the NPV was carried out. Less fuel consumption due to the lightweight design and cost savings for maintenance led to a lower NPV for the SLM. The author strongly recommends the calculation of the LCC to quantify benefits enabled through AM. Although the VDI 2225 was developed for the evaluation of possible solutions for CM, the use for AM can be advantageous too. To include the LCC into the economic evaluation of the VDI 2225 can help to better estimate the potential of AM.

Both, the LCC and the VDI 2225 can be used to quantify the benefits of AM and – along with this – to quantify the often-used term of added value. Again, a systematical and compressible approach – based on figures – helps to settle holistic considerations.

## 3.6 Summary of Chapter 3

In this chapter, SLM was investigated from an economic perspective. The main findings can be summarized as follows:

**Cost modeling:** The importance of knowledge about costs was stated in chapter 3.1. Although cost models for AM have evolved over the past years, there is no generally valid and applicable cost model present in the examined literature. Therefore, cost models have to be adapted and tailored to the own requirements. A comprehensive but also flexible model based on the SLM process chain (including also pre- and post-processing) is highly recommended.

**Platform utilization:** With the IFT cost model (see chapter 3.2), build jobs of three selected parts were investigated in chapter 3.3. First, machine costs could be identified as the main cost driver for SLM. Second, the positive influence of increasing lot size on the manufacturing costs were found. A fully utilized build platform decreases the manufacturing costs per part significantly because indirect costs can be distributed across a higher number of parts. However, this effect nearly disappears after the first build platform.

**Component selection:** In chapter 3.4, the selection process of SLM components was presented based on two use cases. The author emphasizes the importance of a quantifiable method for selection – as the developed selection process model (SPM) in use case 2 (chapter 3.4.2). It identifies promising parts and qualifies them from a technical and economic view and makes the decisions understandable. Since the final part is not determined in this stage, an estimation based on the simplified assumptions is permissible. A possible approach was presented in use case 1 (chapter 3.4.1).

**Lifecycle costing:** Chapter 3.5 showed the effect of LCC on SLM. Despite the higher purchasing costs, the SLM manufactured part revealed an economic advantage compared to the conventional manufactured part, based on the NPV. The author emphasizes the importance of lifecycle considerations for SLM for both – internal (e.g. company, or department) and external (e.g. customer or market). However, these considerations have to

be put in an industrial context where an evaluation based on the purchasing – or manufacturing price is still the norm.

## 4 PARAMETER OPTIMIZATION FOR SLM – “316L ECONOMY”

Findings from chapter 3 show that machine costs are the main cost driver for SLM. The chosen approach in this chapter aims to increase the productivity without additional machine investment. The development and experimental investigation of advanced parameters for 316L stainless steel – internally called “316L economy” will be described in in this chapter. The basic idea as well as preliminary studies are described in chapter 4.1 and 4.2. The goal was to reduce the built time and still keep the relative density in adequate high ranges. This leads to a decrease of machine costs for processing. Thus, a second positive effect of 316L economy has surfaced: the performance of the downskin surface and its corresponding downskin angle was improved significantly. The corresponding experiments and results are described in chapter 4.3. Chapter 4.4 evaluates the findings with regard to their economic impact and chapter 4.5 provides a brief summary of the entire chapter.

### 4.1 Effect of Parameter Settings on the Productivity

The influence of SLM parameter on the productivity of 316L is described relatively rarely in the literature. Metelkova et al. (2018) investigated the influence of laser defocusing of 316L on the productivity of SLM. A defocused laser increases the spot size of the laser beam which further increases the build-up rate. A defocused laser has to be compensated with a higher laser power to achieve a stable melt pool. The authors found a significant increase in productivity by a factor of 8 for  $P_L = 800$  W compared to a conservatively build-up rate of  $7.2 \text{ cm}^3/\text{h}$ . As a drawback, the authors describe a decreased precision due to the bigger spot size. For this, the authors suggest a hull (small laser spot for precision) and core (large spot for speed) strategy. Despite their promising results in terms of productivity, the authors outlined difficulties with the microstructure due to the different cooling rates of hull and core. Furthermore, the authors did not investigate the relative density as an important criterion for their defocused strategies.<sup>197</sup>

Kamath et al. (2014) studied the influence of SLM parameters on the relative density of 316L. Results show that high relative densities (>99 %) can be reached for high scanning speeds up to 1900 mm/s. To prevent lack of fusion, the authors used a laser power of up to 400 W. The

---

<sup>197</sup> Metelkova et al. (2018).

authors used the Archimedes method and scanning electron microscopy (SEM) to evaluate the relative density. However, the increased scanning speed was not transformed into a higher build-up rate as a criterion for their studies. This makes possible statements about the increase of productivity rather difficult.<sup>198</sup>

Sun et al. (2016) stat that there is a direct relationship between laser power and the build-up rate for 316L. They increased the build-up rate by 72 % when using 380 W input laser power instead of 100 W. The relative density remained above 99 %, measured with Archimedes method and image analysis. The authors clearly showed that the productivity can be increased with advanced parameters. Nevertheless, the absolute value for the practical build-up rate was rather small (3.6 cm<sup>3</sup>/h). Still, their study is an important contribution to this topic.

This thesis expands the present knowledge about the positive impact of 316L parameters on the productivity of SLM. Referring to Figure 2.10, productivity is the ratio of a quantifiable output to resources needed (input). The presented approach – hereafter called as introduced 316L economy – decreases the resource input in two ways:

- 1) decrease of build time through higher build-up rates
- 2) minimization of the necessary support structures

Advanced parameters can increase the build-up rate and as a result decrease the build time. The build time is directly related to the machine costs. Therefore, a decrease in time means a decrease in costs and an increase in productivity – assuming the output remains at least the same. For evaluation of the output, the relative density of the fabricated samples was taken into account. Only if the relative density is comparable to the initial state, the advanced parameters can be called “more productive”. By minimization of the support structures 2), three positive effects on the productivity are expected by the author. Minimal use of support structures means:

- I) Less waste: Support structures are scrap. The use of powder for support structures and their disposal cause additional costs during manufacturing.
- II) Decrease of build time: The fabrication of support structures needs time. The use of fewer support structures reduces the build time and furthermore decreases the machine costs.

---

<sup>198</sup> Kamath et al. (2014).

III) Fewer effort for removal: Support structures have to be removed during post-processing – a time consuming and labor-intensive task.

Especially the second possibility – the minimization of support structures – and its positive influence on the productivity has not been found reported on related literature yet. This thesis does not provide in-depth studies of the influence of parameters on the microstructural mechanism of 316L. For this, reference is made to comprehensible studies from relevant literature<sup>199, 200, 201, 202</sup>. The focus of this thesis is put on the economic impact of the presented parameter configurations.

## 4.2 Preliminary Studies

The first internal studies to minimize the amount of support structures for 316L were carried out for the THERMEC Conference in 2018<sup>203</sup>. During these studies, the positive influence on the downskin angle (also called inclination angle) of a novel pre-processing software – called Additive.Designer (AD) – was investigated.

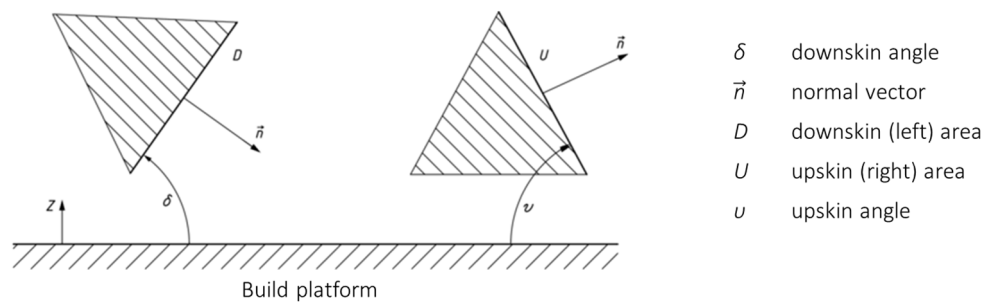


**Figure 4.1:** Designations of angles and surfaces related to AM;  
Source: cf. ISO/ASTM 52911-1:2019 (2019), p. 2 and cf. VDI 3405-3: 2005 p. 5.

The downskin angle  $\delta$  is defined as “angle between the plane of the build platform and the downskin area where the value lies between  $0^\circ$  (parallel to the build platform) and  $90^\circ$  (perpendicular to the build platform)”<sup>204</sup>. The VDI 3405<sup>205</sup> recommends a downskin angle larger than  $45^\circ$  without the need for support structures, depending on the AM process. If the

<sup>199</sup> Cherry et al. (2015).

<sup>200</sup> Liverani et al. (2017).

<sup>201</sup> Choo et al. (2019).

<sup>202</sup> Qiu et al. (2018).

<sup>203</sup> Pichler et al. (2018).

<sup>204</sup> ISO/ASTM 52911-1:2019 (2019).

<sup>205</sup> VDI 3405 Part 3:2015-12 (2015).



downskin angle drops below the value of  $45^\circ$ , the use of support structures is recommended, because the single layers of the SLM are not self-supporting for low angles. For this, support structures fulfill three major tasks<sup>206</sup>:

- 1) heat dissipation
- 2) fixation of the parts to build platform
- 3) absorption of distortion (warping) due to residual stresses

If the downskin angle is too low, the melt pool in the area of the downskin becomes instable. The reason for this is mainly due to too low heat dissipation of the melting zone. Since the loose powder below the downskin acts as thermally insulating, there is excessive heat in the melting zone and a solidification of the surrounding powder of the downskin occurs (balling effect). As a result, the surface roughness of the downskin increases dramatically due to the adhered powder particles. If the downskin angle is further decreased, a sufficient solidification base of the previous layer is missing. As an outcome, the layer cannot connect properly to the previous layer and the build job will collapse. In order to prevent this, support structures are used. Furthermore, support structures act as a solidification base and allow the heat to securely dissipate.<sup>207</sup>

Nevertheless, the goal in terms of productivity is to minimize the necessary amount of support structures. For the studies for the THERMEC conference, the downskin angle was varied between  $30^\circ$  to  $90^\circ$  for cuboid samples. Only standard parameters – provided by the machine manufacturer – were used. Results show the positive influence of the use of the AD on the downskin – compared to the used standard software Materialise Magics (MM). In fact, samples prepared with the AD show lower possible downskin angles of approx.  $35^\circ$  to  $40^\circ$  compared to the approx.  $50^\circ$  of MM (see Figure 4.2). Furthermore – as indicated by the annealing colors – the heat impact was lower for the AD samples. Also, the surface roughness (Ra, Rz, Rq, Sa, Sz and Sq) was lowered by the use of the AD. Additionally, positive effects of a decreased laser power in the second stage of the experiments were observed for both – AD and MM.

---

<sup>206</sup> Cf. VDI 3405 Part 3:2015-12 (2015) pp. 22–23.

<sup>207</sup> Skalon et al. (2020).

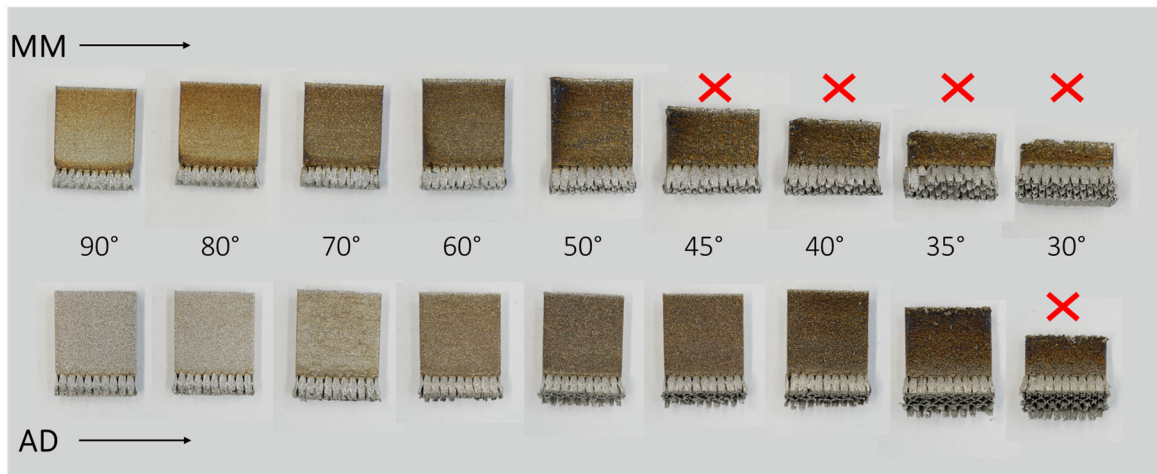


**Figure 4.2:** Comparison of downskin areas for different downskin angles, prepared with AD (above) and MM (below). A red cross marks aborted build jobs;  
Source: modified from R. Pichler et al. (2018).

Out of these first results, a special test specimen was developed to investigate the downskin angle and the surface roughness. Due to its shape and appearance, this test specimen is also called “trombone” internally. The trombone has a varying downskin angle between 15.8° to 78.6°. Furthermore, the trombone allows statements about up- and downskin. The trombone was used for all further investigations of 316L economy that will be described in the following chapters.

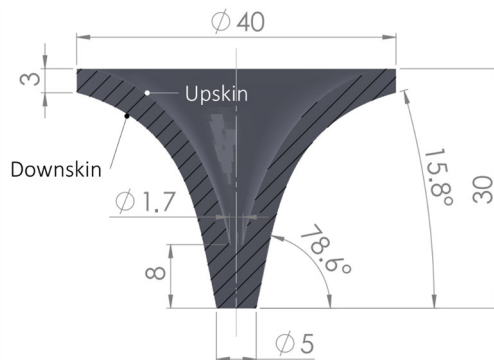


**Figure 4.3:** Trombone specimen;  
Source: own representation.

Within this preliminary study, the successful decrease of the downskin angle to reduce the amount of support structures was shown. The use of the AD as a preparation software decreased the possible downskin angle to 35° when using the default settings for 316L ( $l_z = 50 \mu\text{m}$ ). The reason for this is an alternative scanning strategy in the area of the

downskin (called “retraction”). This strategy will not be described further due to confidential agreements with the inventing company that invented the AD. Also, the use of a decreased laser power of 75 % compared to the standard parameters showed good results for especially low inclination angles. Based on these promising first results, the investigations on 316L economy were deepened.

### 4.3 Studies on 316L Economy

The following chapter describes the development of parameter configurations (PC) for 316L economy. First, the basic methodology is described. After that, the two consecutive test series and their results are presented. Their economic impact is evaluated in the next chapter 4.4.

#### 4.3.1 Methodology

All following experiments were conducted with the SLM 280HL machine from SLM Solutions Group AG at the IFT. The machine operates with a 400 W single-mode continuous wave (CW) Ytterbium fiber laser. As already mentioned, 316L stainless steel powder was used. Since the experiments were conducted over two years, multiple batches of 316L (equal to 1.4404) powder were used. However, an emphasis was put on the chemical composition and on the particle size distribution remaining in similar ranges for the different batches. Along with this, the powder was sieved and recycled multiple times. Findings from the literature indicate that 316L powder is unproblematic for multiple use over a longer period of time from a quality perspective.<sup>208, 209</sup> As for the powder, Oerlikon MetcoAdd 316L-A with a nominal range of  $-45+15 \mu\text{m}$ ,  $D_{50} = 30 \mu\text{m}$  and  $D_{90} = 46 \mu\text{m}$  was used (Figure 4.4). The chemical composition and a comparison with nominal values according to ASTM A276 can be found in Table 4.1.

**Table 4.1:** Chemical composition in weight-% of the used 316L powder.

Lot	C	Cr	Mn	Mo	Ni	Si	Fe
472242	0.01	17.66	0.38	2.34	12.78	0.40	Bal.
482622	0.02	17.76	0.79	2.28	12.62	0.69	Bal.
490578	0.02	17.54	1.36	2.37	12.78	0.64	Bal.
Nominal <sup>210</sup>	≤0.03	16.00-18.00	≤2.00	2.00-2.50	10.00-14.00	≤0.75	Bal.

<sup>208</sup> J. Hajnys et al. (2020).

<sup>209</sup> Whittaker (2017).

<sup>210</sup> Deutsche Edelstahlwerke Specialty Steel GmbH & Co. KG (2016).

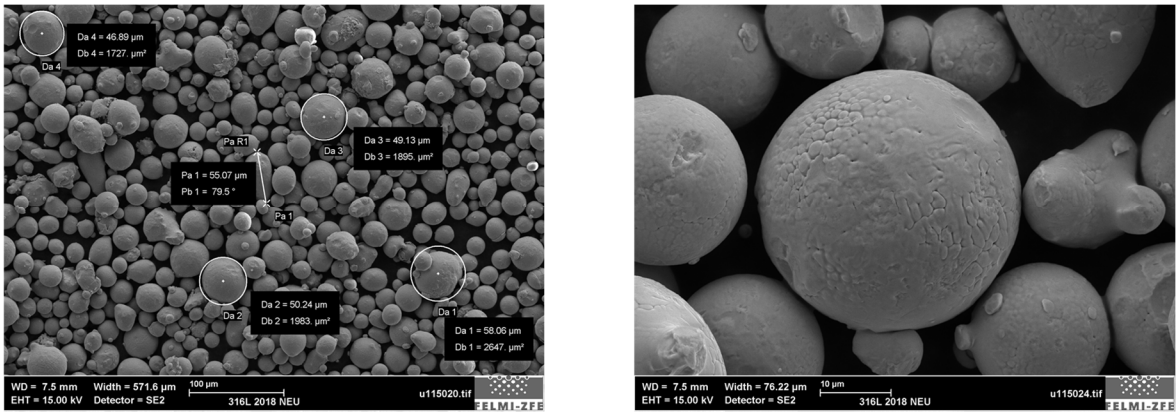


**Figure 4.4:** SEM images of new 316L powder used for 316L economy;  
Source: own representation, with special thanks to FELMI Graz.

Technically pure Argon (Ar) was used as shielding gas. For the build job preparation, again Additive.Designer (vers. 0.0.7b) was used. Materialise Magics (vers. 21) was also used, but for comparison purposes only. If not explicitly mentioned, AD was used for the experiments in chapter 4. A layer thickness  $l_z = 50 \mu\text{m}$  was used throughout the experiments. As stated in chapter 4.1, the aim of 316L economy is to increase the productivity by faster build-up rates and by minimization of the support structures. Both approaches were developed simultaneously and were steadily improved. For a better understanding, the methodical procedure is chronologically described with its different stages. To address both approaches, the experimental work was divided into two test series – test series 1 and 2.

### 4.3.2 Test Series 1 – Improvement of the Downskin Angle

Parameter studies on 316L date back to the time when the SLM280HL machine was first put into operation at the IFT in 2016. Since then, parameter variations based on the default parameters provided by the manufacturer were carried out. The decisive factor for this was the high energy input during the scanning process during the first build jobs where a downskin angle of  $45^\circ$  was impossible to realize. By increasing the scanning speed to 133 % compared to the standard parameters for 316L, an improvement of the downskin angle to approx.  $40^\circ$  was achieved. These first findings were slightly incorporated into the investigations for THERMEC (see chapter 4.2).

#### 4.3.2.1 Methodology and Parameter Configuration for Test Series 1

As a next step, the potential of advanced parameter settings to improve the downskin angle was further investigated. For this, the trombone test specimen (Figure 4.3) was chosen.

Additionally, promising findings from the literature influenced the selection of parameters. Cloots et al. (2017) investigated the positive influence of scanning strategy and process parameters on the overhanging surfaces for two different SLM machines. The authors were able to produce cuboid samples with a downskin angle of  $20^\circ$  with one of their machines. According to the authors, scanning tracks parallel to the downskin surface were exceptionally promising (see Figure 4.5). The authors contribute these findings to the decreased risk of excessive high thermal input. Additionally, the most promising parameter configuration (PC) did neither include a border nor a filling contour (cf. Figure 2.11). This means that hatching was done with standard lines, without rotating from layer to layer and with a volumetric energy density of  $E_V = 52 \text{ J/mm}^3$ .

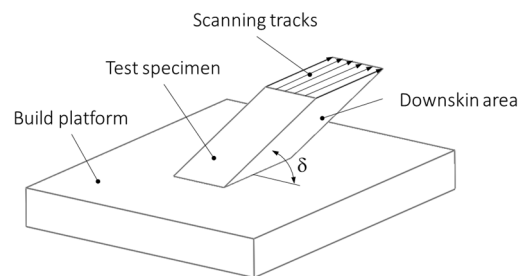


**Figure 4.5:** Scanning tracks parallel to the downskin surface;  
Source: own representation, cf. Cloots et al. (2017) p.363.

However, the study of Cloots et. al. has its limitations. Firstly, for the most promising parameter configuration ( $\delta = 20^\circ$ ,  $R_a = 19 \mu\text{m}$ ), a relative density of only 95.1 % was measured (via Archimedes method). Secondly, a ConceptLaser M2 machine with a relatively low laser power of 200 W was used. Thirdly, the positive impact of the minimization of support structures through smaller downskin angles was only mentioned<sup>211</sup>, but not examined quantitatively. In order to do that, existing findings from this study were extended by the author for 316L economy based on the following considerations.

- 1) The use of the 400 W laser of the SLM 280HL could:
  - a) increase the relative density for similar build-up rates compared to Cloots et al.,
  - b) increase the build-up-rate by using faster scanning speeds ( $>2000 \text{ mm/s}$ ),
  - c) increase both, a) the relative density and b) the build-up rate.

<sup>211</sup> Cf. Cloots et al. (2017) p. 363.

2) The use of trombone (Figure 4.3) as test specimen:

- a) equalizes the orientation (not the position) on the build platform due to its rotational symmetry,
- b) is more practicable because of the continuous variation of the downskin angle within a wide range (15.8° to 78.6°),
- c) allows an evaluation of the positive influence of the minimization of support structures on the productivity.

The first experiments (stage 1) were carried out to test findings of Cloots et al. at our SLM 280HL machine. For this, the SLM standard parameters – and slight deviations based on the THERMEC study – for 316L and  $l_z = 50 \mu\text{m}$  were taken. For each pre-processing software – AD and MM – one build job was carried out. Starting from parameter configuration 10, deviations were developed. In the following, the differences of AD/MM 11-13 to the standard parameter configuration AD/MM 10 are shortly explained and the chosen values can be seen in Table 4.2.

- AD/MM 11: is based on a different downskin strategy, but on same basic SLM parameters and energy density. For AD, the special strategy „retraction“ was enabled and in MM, ten reference layers were taken into account for the downskin strategy.
- AD/MM 12: Due to good experiences in the THERMEC experiments,  $P_L$  was decreased to 207 W to achieve an  $E_V$  of 75 % of the standard value from AD/MM 10.
- AD/MM 13: The scanning speed  $v_s$  was increased to 931 mm/s to achieve an  $E_V$  of 75 % of the standard value from AD/MM 10. This furthermore results in a faster build-up rate compared to AD/MM 10-12 due to the faster  $v_s$ .

Also, the parameter set 9 of Cloots et al. was considered for further investigations. The authors used  $l_z = 30 \mu\text{m}$ . This requires an adaption for  $l_z = 50 \mu\text{m}$ . Since good results for low downskin angles were achieved for THERMEC with lower energy densities,  $E_V$  was set with 75 % of the proposed value from Cloots et al. This results in an intentionally low value of  $E_v = 40 \text{ J/mm}^3$  that was also set as the bottom value for all further experiments (parameter AD/MM 14, Table 4.2).

**Table 4.2:** Overview of parameter configurations for test series 1.

Parameter	PL in W			vs in mm/s			h <sub>s</sub> in μm	Ev in J/mm <sup>3</sup>		
	H	F	B	H	F	B		H	F	B
AD/MM 10	275	150	100	700	400	300	120	65	63	56
AD/MM 11	275	150	100	700	400	300	120	65	63	56
AD/MM 12	207	113	75	700	400	300	120	49	47	42
AD/MM 13	275	150	100	931	532	399	120	49	47	42
AD/MM 14	260	-	-	2000	-	-	65	40	-	-

Contour types: *H* hatching; *F* filling; *B* border

#### 4.3.2.2 Results from Test Series 1

It was not possible to complete the trombone specimens for the standard PC and its deviations. AD 10-13 and MM 10-13 showed excessive warping, which led to the termination of the affected trombones within the build job (Figure 4.6). The annealing colors further show the high thermal load during processing, whereas the trombone built with the PC AD/MM 14 was completed without any problems. Also, the annealing color suggests that the heat impact was less harmful than for AD/MM 10-13.

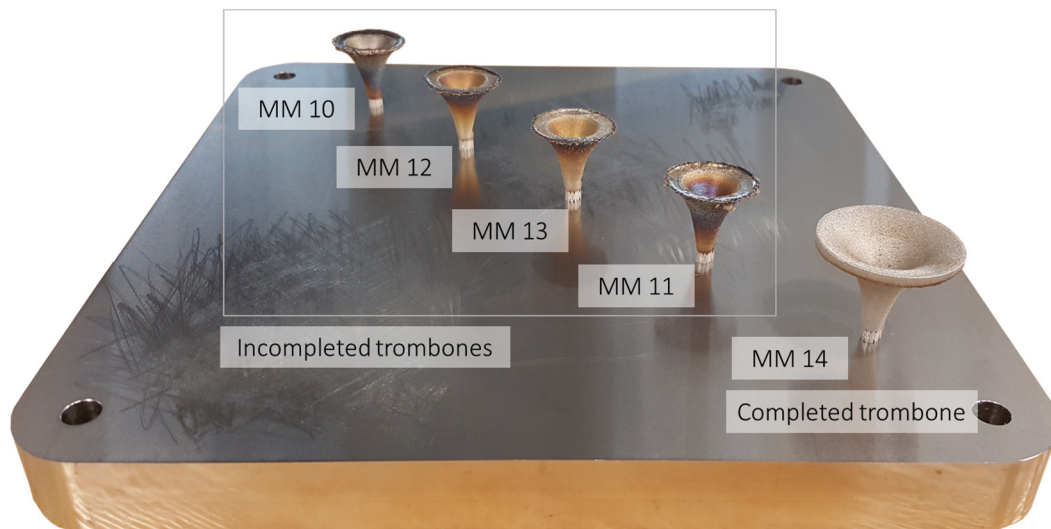


**Figure 4.6:** Overview of stage 1 experiments with trombones, pre-processed with MM;  
Source: own representation.

The results of the trombone studies show similar results for both investigated pre-processing programs AD and MM (Figure 4.7). Only PC 5 was terminated at layer no. 642 of 680 (including support structures) for the AD and at layer no. 635 for the MM build job.

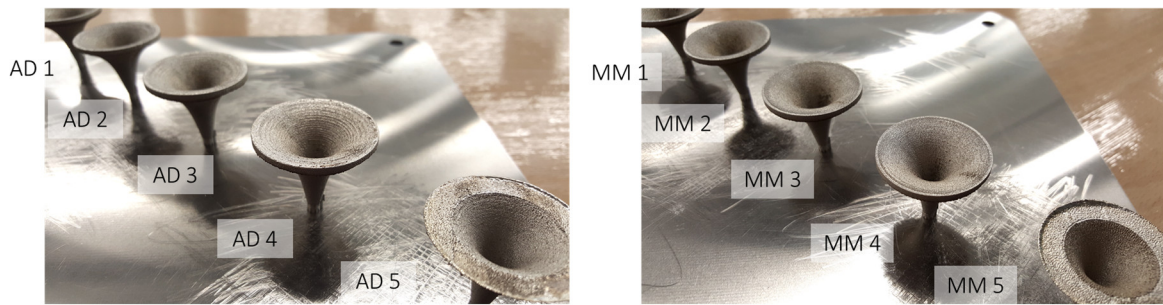


**Figure 4.7:** Similar results for both pre-processing programs for advanced PCs, pre-processed with Additive Designer (left) and Materialise Magics (right);  
Source: own representation.

The trombone studies revealed the potential of advanced parameter configurations to shift the boundaries of the downskin angle to lower values. Completed trombones mean that a downskin angle of roughly  $15^\circ$  was achieved. Standard parameters and their slight deviations in scanning speed  $v_s$  and laser power  $P_L$  were not able to complete the trombones without the use of support structures. Based on the findings from this chapter, the parameter configurations were developed further. Additionally, relative density – as an important evaluation criterion – will be discussed in the next chapter.

### 4.3.3 Test Series 2 – Investigation of the Relative Density

The second test series deals with the investigation of the relative density of selected parameter configurations. Already promising PCs from the trombone studies are evaluated and further configurations are developed. In total, 30 different PCs were investigated. Again, the focus was put on the variation of the main SLM parameters discussed in chapter 2.5.1 and 2.5.3. As main parameters, the laser power  $P_L$ , the scanning speed  $v_s$  and the hatch spacing  $h_s$  were used and modified. According to equation (2.2), the modification of those parameters directly influences the volumetric energy density  $E_v$ . Promising parameter configurations were identified within test series 1 for the trombones. Completed trombones showed advantages concerning downskin but their relative density remains unclear.

#### 4.3.3.1 Methodology and Parameter Configuration for Test Series 2

As test specimen, cubes of  $12 \times 12 \times 12 \text{ mm}^3$  were chosen. Cubes are popular for parameter investigations of SLM for several reasons. For instance, they are perfectly suitable for density measurements according to the Archimedes method. Furthermore, they can be cut easily to



create samples for metallographic analysis. Additionally, a lot of cubes with different PCs can be manufactured at the same time on the same build platform.

So where did the different parameters come from? On the one hand, promising parameters from test series 1 were taken. On the other hand, new PCs were developed to aim a high build-up rate. Basically, two parameters of the investigated ones influence the build-up rate: hatch spacing  $h_s$  and scanning speed  $v_s$ . However, if those parameters are increased to achieve faster build-up rates, the volumetric energy density  $E_v$  drops (see Equation (2.2)). The author postulates that an increased laser power can compensate this issue and helps to prevent balling and lack of fusion porosity. In the following table, only the range of chosen parameters are provided (Table 4.3). A complete overview of the selected parameter configurations can be seen in Table A 6, Appendix.

**Table 4.3:** Overview of the examined parameters and their value ranges.

Parameter		min.	max.
Laser power $P_L$ in W	Hatching	195	400
	Filling	100	150
	Border	75	100
Scanning speed $v_s$ in mm/s	Hatching	700	3080
	Filling	400	625
	Border	300	625
Hatch spacing $h_s$ in $\mu\text{m}$		35	120
Energy density $E_v$ in $\text{J}/\text{mm}^3$		20	80
Scanning strategy	Rotation	no	yes
	Filling	no	yes
	Border	no	yes

Two different methods to determine the relative density are established for SLM samples: Archimedes and image method. Due to its simplicity and its broad acceptance in literature<sup>212</sup>, the Archimedes method was selected. For this, a Kern analytical balance (ABT 320-4NM) with a density measurement kit (YDB-03) was used. As reference liquid, Acetone was used. Before measuring, the support structures were removed completely and the concerned area of the cube was grinded to exclude surface roughness effects from the measurements. In total, six different positions for each PC were chosen on the build platform (Figure 4.12). For each cube, three density measurements were done for two similar builds jobs. Nevertheless,

<sup>212</sup> Spierings et al. (2011).

metallographic specimens were generated for the selected cubes to investigate the microstructure and the appearance of pores for better explanatory power.

#### 4.3.3.2 Results from Test Series 2

The results show a broad range of measured densities. On the one hand, high relative densities above 99 % were measured. On the other hand, some cubes showed open porosities – visible through permanently rising bubbles during the measurements in the liquid. Open porosity was defined as an exclusion criterion and those parameter configurations were not considered further. The mean value of the relative density of the remaining configuration can be seen in Figure 4.8. The parameter configurations with open porosity (AD 9, 17, 18, 20, 24 and 28) are not included in the figure.

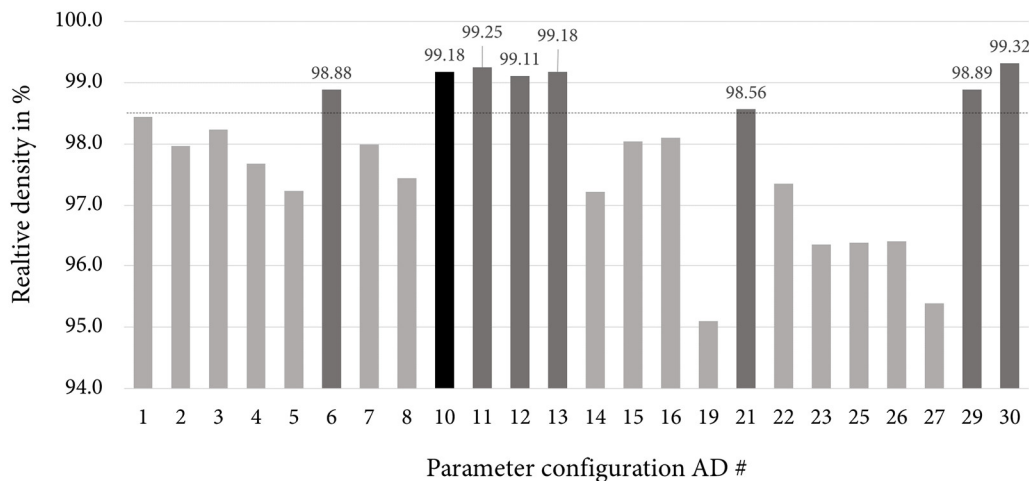


**Figure 4.8:** Results of the density measurements (mean values) for parameter configurations AD 1-30;

Source: own representation.

The selection of the threshold of 98.5 % relative density was based on findings from the literature. Liverani et al. (2017) found that mechanical properties (yield strength and ultimate tensile strength) for SLM 316L with relative densities between 98.4 % to 99.9 % were above the nominal datasheet values. Out of this, eight parameter configurations AD 6, 10, 11, 12, 13, 21, 29 and 30 were considered for further investigations.

For this, metallographic samples (unetched) were made. Results show that very low porosity (small pores, homogenous distribution) is visible for the standard parameter AD 10 and its deviation AD 13 (Figure 4.9).

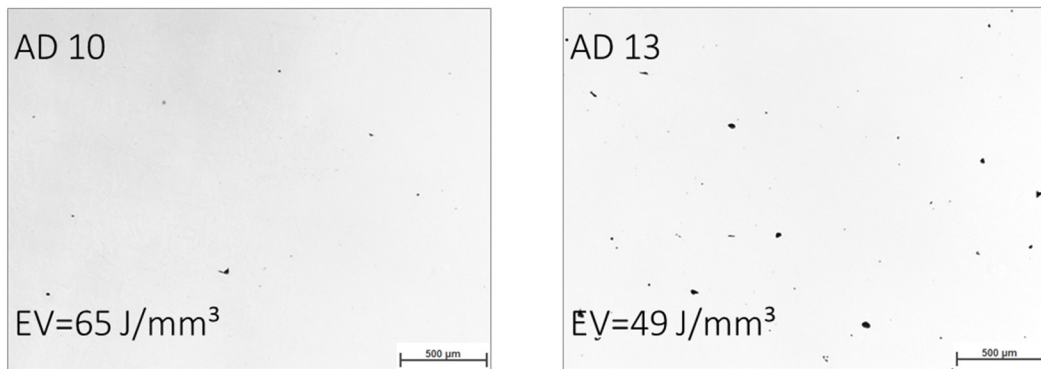


**Figure 4.9:** Microsection of cubical specimens fabricated AD 10 (left) and AD 13 (right);  
Source: own representation.

Furthermore, for AD 6, 29 and 30, visible pores are in low ranges. AD 21 shows a noticeably higher number of pores – especially large-sized lack of fusion pores (Figure 4.10 and Figure 4.11). These results confirm the density measurements from before. Interestingly enough, none of the samples with a hatching  $E_V$  of 40 J/mm<sup>3</sup> achieved densities above the threshold. Whereas cubes made with AD 12 and AD 13 (both  $E_V = 49$  J/mm<sup>3</sup>) showed densities above 99.0 %.

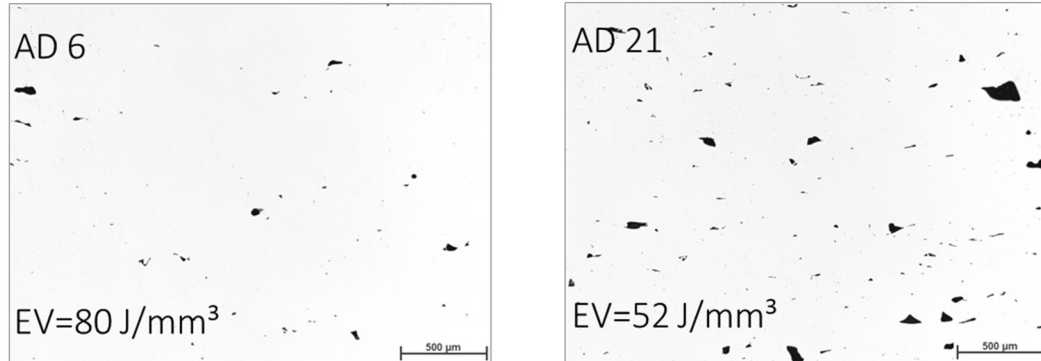


**Figure 4.10:** Microsection of cubical specimens fabricated AD 6 (left) and AD 21 (right);  
Source: own representation.

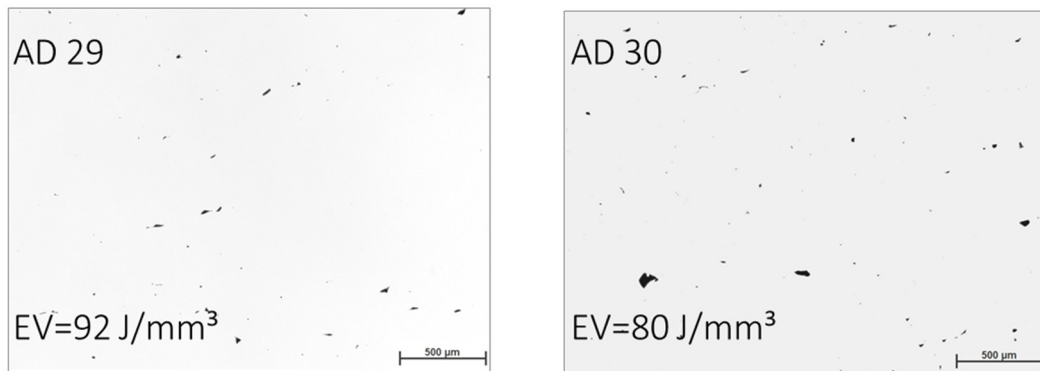


**Figure 4.11:** Microsection of cubical specimens fabricated AD 29 (left) and AD 30 (right); Source: own representation.

Generally, a direct relationship between  $E_v$  and the relative density (higher  $E_v$  means higher relative density) cannot be confirmed within the whole 316L studies. In contrast to that, the interaction between the SLM parameters during the complex melting process has proven to be of great importance. The limited expressiveness of  $E_v$  is a fact that has already been investigated for 316L in literature. The noticed limitations of  $E_v$  as leading design parameter for SLM is consistent within the relevant literature<sup>213</sup>.

Promising results of the developed parameters in terms of relative density were found. To confirm their overall suitability for 316L economy, the downskin angle needs to be investigated. For this, trombones were built once again for AD 6, AD 29 and AD 30 – together with the reference configurations of AD 10 and AD 13. AD 21 was excluded from further considerations due to the observed porosity during the metallographic analysis (Figure 4.10, right).

---

<sup>213</sup> Scipioni Bertoli et al. (2017).

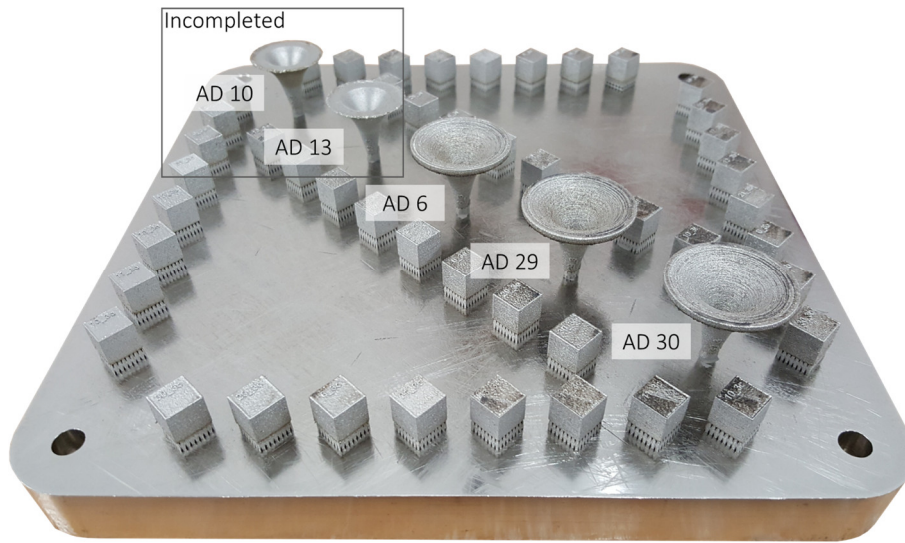


**Figure 4.12:** Overview of the experimental setup for trombones and cubes;  
Source: own representation.

It can be seen that the trombones were successfully completed for the developed PC. At this point, two basic requirements can be fulfilled by the 316L Economy PC:

- 1) Minimization of the downskin angle
- 2) Enabling of high relative density

Nevertheless, the most important question has not been answered yet: What are the economic impacts of the newly developed parameters? This question will be discussed and answered in the following chapter.

#### 4.4 Economic Evaluation of 316L Economy and Discussion

The developed parameter configurations show promising characteristics in terms of downskin angle and relative density. As a third criterion, the practical build-up rate  $\dot{V}_{Pr}$  was determined. As already stated, the  $\dot{V}_{Pr}$  is a measure for the build time and furthermore for the productivity. The determination of the  $\dot{V}_{Pr}$  was carried out in the same way as already described in chapter 2.5.3 – through simulation. For this, the build time and overall volume based on the fabrication of 25 pieces of trombones (correspondent to one full build platform). With equation 2.3, the  $\dot{V}_{Pr}$  was calculated for the investigated parameter configurations. Figure 4.13, left shows the relationship between build-up rate and relative density for the investigated PCs. Here again, AD 10 is the standard PC that serves as a

reference. Of course, a high relative density paired with a high build-up rate results in an optimal parameter configuration (Figure 4.13, left, top right-hand corner). From this perspective, AD 30 shows the most beneficial combination with priority on a high relative density. The percentual increase in build-up rate compared to the standard PC AD 10 can be seen in Figure 4.13, right. From that, especially AD 3 shows a significant increase of the build-up rate of nearly 80 % by keeping the relative density in an adequately high range (approx. 98.25 %).

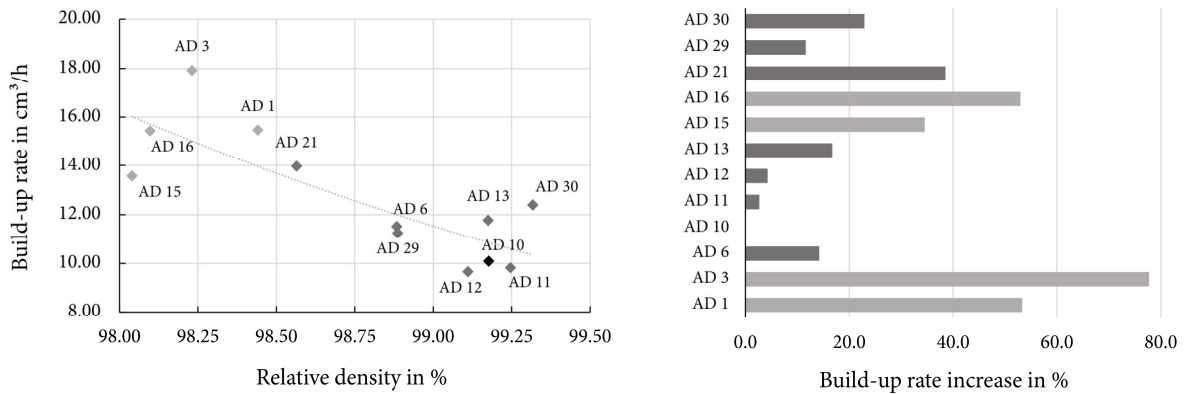


**Figure 4.13:** left: Investigated relationship between relative density and practical build-up rate  $\dot{V}_{Pr}$  for selected parameter configurations;  
 right: Build-up rate increase compared to the standard parameter AD 10;  
 Source: own representation.

In the next step, the economic impact of 316L is rated based on manufacturing costs. The evaluation was done similarly to the rating shown in chapter 3.3. With the use of the IFT cost model, the costs of a fully utilized build job of trombones (25 parts) – for selected parameter configurations – was calculated. Due to its complexity, the calculation was exemplarily done for 1, 3, 8, 16 and 25 pieces of trombones to achieve a meaningful correlation between manufacturing costs per part and lot size. For this calculation, both proposed advantages of 316L were evaluated: 1) the decrease of build time through higher build-up rates and 2) the minimization of support structures. For 2), Figure 4.6 shows that the trombone specimen cannot be completed to its full height with the standard parameters and its deviations. According to this, support structures must be provided to complete build jobs of trombones for AD 10, 11, 12 and 13 (Figure 4.14). In order to do that, support structures were created for the affected PCs. As a starting downskin angle, 40° was considered to ensure a proper heat dissipation along the downskin.

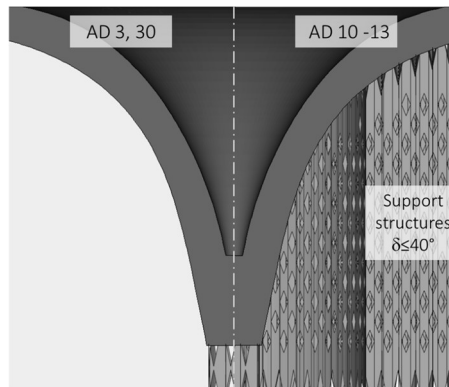


**Figure 4.14:** Additional support structures for AD 10-13 (right half of the trombone) at downskin areas  $\delta \leq 40^\circ$  to prevent build job termination;  
Source: own representation.

Compared to the developed PCs within 316L economy, an increase in manufacturing costs can be expected. The reason for this is the high amount of additional necessary support structures for the standard parameters AD 10, 11, 12 and 13. Following these arguments, the manufacturing costs per piece were calculated and their relation to the lot size is provided in Figure 4.15.

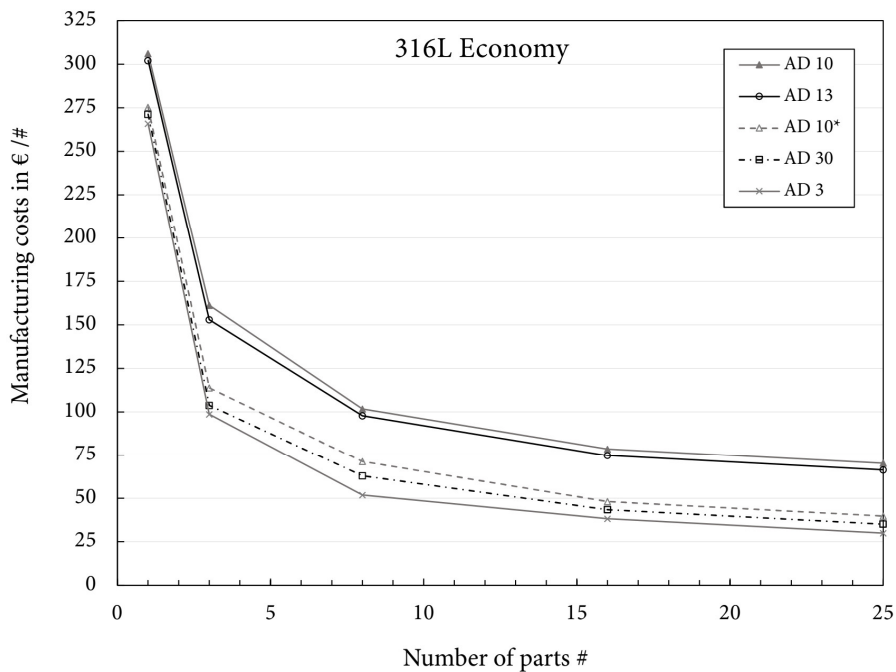


**Figure 4.15:** Comparison of manufacturing costs per trombone for different parameter configurations;  
Source: own representation.

The positive impact of the PCs developed within 316 economy can be clearly seen in Figure 4.15. For AD 30, cost advantages of approx. 45 % were found compared to AD 10 (based on 25 trombones). For AD 3, the economic benefits were even higher (53 %), but accepting a lower density compared to AD 10 and AD 30. It is noteworthy that the positive economic impact of reducing the amount of support structures is much more significant than the impact caused by a higher build-up rate. This can be explained by the massive drop of costs from AD 10 to AD 10\*. AD 10\* is based on the notional assumption that no additional supports are necessary at the downskin area – something that has already been disproved by the trombone studies. AD 10\* shows a decrease of manufacturing costs of approx. 37 % compared to AD 10. This positive impact can be directly attributed to the minimization of the support structures, since the parameter configuration (and therefore the build-up rate) remained the same. Additional support structures for the completion of the trombones mean:

- 1) Additional raw material is needed to support the 25 trombones: 274.4 cm<sup>3</sup> of 316L is required for the support structures. This results in additional direct material costs of 142.72 € based on 60 €/kg and 10 % surcharge for waste material for 316L powder (25 trombones).
- 2) The additional support structures increase the build time. Based on the pre-preparation simulation, the build time is extended by 9 h. This results in additional 361.30 € due to machine costs, increased energy and gas consumption and supervision time for a fully utilized trombone build job.
- 3) The removal of the additional support structures takes 6.25 hours for all 25 trombones (15 min. per trombone compared to 2 min. without additional support). From a monetary perspective, this means an increase of 258.00 € due to additional labor for post-processing.

The effect of the higher build-up rate can be assumed to be approx. 15-18 % when comparing AD 30 to AD 10\*.



## 4.5 Summary of Chapter 4

In this chapter, the positive economic impact of advanced PCs for 316L was presented. For this, the productivity was increased by two effects:

- 1) increase of the practical build-up rate  $\dot{V}_{Pr}$
- 2) decrease of the minimum downskin angle  $\delta$

To investigate 1), a large number of cubical test samples with 30 different parameter configurations were created and investigated. As a result, the  $\dot{V}_{Pr}$  was increased by approx. 23 % compared to the standard PC, while the density remained in similar high ranges (>99 %) for AD 30.

For 2), trombone test specimens were created with promising PCs from 1). 316L economy PCs enabled the completion of the trombone build jobs, whereas trombones built with standard PCs had to be terminated. The reason for this were the lower downskin angles that are achievable with 316L economy PCs. The positive influence of the lower possible downskin angles on the productivity was validated. Fewer necessary support structure for 316L economy PC led to a decrease in manufacturing costs of approx. 43 % for a fully utilized build platform of trombones (n = 25). As a result, the positive effect of lower downskin angles was found to be much more significant than the increase in  $\dot{V}_{Pr}$ .

## 5 DIRECT MACHINING AS A NEW APPROACH TO ECONOMIC POST-PROCESSING

Measures to increase the economic efficiency of pre-processing and processing were presented in chapter 3 and 4. This chapter focuses on the last step of post-processing of the SLM process chain. For this, the novel concept of “direct machining” (DM) was developed. Chapter 5.1 states the initial situation and describes the necessity for SLM post-processing with CNC machines. Further on in chapter 5.1, the concept of DM is introduced. In chapter 5.2, the feasibility studies of DM are presented. Chapter 5.3 describes the load model behind the concept that led to further optimizations of DM, shown in chapter 5.4. The economic relevance of DM is stated in chapter 5.5. Chapter 5.6 summarizes the presented approach of DM.

Selected parts of this chapter 5 were already published and can be found in Höller et al.<sup>214,215</sup>.

### 5.1 Initial Situation

Apart from the limited productivity and the low grade of automatization, the part properties in the as-built state are a significant drawback of SLM. Coarse geometrical and dimensional tolerances as well as high surface roughness demand for additional post-processing, such as CNC machining, heat treatment or polishing processes. These additional efforts significantly increase the manufacturing costs. As shown in chapter 3 and concluded from internal studies at the IFT, post-processing can attribute up to even 30 % to the overall manufacturing costs. To address this problem, the concept of direct machining (DM) was developed and elaborated.

#### 5.1.1 The Geometrical Accuracy of SLM

The limited accuracy of the SLM process is a well-known issue concerning precise industrial applications.<sup>216</sup> The reason for this can be attributed to the process characteristics and the machine setup. Related to this, the scanning system, laser spot size, as well as the layer thickness are reported as influencing factors.<sup>217</sup> Moreover, distortion – caused by residual

---

<sup>214</sup> Höller et al. (2019).

<sup>215</sup> Höller et al. (2020).

<sup>216</sup> Cf. Zhang et al. (2018).

<sup>217</sup> Cf. Ahmed et al. (2019) p. 2.

stresses during the melting process – decreases the geometrical and dimensional accuracy.<sup>218</sup> However, specific scientific literature that provides definite values of the accuracy is rare. Therefore, preliminary studies were carried out at the IFT in order to investigate the accuracy of the SLM process. This should help to understand to what extent CNC post-processing is necessary for the production of highly accurate SLM parts.

For these preliminary studies, test build jobs were developed. The chosen parts (size 1 mm to 50 mm) were supposed to cover typical values of geometric dimensioning and tolerancing (GD&T) and dimensional tolerancing. In total, 49 parts were placed on the test build platform. Out of them, 12 different characteristics were investigated. The evaluation and classification were made according to the ISO 2768-1<sup>219</sup> and ISO 2768-2<sup>220</sup> standards. The test build jobs were fabricated out of 316L stainless steel in the same composition as already described in chapter 4.3. 50 µm was chosen as layer thickness. As preparation software, Additive.Designer (AD) was used.

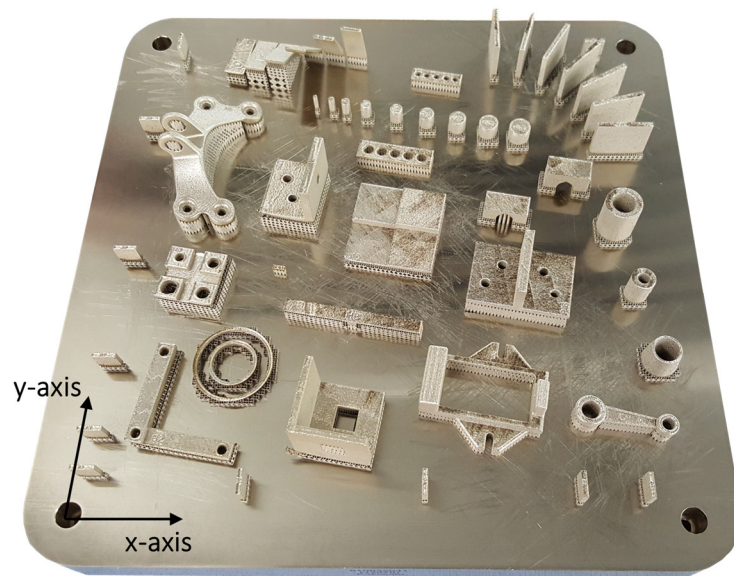


**Figure 5.1:** Overview of the fabricated test build platform including 49 test parts;  
Source: own representation.

After the build process, the geometrical accuracy of the build platform in the as-built state was evaluated. For this, the actual geometry was compared with the target geometry based on the build job preparation with the AD. The actual geometry was measured via optical 3D

<sup>218</sup> Cf. Ahmed et al. (2019) p. 3.

<sup>219</sup> ISO 2768-1:1989 (1989).

<sup>220</sup> ISO 2768-2:1989 (1989).

scanning with a GOM ATOS Triple Scan system (resolution 20  $\mu\text{m}$ ). The evaluation was carried out with GOM Inspect. The basic workflow of the investigations is shown in Figure 5.2. The shown specimen “O15 – Connecting Rod”, for example, allows the evaluation of diameter deviations, distance tolerances according to ISO 2768-1 and the circularity as feature of GD&T.

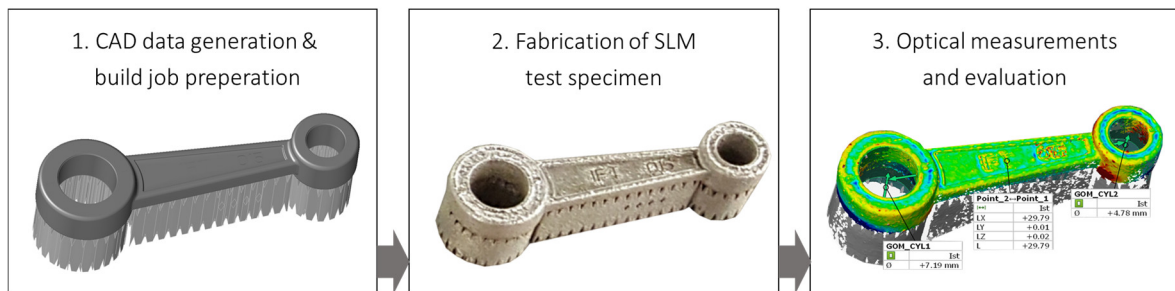


**Figure 5.2:** Basic workflow of preliminary experiments to determine the accuracy of SLM;  
Source: own representation.

Results show that the accuracy of the investigated parts can differ widely from the target value, strongly depending on which feature (diameter, length, cylindricity etc.) was studied. According to ISO 2768-1, the experiments showed accuracies between fine and coarse for length features. Length features include the dimension of the test parts (length in x- and y-direction, height in z-direction) and distances between two significant features (e.g. distance between the center of two holes). However, approx. 51 % of the measurements were in the range of medium and coarse (Figure 5.3). These findings correspond to findings from literature. Otawa et al.<sup>221</sup> reported a geometrical accuracy between fine and coarse – depending on the build direction – according to ISO 2768-1 for SLM.

<sup>221</sup> Otawa et al. (2015).

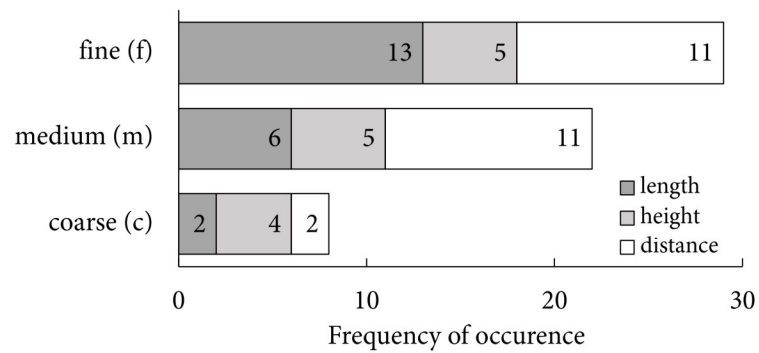


**Figure 5.3:** Classification of the investigated length features (n = 59) according to ISO-2768-1; Source: own representation, cf. Höller et al. (2020).

Results from these basic investigations clearly indicate the need for CNC post-processing to fulfill tight tolerances and GT&D. Although deviations of diameter features were found adequately low, outliers make it hard to predict a general accuracy for SLM (Figure 5.4).

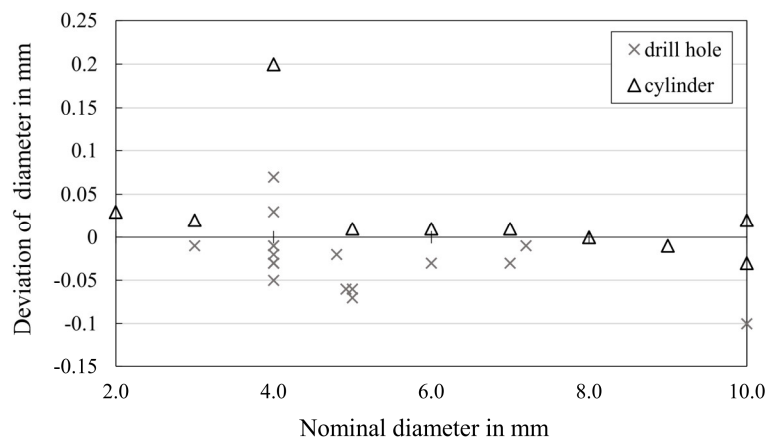


**Figure 5.4:** Measured deviations (n = 29) from the nominal diameter of various holes and cylindrical specimens; Source: own representation, cf. Höller et al. (2020).

As a further example, deviations of flatness and angularity – as examples of GD&T – are shown in Figure 5.5. Deviations of nearly 0.5 mm (flatness) and 0.5° (angularity) were found for small downskin angles. As an outcome, functional surfaces – like fits – cannot be manufactured with SLM directly and require additional post-processing, such as milling or grinding. For further details and results, reference is made to the Bachelor’s Thesis of Thomas Hinterbuchner<sup>222</sup>.

<sup>222</sup> Hinterbuchner (2019).

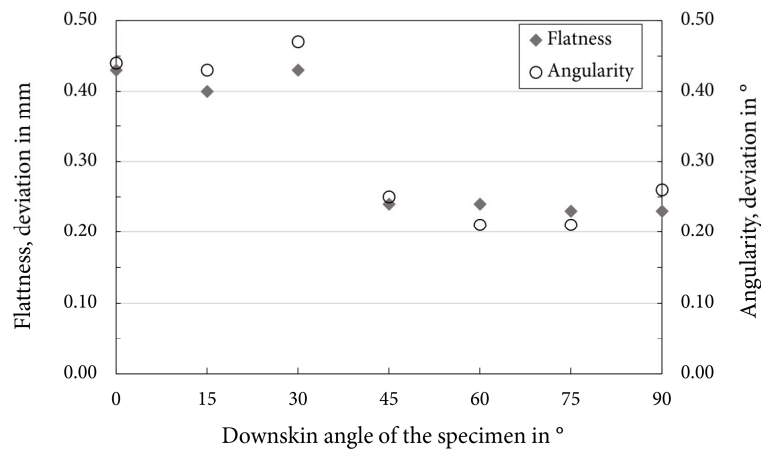


**Figure 5.5:** Measured deviations ( $n = 14$ ) of flatness and angularity for specimens with different downskin angles;

Source: own representation; cf. Hinterbuchner (2019).

These basic experiments confirm the necessity of CNC post-processing for SLM when highly accurate parts are required. Furthermore, results indicate that the geometrical accuracy of the SLM process varies strongly depending on feature size, part orientation etc. This makes the predictability of the accuracy and a uniform classification of the SLM process according to ISO 2768 practically impossible.

### 5.1.2 The Concept of Direct Machining

As described above, for precise SLM geometries, CNC machining has to be performed as an additional step in post-processing. As examples, milling parallel functional surfaces or drilling exactly positioned holes can be mentioned. CNC machining requires proper clamping. For this, every SLM part has to be detached from the build platform and separately clamped in the machine afterwards. Still, this can be challenging. SLM parts often consist of fragile geometries and structures as well as insufficient defined reference areas that could prevent a secure clamping. In order to deal with that problem, special fixtures and clamping tools quite often become necessary to create a good fixation inside the machine. And this requires time for clamping. Together with necessary fixtures, the manufacturing costs for post-processing can rise significantly. These cost effects are even worse for small lot sizes or a single part production where tailor-made fixtures are necessary.

To address this issue, the concept of direct machining was developed. The author defines DM as:

“Direct machining (DM) is the post-processing of SLM parts via machining without prior removal of the parts from the build platform to achieve economic benefits.”<sup>223</sup>

It follows from the definition that the parts are still attached to the build platform during the CNC machining process. This is the main difference to the conventional way where clamping and fixturing take place separately for each part. This should lead to economic benefits due to less clamping time and no additional costs for fixtures. The basic workflow of DM can be seen in Figure 5.6.

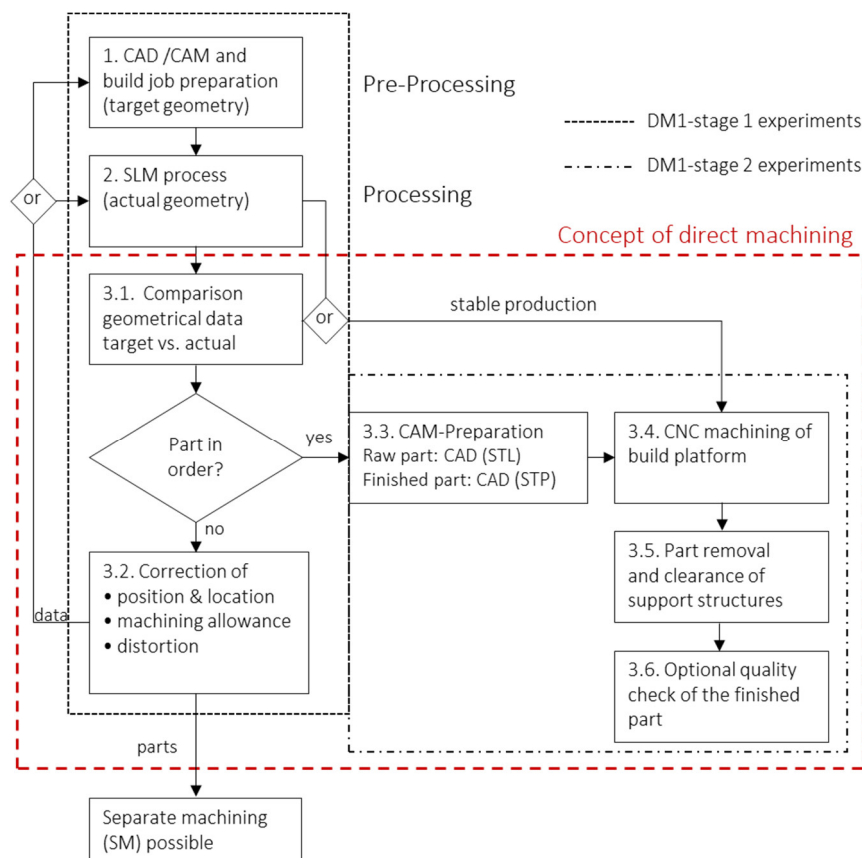


**Figure 5.6:** Basic workflow of direct machining;  
Source: own representation, modified from Höller et al. (2019).

For DM, the support structures have to fulfill the task of proper and secure fixturing. This is a totally different task compared to their original use for heat dissipation and fixation. So the main question arises, whether support structures are capable to withstand cutting forces during machining to act as secure fixtures. To the best of the author's knowledge, this subject has never been studied scientifically before. Only one article was found, where this topic was

<sup>223</sup> Höller et al. (2020) p. 2.

mentioned, not explicitly describing the concept or term DM.<sup>224</sup> Tripathi et al.<sup>225</sup> studied the milling behavior of SLM block supports made of Inconel 718. They concluded that the support structures can cause higher tool wear since interrupted cutting takes place. Furthermore, the authors found that the support structures are unexpectedly rigid if exposed to milling forces. However, the authors focused on the machining of the support structures as a possible post-processing technique to remove them. For DM, the machining of the SLM part is important whereas the removal of the support structure is a follow-up step that can be done in the most efficient way. Bobbio et al.<sup>226</sup> investigated the strength of support structures made of Ti6Al4V. They found out that the structural strength under tensile loads is significantly decreased compared to a normalized fully dense material. They attributed this to the stress concentration in the sharp-edged transition zone between the part and the support structures. For DM, support structures have to absorb the cutting forces and ensure a rigid clamping for CNC machining. For this, the present knowledge about the strength of SLM support structures had to be extended.

### 5.2 Feasibility Study of Direct Machining – DM1

After the concept of DM had been developed, its feasibility was studied within the first series (DM1). For this, two requirements had to be fulfilled:

1. Positioning and repeatability: only a repeatable SLM process can make the machining on the build platform economically possible. The location of the parts on the build platform has to remain constant for consecutive build jobs. Otherwise, an efficient and precise positioning of the milling tool cannot be guaranteed. See Figure 5.6, DM1-stage 1 experiments.
2. Machinability: the support structures have to withstand the cutting forces without permanent deformation. They have to act as fixtures to allow DM. See Figure 5.6, DM1-stage 2 experiments.

Both the requirements and the proof of the DM concept were addressed in Höller et al. (2019). For this thesis, the most relevant findings and results will be discussed in more detail.

---

<sup>224</sup> Hamilton (2016).

<sup>225</sup> Tripathi et al. (2018).

<sup>226</sup> Bobbio et al. (2017).



The first requirement, positioning and repeatability, was investigated by means of the earlier developed test build job (TBJ 1) from chapter 5.1.1. For efficiency reasons, only 14 of the 49 test parts of the build jobs were used for three similar consecutive test build jobs (TBJ 2-4). The particular location of these 14 parts on the build platform was compared for all four TBJ with the CAD target geometry from the preparation step. Again, optical measurement with the GOM ATOS Triple Scan was performed. As reference point, a mounting point on the build platform was used (see Figure 5.8). The results can be seen in the following Figure 5.7.

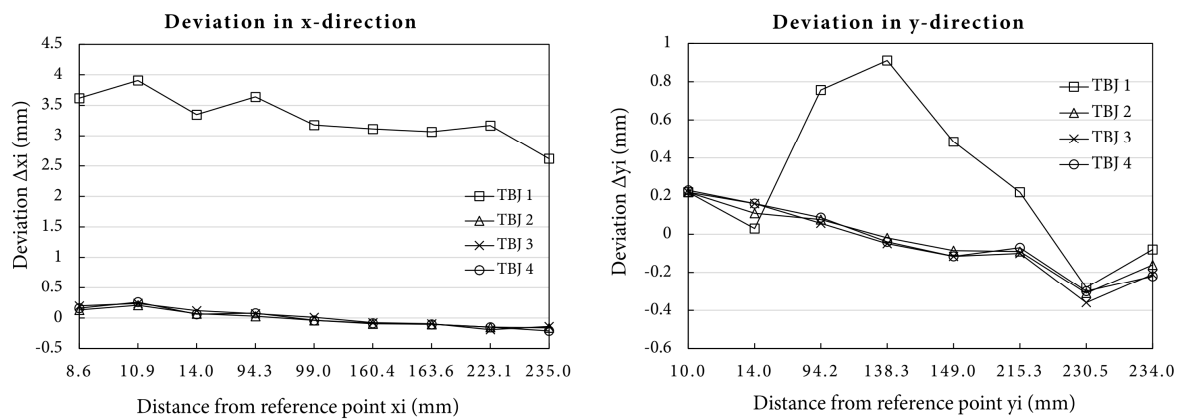


**Figure 5.7:** Deviation of the SLM process in x-direction (left) and y-direction (right) for four consecutive test build jobs (TBJ 1-4);

Source: own representation, cf. Höller et al. (2019).

The first test build job (TBJ 1) showed significantly high deviations up to  $\Delta x_i = 3.91$  mm and  $\Delta y_i = 0.91$  mm from the CAD target positions. Between TBJ 1 and 2, a professional calibration of the laser optics of the SLM 280HL machine was done during the regular maintenance. After this new calibration, the deviations were greatly reduced, but still detectable – especially towards the borders of the build platform. Furthermore, a high repeatability between TBJ 2-4 was investigated for the x- and y-direction. It should be noted that the position accuracy should be seen independently from the geometrical accuracy of the parts itself (as discussed in chapter 5.1.1). However, the observed repeatability fulfills the basic requirement 1 for DM which is the efficient use of DM results in a stable production (see Figure 5.6) and involves the use of CAM to increase the level of automatization. Nevertheless, out of the results, a machining allowance of min. 0.25 mm – to deal with deviations in repeatability – can be recommended.

The basic requirement 2 is the resistance of the support structures against cutting forces during machining of the SLM part. For this, test parts were fabricated and machined (DM1-

stage 2 experiments, Figure 5.6) and the forces during machining were measured. For the milling experiments, cuboidal and spherical SLM test parts were fabricated. Since TBJ 2-4 only contained 14 test parts, the cuboid and cylinders could be placed on TBJ 2-4. Additive.Designer was used as preparation software. The test parts varied in size and type of support structure. An overview of the used test setup is provided in the following.

- Shape of the test parts: cuboidal and cylindrical
- Size of the test parts:
  - Cuboid: 5 x 5 to 20 x 20 mm<sup>2</sup>, height: 15 mm
  - Cylindrical: d = 5 to d = 20 mm, height: 15 mm
- Two support types: block support and the AD specific “Heartcell” support

The CNC machining was carried out with the DMG Mori Linear 30 CNC 5-axis milling machine at the IFT. The cutting forces during machining were measured with a Kistler Multicomponent Dynamometer (type 9129AA) in combination with a Kistler 5070A10100 charge amplifier. The data was collected with a National Instruments data acquisition module NI9223. The evaluation was done with MATLAB (V2017b).

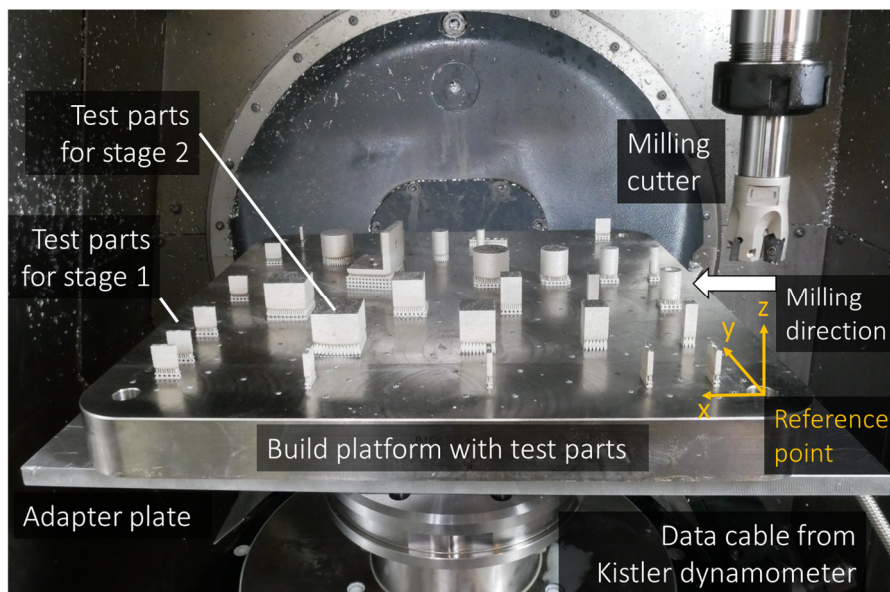
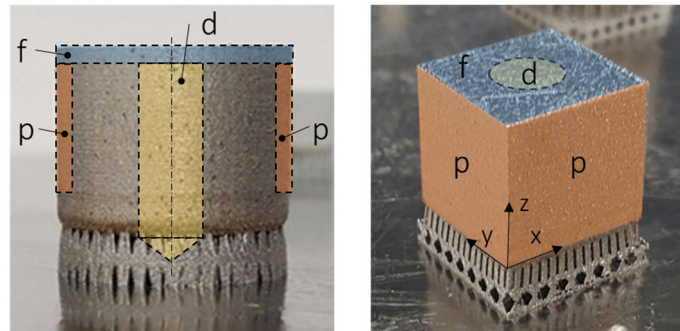


**Figure 5.8:** Experimental setup for the milling experiments (DM1-stage 2); Source: own representation, cf. Höller et al. (2019).

For the machining experiments, the focus was on common machining operations using well-tried cutting parameters (Figure 5.9). The preparation for the CNC machining was done with

computer-aided manufacturing (CAM), see step 3.3 in Figure 5.6, ESPRIT CAM Software vers. 2017.



Operation	Tool	$v_c$ (m/min)	$v_f$ (mm/min)	$a_p$ (mm)
1. Face milling (f)	Insert milling cutter d = 25 mm	100	255	0.1/0.25/ 0.5/1.0
2. Profile milling (p)	Solid carbide milling cutter d = 8 mm	100	636	0.5 (x/y) 10.0 (z)
3. Drilling (d)	HSS-Drill d = 6 mm	10	49	clearance hole

Cutting parameters:  $v_c$  cutting speed;  $v_f$  feed speed;  $a_p$  cutting depth

**Figure 5.9:** Test specimen with schematic overview of machining operations (above) and cutting parameters

above left: cylinder, d = 20 mm, block support structure;  
above right: cuboid, l = 15 mm, Heartcell support structure;  
Source: own representation, cf. Höller et al. (2019).

As already stated, the support structures have to absorb the cutting forces during machining to act as fixtures. Bending stresses were considered to be the most relevant criterion for failure (for details see chapter 5.3). Therefore, cutting forces in x-, y- and z-direction were measured. However, for bending stresses, only  $F_x$  and  $F_y$  were supposed to be relevant. Furthermore,  $F_z$  showed significantly lower values (approx. 20-30 %) – especially for high cutting depths – compared to the combination of  $F_x$  and  $F_y$ . For the evaluation, the resulting force  $F_{res}$  was calculated:

$$F_{res} = \sqrt{F_x^2 + F_y^2} \quad (5.1)$$

In the following, selected results from the experiments are presented to show the feasibility of DM. Clear differences between the single cutting depths were visible. As expected, higher cutting depths lead to higher cutting forces. However, the smallest test part configuration

(cuboid:  $5 \times 5 \text{ mm}^2$  and cylinder:  $d = 5 \text{ mm}$ ) was not able to withstand the lowest cutting depth of  $a_p = 0.1 \text{ mm}$ . The reason for this could be the interruptive cutting process of the insert milling cutter with its four symmetrically arranged cutting edges.

With increasing part and support structure dimensions, the capability of load absorption increases. Figure 5.10 shows the results from the milling experiments of TBJ 2 and TBJ 3 for the cylindrical test parts from  $d = 5$  to  $d = 20 \text{ mm}$ . The data points show mean values of the recorded  $F_{\text{res}}$  and the error bar shows the intermittent maxima of  $F_{\text{res}}$ . The “F” in the graph marks where failure of the support structure for the test part occurred. There were two major observations that indicated failure. First, via optical inspection when a part detaches from the build platform. Second, values for  $F_x$  and  $F_y$  drop to zero.

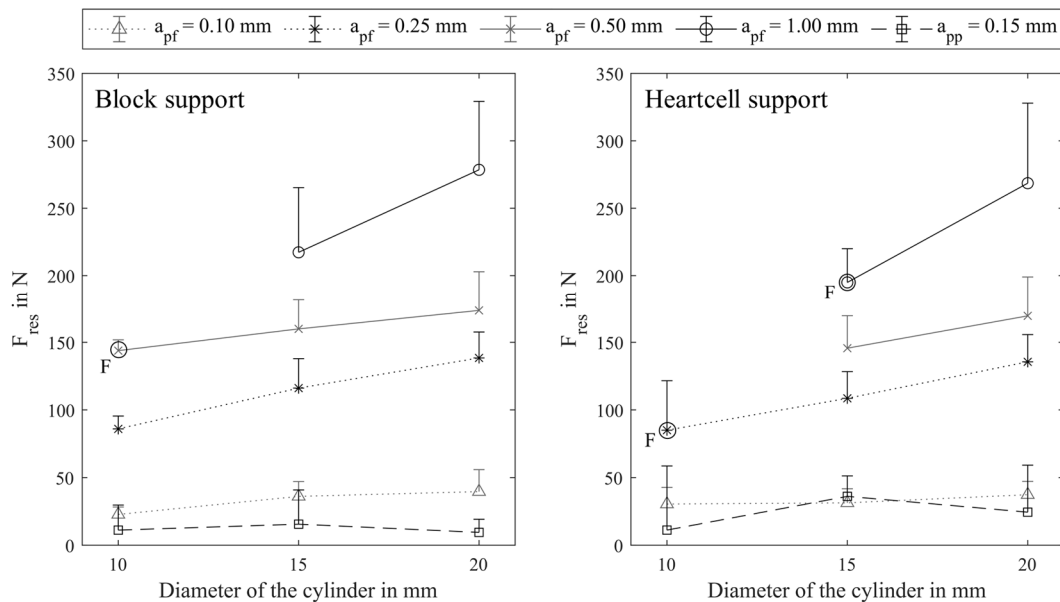


**Figure 5.10:** Mean and maximum cutting forces for cylindrical test parts for face milling ( $a_{pf}$ ) and profile milling ( $a_{pp}$ );

Left: block support structures; right: Heartcell support structures;

Source: own representation, cf. Höller et al. (2019).

Results show that the support structures were able to withstand high cutting forces. Milling with a large cutting depth of  $2.0 \text{ mm}$  was possible for most test parts with a feature size of  $15 \text{ mm}$  and for all test parts with a feature size of  $20 \text{ mm}$ . As expected, more volume of support structures means a higher load capacity. The Heartcell support structure shows clearly less capability of cutting force absorption compared with the block support. The reason for this is the fragile connection zone between support structure and part which should simplify the support structure removal during post-processing. The drilling

experiments with the 6 mm drill bit were quite promising as well. None of the investigated test parts failed due to maximum drilling forces in z-direction  $F_{z,max} > 600$  N (see Figure A 5, Appendix).

It can be concluded, that also the second requirement for DM – the ability of the support structures to act as fixtures – was tested and evaluated positively. Further results and details about this preliminary study can be found in Figure A 6, Appendix.

Of course, these studies are limited. Only a single cutting height of 19 mm in z-direction (15 mm part + 4 mm support structures) was tested. Increasing the cutting height would immediately increase the bending stresses. Additionally, the investigation of influence of the support structure configuration on the load capacity was limited. Due to the positive feasibility, the concept of DM was developed further. To understand the cutting process during DM (step 3.4 in Figure 5.6) better, a simplified theoretical load model was elaborated that is presented in the following chapter 5.3. From that model, typical support structures were optimized and tested towards DM (chapter 5.4).

### 5.3 Modelling of Direct Machining

The previous chapter showed that plain face milling can become crucial for the support structures during DM. Therefore, a focus was set on this milling operation. An understanding of the cutting forces helps to make statements about the load on the support structures during DM.

#### 5.3.1 Cutting Forces for Plain Face Milling

For the chip removal during cutting, the machining force  $F$  has to be overcome. According to DIN 6584<sup>227</sup>, this machining force  $F$  can be broken down into different components (Figure 5.11). Based on the working plane, the active force  $F_a$  is built by the feed force  $F_f$  and the cutting force  $F_c$ . The passive force results from the cutting process perpendicular to the working area but does not contribute to power conversion during cutting.<sup>228</sup> The following equations and calculations were taken from the comprehensive work of Grote and Antonsson<sup>229</sup>.

---

<sup>227</sup> DIN 6584:1982-10 (1982).

<sup>228</sup> Cf. Grote/Antonsson (2009) p. 612.

<sup>229</sup> Cf. Grote/Antonsson (2009) p. 612; pp. 619-624.

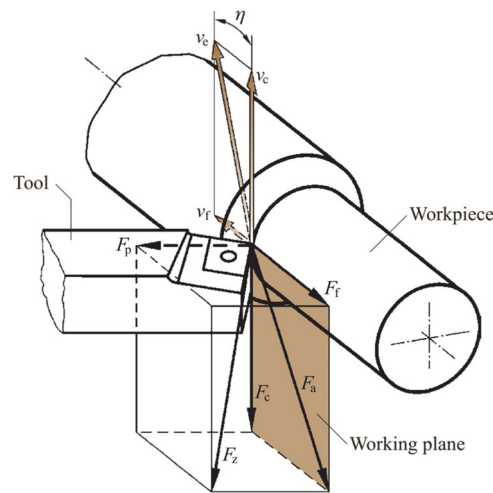


**Figure 5.11:** Components of cutting forces;  
Source: Grote/Antonsson (2009) p. 612.

From basic considerations from the turning process follows the basic relationship for the total machining force  $F$ :

$$F = \sqrt{F_c^2 + F_f^2 + F_p^2} \quad (5.2)$$

The cutting force  $F_c$  can be calculated – based on the well-established method by Otto Kienzle – out of the area of the undeformed chip  $A$  and the specific cutting force  $k_c$ :

$$F_c = A \cdot k_c = h \cdot b \cdot k_c = a_p \cdot f \cdot k_c \quad (5.3)$$

Based on the cutting tool angle  $\kappa$  and the cutting depth  $a_p$ , the undeformed chip width  $b$  and the undeformed chip thickness  $h$  (Figure 5.12) can be calculated:

$$b = \frac{a_p}{\sin(\kappa)} \quad (5.4)$$

$$h = f_z \cdot \sin(\kappa) \cdot \sin(\varphi) \quad (5.5)$$

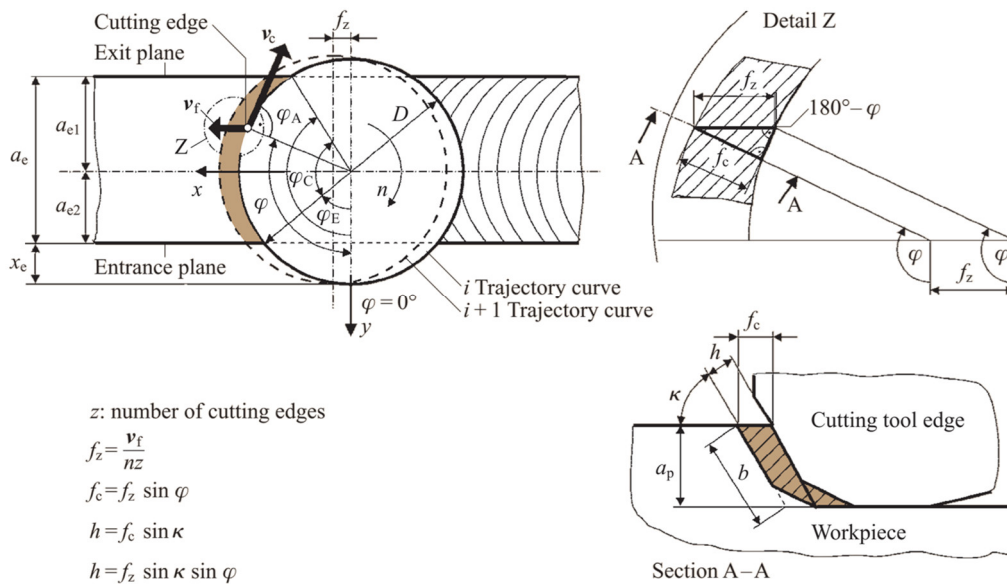


**Figure 5.12:** Variables of plain face milling;  
 Source: Grote/Antonsson (2009) p. 621.

The specific cutting force  $k_c$  can be experimentally determined and depends logarithmically on the undeformed chip thickness  $h$ :

$$k_c = k_{c1.1} \left( \frac{h}{h_0} \right)^{-m_c} \quad (5.6)$$

If  $k_{c1.1}$  is the unit specific cutting force that describes the cutting force based on  $h = 1$  mm and  $b = 1$  mm for a certain tool/material combination, the value  $m_c$  is the exponent of the specific cutting force. Out of it, the cutting force formula can be concluded:

$$F_c = k_{c1.1} \cdot b \cdot h^{1-m_c} \quad (5.7)$$

For  $k_{c1.1}$  and  $1-m_c$ , extensive experimental investigations led to tables that allow the determination of both values depending on material und cutting parameters.

The general formula for the cutting force by Kienzle can be transferred to milling as well. For milling, the cutting force  $F_c$  and its perpendicular component  $F_{cN}$  are constantly co-rotating as the milling tool rotates. Whereas the coordinate system for the feed force  $F_f$  and its perpendicular component  $F_{fN}$  remain fixed. The passive force  $F_p$  again acts in a direction perpendicular to the working plane. A general equation for face milling can be noted as follows:

$$F_i = A \cdot k_i \quad (5.8)$$

If the indices  $i = c, cN, \text{ or } p$ . Again,  $A$  is the undeformed chip cross section and  $k_i$  the specific machining force for the related direction.

Up to now, only tool specific forces were discussed. In practice, the measurement of the cutting forces is done with a multi-component dynamometer between machine bed and tool.<sup>230</sup> This method was also used for the experiments of DM, as described in chapter 5.2 and 5.4. For the transformation of  $F_c, F_{cN}$  and  $F_p$  into the fixed coordinate system of  $F_x, F_y$  and  $F_z$ , the following transformation<sup>231</sup> has to be used:

$$\begin{bmatrix} F_c \\ F_{cN} \\ F_p \end{bmatrix} = \begin{bmatrix} \sin(\varphi) & -\cos(\varphi) & 0 \\ \cos(\varphi) & \sin(\varphi) & 0 \\ 0 & 0 & 1 \end{bmatrix} \cdot \begin{bmatrix} F_x \\ F_y \\ F_z \end{bmatrix} \quad (5.9)$$

The relationship between active Forces  $F_c, F_{cN}$  and the workpiece specific forces  $F_x, F_y$  can be seen in Figure 5.13.

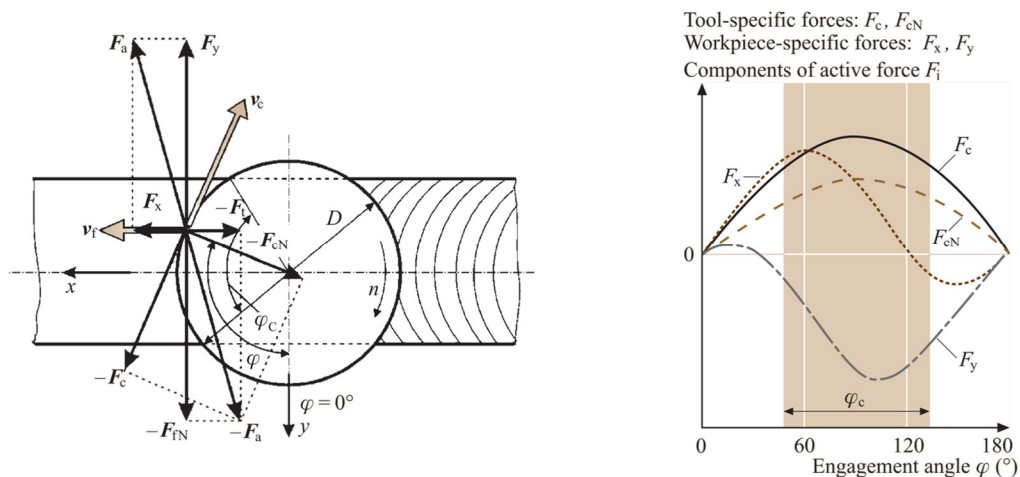


**Figure 5.13:** Components of the cutting force for plain face milling;

Source: Grote/Antonsson (2009) p. 622.

The described cutting forces  $F_c, F_{cN}$  and  $F_p$  are only valid for a certain point of contact for a single cutting edge in operation. With the mean undeformed chip thickness  $h_m$ , the average cutting force and average passive force per cutting edge is:

<sup>230</sup> Cf. Denkena/Tönshoff (2011) pp. 81–82.

<sup>231</sup> Cf. Denkena/Tönshoff (2011) p. 82.



$$F_i = b \cdot k_{i1.1} \cdot h_m^{1-m_c} \cdot K \quad (5.10)$$

If the indices  $i = \text{cmz}, \text{cNmz}, \text{or pmz}$ . The factor  $K$  includes various different correction factors for the considered manufacturing process, such as  $K_{\text{TW}}$ , the correction factor for tool wear. In practical use, more than one cutting edge is in operation at the same time. Therefore, the forces from equation (5.10) have to be multiplied with the number of cutting edges in operation  $z_{iE}$ . The total average cutting force is then:

$$F_{cm} = F_{cmz} \cdot z_{iE} \quad (5.11)$$

However, the use of a single tooth cutter is reported as beneficial for cutting force measurements<sup>232</sup>. Thus, the measured forces  $F_x$ ,  $F_y$  and  $F_z$  can be directly transferred into  $F_c$ ,  $F_{cN}$  and  $F_p$ . Nevertheless, DM focuses on the workpiece (SLM test part) and not on the tool (milling cutter). Therefore, the statements about the cutting forces were of minor interest for the presented studies.

### 5.3.2 Cutting Forces for Direct Machining

For DM, the workpiece specific forces  $F_x$  and  $F_y$  are most relevant because they cause critical bending stresses. This means that the forces which were measured by the dynamometer in the experiments can be directly used for the load model of the support structures.

In this chapter, the theoretical load model with regard to the support structures is elaborated further. For this, a random contact point  $p_i$  between the cutting edge and the SLM test specimen during milling is observed (Figure 5.1). As stated in the previous chapter, the cutting process causes forces in  $x$ - and  $y$ -direction of the working plane. With equation (5.1),  $F_{\text{res}}$  can be calculated out of  $F_x$  and  $F_y$ .

---

<sup>232</sup> Cf. Denkena/Tönshoff (2011) p. 82.

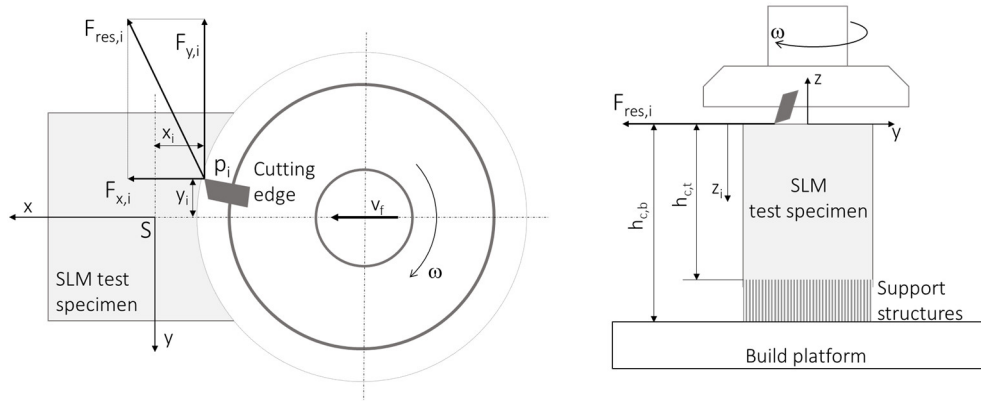


**Figure 5.14:** Forces during plain face milling in a random point  $p_i$ ;  
Source: own representation.

The forces cause two main types of loads: Bending moments and torsional moments. The bending moment in both axes at a random point is:

$$M_{bx,i} = F_{y,i} \cdot z_i \quad (5.12)$$

$$M_{by,i} = F_{x,i} \cdot z_i \quad (5.13)$$

In which  $z_i$  is a random position in  $z$ -direction. The torsional moment regarding the shear center  $S$  for both forces  $F_{x,i}$  and  $F_{y,i}$  is:

$$M_{t,S} = F_{x,i} \cdot y_i + F_{y,i} \cdot x_i \quad (5.14)$$

With the perpendicular distance to the neutral axis  $e_i$  and the second area of inertia  $I$ , the bending stress  $\sigma_b$  for both axes is:

$$\sigma_{bzx,i} = \frac{M_{by,i} \cdot e_{x,i}}{I_y} \quad (5.15)$$

$$\sigma_{bzy,i} = \frac{M_{bx,i} \cdot e_{y,i}}{I_x} \quad (5.16)$$

The shear stress  $\tau$  can be calculated with the forces  $F_{x,i}$  and  $F_{y,i}$  and the related cross section  $A_{x,i}$  and  $A_{y,i}$ :

$$\tau_{zx,i} = \frac{F_{x,i}}{A_{x,i}} \quad (5.17)$$

$$\tau_{zy,i} = \frac{F_{y,i}}{A_{y,i}} \quad (5.18)$$

However, for DM, the maximum bending and shear stresses are clearly expected inside of the support structures. Support structures for SLM are usually thin and fragile. Therefore, the determination of shear stresses due to  $F_{x,i}$  and  $F_{y,i}$  based on equation (5.17) and (5.18) is only valid for the test specimen themselves. For the support structures, the calculation of shear stresses based on thin-walled, open structures is recommended. Also, the determination of torsional shear stresses for typical support structures is not possible with simple approaches from mechanics. As a result, the focus was placed on bending stress as the most critical failure criterion during DM. The occurrence of shear stresses as failure criterion will be discussed qualitatively based on fracture patterns.

With this basic load model, DM was investigated further. Three different types of support structures were examined with regard to their load capacity. The experimental procedure and results are described in the next chapter.

## 5.4 Optimization of Support Structures for Direct Machining – DM2

Experiments from the feasibility studies (chapter 5.2) showed fundamental differences in the load capacity of the support structures during DM. Therefore, the role of the support structures was studied more closely during the second round of DM experiments (DM2). The experiments were supposed to clarify which support types could fulfill the following three requirements:

1. High load capacity in order to withstand the cutting forces during DM
2. Sufficient heat dissipation and fixation as original task of SLM support structures
3. Low amount of necessary raw material and easy removability

### 5.4.1 Experimental Setup

The basic experimental setup corresponds to that of the feasibility studies in chapter 5.2. Again, the SLM 280HL was used and all test specimen were fabricated out of 316L stainless steel powder. The build job preparation was done with the software Additive.Designer.

Cuboid samples with a cross section of  $14 \times 14 \text{ mm}^2$  were chosen. The experimental setup involves the variation of three parameters:

1. Support type (ST): cross support (C), rod support (R) and block support (B)
2. Filling level (FL): weak (W), medium (M) and strong (S)
3. Bottom cutting height ( $h_{c,b}$ ): 19 mm, 34 mm and 64 mm

The three chosen support types are standard configurations provided by the preparation software (Figure 5.15). As stated in chapter 4.3.2, the minimum use of support structures should be targeted for economic reasons. This was addressed by the filling level that considers the volume of necessary support structure and the second moment of inertia. The bottom cutting high ( $h_{c,b}$ ) marks the distance from the build platform to the contact point of cutting in z-direction – including the height of the support structures of 4 mm (Figure 5.14). In total, 27 different configurations of SLM samples were investigated and two similar test build jobs were fabricated.

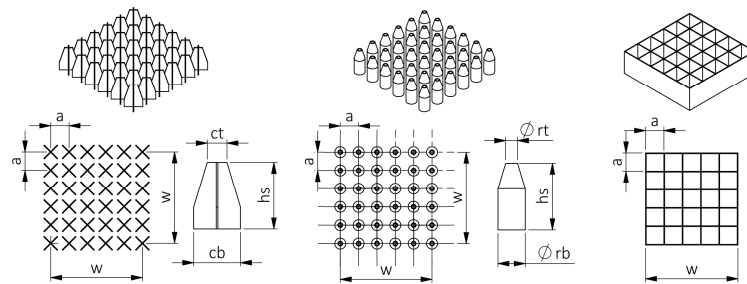


**Figure 5.15:** Different support types (ST) and characteristic values of the grid;  
Source: cf. Höller et al. (2020).

**Table 5.1:** Overview of the 27 different test specimen configurations for DM2 experiments.

Cutting height $h_{c,b}$	Type of support structure								
	Cross (C)			Rod (R)			Block (B)		
19 mm	W	M	S	W	M	S	W	M	S
34 mm	W	M	S	W	M	S	W	M	S
64 mm	W	M	S	W	M	S	W	M	S

To make the results comparable, all ST with the same FL had nearly the same volume. Due to the regular grid and its characteristics, it was impossible to avoid slight differences between the volumes.

**Table 5.2:** Overview of geometrical values for the ST configurations.

	Filling level		
	W	M	S
<b>General</b>			
Grid pattern	6x6	8x8	10x10
Grid distance a (mm)	2.74	1.96	1.52
Grid thickness t (μm)	100	100	100
Support height h <sub>s</sub> (mm)	4	4	4
Total grid width w (mm)	13.7	13.7	13.7
<b>Cross support</b>			
Volume V <sub>SC</sub> (mm <sup>3</sup> )	63.32	85.22	106.81
Cross length top c <sub>t</sub> (mm)	1.18	0.85	0.68
Cross length bottom c <sub>b</sub> (mm)	2.79	1.98	1.54
<b>Rod support</b>			
Volume V <sub>SR</sub> (mm <sup>3</sup> )	61.26	80.54	98.95
Rod diameter top Ø <sub>rt</sub> (mm)	0.71	0.54	0.44
Rod diameter bottom Ø <sub>rb</sub> (mm)	1.63	1.19	0.94
<b>Block support</b>			
Volume V <sub>SB</sub>	64.80	85.76	106.40

As can be seen in equation (5.15) and (5.16), the second moment of inertia  $I_x$  and  $I_y$  of the observed cross section has great influence for the bending stress. Failure due to bending stresses will most likely occur at two points. First, at the connection of the support structure with build platform at  $z_i = h_{c,b}$  (bottom cutting height). Second, at the transition zone between support structures and the SLM part at  $z_i = h_{c,t}$  (top cutting height), see Figure 5.14. The second area of inertia for the three ST was calculated with the theorem of Steiner, where  $n_{sx}$  and  $n_{sy}$  are the number of uniform cells along the cross section:

$$I_x = \sum_{i=1}^{n_{sx} * n_{sy}} (I_{x,i} + A_i * y_{ca}^2) \quad (5.19)$$

$$I_y = \sum_{i=1}^{n_{sx} * n_{sy}} (I_{y,i} + A_i * x_{ca}^2) \quad (5.20)$$

All three ST are symmetrical to their x- and y-axis. Therefore, the second area of inertia is

$$I_x = I_y = I_{x,y} \quad (5.21)$$

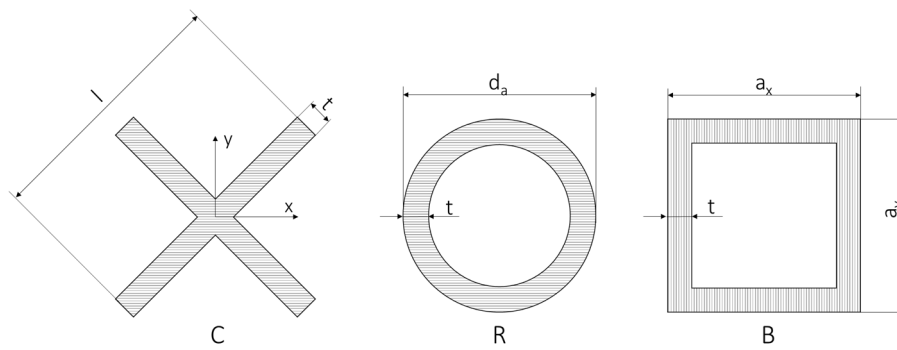


**Figure 5.16:** Single cell of cross, rod and block support;  
Source: own representation, based on Tiefnig (2019).

The  $I_{x,y}$  for a single support element (Figure 5.16) of C, R and B can be calculated as follows:

$$I_{x,y,cross} = (l^3 + (l - t) * t^2) * \frac{t}{12} \quad (5.22)$$

$$I_{x,y,rod} = \frac{\pi}{64} * (d_a^4 - (d_a - 2 * t)^4) \quad (5.23)$$

$$I_{x,y,block} = \frac{a_x * a_y^3}{12} - \frac{(a_x - t) * (a_y - t)^3}{12} \quad (5.24)$$

With equation (5.22)-(5.24), the second moment of inertia at both relevant positions –  $h_{c,b}$  and  $h_{c,t}$  – was calculated.

**Table 5.3:** Second moment of inertia  $I_{x,y}$  for the ST configurations.

	Filling level		
	W	M	S
<b>Cross support</b>			
$I_{x,y}$ top total (mm <sup>4</sup> )	178.63	206.28	241.03
$I_{x,y}$ bottom total (mm <sup>4</sup> )	438.51	500.94	572.71
<b>Rod support</b>			
$I_{x,y}$ top total (mm <sup>4</sup> )	151.43	177.99	204.10
$I_{x,y}$ bottom total (mm <sup>4</sup> )	383.99	444.00	506.82
<b>Block support</b>			
$I_{x,y}$ top/bottom total (mm <sup>4</sup> )	304.84	384.35	463.69

The values in Table 5.4 immediately reveal that the  $I_{x,y}$  for the C and R supports is significantly lower at the top compared to the B support. This indicates a critical zone for failure at the top of those support structures. The reason for the decrease of size in this area for C and R can be attributed to the idea of an easier removal of the support structures from the part. For DM, the load capacity is expected to be limited in this area.

For the milling experiments, the cutting parameters were adapted. An insert milling cutter with one insert (means one cutting edge) was chosen. The cutting parameters were supposed to represent practical values for cutting of 316L stainless steel. Again, the cutting depth  $a_{pf}$  was increased step by step from 0.1 mm to 1.5 mm. The experimental setup for the DM2 experiments can be seen in Figure 5.17.

**Table 5.4:** Cutting parameters for the DM2 experiments.

Tool	$v_c$ (m/min)	$f_z$ (mm/min)	$a_{pf}$ (mm)
Insert milling cutter d = 25 mm, one insert	100	0.05	0.1/0.25/0.5/ 1.0/1.5

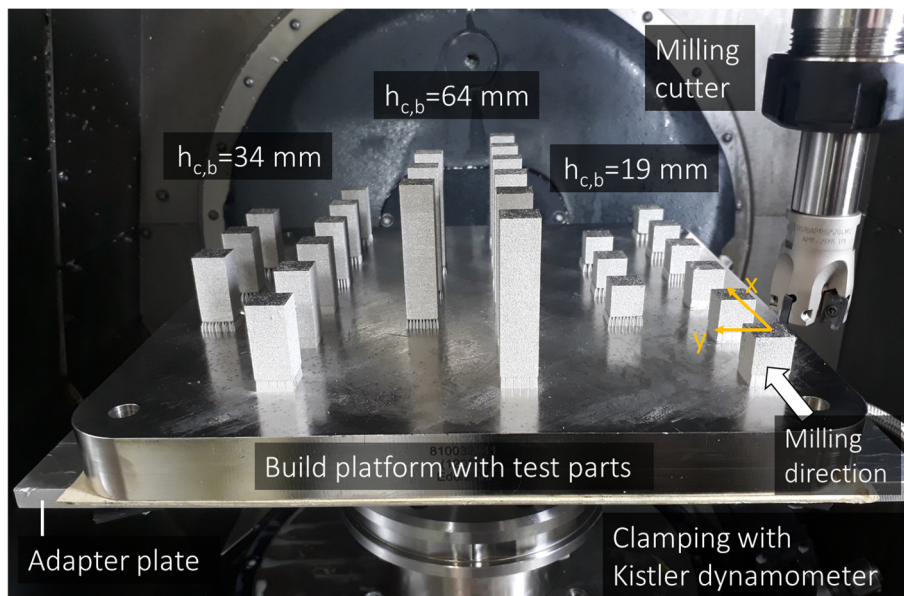


**Figure 5.17:** Experimental setup for the milling experiments (DM2);  
Source: own representation, modified from Höller et al. (2020).

#### 5.4.2 Results and Discussion of the Milling Experiments

The results of the plain face milling experiments revealed interesting findings regarding the load capacity of the observed configurations. Again,  $F_{res}$  rises with increasing  $a_{pf}$ . This clearly corresponds with the theoretical load model, since  $a_p$  directly influences the cutting force (see equation (5.3)). As expected, the filling level FL and the bottom cutting high  $h_{c,b}$  did not influence  $F_{res}$  significantly. However, in terms of load capacity, the different support structure configurations showed clearly different behaviors. Figure 5.18 shows the mean maximum

forces of  $F_{res}$  out of both observed TBJ 5 and 6 for test series DM2. The values for the maximum forces were derived from the recorded force time graph (Figure A 7, Appendix). For  $h_{c,b} = 19$  mm, failure (again marked with an “F”) occurred for  $a_{pf} = 0.5$  mm and FL weak – for the cross support type. The rod support failed later – at  $a_{pf} = 1.0$  mm for its weak configuration. The block support showed no failure for  $h_{c,b} = 19$  mm at all. The cutting forces were absorbed even for deep cutting depths of  $a_{pf} = 1.5$  mm for the block support.

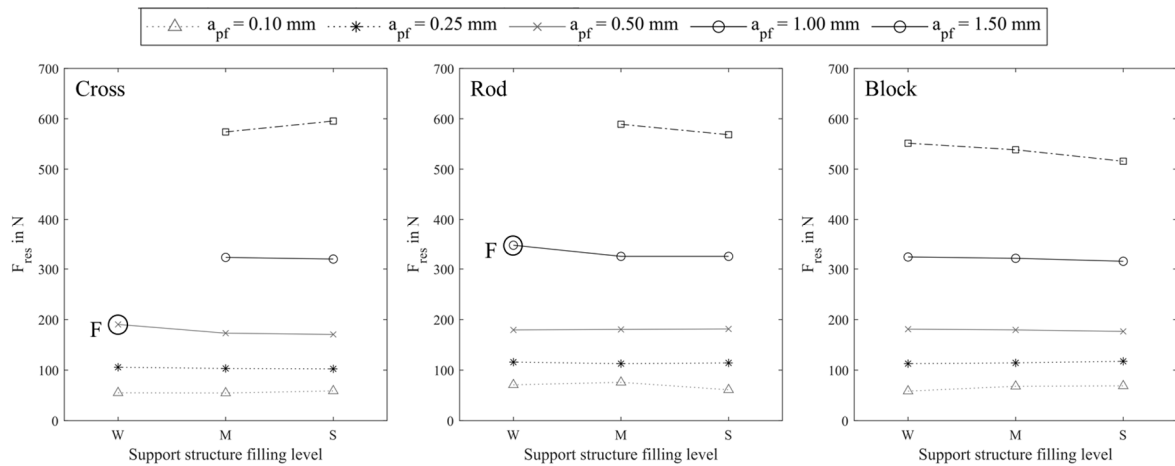


**Figure 5.18:** Maxima of  $F_{res}$  for  $h_{c,b} = 19$  mm for C, R and B supports and different filling levels; Source: own representation, cf. Höller et al. (2020).

Figure 5.19 shows the mean maximum forces of  $F_{res}$  for the  $h_{c,b} = 34$  mm. The increased cutting height clearly affects the failure behavior of the support structure configurations. Failure was observed earlier and more frequently compared to  $h_{c,b} = 19$  mm. The reason for this is that the cutting height directly influences the bending stress inside the support structures. Failures for the cross support were detected for all FL and none of the FL of the C support were able to withstand the cutting forces at  $a_{pf} = 1.5$  mm. For the rod support, only the strong filling level did not show any failure during the experiments for  $h_{c,b} = 34$  mm. However, the block support structure once more showed superior resistance against the cutting forces with the same volume of support structure.



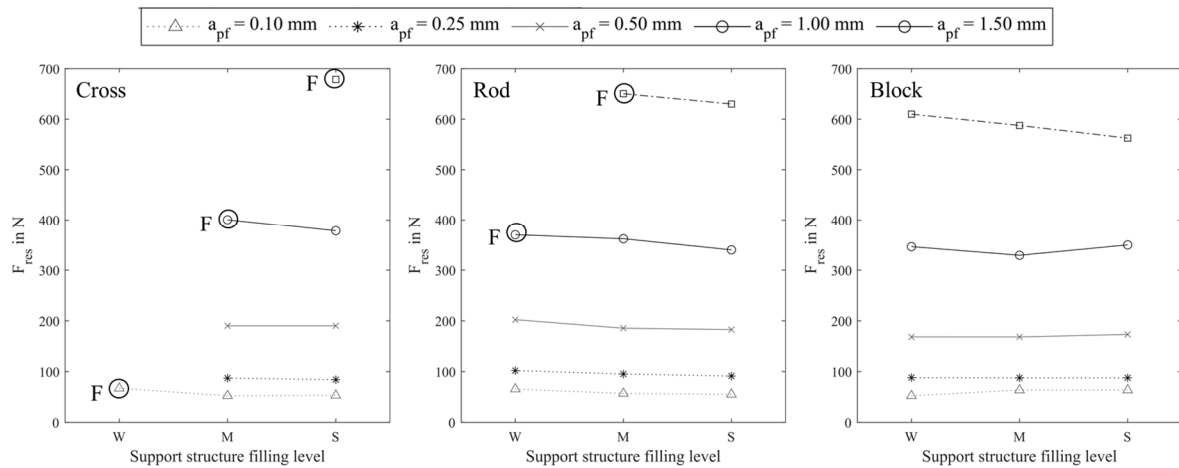


**Figure 5.19:** Maxima of  $F_{res}$  for  $h_{c,b} = 34$  mm for C, R and B supports and different filling levels; Source: own representation, cf. Höller et al. (2020).

An overview of the conducted results out of the DM2 experiments are shown in Table 5.5 which shows the values for  $a_{pf}$  and  $F_{res}$  where failure occurred and those configurations where no failure occurred– even for the highest cutting depth  $a_p = 1.5$  mm (marked in bold). It can be seen that the block support showed the highest load capacity of all configurations. Whereas the cross support showed the least ability to withstand the cutting forces. The rod support structure is preferable to the cross support when it comes to absorption of cutting forces. However, the values for  $h_{c,b} = 64$  mm should be interpreted with care. One reason for this is that failure occurred immediately at the first contact between the cutting edge and the test specimen. The other reason is that the presence of vibrations for this cutting high was clearly visible during the force measurements.

**Table 5.5:** Overview of results for DM2 experiments,  $F_{res}$  in N,  $a_{pf}$  in mm.

$h_{c,b}$	Filling level (FL)	Type of support structure (ST)					
		Cross (C)		Rod (R)		Block (B)	
		$a_{pf}$	$F_{res}$	$a_{pf}$	$F_{res}$	$a_{pf}$	$F_{res}$
19	W	0.5	190.3	1.0	347.1	<b>P</b>	<b>551.0</b>
	M	<b>P</b>	<b>574.5</b>	<b>P</b>	<b>589.2</b>	<b>P</b>	<b>538.5</b>
	S	<b>P</b>	<b>595.0</b>	<b>P</b>	<b>568.7</b>	<b>P</b>	<b>516.4</b>
34	W	0.1	67.2	1.0	375.1	<b>P</b>	<b>610.8</b>
	M	1.0	400.6	1.5	650.5	<b>P</b>	<b>588.8</b>
	S	1.5	678.6	<b>P</b>	<b>628.8</b>	<b>P</b>	<b>562.7</b>
64	W	0.1	63.1	0.1	79.6	0.25	150.3
	M	0.25	ND	0.25	148.3	1.0	358.1
	S	0.25	ND	1.5	462.2	1.5	746.0

*P* passed (no failure); *ND* not detectable;

With the results of Table 5.5, the theoretical bending stresses can be calculated for x- and y-axis of the specimens. The calculation follows the assumption, that both components –  $F_x$  and  $F_y$  – equally contribute to the formation of  $F_{res}$ . This means:

$$F_{x,i} = F_{y,i} = \frac{F_{res}}{\sqrt{2}} \quad (5.25)$$

This results in similar bending moments and – consequently – in similar bending stresses for the x- and y-axis:

$$\sigma_{bzx,i} = \sigma_{bzy,i} = \sigma_{bz,i} \quad (5.26)$$

Both bending stresses can be added to a total theoretical bending stress  $\sigma_{bzes,i}$  in any test specimen cross section:

$$\sigma_{bzes,i} = 2 \cdot \sigma_{bz,i} \quad (5.27)$$

Following that, the maximum theoretical bending stresses in the critical transition zone  $\sigma_{bzes,t}$  can be calculated with the values for  $F_{res}$  from Table 5.5, the second moment of inertia (top) from Table 5.2 and the perpendicular distance to the neutral axis  $e_{x,y} = 7$  mm (because of the side length of 14 mm square). For the calculation, only test specimens were considered that passed the DM2 experiments with the maximum cutting depth  $a_{pf} = 1.5$  mm (see Table 5.5). The top 5 configurations with regard to the highest values for  $\sigma_{bzes,t}$  can be seen in Table 5.6. Two machined surfaces (including failure) can be seen in the Appendix, Figure A 8.

**Table 5.6:** Highest calculated theoretical bending stress at  $h_{c,t}$ .

Config.	ST	FL	$h_{c,b}$ in mm	$h_{c,t}$ in mm	$I_{x,y}$ (top) in mm <sup>4</sup>	$F_{res}$ in N	$\sigma_{bzes,t}$ in N/mm <sup>2</sup>
1	R	S	34	30	204.10	628.8	<b>915.0</b>
2	B	W	34	30	304.84	610.8	<b>595.1</b>
3	R	M	19	15	177.99	589.2	<b>458.8</b>
4	B	S	34	30	463.69	588.8	<b>455.0</b>
5	C	M	19	15	206.28	574.5	<b>386.0</b>

The calculation of  $\sigma_{bzes,t}$  shows high theoretical bending stresses of the support structures in the critical zones. The values for  $\sigma_{bzes,t}$  are in the range of the as-built tensile strength ( $R_m = 582-648$  N/mm<sup>2</sup>,  $SD = 15$  N/mm<sup>2</sup>) and offset yield strength of SLM 316L ( $R_e = 470-$

510 N/mm<sup>2</sup>, SD = 5-31 N/mm<sup>2</sup>).<sup>233</sup> This strengthens the theory that support structures are able to deal with high loads due to the cutting process. However, the values for  $\sigma_{b_{zres,t}}$  should be seen as indicative for the load capacity only. First, they are calculated based on the maximum values for  $F_{res}$ . These maximum values of  $F_{res}$  are peak values that occur for a short time during the cutting operation. This also explains the high bending stress for configuration 1 from table Table 5.6, where the responsible  $F_{res}$  was of very short duration. Second, the complex process of cutting was simplified and only a single point of application was observed. During the plain face milling of a surface, the lines of action as well as the magnitudes of the involved forces constantly change. Together with the complex geometry of the support structures, DM is a challenging mechanical system. Therefore, torsional stresses were not calculated. This system demands for FE-analysis to fully understand the load situation. Initial FE simulations of DM were already carried out at the IFT (“Support Optimizer”) to understand the differences in the notch effect of C, R and B.<sup>234</sup> However, there is a need for further research to cover the topic of DM.

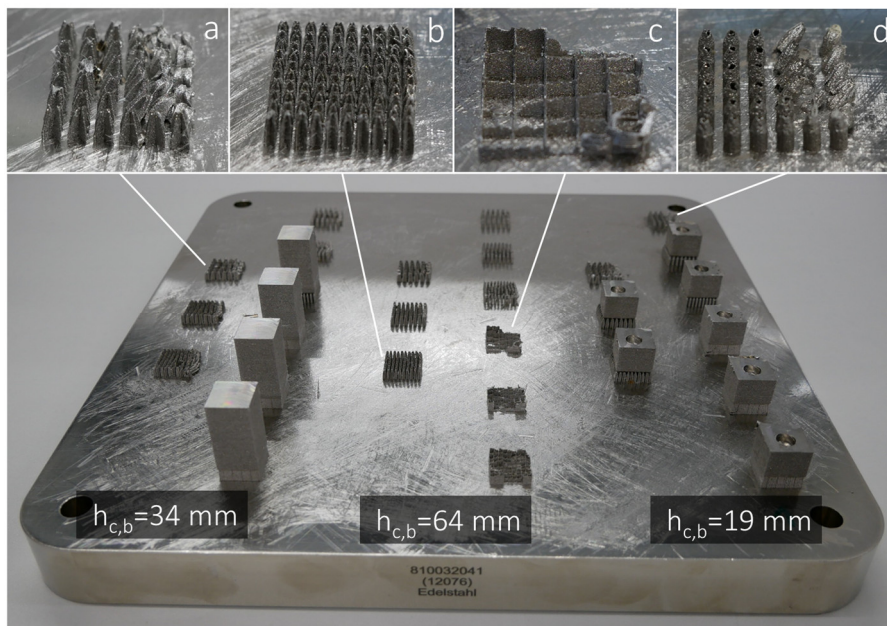


**Figure 5.20:** SLM build platform (TBJ 5) after DM2 milling experiments;  
Source: own representation, modified from Höller et al. (2020).

Findings from the visual inspection of the fracture zones confirm that breakage – as expected – primarily occurred at the transition zone between support structure and the cuboidal part

<sup>233</sup> SLM Solutions Group AG (2019).

<sup>234</sup> Tiefnig (2019).

at  $h_{c,t}$  for C and R support structures. This indicates that the lower  $I_{x,y}$  in this area favors breakage. For the block support,  $I_{x,y}$  is constant along the z-direction and breakage occurs more unevenly along the support structures (Figure 5.20).

The rod support structure showed higher load capacities compared to the cross support – despite the nearly similar  $I_{x,y}$ . This indicates that bending stresses are not the single failure criterion during face milling. Especially for torsional shear stresses, closed profiles are preferable when it comes to resistance against failure. This could explain the differences between rods – that are considered individually as closed profiles – and the cross supports (open profile, see Figure 5.15).

From a technical perspective, DM should produce milled surfaces that are comparable in terms of surface roughness with those of conventional milling. This requirement was investigated for the DM2 test series. For this, random test specimens of TBJ 5 and 6 were chosen and their surface roughness was exemplarily measured. In total, 30 measurements in longitudinal and transversal direction to the milling direction were conducted. The measurements were performed on intact surfaces, before failure could occur. The measurements were carried out with a Jenoptik Waveline W20 tactile roughness measurement device in accordance with the standard DIN EN ISO 4288<sup>235</sup> ( $\lambda_c = 0.8$  mm,  $l_n = 4$  mm,  $l_t = 4.8$  mm).

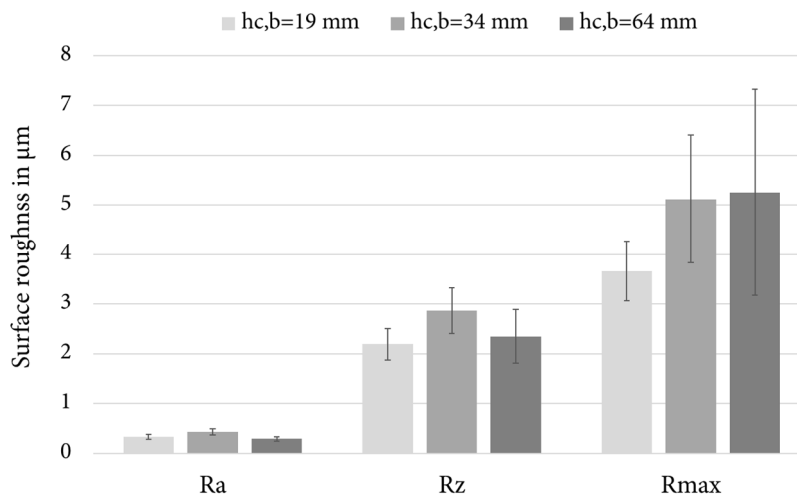


**Figure 5.21:** Mean values and SEM for Ra, Rz and Rmax for different bottom cutting heights;  
Source: own representation.

<sup>235</sup> DIN EN ISO 4288:1998-04 (1998).

Results show low surface roughness after DM (Figure 5.21). There was no clear influence of the cutting high  $h_{c,b}$  on the surface roughness detectable – same with the support structure type. The mean values for the observed surface roughness were:

- Arithmetic average roughness  $R_a = 0.288\text{-}0.429 \mu\text{m}$
- Average roughness depth  $R_z = 2.193\text{-}2.866 \mu\text{m}$
- Maximum roughness depth  $R_{\text{max}} = 3.664\text{-}5.255 \mu\text{m}$

These promising values correspond to those of finishing operations for traditional (face) milling ( $R_a = 0.2\text{-}2 \mu\text{m}^{236}$  and  $R_{\text{max}} = 10 \mu\text{m}^{237}$ ). These results encourage the use of DM for post-processing and finishing of SLM surfaces from a technical point of view.

## 5.5 Economic Evaluation of Direct Machining

The idea and the technical feasibility – including first optimizations – of DM were stated in the previous chapters. In this chapter, the economic reasonability will be discussed. For this, the expected savings in setup time for clamping or tactile touching will be quantified and evaluated.

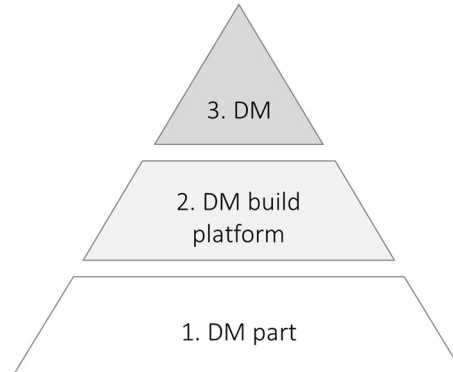


**Figure 5.22:** Levels of productivity for DM;  
Source: own representation.

For the evaluation of DM, three levels of productivity can be defined. It follows the assumption of a small series production where several successive build platforms with the same part arrangement are manufactured. The task of mounting the build platform on the

---

<sup>236</sup> Cf. Bartz et al. (2000) p. 617.

<sup>237</sup> Cf. Dietrich (2016) p. 221.

machine bed (manually or automatically by a transport system) is not considered for these levels – only the step of machining is discussed.

### 1. Level: DM part

At this level, the location and orientation of each part on the mounted build platform has to be determined. This is usually done by tactile touching inside a CNC machine. After that, the CNC program is started and machining of each part takes place. This level is not efficient, since only the task of clamping is eliminated, but not the determination of the positions and orientations of the parts. Furthermore, the task of touching has to be repeated for every new build platform.

### 2. Level: DM build platform

The second level decreases the efforts for the positioning. The actual location of all parts on the build platform has to be checked for the first build platform (e.g. optically). For every consecutive build platform, only significant points (e.g. mounting holes) or parts on the build platform can be used. The validation of this significant points provides conclusions about the entire build platform. However, knowledge about the repeatability is a fundamental requirement. This level was achieved during experiments within the DM1 test series, where CAM was used for programming.

### 3. Level: DM

The highest level of DM productivity can be achieved if the machining of the parts on the build platform and the evaluation of the position and orientation has to be done only once – for checking reasons at the very first build platform. The mounting of the build platform is done with a zero-point clamping system. This ensures fast handling and exact positioning inside the CNC machine. Afterwards, the CAM machining process takes place. This level requires a high repeatability of the SLM process as well as well-considered machining allowances.

To evaluate the economic potential of DM, the IFT cost model was used. Furthermore, DM in level 3 was chosen for the calculation. This means a stable and accurate SLM production. For the evaluation, a mock build job of the jet engine bracket (chapter 3.3.2) was selected and CNC milling and drilling were considered as necessary post-processing procedures.

#### **Initial situation:**

- Number of parts per build platform: 16 jet engine brackets

- Milling operations: profile milling, pocket milling and drilling (Figure 5.23)

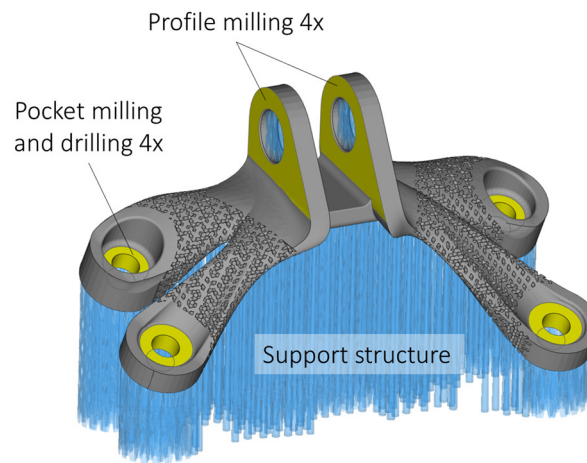


**Figure 5.23:** Machining operations for the jet engine bracket;  
Source: own representation.

For the calculation, assumptions and simplification were made to consider the differences between DM and separate machining (SM). The considered differences and their related estimations are listed in Table 5.7 for DM and in Table 5.8 for SM. These assumptions also consider learning effects, for instance for the adjustment of the CAM program or for faster clamping due to gained routine. Since less tool paths and tool changes are necessary, the machining time per bracket for DM is lower compared to SM. All operations during the manufacturing process that are not explicitly mentioned here, such as the build process, heat treatment or the removal of support structures are similar for both – DM and SM.

**Table 5.7:** Assumptions for DM.

	Affected costs	Number of build jobs					
		1	2	3	4	5	6
<b>1. Preprocessing</b>							
1.1 CAM programming in h	$C_{Pre,L} / C_{Pre,HS}$	5.00	3.00	0.50	0	0	0
<b>2. Processing</b>							
assumption: no differences DM/SM							
<b>3. Post-processing</b>							
3.1 Measurement (accuracy check), time in h for labor and the measurement device	$C_{Pos,M} / C_{Pos,L}$	6.00	3.00	0	0	0	0
3.2 Clamping and Positioning in h, labor and machine	$C_{Pos,M} / C_{Pos,L}$	0.50	0.30	0.10	0.10	0.10	0.10
3.3 Machining process in h, based on 6 min/#	$C_{Pos,M}$	1.77	1.90	1.60	1.60	1.60	1.60

**Table 5.8:** Assumptions for SM.

	Affected costs	Number of build jobs					
		1	2	3	4	5	6
<b>1. Preprocessing</b>							
1.1 CAM programming in h	$C_{Pre,L} / C_{Pre,HS}$	2.00	0.50	0.10	0	0	0
<b>2. Processing</b>							
assumption: no differences DM/SM							
<b>3. Post-processing</b>							
3.1 Measurement (accuracy check), time in h for labor and the measurement device	$C_{Pos,M} / C_{Pos,L}$	2.00	1.00	0	0	0	0
3.2 Clamping and Positioning in h, labor and machine	$C_{Pos,M} / C_{Pos,L}$	3.40	2.40	2.08	1.92	1.60	1.60
3.3 Machining process in h, based on 8 min/#	$C_{Pos,M}$	2.30	2.13	2.13	2.13	2.13	2.13

The evaluation of the manufacturing costs shows that DM can be seen as economically beneficial after the third consecutive build job (Figure 5.24). A closer look at the main cost shares in Figure 5.25 reveals the differences between DM and SM. At the beginning, additional efforts for CAM programming (pre-processing) and validation of the accuracy after the build process (post-processing) result in higher costs for DM. However, once a stable process is achieved, these costs no longer need to be taken into account.

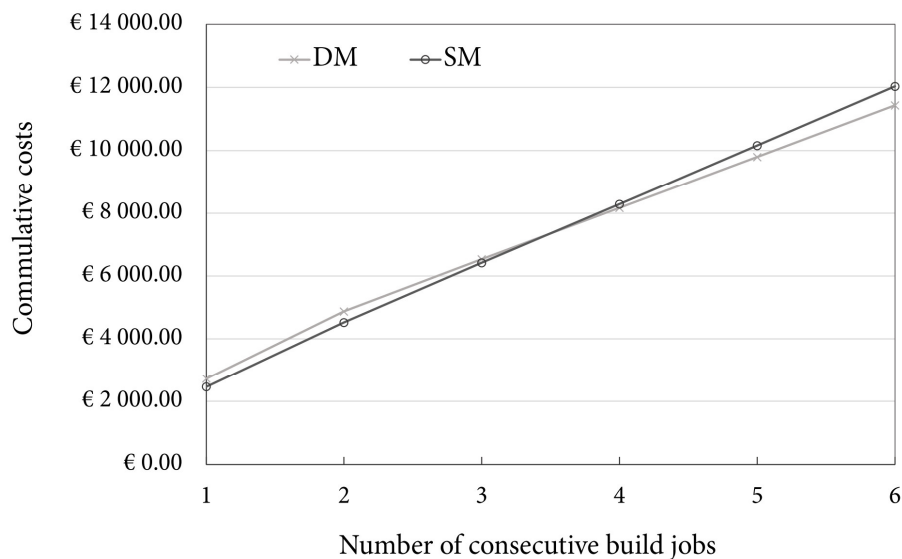


**Figure 5.24:** Accumulative costs for DM and SM for six consecutive build jobs; Source: own representation.



Furthermore, Figure 5.25 shows the positive impact of DM for post-processing. For SM, especially the clamping and positioning of fragile parts like the jet engine bracket takes time for the worker and increases the time where the CNC machine is occupied (post-processing). Also, costs for a special fixture for SM may become necessary to ensure proper clamping for SM (was not considered for this example).

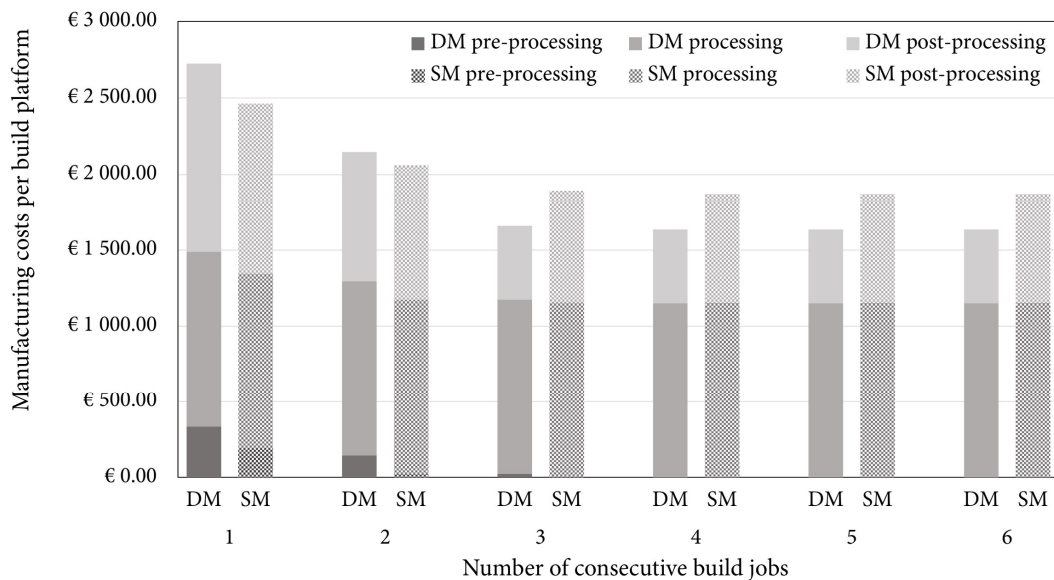


**Figure 5.25:** Comparison of main cost shares for DM and SM for six build jobs;  
Source: own representation.

Up to now, only a stable small series process of consecutive, similar build jobs was considered for DM. Nevertheless, the range of a beneficial use of DM can be extended. Especially for complex and highly individualized parts, special fixtures for CNC machining may become necessary for SM. The fabrication of the fixture can significantly increase the manufacturing costs, most notably for small quantities of SLM parts. For DM, special fixtures are not required because the support structures cover their task.

However, DM as a concept also has its limitations which will be addressed in the following:

1) Part orientation and accessibility:

If DM is considered for post-processing, the orientation of the parts on the build platform has to be adjusted to that. This DM related orientation can differ from positions that will be chosen for economic or anisotropic reasons. The accessibility of the tools on the concerning areas on the part have to be ensured and possible collisions between part and

tool must be prevented under all circumstances – especially for the use of 5-axis machining. Also, downfacing surfaces can only be machined in rare cases.

### 2) Removal of support structures:

DM does not make the removal of support structures obsolete – it will just take place in a later step of the process chain. If supported areas or downfacing surfaces from 1) have to be machined, SM must be done additionally. This would make DM and its benefits obsolete.

### 3) Geometrical accuracy:

Geometrical accuracy can be seen from two perspectives. On the one hand, the SLM process has to produce repeatable, accurate build jobs to ensure unerring DM post-processing. Nevertheless, adequate machining allowance has to be included in the part design.

On the other hand, the accuracy concerns also the parts after DM took place. Elastic deformation of the support structure during machining can lead to geometrical deviations. This effect was not studied within the presented test series. However, a rigid support structure (e.g. connected block support) and adequate cutting parameters decrease this risk. Furthermore, the mounting of a standard sized SLM build platform (280 x 280 mm<sup>2</sup>) can be challenging in terms of size and stability in common CNC machines. For this, a segmentation of the build platform and/or the use of a special zero-point clamping system must be considered. At the moment of writing, the author is aware of one recently launched system<sup>238</sup>.

From an economical perspective, the use of DM is a possible measure to increase economic efficiency. As a possible scenario, single part production – where special fixtures are required – can be named. But DM can also attribute to the request for a higher degree of automatization of SLM. Once a stable process is established, handling times can be decreased. And with the use of innovative clamping systems, the transferability between SLM and CNC machines can be managed efficiently.

---

<sup>238</sup> Peter Lehmann AG (2020).

## 5.6 Summary of Chapter 5

In this chapter, the novel approach of direct machining was introduced and studied scientifically. Limited part properties, like surface roughness or dimensional accuracy, require a machine finishing of the as-built SLM parts (see chapter 5.1.1).

DM allows the machining of SLM parts directly on the build platform if the support structures act as fixtures. For this, the occurring cutting forces and the stresses must be absorbed by the support structures. Results show, that the investigated support structures made of 316L are able to withstand high bending stresses and allow cutting with practically relevant speeds. Furthermore, the load capacity of different support structure configurations was investigated. When it comes to DM, a rigid and connected support type – like the block support – should be chosen. This support type showed high resistance and stability during the experiments – even for the lowest filling level. Measurements of the surface roughness showed that the machined surfaces with DM plain face milling are equivalent to those from traditional milling. Both, the load capacity of the support structures and the smooth surface confirm the technical feasibility of DM.

From an economic perspective, DM was shown advantageous after three consecutive build jobs compared to separate machining for a representative build job. However, the importance of a stable process (repeatability of build jobs) for DM is emphasized by the author. When special fixtures are necessary for machining, DM can be beneficial also for small quantities or single part production, where a stable process is not a key requirement.

## 6 CONCLUSION AND OUTLOOK

SLM offers unique possibilities for the design and production of parts and products. It has the ability to change and create new business models and to complement the spectrum of established manufacturing technologies. Remarkable annual growth rates underline the increasing interest in this technology. However, the dissemination of SLM as a manufacturing technology is still low within the manufacturing industry – for two main reasons. First, the economic efficiency of SLM is limited. Apart from its disruptive potential, SLM is associated with high manufacturing costs and low productivity – two issues that are highly disadvantageous for modern production. Second, companies quite often lack technical expertise. AM – and SLM in particular – require specific design and cost considerations beyond the realm of traditional manufacturing.

This thesis addresses these issues and presents concepts to increase the productivity as well as approaches towards a more efficient use of SLM. For this, the whole SLM process chain was observed. For each main process step, a research question was developed and investigated (see chapters 3, 4 and 5). The main findings will be presented and research questions will be answered in the following subchapters.

### 6.1 Pre-Processing: Costs and Economic Appraisal

**RQ1: “How can pre-processing – and especially design for additive manufacturing (DfAM) in particular – positively influence the economic perspective on SLM parts?”**

Chapter 3 covered the production costs on SLM. Findings from literature show that a cause-based allocation of costs during the manufacturing is essential for SLM and its flexibility in production. With the use of the IFT cost model, main cost drivers for SLM were identified for three representative build jobs.

Machine costs were found as a main cost driver. They attribute 36-67 % to the manufacturing costs, followed by labor costs (29-45 %). Especially the high labor costs emphasize the low grade of automatization of SLM. Further results show, that scale effects – named as micro-economies of scale – are achievable with SLM. These effects were highly significant for the very first build platform where manufacturing costs fell up to 85 % from single part manufacturing to a fully utilized build platform. However, the effect of micro-economies of scale decreased dramatically after the first build platform. Along with that, the often cited

cost independence from the lot size for AM was refuted. These facts should be taken into account when it comes to cost considerations during pre-processing.

The importance of the selection process of potential SLM parts during pre-processing was understood by looking at two cases from industry. This selection has to be structured, quantifiable and should also include cost estimations. The use of a replicable assessment method – as the developed screening process model (SPM) – has proven as highly beneficial. With the use of this model, it was possible to select five highly potential parts out of 120 possible parts. The identification of promising parts reduces the risk of unnecessary consequential costs for development and increases the possibility of creating successful parts – also from an economic viewpoint.

During pre-processing, the design of the SLM part is defined. The use of SLM can rarely be justified by lower initial manufacturing costs. Accordingly, the importance of DfAM is frequently emphasized in the literature but its economic implication is rarely studied. Thus, DfAM should not be carried out for its own sake. Benefits, that are enabled by DfAM, have to be made quantifiable as good as possible. Lifecycle costing, as shown in chapter 3, is an adequate method to quantify the DfAM enabled benefits beyond manufacturing costs.

In conclusion, the answer to **RQ1** can be summarized as follows:

DfAM and its related benefits have to be complemented with an economic appraisal. Within the pre-processing phase, cost estimations (early stage) and cost calculations (later stage) evaluate the economic potential of SLM as a manufacturing technology, as soon as suitable parts have been identified. Without that, frequently used terms related to SLM, like added-value, will remain blurred. Nevertheless, economically reasonable SLM parts are achievable. Along with DfAM, two basic requirements are necessary:

1. Know your costs and their interrelationships (cost driver, lot size dependency etc.)
2. Select the right parts via a structured approach before DfAM is carried out

## 6.2 Processing: 316L Economy

**RQ2: “How can the choice of newly developed parameters for 316L stainless steel have a positive influence on economic efficiency?”**

Published literature describes how the development of new SLM parameters for various materials can increase the build-up rate. Similar research can be found concerning the

reduction of the downskin angle. However, only a limited number of studies properly discusses the increase of productivity. Especially, the positive impact of the downskin angle on the manufacturing costs has been identified as a research gap.

To answer **RQ2**, the positive impact of 316L on the productivity is clearly stated. For 316L, a comparable output of trombones (criteria: relative density) was achieved through lower input (criteria: less manufacturing costs). Depending on the lot size, an increase in productivity of 40-50 % was observed. The positive effect of the minimization of the support structures contributes about 2/3 of the overall increase in productivity whereas the increase of the build-up rate is responsible for the remaining 1/3. Once again, all savings can be achieved without additional machine investment – just by the conscious variation of SLM parameters. Of course, this requires knowledge, experimental efforts and most of all the possibility to adjust parameters on the SLM machine, which only few manufactures on the market allow. Knowledge also means target-oriented use of SLM technology. It should be critically questioned whether full part density is always necessary. If 98.5 % or less is sufficient, even higher cost benefits can be realized through adapted parameter configurations for SLM.

### 6.3 Post-Processing: Direct Machining

**RQ3: “How can the step of subtractive post-processing be made more efficient?”**

Post-processing with machining procedures was identified as a crucial cost factor for SLM in chapter 3. The often insufficient as-built quality of SLM parts demands for machining processes. In practical applications, functional surfaces, accurately positioned features and part tolerances are created with CNC machines after the build process. Today, this requires many manual tasks, like clamping, positioning and touching of the SLM parts. Looking towards a higher level of automatization, the novel concept of direct machining was elaborated.

Two basic prerequisites for the feasibility of DM were identified:

1. Sufficiently high repeatability of the SLM process
2. Absorption of the cutting forces by support structures

Findings from chapter 5 show that both requirements were fulfilled during the experiments of DM test series 1. Along with this, the importance of a calibrated laser system should be

emphasized. Block support structure was found as especially preferable for DM. Its rigid, connected structure allows the absorption of high cutting forces- even for low filling levels. This corresponds with the developed theoretical load model. From the perspective of quality, machined surfaces after DM showed low surface roughness, comparable with the finishing process of traditional milling.

From an economical perspective, DM increases the productivity due to less handling time. Because of higher initial efforts for accuracy checks and pre-processing, DM requires multiple consecutive build jobs to be more efficient than the separate machining of SLM parts.

To answer **RQ3**, fundamental findings from the research conducted confirm that DM is

- a) technically feasible and
- b) can increase the efficiency of SLM post-processing. An increase of economic efficiency can be reached if:
  - higher initial costs for DM (CAM, measurement tasks) compared to SM are compensated by cost advantages due to less handling times (stable production) and/or
  - fixtures are eliminated.

It should be emphasized that all features to be machined must be accessible for DM. If separate machining is still required to obtain the final contour, the concept of DM becomes obsolete.

### 6.4 Synthesis of the Approaches

For reasons of clarity, the three approaches were described separately throughout this thesis. This chapter should link these approaches for a joint conclusion.

As intended, these approaches were worked out chronologically along the SLM process chain. Thus, they can be used individually but also in any possible combination. The central statements and recommendations out of the conducted research are listed in Figure 6.1.

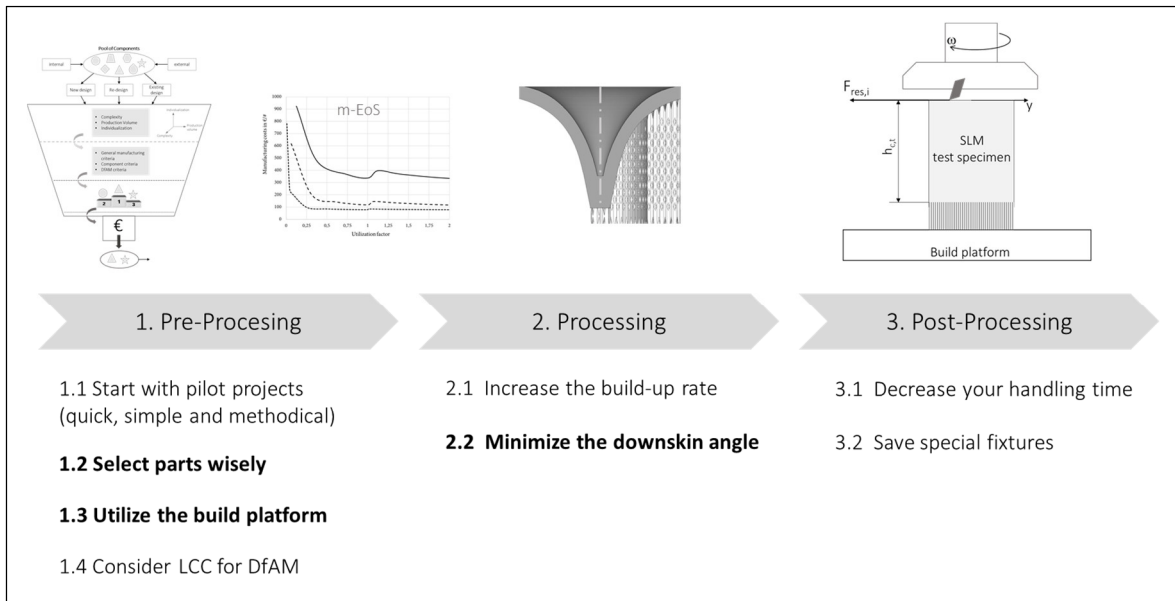


**Figure 6.1:** Central statements of the thesis along the SLM process chain;  
Source: own representation.

However, the potential towards higher productivity for the different approaches differs. For this, the top three approaches with regard to productivity – in the opinion of the author – are listed in bold in Figure 6.1.

#### ad 1.2 Select parts wisely

A well-executed selection process prepares the basis for successful SLM components and at the same time reduces the effort for those parts that are not promising. Although its impact on the productivity is hard to quantify by numbers, the selection process – once established – attributes absolutely positive to pre-processing.

#### ad 1.3 Utilize your build platform

Utilization of the first build platform leads to direct and immediate cost advantages. Of course, this has to be done in accordance with the order situation in a company. Nevertheless, scale effects should be used – also for SLM.

#### ad 2.2 Minimize the downskin angle

Economic benefits due to less support structures are a direct way to increase the productivity significantly. Of course, if DM is planned for post-processing, the amount of support structures has to be adapted.

The reason why DM was not chosen for the top three list is that there is still a way to go to fully identify its economic potential. Whereas a direct quantification of cost savings is simple



for the reduction of fixtures, it is more difficult for a full implementation of DM in a small series production. Statements about cost benefits from that scenario are limited in this study, because they are based on estimations only. From a technical perspective, the part accuracy – in addition to the surface roughness – should be investigated.

How this thesis contributes to the issue of higher productivity for SLM was presented up to now. Great importance was attached to the fact that the concepts were developed for a standard SLM infrastructure. Therefore, the described approaches are not restricted to a specific target group and can be beneficial to every SLM user who is interested in improving their productivity. Depending on the existing infrastructure, these approaches can be implemented directly or can serve as a basis for further developments.

### **6.5 Outlook and Future Tasks**

Starting with concepts for pre-processing, the developed screening process model (SPM) should be utilized in further use cases to test its suitability in different companies and to elaborate it further. Generally, the implementation of SLM and the transfer of necessary knowledge into companies should be accompanied more often by academic and other comparable institutions. Aided by an independent academic perspective, first pilot projects could be started and elaborated together and awareness would be created. As a result, a steep learning curve – in terms of rapid growth of knowledge – could be achieved and an economically reasonable use of SLM could be reached earlier.

For the step of processing, the presented findings are limited to 316L stainless steel. Clearly, the study of advanced parameter configurations and their economic impact can be expanded to further SLM materials. Thinking ahead, the adjustment of parameters should be more individualized. Freedom of design for SLM also means unique part properties, like graded porosity inside a part or a different local surface morphology. Therefore, the adjustment of parameters during pre-processing should be made possible by sections instead of the whole part. What is possible today only with detours, will hopefully become easier in the future, by the use of modern pre-processing software. This corresponds with the concept of DfAM and leads to a better exploitation of SLM potentials.

The feasibility of DM was demonstrated, now the time has come to test the concept within a production environment. The elaboration of further studies with more complex SLM parts in combination with innovative clamping systems is necessary to study its practical

relevance. A good opportunity for this would be in modern research environments, as available at the IFT, where the whole DM process chain can be covered – from data generation to measurement and up to CNC machining.

Regarding software application, the implementation of DM into a program for build job preparation would be highly interesting. This means two things. First, the generation of the support structure is done with regard to later DM, not only due to downskin specifications and heat dissipation. Second, CAM functionalities are already implemented in the preparation software. This means, that the later CNC machining processes are already defined during build job preparation and no additional CAM software is required. With knowledge of the load capacity – as studied in this thesis – a sort of heat map could be created by the software based on FEA. This heat map could show critical zones caused by the expected cutting forces for the previous selected machining processes. As a result, additive and subtractive manufacturing could be prepared simultaneously with the same software. These are not just thoughts about the future; initial discussions on this subject have already been held with an established software developer.

From prototyping to production – SLM has made rapid progress in recent years. And still there is a way to go. Productivity and economic efficiency are crucial for the future success of the technology. However, the growing interest and the extensive efforts of industry and academia are pushing SLM forward. Moreover, its flexibility and adaptability fit the requirements of the tomorrow's digital factory – good prerequisites for the future of SLM.



## LIST OF FIGURES

Figure 1.1: Basic structure of the thesis; Source: own representation. ....	8
Figure 2.1: Basic classification of manufacturing technologies; Source: own representation.....	10
Figure 2.2: Main categories of manufacturing technologies based on DIN 8580; Source: own representation, based on DIN 8580:2003-09 (2003).....	11
Figure 2.3: Classification of AM processes based on the initial state of raw material; Source: own representation. ....	12
Figure 2.4: General process chain of AM; Source: modified from Kumke (2018) p. 10.....	14
Figure 2.5: Relationship between costs and complexity (left) and production volume (right) of AM and CM; Source: own representation, adapted from Klahn et al. (2018) p. 14 and Poprawe et al. (2015) p. 51. ....	19
Figure 2.6: Fields of application and possible benefits of AM along the value chain; Source: own representation, adapted from Klahn et al. (2018) p. 73.....	21
Figure 2.7: Schematic principle of the SLM build process – layer-by-layer sequence; Source: own representation. ....	25
Figure 2.8: Schematic melting process and basic parameters for SLM; Source: own representation. ....	27
Figure 2.9: Stair-step effect for high layer thickness (left) and small layer thickness (right); Source: own representation. ....	29
Figure 2.10: General definition of productivity with examples for output and input; Source: own representation, adapted from Durdyev et al. ....	32
Figure 2.11: Schematic sequence of the laser scanning; Source: own representation. ....	35
Figure 2.12: Selection of typical hatching patterns for SLM; Source: own representation.....	36
Figure 2.13: Classification of DfAM approaches; Source: own representation, adapted and modified from Kumke (2018) p. 43. ....	39
Figure 3.1: Cost comparison of AM with IM for the small lever; Source: Hopkinson and Dickens (2003) p. 38. ....	44
Figure 3.2: Saw tooth curve of costs per part for the lever; Source: Ruffo et al. (2006) p. 1423.....	45
Figure 3.3: Schematic structure of the lifecycle costs; Source: own representation, modified from Ehrlenspiel et al. (2007) p. 113.....	49
Figure 3.4: Main types of costs along the SLM process chain for the calculation of the manufacturing costs with IFT cost model; Source: own representation.....	52
Figure 3.5: Overview of the prepared jet engine brackets (16 parts) for SLM; Source: own representation. ....	59
Figure 3.6: Cost shares of manufacturing costs of one jet engine bracket ( $l_z = 50 \mu\text{m} / t_w = 0 \text{ s} / 16$ parts); Source: own representation. ....	60
Figure 3.7: Influence of different parameter configurations on the relationship between manufacturing costs and lot size for the jet engine bracket; Source: own representation.....	61
Figure 3.8: Overview of the prepared filter heads (8 parts) for SLM; Source: own representation.....	62

## List of Figures

---

Figure 3.9: Cost shares of manufacturing costs of one filter head ( $l_z = 50 \mu\text{m} / t_w = 0\text{s} / 8 \text{ parts}$ ); Source: own representation. ....	63
Figure 3.10: Influence of different parameter configurations on the relationship between manufacturing costs and lot size for the filter head; Source: own representation. ....	64
Figure 3.11: Overview of the prepared pipe sections (117 parts) for SLM; Source: own representation. ....	65
Figure 3.12: Cost shares of manufacturing costs of one pipe section ( $l_z = 50 \mu\text{m} / t_w = 0\text{s} / 117 \text{ parts}$ ); Source: own representation. ....	66
Figure 3.13: Influence of different parameter configurations on the relationship between manufacturing costs and lot size for the pipe section; Source: own representation. ....	66
Figure 3.14: Cost comparison for three different parts and micro-economies of scale effect; Source: own representation. ....	68
Figure 3.15: Comparison of cost shares of the three representative SLM parts of this chapter; Source: own representation. ....	71
Figure 3.16: Comparison of the initial design and the optimized SLM design. All values in the graph are related to one component; Source: own representation; modified from Karanovic (2018), p. 99. ....	76
Figure 3.17: The metal-AM transfer model (m-AMTM) for use case 2; Source: cf. Leitner (2020) p. 33. ....	81
Figure 3.18: Screening process model (SPM) for suitable AM components; Source: own representation, cf. Leitner (2020). ....	82
Figure 3.19: Main landing gear of the Piaggio P.180 Avanti II airplane; Source: Atzeni and Salmi (2012) p. 1151. ....	87
Figure 3.20: Comparison between design 1 (CM) and design 8 (SLM) for the major support component; Source: own representation, based on Hochreiter (2018). ....	89
Figure 3.21: Evaluation according to VDI 2225 for design 1 and design 8. The direction of the dotted arrow marks the impact of the LCC; Source: Own representation, based on VDI 2225. ....	93
Figure 4.1: Designations of angles and surfaces related to AM; Source: cf. ISO/ASTM 52911-1:2019 (2019), p. 2 and cf. VDI 3405-3: 2005 p. 5. ....	98
Figure 4.2: Comparison of downskin areas for different downskin angles, prepared with AD (above) and MM (below). A red cross marks aborted build jobs; Source: modified from R. Pichler et al. (2018). ....	100
Figure 4.3: Trombone specimen; Source: own representation. ....	100
Figure 4.4: SEM images of new 316L powder used for 316L economy; Source: own representation, with special thanks to FELMI Graz. ....	102
Figure 4.5: Scanning tracks parallel to the downskin surface; Source: own representation, cf. Cloots et al. (2017) p.363. ....	103
Figure 4.6: Overview of stage 1 experiments with trombones, pre-processed with MM; Source: own representation. ....	105
Figure 4.7: Similar results for both pre-processing programs for advanced PCs, pre-processed with Additive.Designer (left) and Materialise Magics (right); Source: own representation. ....	106
Figure 4.8: Results of the density measurements (mean values) for parameter configurations AD 1-30; Source: own representation. ....	108
Figure 4.9: Microsection of cubical specimens fabricated AD 10 (left) and AD 13 (right); Source: own representation. ....	109

## List of Figures

---

Figure 4.10: Microsection of cubical specimens fabricated AD 6 (left) and AD 21 (right); Source: own representation. ....	109
Figure 4.11: Microsection of cubical specimens fabricated AD 29 (left) and AD 30 (right); Source: own representation. ....	110
Figure 4.12: Overview of the experimental setup for trombones and cubes; Source: own representation. ....	111
Figure 4.13: left: investigated relationship between relative density and practical build-up rate VPr for selected parameter configurations; right: build-up rate increase compared to the standard parameter AD 10; Source: own representation. ....	112
Figure 4.14: Additional support structures for AD 10-13 (right half of the trombone) at downskin areas $\delta \leq 40^\circ$ to prevent build job termination; Source: own representation. ....	113
Figure 4.15: Comparison of manufacturing costs per trombone for different parameter configurations; Source: own representation. ....	113
Figure 5.1: Overview of the fabricated test build platform including 49 test parts; Source: own representation. ....	117
Figure 5.2: Basic workflow of preliminary experiments to determine the accuracy of SLM; Source: own representation. ....	118
Figure 5.3: Classification of the investigated length features (n = 59) according to ISO-2768-1; Source: own representation, cf. Höller et al. (2020). ....	119
Figure 5.4: Measured deviations (n = 29) from the nominal diameter of various holes and cylindrical specimens; Source: own representation, cf. Höller et al. (2020). ....	119
Figure 5.5: Measured deviations (n = 14) of flatness and angularity for specimens with different downskin angles; Source: own representation; cf. Hinterbuchner (2019). ....	120
Figure 5.6: Basic workflow of direct machining; Source: own representation, modified from Höller et al. (2019). ....	121
Figure 5.7: Deviation of the SLM process in x-direction (left) and y-direction (right) for four consecutive test build jobs (TBJ 1-4); Source: own representation, cf. Höller et al. (2019). ....	123
Figure 5.8: Experimental setup for the milling experiments (DM1-stage 2); Source: own representation, cf. Höller et al. (2019). ....	124
Figure 5.9: Test specimen with schematic overview of machining operations (above) and cutting parameters above left: cylinder, d = 20 mm, block support structure; above right: cuboid, l = 15 mm, Heartcell support structure; Source: own representation, cf. Höller et al. (2019). ....	125
Figure 5.10: Mean and maximum cutting forces for cylindrical test parts for face milling ( $a_{pf}$ ) and profile milling ( $a_{pp}$ ); Left: block support structures; right: Heartcell support structures; Source: own representation, cf. Höller et al. (2019). ....	126
Figure 5.11: Components of cutting forces; Source: Grote/Antonsson (2009) p. 612. ....	128
Figure 5.12: Variables of plain face milling; Source: Grote/Antonsson (2009) p. 621. ....	129
Figure 5.13: Components of the cutting force for plain face milling; Source: Grote/Antonsson (2009) p. 622. ....	130
Figure 5.14: Forces during plain face milling in a random point p; Source: own representation. ....	132
Figure 5.15: Different support types (ST) and characteristic values of the grid; Source: cf. Höller et al. (2020). ....	134
Figure 5.16: Single cell of cross, rod and block support; Source: own representation, based on Tiefnig (2019). ....	136

## List of Figures

---

Figure 5.17: Experimental setup for the milling experiments (DM2); Source: own representation, modified from Höller et al. (2020).....	137
Figure 5.18: Maxima of $F_{res}$ for $h_{c,b} = 19$ mm for C, R and B supports and different filling levels; Source: own representation, cf. Höller et al. (2020).....	138
Figure 5.19: Maxima of $F_{res}$ for $h_{c,b} = 34$ mm for C, R and B supports and different filling levels; Source: own representation, cf. Höller et al. (2020).....	139
Figure 5.20: SLM build platform (TBJ 5) after DM2 milling experiments; Source: own representation, modified from Höller et al. (2020).....	141
Figure 5.21: Mean values and SEM for $R_a$ , $R_z$ and $R_{max}$ for different bottom cutting heights; Source: own representation.....	142
Figure 5.22: Levels of productivity for DM; Source: own representation.....	143
Figure 5.23: Machining operations for the jet engine bracket; Source: own representation.....	145
Figure 5.24: Accumulative costs for DM and SM for six consecutive build jobs; Source: own representation.....	146
Figure 5.25: Comparison of main cost shares for DM and SM for six build jobs; Source: own representation.....	147
Figure 6.1: Central statements of the thesis along the SLM process chain; Source: own representation.....	154
Figure A 1: Hierarchy of problem statement for step 1 of the screening process model (SPM); Source: cf. Leitner (2020) p. 44.....	176
Figure A 2: Assessment of two possible parts; Source: Leitner (2020) p. 56.....	177
Figure A 3: Lifecycle analysis of the CM major support component; Source: cf. Hochreiter (2018) p. 63.....	178
Figure A 4: Lifecycle analysis of the AM major support component; Source: cf. Hochreiter (2018) p. 64.....	179
Figure A 5: Time-force graph for the drilling experiments for DM1 test series; Source: own representation.....	181
Figure A 6: Mean and maximum cutting forces for cuboid test parts for face milling ( $a_{pf}$ ) and profile milling ( $a_{pp}$ ); Left: block support structures; right: Heartcell support structures; Source: own representation, cf. Höller et al. (2019).....	181
Figure A 7: Force-time graph for two revolutions of the milling cutter with a single insert; Source: own representation, cf. Höller et al. (2020).....	182
Figure A 8: Exemplary macro pictures of two machined surfaces of different ST and FL during DM2 experiments; Source: own representation.....	182

## LIST OF TABLES

Table 2.1: Classification of AM processes into seven categories according to ISO/ASTM 52900 with a brief explanation and processable materials; Source: own representation, based on '.....	11
Table 2.2: Specific AM benefits as driver for added value; Source: cf. Klahn et al. (2018) p. 71.....	19
Table 2.3: Selection of processable materials for SLM; Source: based on Yap et al. (2015).....	29
Table 3.1: Primary input variables for the IFT cost model. ....	52
Table 3.2: Main type of costs for step 1: pre-processing.....	53
Table 3.3: Main type of costs for step 2: processing.....	53
Table 3.4: Main type of costs for step 3: post-processing.....	54
Table 3.5: Comparison of computed and real build time for 18 build jobs.....	57
Table 3.6: Overview of parameter variation for the three investigated parts. ....	58
Table 3.7: Parameter configuration and simulated build times for the jet engine bracket. ....	59
Table 3.8: Parameter configuration and simulated build times for the filter head.....	63
Table 3.9: Parameter configuration and simulated build times for the pipe section. ....	65
Table 3.10: Scheme of the developed assessment method with exemplary rating.....	74
Table 3.11: Overview of direct monetary (DM) and indirect monetary (IDM) benefits for SLM inlet-outlet manifold.....	77
Table 3.12: Estimation of assembly and supply chain costs for the initial manifold.....	78
Table 3.13: Estimation of assembly and supply chain costs for the optimized SLM manifold.....	78
Table 3.14: Summarized calculation of the NPV for design 1 and design 8.....	91
Table 4.1: Chemical composition in weight-% of the used 316L powder.....	101
Table 4.2: Overview of parameter configurations for test series 1.....	105
Table 4.3: Overview of the examined parameters and their value ranges.....	107
Table 5.1: Overview of the 27 different test specimen configurations for DM2 experiments. ....	134
Table 5.2: Overview of geometrical values for the ST configurations. ....	135
Table 5.3: Second moment of inertia $I_{x,y}$ for the ST configurations.....	136
Table 5.4: Cutting parameters for the DM2 experiments. ....	137
Table 5.5: Overview of results for DM2 experiments, $F_{res}$ in N, $a_{pf}$ in mm. ....	139
Table 5.6: Highest calculated theoretical bending stress at $h_{c,t}$ .....	140
Table 5.7: Assumptions for DM.....	145
Table 5.8: Assumptions for SM.....	146
Table A 1: Overview of the manufacturing costs for the jet engine bracket.....	175
Table A 2: Overview of the manufacturing costs for the filter head.....	175
Table A 3: Overview of the manufacturing costs for the pipe section.....	176
Table A 4: Technical value of the compared design 1 and 8 for the major support component; source: Hochreiter (2018). ....	180



## List of Tables

---

Table A 5: Economic value of the compared design 1 and 8 for the major support component; source: Hochreiter (2018). .....	180
Table A 6: Overview of all investigated parameter configurations for 316L economy.....	180

---

## REFERENCES

- Adam, G. (2015): Systematische Erarbeitung von Konstruktionsregeln für die additiven Fertigungsverfahren Lasersintern, Laserschmelzen und Fused Deposition Modeling, Dissertation, Paderborn University, Paderborn
- Afshari, E. / Ghambari, M. / Abdolmalek, H. (2017): Production of CuSn10 bronze powder from machining chips using jet milling, in: *The International Journal of Advanced Manufacturing Technology*, 92/1-4, pp. 663–672
- Ahmed / Majeed / Atta / Guozhu (2019): Dimensional Quality and Distortion Analysis of Thin-Walled Alloy Parts of AlSi10Mg Manufactured by Selective Laser Melting, in: *Journal of Manufacturing and Materials Processing*, 3/2, pp. 1–13
- Ameri, F. / Stecke, K. / Cieminski, G. von (2019): *Advances in Production Management Systems. Production Management for the Factory of the Future. IFIP WG 5.7 International Conference, APMS 2019, Austin, TX, USA, September 1–5, 2019, Proceedings, Part I, IFIP Advances in Information and Communication Technology*, Basel: Springer Nature Switzerland AG
- Ampower (2019): *Metal Additive Additive Manufacturing Report 2019, 2019*, retrieved from <https://additive-manufacturing-report.com/>, accessed February 19, 2020
- Atzeni, E. / Salmi, A. (2012): Economics of additive manufacturing for end-usable metal parts, in: *The International Journal of Advanced Manufacturing Technology*, 62/9-12, pp. 1147–1155
- Averkamp, H. (2020): What are production costs?, retrieved from <https://www.accountingcoach.com/blog/what-are-production-costs>, accessed September 9, 2020
- Barclift, M. / Joshi, S. / Simpson, T. / Dickman, C. (2016): Cost Modeling and Depreciation for Reused Powder Feedstocks in Powder Bed Fusion Additive Manufacturing, in: *Proceedings of the 27th Annual International Solid Freeform Fabrication Symposium*, pp. 2007–2028
- Bartz, W. / Springer, G. / Blanke, H.-J. (eds.) (2000): *Expert Praxis-Lexikon Tribologie plus. 2010 Begriffe für Studium und Beruf*, 2<sup>nd</sup> ed., Renningen-Malmsheim: expert-Verl.
- Baumers, M. / Dickens, P. / Tuck, C. / Hague, R. (2016): The cost of additive manufacturing: machine productivity, economies of scale and technology-push, in: *Technological Forecasting and Social Change*, 102, pp. 193–201
- Baumers, M. / Holweg, M. (2019): On the economics of additive manufacturing: Experimental findings, in: *Journal of Operations Management*, 65/8, pp. 794–809
- Berger, U. / Hartmann, A. / Schmid, D. (2019): *3D-Druck - Additive Fertigungsverfahren. Rapid Prototyping, Rapid Tooling, Rapid Manufacturing*, 3<sup>rd</sup> ed., Haan-Gruiten: Verlag Europa-Lehrmittel
- Bhavar, V. / Kattire, P. / Patil, V. / Khot, S. / Gujar, K. / Singh, R. (2017): A review on powder bed fusion technology of metal additive manufacturing, in: Badiru, A. / Valencia, V. / Liu, D. (Hrsg.): *Additive Manufacturing Handbook*, CRC Press, pp. 251–253
- Bobbio, L. / Qin, S. / Dunbar, A. / Michaleris, P. / Beese, A. (2017): Characterization of the strength of support structures used in powder bed fusion additive manufacturing of Ti-6Al-4V, in: *Additive Manufacturing*, 14, pp. 60–68

## References

---

- Brecher, C. (ed.) (2015): *Advances in production technology*, Lecture Notes in Production Engineering, Cham: Springer Open, retrieved from <http://hdl.handle.net/10419/182307>
- Brecher, C. / Özdemir, D. (eds.) (2017): *Integrative production technology. Theory and applications*, Cham, Switzerland: Springer, retrieved from <http://www.springer.com/>
- Bremen, S. / Buchbinder, D. / Meiners, W. / Wissenbach, K. (2011): *Mit Selective Laser Melting auf dem Weg zur Serienproduktion?*, in: *Laser Technik Journal*, 8/6, pp. 24–28
- Brischetto, S. / Maggiore, P. / Ferro, C. (eds.) (2017): *Additive manufacturing technologies and applications*, Basel et al.: MDPI, retrieved from <https://www.doabooks.org/doab?func=fulltext&uiLanguage=en&rid=24927>
- Buchbinder, D. / Schleifenbaum, H. / Heidrich, S. / Meiners, W. / Bültmann, J. (2011): *High Power Selective Laser Melting (HP SLM) of Aluminum Parts*, in: *Physics Procedia*, 12, pp. 271–278
- Burns, M. (1993): *Automated fabrication. Improving productivity in manufacturing*, Englewood Cliffs, N.J.: PTR Prentice Hall
- Campbell, I. / H. Jee / Y.S. Kim (2013): *Adding product value through additive manufacturing*
- Chekurov, S. (2019): *Categorization of Design for Additive Manufacturing Concepts*, in: *Conference Proceedings - ASME 2019 International Mechanical Engineering Congress and Exposition, Volume 14: Design, Systems, and Complexity*
- Cherry, J. / Davies, H. / Mehmood, S. / Lavery, N. / Brown, S. / Sienz, J. (2015): *Investigation into the effect of process parameters on microstructural and physical properties of 316L stainless steel parts by selective laser melting*, in: *The International Journal of Advanced Manufacturing Technology*, 76/5-8, pp. 869–879
- Choo, H. / Sham, K.-L. / Bohling, J. / Ngo, A. / Xiao, X. / Ren, Y. / Depond, P. / Matthews, M. / Garlea, E. (2019): *Effect of laser power on defect, texture, and microstructure of a laser powder bed fusion processed 316L stainless steel*, in: *Materials & Design*, 164, p. 107534
- Chua, C. / Leong, K. (2014): *3D Printing and Additive Manufacturing*, Singapore: World Scientific
- Cloots, M. / Zumofen, L. / Spierings, A. / Kirchheim, A. / Wegener, K. (2017): *Approaches to minimize overhang angles of SLM parts*, in: *Rapid Prototyping Journal*, 23/2, pp. 362–369
- Conner, B. / Manogharan, G. / Martof, A. / Rodomsky, L. / Rodomsky, C. / Jordan, D. / Limperos, J. (2014): *Making sense of 3-D printing: Creating a map of additive manufacturing products and services*, in: *Additive Manufacturing*, 1-4, pp. 64–76
- Cordovilla, F. / García-Beltrán, Á. / Garzón, M. / Muñoz, D. / Ocaña, J. (2018): *Numerical-Experimental Study of the Consolidation Phenomenon in the Selective Laser Melting Process with a Thermo-Fluidic Coupled Model*, in: *Materials (Basel, Switzerland)*, 11/8
- Denkena, B. / Tönshoff, H. (2011): *Spanen*, Berlin, Heidelberg: Springer Berlin Heidelberg
- Deutsche Edelstahlwerke Specialty Steel GmbH & Co. KG (2016): *Material Datasheet X2CrNiMo17-12-21.4404*, retrieved from [https://www.dew-stahl.com/fileadmin/files/dew-stahl.com/documents/Publikationen/Werkstoffdatenblaetter/RSH/1.4404\\_de.pdf](https://www.dew-stahl.com/fileadmin/files/dew-stahl.com/documents/Publikationen/Werkstoffdatenblaetter/RSH/1.4404_de.pdf), accessed September 9, 2020
- Dietrich, J. (2016): *Praxis der Zerspantechnik*, Wiesbaden: Springer Fachmedien Wiesbaden

## References

---

- DIN 6584:1982-10 (1982): Terms of the cutting technique; forces, energy, work, power, 1982, Berlin: Beuth Verlag GmbH
- DIN 8580:2003-09 (2003): Manufacturing processes - Terms and definitions, division, 2003, Berlin: Beuth Verlag GmbH
- DIN EN ISO 4288:1998-04 (1998): Geometrical Product Specifications (GPS) - Surface texture: Profile method - Rules and procedures for the assessment of surface texture (ISO 4288:1996), 1998, Berlin: Beuth Verlag GmbH
- Durdyev, S. / Ismail, S. / Kandymov, N. (2018): Structural Equation Model of the Factors Affecting Construction Labor Productivity, in: Journal of Construction Engineering and Management, 144/4, p. 4018007
- Ehrlenspiel, K. / Kiewert, A. / Hundal, M. / Lindemann, U. (2007): Cost-efficient design, Heidelberg/New York: Springer
- Ehrlenspiel, K. / Kiewert, A. / Lindemann, U. / Mörtl, M. (2014): Kostengünstig Entwickeln und Konstruieren, Berlin, Heidelberg: Springer Berlin Heidelberg
- EOS GmbH (2019): EOS M 400 Series, Production Platform for Additive Manufacturing of High-Quality Metal Parts, retrieved from [https://www.eos.info/03\\_system-related-assets/system-related-contents/\\_pdf\\_system-data-sheets/eos\\_system\\_data\\_sheet\\_eos\\_m\\_400-4\\_en.pdf](https://www.eos.info/03_system-related-assets/system-related-contents/_pdf_system-data-sheets/eos_system_data_sheet_eos_m_400-4_en.pdf), accessed September 9, 2020
- Esmailian, B. / Behdad, S. / Wang, B. (2016): The evolution and future of manufacturing: A review, in: Journal of Manufacturing Systems, 39, pp. 79–100
- Fayazfar, H. / Salarian, M. / Rogalsky, A. / Sarker, D. / Russo, P. / Paserin, V. / Toyserkani, E. (2018): A critical review of powder-based additive manufacturing of ferrous alloys: Process parameters, microstructure and mechanical properties, in: Materials & Design, 144, pp. 98–128
- Ferrage, L. / Bertrand, G. / Lenormand, P. / Grossin, D. / Ben-Nissan, B. (2017): A review of the additive manufacturing (3DP) of bioceramics: alumina, zirconia (PSZ) and hydroxyapatite, in: Journal of the Australian Ceramic Society, 53/1, pp. 11–20
- Forbes (2019): Global 3D printing products and services market size from 2020 to 2024 (in billion U.S. dollars), March 27, 2019, retrieved from <https://www.statista.com/statistics/315386/global-market-for-3d-printers/>, accessed September 9, 2020
- Frenz, W. (1963): Beitrag zur Messung der Produktivität und deren Vergleich auf der Grundlage technischer Mengengrößen, Forschungsberichte des Landes Nordrhein-Westfalen, vol. 1228, Wiesbaden: VS Verlag für Sozialwissenschaften
- Gabler Wirtschaftslexikon (2020): Wirtschaftlichkeit, retrieved from <https://wirtschaftslexikon.gabler.de/definition/wirtschaftlichkeit-47252/version-270518>, accessed September 9, 2020
- GE Additive (2020): Direct Metal Laser Melting (DMLM) machines, retrieved from <https://www.ge.com/additive/additive-manufacturing/machines/dmlm-machines/x-line-2000r>, accessed September 9, 2020
- Gebhardt, A. (2011): Understanding additive manufacturing. Rapid prototyping, rapid tooling, rapid manufacturing, München: Hanser

## References

---

- Gebhardt, A. / Hötter, J.-S. (2016): Additive manufacturing. 3D printing for prototyping and manufacturing, Munich et al.: Hanser Publications
- Gehrke, L. / Kühn, A. / Rule, D. / Moore, P. / Bellmann, C. / Siemes, S. / Dawood, D. / Kulik, J. / Standley, M. (2015): A Discussion of Qualifications and Skills in the Factory of the Future: A German and American Perspective, in:
- German Machine Tool Builders' Association (2019): Market Report 2018. The German Machine Tool Industry and its Position in the World Market, 2019, retrieved from [https://vdw.de/wp-content/uploads/2019/07/pub\\_vdw-marktbericht\\_2018-2.pdf](https://vdw.de/wp-content/uploads/2019/07/pub_vdw-marktbericht_2018-2.pdf), accessed February 19, 2020
- Gibson, I. / Rosen, D. / Stucker, B. (2015): Additive Manufacturing Technologies, New York, NY: Springer New York
- Glossary of Industrial Organisation Economics and Competition Law (1993), 1993, retrieved from <http://www.oecd.org/regreform/sectors/2376087.pdf>
- Goharian, A. (2019): Porous Osseointegrative Layering for Enhancement of Osseointegration, in: : Osseointegration of Orthopaedic Implants, Elsevier, pp. 141–162
- GrabCAD (2013): GE Challenge - Charlie Pyott, retrieved from <https://grabcad.com/library/ge-challenge-charlie-pyott-1>, accessed September 9, 2020
- Groover, M. (2013): Fundamentals of modern manufacturing. Materials, processes, and systems, 5<sup>th</sup> ed., Hoboken, NJ: Wiley
- Grote, K.-H. / Antonsson, E. (2009): Springer handbook of mechanical engineering, Berlin: Springer
- Gu, D. / Meiners, W. / Wissenbach, K. / Poprawe, R. (2012): Laser additive manufacturing of metallic components: materials, processes and mechanisms, in: International Materials Reviews, 57/3, pp. 133–164
- Gu, H. / Gong, H. / Pal, D. / Rafi, H. / Starr, T. / Stucker, B. (2013): Influences of Energy Density on Porosity and Microstructure of Selective Laser Melted 17-4PH Stainless Steel, in: 24th International SFF Symposium - An Additive Manufacturing Conference, SFF 2013
- Gupta, M. (ed.) (2019): 3d printing of Metals, Basel: MDPI, retrieved from <http://www.mdpi.com/books/pdfview/book/1485>, accessed September 9, 2020
- Gusarov, A. / Grigoriev, S. / Volosova, M. / Melnik, Y. / Laskin, A. / Kotoban, D. / Okunkova, A. (2018): On productivity of laser additive manufacturing, in: Journal of Materials Processing Technology, 261, pp. 213–232
- Hamilton, K. (2016): Planning, preparing and producing: Walking the tightrope between additive and subtractive manufacturing, in: Metal AM, Vol. 2/1, pp. 39–56
- Hannibal, M. / Knight, G. (2018): Additive manufacturing and the global factory: Disruptive technologies and the location of international business, in: International Business Review, 27/6, pp. 1116–1127
- Hedberg, Y. / Qian, B. / Shen, Z. / Virtanen, S. / Wallinder, I. (2014): In vitro biocompatibility of CoCrMo dental alloys fabricated by selective laser melting, in: Dental materials : official publication of the Academy of Dental Materials, 30/5, pp. 525–534
- Hinterbuchner, T. (2019): Post-processing of Metal-based 3D-printed Parts with Subtractive Manufacturing [Bachelor's Thesis, TU Graz - not published]

## References

---

- Hochreiter, K. (2018): Technical and Economic Analysis of Metal-based 3D-printing and Improvement Potentials [Bachelor's Thesis, TU Graz - not published]
- Hoeges, S. / Lindner, M. / Fischer, H. / Meiners, W. / Wissenbach, K. (2009): Manufacturing of bone substitute implants using Selective Laser Melting, in: Magjarevic, R. / Hauelsen, J. / Nagel, J. / Nyssen, M. / Sloten, J. / Verdonck, P. (Hrsg.): 4th European Conference of the International Federation for Medical and Biological Engineering. ECIFMBE 2008 23-27 November 2008 Antwerp, Belgium, Berlin, Heidelberg: Springer Berlin Heidelberg, pp. 2230–2234
- Höller, C. / Hinterbuchner, T. / Schwemberger, P. / Zopf, P. / Pichler, R. / Haas, F. (2019): Direct Machining of selective laser melted components with optimized support structures, in: *Procedia CIRP*, 81, pp. 375–380
- Höller, C. / Zopf, P. / Schwemberger, P. / Pichler, R. / Haas, F. (2020): Load Capacity of Support Structures for Direct Machining of Selective Laser Melted Parts, in: *Conference Proceedings - ASME 2019 International Mechanical Engineering Congress and Exposition, Volume 2A: Advanced Manufacturing*
- Hopkinson, N. / Dickens, P. (2003): Analysis of rapid manufacturing—using layer manufacturing processes for production, in: *Proceedings of the Institution of Mechanical Engineers, Part C: Journal of Mechanical Engineering Science*, 217/1, pp. 31–39
- Hopkinson, N. / Dickens, P. / Hague, R. (2006): *Rapid manufacturing. An industrial revolution for the digital age*, Chichester, England: John Wiley
- Horsch, J. (2020): *Kostenrechnung. Klassische und neue Methoden in der Unternehmenspraxis*, 4<sup>th</sup> ed., Wiesbaden: Springer Gabler
- Hu, Z. / Zhu, H. / Zhang, H. / Zeng, X. (2017): Experimental investigation on selective laser melting of 17-4PH stainless steel, in: *Optics & Laser Technology*, 87, pp. 17–25
- IDC (2020): 3D printing spending forecast worldwide in 2019 and 2022, by segment (in billion U.S. dollars), September 9, 2020, retrieved from <https://www.statista.com/statistics/891764/worldwide-3d-printing-spending/>
- Industrieverband Massivumformung e.V. (2014): *Der technische Fortschritt in den Händen der Schmiede*, retrieved from <https://www.massivumformung.de/branche/geschichte-der-branche/der-technische-fortschritt-in-den-haenden-der-schmiede/>, accessed September 9, 2020
- ISO 2768-1:1989 (1989): *General tolerances — Part 1: Tolerances for linear and angular dimensions without individual tolerance indications*, 1989, Geneva
- ISO 2768-2:1989 (1989): *General tolerances — Part 2: Geometrical tolerances for features without individual tolerance indications*, 1989, Geneva
- ISO/ASTM 52900:2015 (2015): *Additive manufacturing — General principles — Terminology*, 2015, Geneva
- ISO/ASTM 52911-1:2019 (2019): *Additive manufacturing — Design — Part 1: Laser-based powder bed fusion of metals*, Number 1/2019, Geneva
- J. Hajnys / M. Pagac / J. Mesicek / J. Petru / F. Spalek (2020): Research of 316L Metallic Powder for Use in SLM 3D Printing, in: *Advances in Materials Science*, 20/1, pp. 5–15
- Jardim-Goncalves, R. / Sarraipa, J. / Agostinho, C. / Panetto, H. (2011): Knowledge framework for intelligent manufacturing systems, in: *Journal of Intelligent Manufacturing*, 22/5, pp. 725–735

## References

---

- Javaid, M. / Haleem, A. (2018): Additive manufacturing applications in medical cases: A literature based review, in: *Alexandria Journal of Medicine*, 54/4, pp. 411–422
- Jhabvala, J. / Boillat, E. / Antignac, T. / Glardon, R. (2010): On the effect of scanning strategies in the selective laser melting process, in: *Virtual and Physical Prototyping*, 5/2, pp. 99–109
- Kai, C. / Jacob, G. / Mei, T. (1997): Interface between CAD and Rapid Prototyping systems. Part 1: A study of existing interfaces, in: *The International Journal of Advanced Manufacturing Technology*, 13/8, pp. 566–570
- Kamath, C. / El-dasher, B. / Gallegos, G. / King, W. / Sisto, A. (2014): Density of additively-manufactured, 316L SS parts using laser powder-bed fusion at powers up to 400 W, in: *The International Journal of Advanced Manufacturing Technology*, 74/1-4, pp. 65–78
- Karanovic, S. (2018): Evaluation of Metal-based Selective Laser Melting Technology for Innovative Automotive Test and Measurement Solutions [Master's Thesis, TU Graz - not published]
- Kempen, K. / Thijs, L. / van Humbeeck, J. / Kruth, J.-P. (2012): Mechanical Properties of AlSi10Mg Produced by Selective Laser Melting, in: *Physics Procedia*, 39, pp. 439–446
- Kempen, K. / Yasa, E. / Thijs, L. / Kruth, J.-P. / van Humbeeck, J. (2011): Microstructure and mechanical properties of Selective Laser Melted 18Ni-300 steel, in: *Physics Procedia*, 12, pp. 255–263
- Kim, S. / Moon, S. (2020): A Part Consolidation Design Method for Additive Manufacturing based on Product Disassembly Complexity, in: *Applied Sciences*, 10/3, p. 1100
- Kingsley-Jones, M. (2018): NBAA: Business jet designs that changed the industry, September 9, 2020, retrieved from <https://www.flightglobal.com/business-aviation/nbaa-business-jet-designs-that-changed-the-industry/129766.article>
- Klahn, C. / Meboldt, M. / Fontana, F. / Leutenecker-Twelsiek, B. / Jansen, J. (eds.) (2018): *Entwicklung und Konstruktion für die Additive Fertigung. Grundlagen und Methoden für den Einsatz in industriellen Endkundenprodukten*, Würzburg: Vogel Business Media
- Kranz, J. (2017): *Methodik und Richtlinien für die Konstruktion von laseradditiv gefertigten Leichtbaustrukturen*, Dissertation, Hamburg University of Technology, Hamburg
- Krauss, H. (2017): *Qualitätssicherung beim Laserstrahlschmelzen durch schichtweise thermografische In-Process-Überwachung*, Dissertation, Technical University of Munich, Munich
- Krauss, H. / Eschey, C. / Götzfried, A. / Teufelhart, S. / Westhäuser, S. / Zäh, M. / Reinhart, G. (2011): Modellgestützte und hierarchische Prozesskettenbetrachtung für die additive Fertigung, in: *RTjournal - Forum für Rapid Technologie*, 8/1
- Kritzinger, W. / Steinwender, A. / Lumetzberger, S. / Sihm, W. (2018a): Impacts of Additive Manufacturing in Value Creation System, in: *Procedia CIRP*, 72, pp. 1518–1523
- Kritzinger, W. / Steinwender, A. / Lumetzberger, S. / Sihm, W. (2018b): Impacts of Additive Manufacturing in Value Creation System, in: *Procedia CIRP*, 72, pp. 1518–1523
- Kruth, J.-P. / Mercelis, P. / van Vaerenbergh, J. / Froyen, L. / Rombouts, M. (2005): Binding mechanisms in selective laser sintering and selective laser melting, in: *Rapid Prototyping Journal*, 11/1, pp. 26–36
- Kumke, M. (2018): *Methodisches Konstruieren von additiv gefertigten Bauteilen*, Dissertation, Technische Universität Braunschweig, Braunschweig

- Kurzynowski, T. / Chlebus, E. / Kuźnicka, B. / Reiner, J. (2012): Parameters in selective laser melting for processing metallic powders, in: Beyer, E. / Morris, T. (Hrsg.): High Power Laser Materials Processing: Lasers, Beam Delivery, Diagnostics, and Applications, SPIE, pp. 1–7
- Lachmayer, R. / Lippert, R. / Fahlbusch, T. (2016): 3D-Druck beleuchtet, Berlin, Heidelberg: Springer Berlin Heidelberg
- Laverne, F. / Segonds, F. / Anwer, N. / Le Coq, M. (2015): Assembly Based Methods to Support Product Innovation in Design for Additive Manufacturing: An Exploratory Case Study, in: Journal of Mechanical Design, 137/12, 21701/1-8
- Lee, H. / Lim, C. / Low, M. / Tham, N. / Murukeshan, V. / Kim, Y.-J. (2017): Lasers in additive manufacturing: A review, in: International Journal of Precision Engineering and Manufacturing-Green Technology, 4/3, pp. 307–322
- Leitner, C. (2020): Determination of Key Factors to Enable the Economic Use of Selective Laser Melting for Innovative Measurement Devices [Master's Thesis, TU Graz - not published]
- Leutenecker-Twelsiek, B. / Ferchow, J. / Klahn, C. / Meboldt, M. (2018): The Experience Transfer Model for New Technologies - Application on Design for Additive Manufacturing, in: Meboldt, M. / Klahn, C. (Hrsg.): Industrializing Additive Manufacturing - Proceedings of Additive Manufacturing in Products and Applications - AMPA2017, Cham: Springer International Publishing, pp. 337–346
- Li, R. / Liu, J. / Shi, Y. / Wang, L. / Jiang, W. (2012): Balling behavior of stainless steel and nickel powder during selective laser melting process, in: The International Journal of Advanced Manufacturing Technology, 59/9-12, pp. 1025–1035
- Lindemann, C. / Jahnke, U. / Habdank, M. / Koch, R. (2012): Analyzing Product Lifecycle Costs for a Better Understanding of Cost Drivers in Additive Manufacturing, in: 23rd Annual International Solid Freeform Fabrication Symposium - An Additive Manufacturing Conference, SFF 2012, pp. 177–188
- Lindemann, C. / Reiher, T. / Jahnke, U. / Koch, R. (2015): Towards a sustainable and economic selection of part candidates for additive manufacturing, in: Rapid Prototyping Journal, 21/2, pp. 216–227
- Lipson, H. / Kurman, M. (2013): Fabricated. The new world of 3D printing ; the promise and peril of a machine that can make (almost) anything, Indianapolis, Ind: J. Wiley & Sons
- Liverani, E. / Toschi, S. / Ceschini, L. / Fortunato, A. (2017): Effect of selective laser melting (SLM) process parameters on microstructure and mechanical properties of 316L austenitic stainless steel, in: Journal of Materials Processing Technology, 249, pp. 255–263
- Lodhi, M.J.K. / Deen, K. / Greenlee-Wacker, M. / Haider, W. (2019): Additively manufactured 316L stainless steel with improved corrosion resistance and biological response for biomedical applications, in: Additive Manufacturing, 27, pp. 8–19
- Measuring Productivity - OECD Manual. Measurement of Aggregate and Industry-level Productivity Growth (2001), Paris: OECD Publishing
- Metelkova, J. / Kinds, Y. / Kempen, K. / Formanoir, C. de / Witvrouw, A. / van Hooreweder, B. (2018): On the influence of laser defocusing in Selective Laser Melting of 316L, in: Additive Manufacturing, 23, pp. 161–169
- Milewski, J. (2017): Additive Manufacturing of Metals. From Fundamental Technology to Rocket Nozzles, Medical Implants, and Custom Jewelry, Springer Series in Materials Science, v.258, Cham: Springer International Publishing



## References

---

- Morgan, D. / Levatti, H. / Sienz, J. / Gil, A. / Bould, D. (2016): (2016) GE Jet Engine Bracket Challenge: A Case Study in Sustainable Design, in: *The Journal of Innovation Impact*, 7, pp. 95–107
- Otawa, N. / Sumida, T. / Kitagaki, H. / Sasaki, K. / Fujibayashi, S. / Takemoto, M. / Nakamura, T. / Yamada, T. / Mori, Y. / Matsushita, T. (2015): Custom-made titanium devices as membranes for bone augmentation in implant treatment: Modeling accuracy of titanium products constructed with selective laser melting, in: *Journal of cranio-maxillo-facial surgery : official publication of the European Association for Cranio-Maxillo-Facial Surgery*, 43/7, pp. 1289–1295
- Peter Lehmann AG (2020): Nullpunktspannsystem für 3D-Metalldruck, retrieved from <https://www.lehmann-additive.com/Deutsch/Downloads/>, accessed September 9, 2020
- Petrou, A. (2014): Economic Efficiency, in: Michalos, A. (Hrsg.): *Encyclopedia of Quality of Life and Well-Being Research*, Dordrecht: Springer Netherlands, pp. 1793–1794
- Pichler, R. / Stadlmayr, D. / Höller, C. / Schwemberger, P. / Malý, M. (2018): Economisation of Selective Laser Melting Processes via new Software Based Reductions of Support Structures and Enhanced Laser Strategies, July 12, 2018, Paris
- Piili, H. / Happonen, A. / Väistö, T. / Venkataramanan, V. / Partanen, J. / Salminen, A. (2015): Cost Estimation of Laser Additive Manufacturing of Stainless Steel, in: *Physics Procedia*, 78, pp. 388–396
- Piller, F. / Weller, C. / Kleer, R. (2015): Business Models with Additive Manufacturing—Opportunities and Challenges from the Perspective of Economics and Management, in: Brecher, C. (Hrsg.): *Advances in Production Technology*, Cham: Springer International Publishing, pp. 39–48
- Poprawe, R. / Hinke, C. / Meiners, W. / Schrage, J. / Bremen, S. / Merkt, S. (2015): SLM Production Systems: Recent Developments in Process Development, Machine Concepts and Component Design, in: Brecher, C. (Hrsg.): *Advances in Production Technology*, Cham: Springer International Publishing, pp. 49–65
- Prokopenko, J. (1987): *Productivity management. A practical handbook*, Geneva: Internat. Labour Off
- Qiu, C. / Kindi, M. / Aladawi, A. / Hatmi, I. (2018): A comprehensive study on microstructure and tensile behaviour of a selectively laser melted stainless steel, in: *Scientific reports*, 8/1, p. 7785
- Quinz, G. (2016): Erstellen eines Kalkulationsschemas für Bauteile auf Universitäten hergestellt mittels einer Laserschmelzanlage [Bachelor's Thesis, TU Graz - not published]
- Ravi, B. (2006): *Metal casting. Computer-aided design and analysis*, New Delhi: Prentice-Hall
- Revision der Grundlagennorm DIN 8580 „Fertigungsverfahren - Begriffe, Einteilung (2018). press release, retrieved from <https://www.din.de/resource/blob/276578/23c4645f41a507da734b2221b488c42f/pressemitteilung-revision-din-8580-data.pdf>, accessed March 5, 2020
- Rickenbacher, L. / Spierings, A. / Wegener, K. (2013): An integrated cost-model for selective laser melting (SLM), in: *Rapid Prototyping Journal*, 19/3, pp. 208–214
- Rowley, J. (2007): The wisdom hierarchy: representations of the DIKW hierarchy, in: *Journal of Information Science*, 33/2, pp. 163–180
- RUAG Group (2020): Piaggio P.180 Avanti II - first retrofit of Magnaghi Aeronautica landing gear upgrade, September 9, 2020, retrieved from <https://propeller-aircraft.ruag.com/en/piaggio-p180-avanti-ii-landing-gear-upgrade-retrofit-magnaghi>

## References

---

- Ruffo, M. / Hague, R. (2007): Cost estimation for rapid manufacturing ' simultaneous production of mixed components using laser sintering, in: Proceedings of the Institution of Mechanical Engineers, Part B: Journal of Engineering Manufacture, 221/11, pp. 1585–1591
- Ruffo, M. / Tuck, C. / Hague, R. (2006): Cost estimation for rapid manufacturing - laser sintering production for low to medium volumes, in: Proceedings of the Institution of Mechanical Engineers, Part B: Journal of Engineering Manufacture, 220/9, pp. 1417–1427
- Savalani, M. / Pizarro, J. (2016): Effect of preheat and layer thickness on selective laser melting (SLM) of magnesium, in: Rapid Prototyping Journal, 22/1, pp. 115–122
- Savolainen, J. / Collan, M. (2020): How Additive Manufacturing Technology Changes Business Models? – Review of Literature, in: Additive Manufacturing, 32, p. 101070
- Schleifenbaum, H. / Meiners, W. / Wissenbach, K. / Hinke, C. (2010): Individualized production by means of high power Selective Laser Melting, in: CIRP Journal of Manufacturing Science and Technology, 2/3, pp. 161–169
- Schmelzle, J. / Kline, E. / Dickman, C. / Reutzel, E. / Jones, G. / Simpson, T. (2015): (Re)Designing for Part Consolidation: Understanding the Challenges of Metal Additive Manufacturing, in: Journal of Mechanical Design, 137/11, p. 255
- Schröder, M. / Falk, B. / Schmitt, R. (2015): Evaluation of Cost Structures of Additive Manufacturing Processes Using a New Business Model, in: Procedia CIRP, 30, pp. 311–316
- Scipioni Bertoli, U. / Wolfer, A. / Matthews, M. / Delplanque, J.-P. / Schoenung, J. (2017): On the limitations of Volumetric Energy Density as a design parameter for Selective Laser Melting, in: Materials & Design, 113, pp. 331–340
- Skalon, M. / Meier, B. / Gruberbauer, A. / Amancio-Filho, S. / Sommitsch, C. (2020): Stability of a Melt Pool during 3D-Printing of an Unsupported Steel Component and Its Influence on Roughness, in: Materials (Basel, Switzerland), 13/3
- SLM Solutions Group AG (2019): Material Data Sheet - Stainless Steel 316L / 1.4404 / A276, retrieved from [https://slm-solutions.us/wp-content/uploads/2019/02/Stainless\\_Steel\\_316L.pdf](https://slm-solutions.us/wp-content/uploads/2019/02/Stainless_Steel_316L.pdf), accessed September 9, 2020
- SLM Solutions Group AG (2020a): Large Format Selective Laser Melting, retrieved from [https://www.slm-solutions.com/fileadmin/user\\_upload/SLM\\_R\\_800\\_Machine\\_EN.pdf](https://www.slm-solutions.com/fileadmin/user_upload/SLM_R_800_Machine_EN.pdf), accessed September 9, 2020
- SLM Solutions Group AG (2020b): Versatile Selective Laser Melting, High Power Laser in a Compact Footprint for Flexible Manufacturing, retrieved from [https://www.slm-solutions.com/fileadmin/user\\_upload/SLM\\_R\\_125\\_Machine\\_EN.pdf](https://www.slm-solutions.com/fileadmin/user_upload/SLM_R_125_Machine_EN.pdf), accessed September 9, 2020
- SmarTech Analysis (2019): The Future of Metal 3D Printing Technologies from a New Perspective, retrieved from <https://www.smartechanalysis.com/blog/category/additive-manufacturing/>, accessed September 9, 2020
- Sola, A. / Nouri, A. (2019): Microstructural porosity in additive manufacturing: The formation and detection of pores in metal parts fabricated by powder bed fusion, in: Journal of Advanced Manufacturing and Processing, 1/3, pp. 1–21
- Spierings, A. / Schneider, M. / Eggenberger, R. (2011): Comparison of density measurement techniques for additive manufactured metallic parts, in: Rapid Prototyping Journal, 17/5, pp. 380–386

## References

---

- Tang, Y. / Zhao, Y. (2016): A survey of the design methods for additive manufacturing to improve functional performance, in: *Rapid Prototyping Journal*, 22/3, pp. 569–590
- Tao, F. / Cheng, Y. / Zhang, L. / Nee, A. (2017): Advanced manufacturing systems: socialization characteristics and trends, in: *Journal of Intelligent Manufacturing*, 28/5, pp. 1079–1094
- Thijs, L. / Verhaeghe, F. / Craeghs, T. / van Humbeeck, J. / Kruth, J.-P. (2010): A study of the microstructural evolution during selective laser melting of Ti–6Al–4V, in: *Acta Materialia*, 58/9, pp. 3303–3312
- Tiefnig, R. (2019): Berechnung und Optimierung von Supportstrukturen bei additiver Fertigung [Bachelor's Thesis, TU Graz - not published]
- Tripathi, V. / Armstrong, A. / Gong, X. / Manogharan, G. / Simpson, T. / Meter, E. de (2018): Milling of Inconel 718 block supports fabricated using laser powder bed fusion, in: *Journal of Manufacturing Processes*, 34, pp. 740–749
- VDI 2225 Part 3:1998-11 (1998): Design engineering methodics - Engineering design at optimum cost - Valuation of costs, 1998, Düsseldorf
- VDI 2884 (2005): Purchase, operating and maintenance of production equipment using Life Cycle Costing (LCC), 2005, Düsseldorf
- VDI 3405 Part 3:2015-12 (2015): Additive manufacturing processes, rapid manufacturing - Design rules for part production using laser sintering and laser beam melting, 2015, Düsseldorf
- VDI 3405:2014-12 (2014): Additive manufacturing processes, rapid manufacturing - Basics, definitions, processes, 2014, Düsseldorf
- Wang, B. (2018): The Future of Manufacturing: A New Perspective, in: *Engineering*, 4/5, pp. 722–728
- Whittaker, D. (2017): Understanding the impact of powder reuse in metal Additive Manufacturing, in: *Metal AM*, 3/3, pp. 115–125
- Wong, H. / Dawson, K. / Ravi, G. / Howlett, L. / Jones, R. / Sutcliffe, C. (2019): Multi-Laser Powder Bed Fusion Benchmarking—Initial Trials with Inconel 625, in: *The International Journal of Advanced Manufacturing Technology*, 105/7-8, pp. 2891–2906
- Yadroitsev, I. / Krakhmalev, P. / Yadroitsava, I. (2014): Selective laser melting of Ti6Al4V alloy for biomedical applications: Temperature monitoring and microstructural evolution, in: *Journal of Alloys and Compounds*, 583, pp. 404–409
- Yadroitsev, I. / Shishkovsky, I. / Bertrand, P. / Smurov, I. (2009): Manufacturing of fine-structured 3D porous filter elements by selective laser melting, in: *Applied Surface Science*, 255/10, pp. 5523–5527
- Yakout, M. / Elbestawi, M. / Veldhuis, S. (2018): On the characterization of stainless steel 316L parts produced by selective laser melting, in: *The International Journal of Advanced Manufacturing Technology*, 95/5-8, pp. 1953–1974
- Yang, S. / Zhao, Y. (2015): Additive manufacturing-enabled design theory and methodology: a critical review, in: *The International Journal of Advanced Manufacturing Technology*, 80/1-4, pp. 327–342
- Yap, C. / Chua, C. / Dong, Z. / Liu, Z. / Zhang, D. / Loh, L. / Sing, S. (2015): Review of selective laser melting: Materials and applications, in: *Applied Physics Reviews*, 2/4, pp. 1–21
- Yasa, E. / Kempen, K. / Kruth, J.-P. / Thijs, L. / Van, H. (2010): Microstructure and mechanical properties of maraging steel 300 after selective laser melting, in: *21st Annual International Solid Freeform Fabrication Symposium - An Additive Manufacturing Conference, SFF 2010*, pp. 383–396

- Zäh, M. (2013): Wirtschaftliche Fertigung mit Rapid-Technologien. Anwender-Leitfaden zur Auswahl geeigneter Verfahren, München: Hanser
- Zäh, M. / Schilp, J. / Weirather, J. / Zeller, C. / Schmiegel, B. / Ott, M. / Westhäuser, S. (2018): Additive Fertigungsverfahren, in: Rieg, F. / Steinhilper, R. (Hrsg.): Handbuch Konstruktion, München: Carl Hanser Verlag GmbH & Co. KG, pp. 995–1013
- Zhang, L. / Zhang, S. / Zhu, H. / Hu, Z. / Wang, G. / Zeng, X. (2018): Horizontal dimensional accuracy prediction of selective laser melting, in: Materials & Design, 160, pp. 9–20

## APPENDIX

**Table A 1:** Overview of the manufacturing costs for the jet engine bracket.

Number of parts	Manufacturing costs per part in €			
	30 µm / 0 s	30 µm / 30 s	50 µm / 0 s	50 µm / 30 s
1	695.19	1094.82	617.20	914.18
5	209.44	253.09	201.66	218.04
10	145.53	158.69	140.96	145.93
16	121.52	126.97	118.33	120.21
17	152.58	181.22	144.99	164.24
21	140.28	154.83	135.99	141.33
26	129.00	137.42	125.28	128.35
32	120.09	125.55	116.90	118.79
33	136.14	153.54	130.68	141.51
37	130.93	141.55	127.12	130.97
42	125.06	132.35	121.54	124.17
48	119.75	125.21	116.56	118.45

**Table A 2:** Overview of the manufacturing costs for the filter head.

Number of parts	Manufacturing costs per part in €			
	30 µm / 0 s	30 µm / 30 s	50 µm / 0 s	50 µm / 30 s
1	1060.48	1732.65	924.16	1298.86
3	559.15	655.62	477.22	530.72
6	433.59	459.33	365.21	379.42
8	401.73	415.49	336.84	343.73
9	469.85	556.78	397.03	444.79
11	440.51	476.84	370.98	390.58
14	412.13	431.02	345.74	355.77
16	398.88	412.64	333.99	340.88
17	435.11	487.61	366.03	394.55
19	421.78	448.61	354.21	368.45
22	406.27	423.30	340.43	349.32
24	398.10	411.87	333.22	340.10

**Table A 3:** Overview of the manufacturing costs for the pipe section.

Number of parts	Manufacturing costs per part in €			
	30 µm / 0 s	30 µm / 30 s	50 µm / 0 s	50 µm / 30 s
1	909.44	1977.80	781.18	1433.88
5	396.69	550.41	244.88	353.72
10	252.00	277.25	201.34	221.39
30	125.50	127.47	96.49	96.72
59	112.51	112.51	85.08	85.08
88	107.70	107.70	80.98	80.98
117	105.43	105.43	79.02	79.02
118	111.86	120.91	84.59	90.12
147	109.21	109.62	82.28	82.32
176	107.54	107.54	80.79	80.79
205	106.18	106.18	79.64	79.64
234	105.23	105.23	78.83	78.83
235	108.46	113.01	81.62	84.40
264	107.36	107.59	80.66	80.69

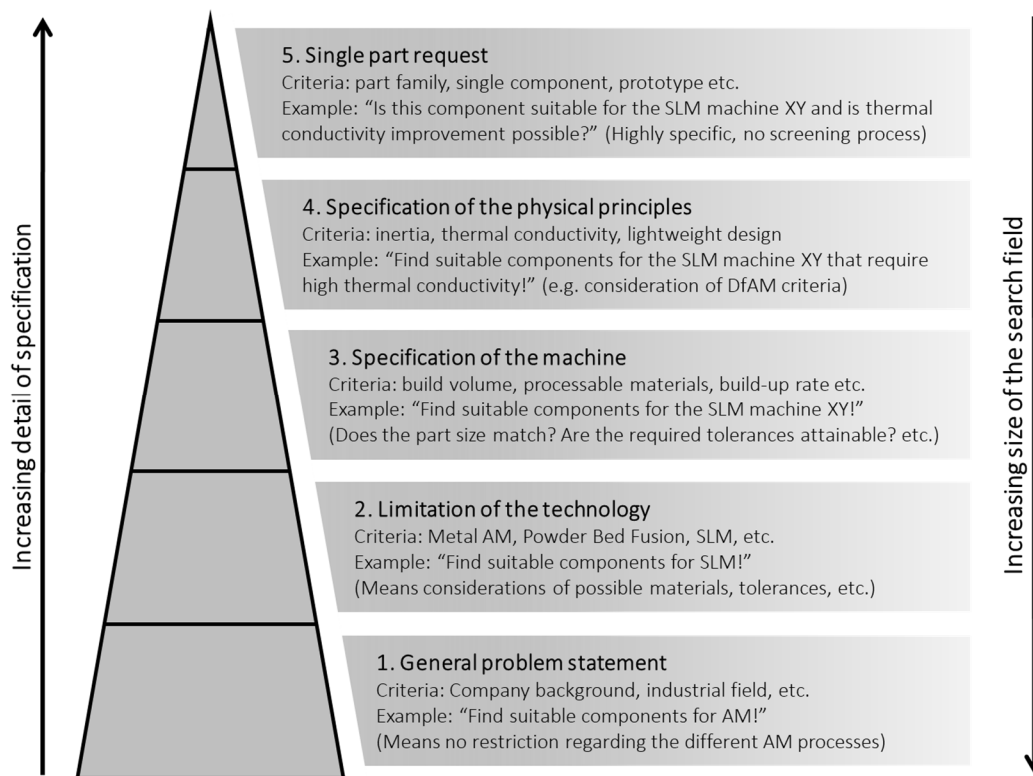


**Figure A 1:** Hierarchy of problem statement for step 1 of the screening process model (SPM);  
Source: cf. Leitner (2020) p. 44.

## Appendix

Criteria (1)	Weighting Factor Main Criteria (2)	Weighting Factor Specific Criteria (3)	Weighting Factor (4)	Measurement cell lock		Measurement body	
				Rating	Utility Value	Rating	Utility Value
<b>General Manufacturing Criteria</b>	35%						
Production Volume		40%	14	5	70	5	70
Individualization		15%	5	1	5	1	5
Complexity		40%	14	2	28	5	70
Scrap		5%	2	2	4	2	4
		100%	35		107		149
<b>Component Criteria</b>	30%						
Material		22%	7	5	33	5	33
Size		22%	7	4	26	5	33
Tolerances		20%	6	3	18	2	12
Surface Quality		20%	6	3	18	3	18
Density		11%	3	5	17	5	17
Stress/Fatigue Resistance		2,5%	1	4	3	2	2
Safety		2,5%	1	5	4	5	4
		100%	30		119		118
<b>DfAM Criteria</b>	35%						
Material Gradient		25%	9	1	9	1	9
Lightweight Design		25%	9	1	9	5	44
Integrated Design		25%	9	1	9	5	44
Surface/Lattice Structure		25%	9	1	9	1	9
		100%	35		35		105
	100%						
					260		372

Max. Value	500	
Min. Value	100	
Limit Value (5)	325	65%

**Figure A 2:** Assessment of two possible parts;  
Source: Leitner (2020) p. 56.

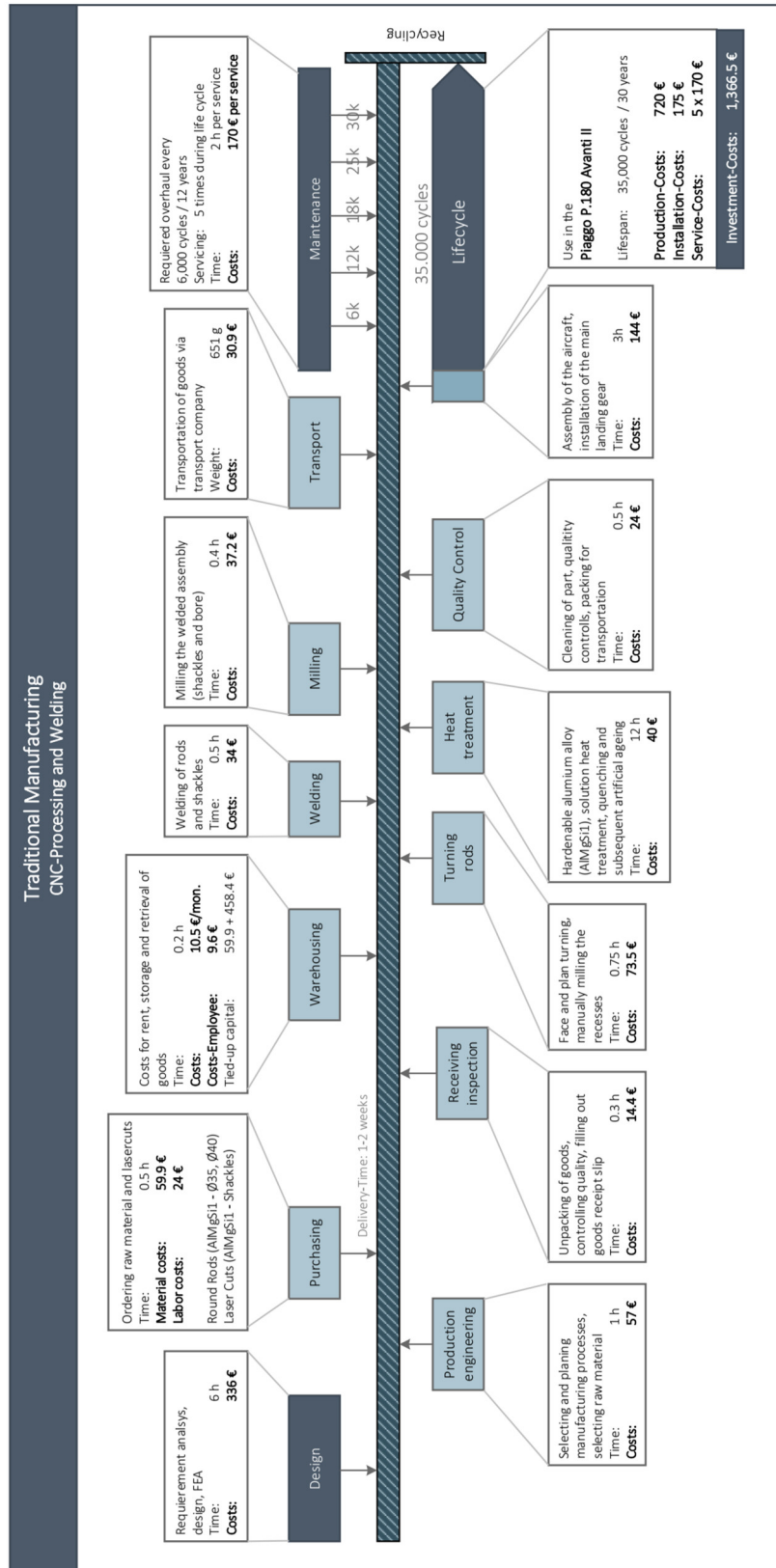


Figure A 3: Lifecycle analysis of the CM major support component; Source: cf. Hochreiter (2018) p. 63.



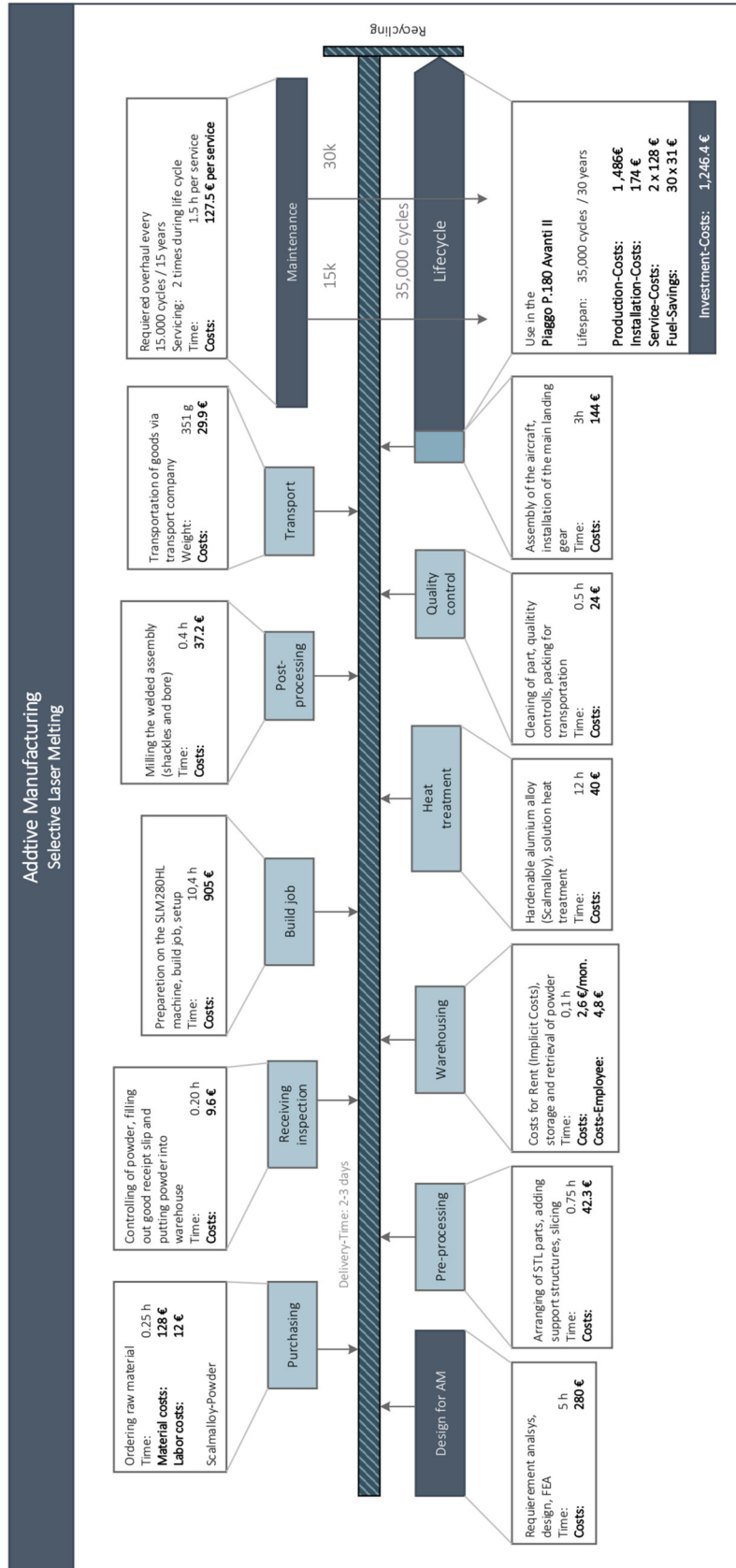


Figure A 4: Lifecycle analysis of the AM major support component; Source: cf. Hochreiter (2018) p. 64.

## Appendix

**Table A 4:** Technical value of the compared design 1 and 8 for the major support component;  
Source: based on Hochreiter (2018).

Technical specifications	Design 1	Design 2	Ideal Design
Lightweight	1	3	4
Material waste	2	3	4
Stress distribution	3	4	4
Stiffness	2	4	4
Manufacturability	3	2	4
Few process steps	2	3	4
Total	13	19	24
<b>Technical value</b>	<b>0.54</b>	<b>0.79</b>	<b>1.00</b>

**Table A 5:** Economic value of the compared design 1 and 8 for the major support component;  
Source: based on Hochreiter (2018).

Economic specifications	Design 1	Design 2
Manufacturing costs H in €	720	1486
Maximal manufacturing costs H <sub>zul</sub> in €	850	850
<b>Economic value</b>	<b>0.83</b>	<b>0.40</b>
Manufacturing costs H in €, LCC	1366	1246
Maximal manufacturing costs H <sub>zul</sub> in €, LCC	1300	1300
<b>Economic value for AM</b>	<b>0.67</b>	<b>0.73</b>

**Table A 6:** Overview of all investigated parameter configurations for 316L economy.

Sample	Laser power P <sub>L</sub> in W			Scan speed v <sub>s</sub> in mm/s			Hatch spacing h <sub>s</sub> in μm	Layer thicknes t <sub>z</sub> in μm	Volumetric energy density E <sub>v</sub> in J/mm <sup>3</sup>			Rotation hatching
	H	F	B	H	F	B	H	F	B			
AD 1	260	none	none	2000	none	none	65	50	40	none	none	yes
AD 2	400	none	none	2000	none	none	100	50	40	none	none	no
AD 3	330	none	none	2540	none	none	65	50	40	none	none	no
AD 4	400	none	none	3080	none	none	65	50	40	none	none	no
AD 5	260	100	100	2000	625	625	65	50	40	49	49	yes
AD 6	350	none	none	1450	none	none	60	50	80	none	none	yes
AD 7	350	none	none	1450	none	none	120	50	40	none	none	yes
AD 8	350	none	none	2900	none	none	60	50	40	none	none	yes
AD 9	350	none	none	2900	none	none	120	50	20	none	none	yes
AD 10	275	150	100	700	400	300	120	50	65	63	56	yes
AD 11	275	150	100	700	400	300	120	50	65	63	56	yes
AD 12	207	113	75	700	400	300	120	50	49	47	42	yes
AD 13	275	150	100	931	532	399	120	50	49	47	42	yes
AD 14	260	none	none	2000	none	none	65	50	40	none	none	no
AD 15	260	100	100	2000	625	625	65	50	40	49	49	yes
AD 16	260	none	none	2000	none	none	65	50	40	none	none	no
AD 17	195	100	100	3000	625	625	65	50	20	49	49	yes
AD 18	260	none	none	2000	none	none	50	50	52	none	none	yes
AD 19	260	none	none	2000	none	none	35	50	74	none	none	yes
AD 20	330	none	none	2540	none	none	50	50	52	none	none	no
AD 21	330	none	none	2540	none	none	50	50	52	none	none	no
AD 22	330	none	none	2540	none	none	35	50	74	none	none	no
AD 23	400	none	none	3080	none	none	65	50	40	none	none	yes
AD 24	400	none	none	3080	none	none	50	50	52	none	none	no
AD 25	400	none	none	3080	none	none	35	50	74	none	none	no
AD 26	260	100	100	2000	625	625	65	50	40	49	49	yes
AD 27	260	100	100	2000	625	625	65	50	40	49	49	yes
AD 28	400	none	none	2540	none	none	65	50	48	none	none	no
AD 29	400	none	none	1450	none	none	60	50	92	none	none	yes
AD 30	400	none	none	1667	none	none	60	50	80	none	none	yes

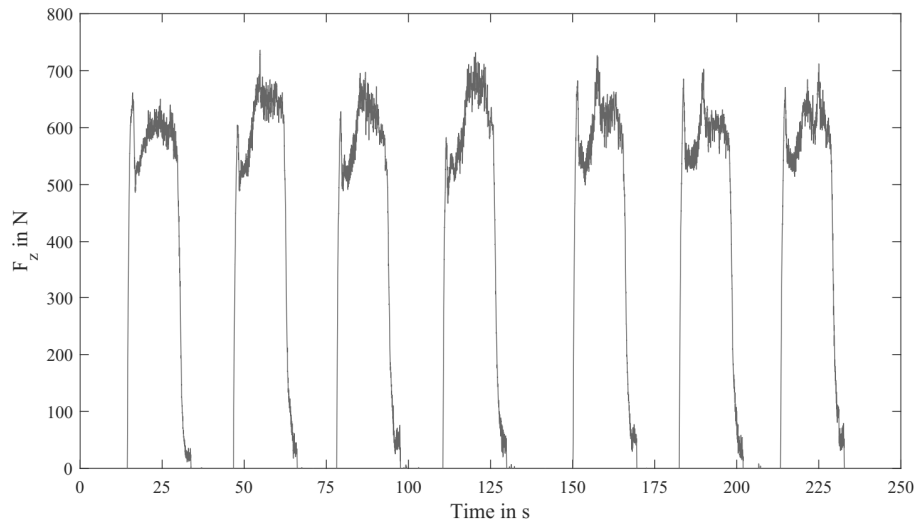


**Figure A 5:** Time-force graph for the drilling experiments for DM1 test series;  
Source: own representation.

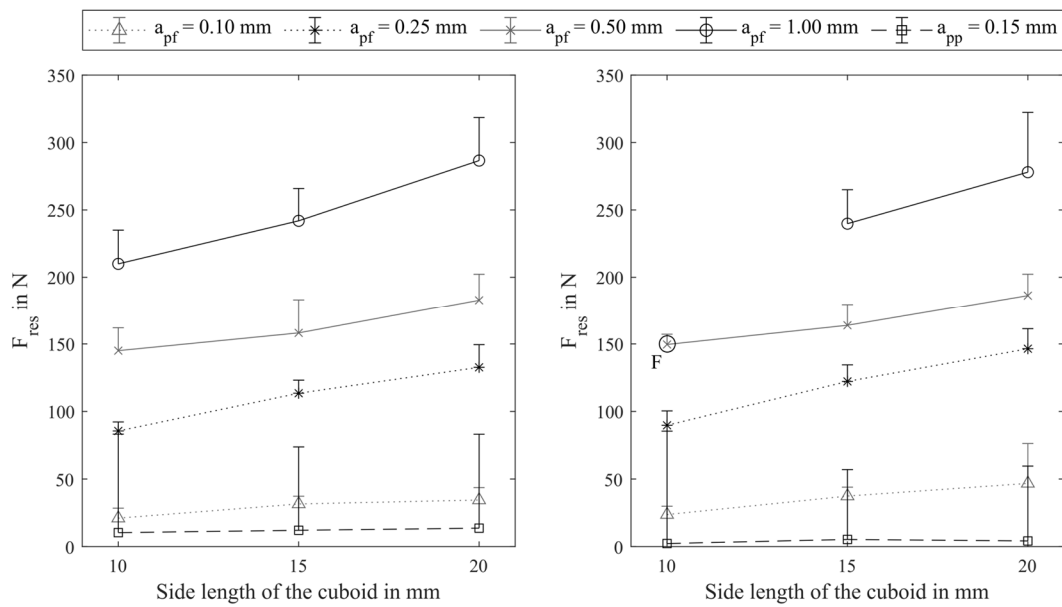


**Figure A 6:** Mean and maximum cutting forces for cuboid test parts for face milling ( $a_{pf}$ ) and profile milling ( $a_{pp}$ );  
Left: block support structures; right: Heartcell support structures;  
Source: own representation, cf. Höller et al. (2019).

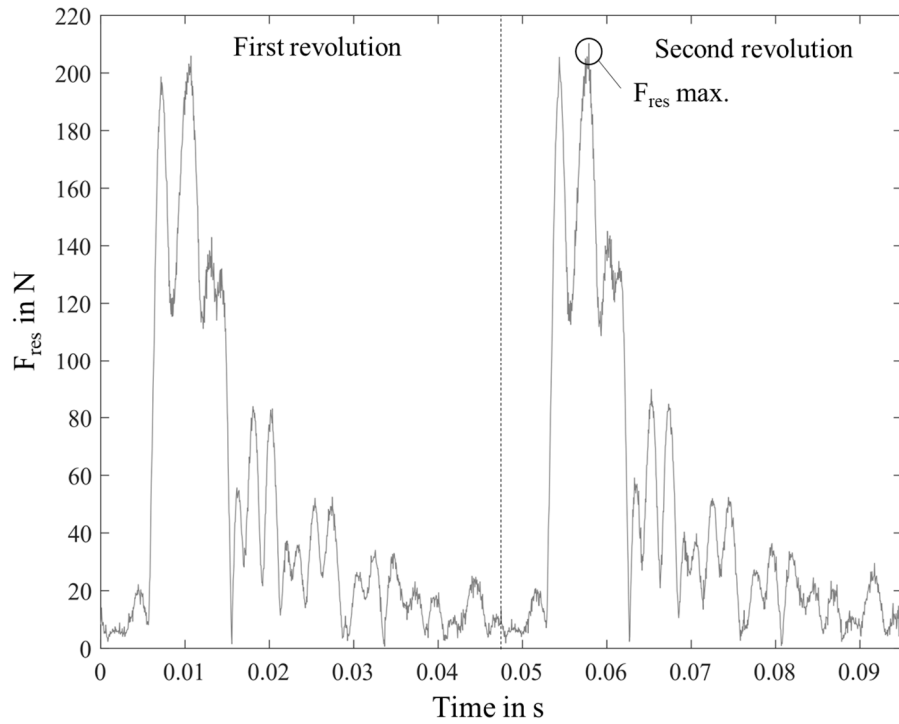


**Figure A 7:** Force-time graph for two revolutions of the milling cutter with a single insert;  
Source: own representation, cf. Höller et al. (2020).

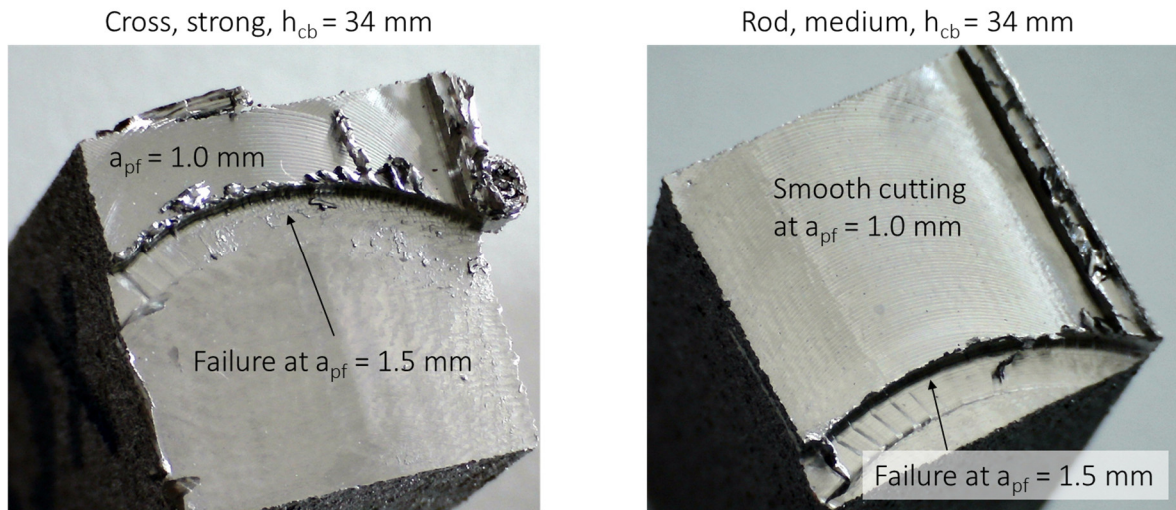


**Figure A 8:** Exemplary macro pictures of two machined surfaces of different ST and FL during DM2 experiments;  
Source: own representation.

*Ein Stift und ein Zettel und der Rest ergibt sich.  
Das Leben ist kein Highway, es ist die B73.*

– Thees Uhlmann –